

**TECTONIC SIGNIFICANCE OF THE AKAITCHO
GROUP, WOPMAY OROGEN, NORTHWEST
TERRITORIES, CANADA**

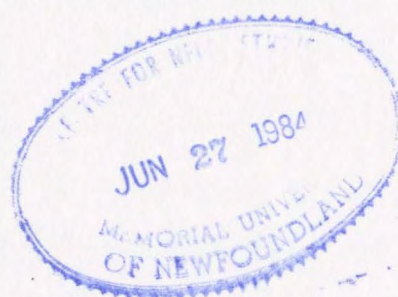
CENTRE FOR NEWFOUNDLAND STUDIES

**TOTAL OF 10 PAGES ONLY
MAY BE XEROXED**

(Without Author's Permission)

ROBERT MICHAEL EASTON

41050



CANADIAN THESES ON MICROFICHE

I.S.B.N.

THESES CANADIENNES SUR MICROFICHE



National Library of Canada
Collections Development Branch

Canadian Theses on
Microfiche Service

Ottawa, Canada
K1A 0N4

Bibliothèque nationale du Canada
Direction du développement des collections

Service des thèses canadiennes
sur microfiche

NOTICE

The quality of this microfiche is heavily dependent upon the quality of the original thesis submitted for microfilming. Every effort has been made to ensure the highest quality of reproduction possible.

If pages are missing, contact the university which granted the degree.

Some pages may have indistinct print especially if the original pages were typed with a poor typewriter ribbon or if the university sent us a poor photocopy.

Previously copyrighted materials (journal articles, published tests, etc.) are not filmed.

Reproduction in full or in part of this film is governed by the Canadian Copyright Act, R.S.C. 1970, c. C-30. Please read the authorization forms which accompany this thesis.

THIS DISSERTATION
HAS BEEN MICROFILMED
EXACTLY AS RECEIVED

AVIS

La qualité de cette microfiche dépend grandement de la qualité de la thèse soumise au microfilmage. Nous avons tout fait pour assurer une qualité supérieure de reproduction.

S'il manque des pages, veuillez communiquer avec l'université qui a conféré le grade.

La qualité d'impression de certaines pages peut laisser à désirer, surtout si les pages originales ont été dactylographiées à l'aide d'un ruban usé ou si l'université nous a fait parvenir une photocopie de mauvaise qualité.

Les documents qui font déjà l'objet d'un droit d'auteur (articles de revue, examens publiés, etc.) ne sont pas microfilmés.

La reproduction, même partielle, de ce microfilm est soumise à la Loi canadienne sur le droit d'auteur, SRC 1970, c. C-30. Veuillez prendre connaissance des formules d'autorisation qui accompagnent cette thèse.

LA THÈSE A ÉTÉ
MICROFILMÉE TELLE QUE
NOUS L'AVONS REÇUE

TECTONIC SIGNIFICANCE OF THE AKAITCHO GROUP,
WOPMAY OROGEN, NORTHWEST TERRITORIES, CANADA

by

© Robert Michael Easton, B.Sc. (Hons.), M.Sc.

A Thesis submitted in partial fulfillment of the
requirements for the degree of Doctor of Philosophy

Department of Earth Sciences
Memorial University of Newfoundland

May, 1982

St. John's

Newfoundland

ABSTRACT

The early Proterozoic Akaitcho Group consists of 6 to 8 km of metasedimentary and metavolcanic rocks located in the central metamorphic core zone of the Wopmay Orogen (Bear Province). In the northern part of the orogen, the following generalized stratigraphic sequence has been recognized: 1) a lower mainly basaltic sequence, 2) 1-2 km of arkosic turbidites intruded by sills of rhyolite porphyry, 3) basalt and rhyolite volcanic complexes, and 4) 1 to 2 km of pelite and tuffaceous sedimentary rocks; locally, intruded by gabbro sills. The Akaitcho Group is conformably overlain by the Odjick Formation, part of an inferred passive-continental margin sequence (the Epworth Group).

Two types of chondrite-normalized REE patterns are present in the Akaitcho Group basalts: a sloping pattern similar to recent continental tholeiites, and a flat pattern similar to type II ocean tholeiites. The basalt geochemistry in the Akaitcho Group evolves from older, evolved continental tholeiites, through continental tholeiites, to younger oceanic tholeiites. The Akaitcho Group rhyolites are probably crustally-derived. REE patterns of the Akaitcho Group sedimentary rocks indicate that the arkosic turbidites were derived from a granodiorite source terrane (i.e. average continental crust), whereas the upper pelites were derived from a volcanic source terrane similar to the Akaitcho Group volcanic complexes and a granodiorite source terrane.

Bimodal volcanism (subalkaline basalt and rhyolite) in association with continent-derived sediments, the temporal evolution of the basalt geochemistry, and the similarity of the Akaitcho Group to recent rift sequences indicate that the Akaitcho Group was deposited in a rift. The stratigraphic position of the Akaitcho Group beneath the Epworth Group suggests that the Akaitcho Group is related to continental break-up along the western Slave Craton about 1.9 Ga. Zircon dates from central Wopmay Orogen indicate that sea-floor spreading associated with continental break-up was short-lived.

ACKNOWLEDGEMENTS

During the course of this study I have been helped by many people whom I wish to acknowledge and thank:

- my supervisors, Brian Fryer, Dave Strong, and Rick Hiscott, for guidance, advice, and review of this manuscript in addition to several of the other publications resulting from this thesis.
- to Paul Hoffman, who initially suggested the project, for providing field support and constructive criticism on various aspects of the project.
- to Marc St-Onge for his companionship during two field seasons in the Hepburn Lake area, and for introducing me to the value of metamorphic petrology.
- to J.C. McGlynn of the Geological Survey of Canada, and to W.A. Padgham of the Department of Indian and Northern Affairs, Yellowknife, for field support and encouragement throughout the course of this study.
- to Sam Bowring and Randy Van Schmus for the zircon dates reported in Table 5.5.
- to D. Press, G. Andrews, P. Davis, H. Longerich, W. Marsh and J. Vahtra for their assistance in geochemical and isotopic analysis and the preparation of this thesis.
- to my field assistants D. Furey (1979) and P. de Bie (1980).
- to the faculty and graduate students of the department for assistance and stimulating conversation.
- to Teresa Barker for typing the final manuscript.

Financial support was provided by a Memorial University of Newfoundland Graduate Fellowship (1979-1982); Energy, Mines and Resources Research Agreements 23233-9-0126 and 23233-0-0057; and a NSERC operating grant to B.J. Fryer. The author acknowledges and appreciates these sources of funding.

Finally, I wish to thank my wife, Monica, for typing parts of successive drafts of the thesis, and the tables in the final manuscript, and for her help and encouragement throughout our stay in Newfoundland.

TABLE OF CONTENTS

	Page
ABSTRACT	ii
ACKNOWLEDGEMENTS	iv
LIST OF TABLES	xiii
LIST OF FIGURES	xvi

CHAPTER 1

INTRODUCTION

1.1 INTRODUCTION	1
1.2 PREVIOUS WORK	2
1.3 PRESENT STUDY	6
1.4 NOMENCLATURE, METHODS AND MATERIALS	10

CHAPTER 2

GENERAL GEOLOGY

2.1 WOPMAY OROGEN - REGIONAL GEOLOGY	13
2.1.1 Sedimentary Prism	19
2.1.2 Great Bear Arc	21
2.1.3 Development of the Wopmay Orogen - The Two Collision Model of Hoffman	21
2.2 GEOLOGY OF ZONE 3	27
2.2.1 Overview	27
2.2.2 Northern Zone 3 (north of 65°N)	27
Hepburn Lake map area (N.T.S. 86J)	35

Four Corners map area.	39
Wopmay-Grant Lake map area	39
2.2.3 Southern Zone 3 (south of 65°N).	39

CHAPTER 3 STRATIGRAPHY

3.1 INTRODUCTION.	50
3.2 SITIYOK COMPLEX	51
3.3 AKAITCHO GROUP.	55
3.3.1 Ipiutak Subgroup	55
3.3.2 Zephyr Formation	68
3.3.3 Okrark Sills	68
3.3.4 Nasittok Subgroup.	71
3.3.5 Aglerok Formation.	81
3.3.6 Tallerk Formation.	88
McGregor Amphibolite Member.	88
Tallerk Sills.	88
3.3.7 Grant Subgroup	89
3.3.8 Zone 2/3 Boundary.	94
Drill Formation.	103
Vaillant Formation	103
Stanbridge Formation	105
3.4 EPWORTH GROUP	105
3.4.1 Odjick Formation	112
External Zone.	112

	viii
	Page
Interhal Zone	112
3.4.2 Rocknest Formation.	112
3.5 AKAITCHO/EPWORTH GROUP RELATIONS.	112
3.5.1 Area 1.	113
3.5.2 Area 2.	113
3.5.3 Area 3.	118
3.5.4 Area 4.	118
3.5.5 Summary	118
3.6 SNARE GROUP.	119
3.7 REGIONAL CORRELATION	120
3.8 SUMMARY: STRATIGRAPHIC CONSTRAINTS ON THE DEVELOPMENT OF THE AKAITCHO GROUP.	122

CHAPTER 4 GEOCHEMISTRY

4.1 INTRODUCTION	126
4.2 EXTRUSIVE ROCKS.	136
4.2.1 Basalts	136
4.2.2 Ipiutak Subgroup Basalts.	146
4.2.3 Tuertok Volcanic Complex Basalts.	154
4.2.4 Kapvik Volcanic Complex Basalts	164
4.2.5 Tallerk Sills	171
4.2.6 Belleau Volcanic Complex Basalts and the Grant Subgroup Basalts.	171
4.2.7 Akaitcho Group Basalts - Overall Trends	180

4.2.8	Rhyolites	180
4.2.9	Vaillant Formation.	187
4.3	SEDIMENTARY ROCKS.	196
4.3.1	Introduction.	196
4.3.2	Lower Akaitcho Group Sedimentary Rocks.	200
4.3.3	Upper Akaitcho Group Sedimentary Rocks.	210
4.3.4	Upper Akaitcho/Lower Epworth Group.	212
4.3.5	Effects of Metamorphic Grade.	224
4.3.6	Comparison With Other Post-Archean Sedimentary Rocks	224
4.4	SUMMARY.	224

CHAPTER 5

ISOTOPE GEOCHEMISTRY AND THE AGE OF
THE AKAITCHO GROUP

5.1	INTRODUCTION	230
5.2	Rb-Sr DATING	231
5.3	SITIYOK COMPLEX.	231
	Gneiss	231
	Granite.	232
	Amphibolite Dykes.	233
5.4	VAILLANT BASALTS	239
5.5	BELLEAU BASALTS.	240
5.6	EDJUVIT MYLONITE ZONE.	244
5.7	OKRARK SILLS	247

	x
	Page
5.8 TUERTOK RHYOLITES:	247
5.9 RIB GRANITE.	248
5.10 OTHER AGE CONTROLS ON THE AKAITCHO GROUP.	254
5.11 U-Pb ZIRCON DATES FROM THE WOPMAY OROGEN.	259
5.12 DISCUSSION.	261
5.12.1 Zircon Dates.	261
5.12.2 Regional Resetting of Rb-Sr Systems	264
5.12.3 Rb-Sr Mobility - Implications For Other Elements?	272
Belleau Basalt.	273
Tuertok Rhyolite.	274
Vaillant Basalt	274
Summary	276
5.13 SUMMARY	277

CHAPTER 6

HISTORY AND SIGNIFICANCE OF THE AKAITCHO GROUP

6.1 INTRODUCTION	278
6.2 THICKNESS OF THE CRUST DURING NASITTOK SUBGROUP DEPOSITION.	279
6.3 PHYSICAL VOLCANOLOGY OF THE AKAITCHO GROUP	286
6.3.1 Basalts	286
6.3.2 Rhyolite.	289
6.3.3 Tallerk Sills	295

6.3.4	Summary	295
6.4	ORIGIN AND SIGNIFICANCE OF THE AKAITCHO GROUP. . .	296
6.5	U-Pb ZIRCON DATES AND MODELS OF THE DEVELOPMENT OF THE WOPMAY OROGEN	300
6.5.1	Introduction.	300
6.5.2	Subsidence Rates and the Deposition of the Akaitcho and Epworth Groups	301
6.5.3	Emplacement of the Hepburn Batholith.	305
6.5.4	Discussion.	306
	Strike-Slip (Pull-Apart) Basin.	306
	Marginal Basin.	307
	Continental Rifting Leading to Limited Sea-Floor Spreading	308
6.6	DEPOSITIONAL HISTORY OF THE AKAITCHO GROUP	311

CHAPTER 7

THE AKAITCHO GROUP AND THE DEVELOPMENT OF CONTINENTAL MARGINS

7.1	INTRODUCTION	316
7.2	CLASSIFICATION OF PROTEROZOIC RIFT SEQUENCES . .	316
7.3	THE AKAITCHO GROUP	317
7.4	CLASS ONE RIFTS - COMPARISON WITH THE AKAITCHO GROUP	321
7.4.1	Labrador Trough	321
7.4.2	Cape Smith Foldbelt	323

7.4.3 Burin Group	325
7.5 DISCUSSION: CRUSTAL STRUCTURE OF CONTINENTAL MARGINS.	326
7.6 CONCLUSIONS.	330

CHAPTER 8

SUMMARY AND CONCLUSIONS	331
-------------------------	-----

REFERENCES.	337
---------------------	-----

APPENDICES

APPENDIX A ANALYTICAL METHODS.	369
A.1 Sample Collection and Preparation.	369
A.2 Major Element Analysis	369
A.3 Trace Element Analysis	371
A.4 Rare-Earth Element Analysis.	372
APPENDIX B RUBIDIUM-STRONTIUM DATING METHODS AND ANALYTICAL RESULTS.	380
B.1 Sample Preparation	380
B.2 Strontium Separation	380
B.3 Rubidium-Strontium Analysis.	381
APPENDIX C STRAIN MEASUREMENTS ON CONGLOMERATES OVERLYING THE TUERTOK VOLCANIC COMPLEX.	392
APPENDIX D CHEMICAL ANALYSES	396

LIST OF TABLES

	Page
Table 1.1 Publications Related to Thesis	10
Table 2.1 Stratigraphic nomenclature and regional correlation chart: Foreland Wopmay Orogen and associated basins.	17
Table 2.2 Comparison between stratigraphic nomenclature in northern (above 65°N) and southern (below 65°N) Wopmay Orogen.	47
Table 3.1 Lithological correlation of strata between the Wopmay Orogen and the Athapuscow Aulacogen	121
Table 4.1 Representative chemical analyses of Akaitcho Group basalts	140
Table 4.2 Representative chemical analyses of Akaitcho Group rhyolites	184
Table 4.3 Representative chemical analyses of Vaillant Formation mafic rocks	190
Table 4.4 Representative chemical analyses of Akaitcho Group sedimentary rocks	201
Table 4.5 Comparison of several post-Archean shale composites	213
Table 5.1 Isochron regressions for samples from the Sityok Igneous Complex	234

Table 5.2	Isochron regressions for samples from the Vaillant Formation and the Belleau volcanic complex	241
Table 5.3	Isochron regressions for samples from the Okrark sills, the Tuertok rhyolites, and the Rib granite	249
Table 5.4	Age controls on the Akaitcho Group and related events and units in the Wopmay Orogen.	255
Table 5.5	U-Pb zircon dates from the Wopmay Orogen	260
Table 5.6	Outcrop scale variation in eight samples of a Tuertok volcanic complex rhyolite flow.	275
Table A.1	Distribution of analyzed samples between stratigraphic units.	371
Table A.2	Comparison of XRF and AA methods for major element determinations on sample F405.78 - a basalt.	373
Table A.3	Comparison of contaminated and uncontaminated sample pellets.	373
Table A.4	Comparison of trace element results for four pellets made from one jar of rock powder for sample F412B.80 - a basalt.	374

Table A.5	Trace element variation in pellets prepared from two splits of sample F464.79 - a gabbro.	374
Table B.1	Results of rubidium and strontium analyses for samples from the Sitiyok Igneous Complex.	382
Table B.2	Results of rubidium and strontium analyses for samples from the Belleau volcanic complex and the Vaillant Formation basalts	383
Table B.3	Results of rubidium and strontium analyses for samples from the Edjuvit mylonite zone.	384
Table B.4	Results of rubidium and strontium analyses for samples from the Okrark sills and a rhyolite from the Tuertok volcanic complex	385
Table B.5	Results of rubidium and strontium analyses for samples from the Rib Pluton	386
Table C.1	Measured strain ratios in conglomerate overlying the Tuertok volcanic complex	394

LIST OF FIGURES

	Page
Figure 1.1	Northwestern Canadian Shield 4
Figure 1.2	Location of areas studied by the author in central Wopmay Orogen. May 1978 to September 1981 9
Figure 2.1	Tectonic subdivisions of the Wopmay Orogen. 15
Figure 2.2	Model for the development of the Wopmay Orogen. 24
Figure 2.3	Geological map of the central metamorphic core zone (Zone 3) of northern Wopmay Orogen. 29
Figure 2.4	Geological compilation map of Zone 3 in southern Wopmay Orogen . . . 31
Figure 2.5	Major faults and structural blocks (A-G) in the northern part of the Wopmay Orogen 34
Figure 2.6	Simplified geological map of the Hepburn Lake map area (N.T.S. 86J/W ₂), showing distribution of the Akaitcho Group. 37
Figure 2.7	Major tectonic elements of the Hepburn Lake map area (N.T.S. 86J). . . 41

Figure 2.8	Generalized cross-section across the Hepburn Lake map area at 66°25'N, showing synclinoria-anticlinoria pairs and thrusts within the Akaitcho and Epworth Groups.	43
Figure 2.9	Metamorphic mineral assemblages and distribution of isograds in the Hepburn Lake map area (N.T.S.86J/W½)	45
Figure 3.1	Geology of the northern half of the Sityok Igneous Complex.	54
Figure 3.2	Generalized stratigraphic column for the Akaitcho Group	56
Figure 3.3	Stratigraphic column for the Akaitcho Group in block B and suggested lithological correlations with the volcanic and sedimentary rocks in Cloos Nappe and the Grant block.	58
Figure 3.4	Geological sketch map showing distribution of volcanic rocks interbedded with the lower Zephyr Formation in crustal block B	62
Figure 3.5	Stratigraphic sequences present in crustal block D	64
Figure 3.6	Distribution of metamorphic mineral assemblages in crustal block D	66

Figure 3.7	Bedding in typical Zephyr Formation turbidites north of Akaitcho Lake.	70
Figure 3.8	Detail of base of a sandy turbidite bed.	70
Figure 3.9	Okrark sill overlying Zephyr Formation turbidites near Akaitcho Lake.	73
Figure 3.10	Typical outcrop surface of a plagioclase-porphyrific sill showing strong deformation of grains	73
Figure 3.11	a) Distribution of volcanic rocks and location of volcanic complexes in the Hepburn Lake map area :	75
	b) Distribution of volcanic facies within the Akaitcho Group volcanic complexes in the Hepburn Lake map area	75
Figure 3.12	Pillowed basalt flows in the Nasittok Subgroup, Tuertok volcanic complex . . .	77
Figure 3.13	Bedded mafic tuffs in the Nasittok Subgroup, Kapvik volcanic complex. . .	77
Figure 3.14	Generalized facies relationships: between the Tuertok and Kapvik volcanic complexes	79
Figure 3.15	Generalized facies relationships in rhyolite centres overlying the Sinister, Tuertok, and Kapvik volcanic complexes.	79

Figure 3.16	Volcanic breccia derived from a rhyolite dome in the Tuertok volcanic complex	83
Figure 3.17	Conglomerate	83
Figure 3.18	Outcrop of marble, Tuertok volcanic complex	85
Figure 3.19	Typical Aglerok Formation pelites, biotite metamorphic grade.	85
Figure 3.20	Mafic tuffaceous mudstone from the Kapvik volcanic complex, biotite metamorphic grade.	87
Figure 3.21	Felsic tuffaceous mudstone, Kapvik volcanic complex.	91
Figure 3.22	Bedded rhyolite tuff, Kapvik volcanic complex.	91
Figure 3.23	Geological map of the southern half of the McGregor Lake area (N.T.S. 86J/14)	93
Figure 3.24	Finely laminated mudstone of the Grant Subgroup	96
Figure 3.25	Siltstone interbed in Grant Subgroup mudstone.	96
Figure 3.26	Dolomite beneath volcanic rocks of the Grant Subgroup, Wopmay Lake.	98
Figure 3.27	Pillowed basalt in the Grant Subgroup	98

Figure 3.28	Distribution of the Grant Subgroup in western Zone 3	100
Figure 3.29	Comparative stratigraphic sections of the Grant Subgroup.	102
Figure 3.30	Distribution of the Drill, Vaillant, and Stanbridge Formations near the Zone 2/3 boundary	107
Figure 3.31	Pillowed basalt flow in the Vaillant Formation near Stanbridge Lake	109
Figure 3.32	Fragmental basalt, "Vaillant Formation, near Stanbridge Lake.	109
Figure 3.33	Vesicles in Vaillant Formation aa basalt flows, Vaillant Lake	111
Figure 3.34	Stanbridge Formation dolomite, Vaillant Lake.	111
Figure 3.35	Geological sketch map showing Akaitcho/Epworth Group relationships 10 km NNE of Hepburn Lake.	115
Figure 3.36	Geological sketch map showing Akaitcho/Epworth Group relationships 20 km SSE of Hepburn Lake.	117
Figure 4.1	Plot of SiO_2 versus frequency for flow rocks of the Akaitcho Group (Ipiutak and Nasittok Subgroups)	129
Figure 4.2	Plot of Zr versus SiO_2 for Akaitcho Group rhyolites	129

Figure 4.3	Chondrite-normalized plot of REE for lower Kapvik rhyolites	131
Figure 4.4	a) $\text{TiO}_2\text{-K}_2\text{O}_5\text{-P}_2\text{O}_5$ plot for Ipiutak and Nasittok Subgroup basalts, and Tallerk sills.	133
	b) $\text{Ti}/100\text{-Zr-Yx3}$ plot for Ipiutak and Nasittok Subgroup basalts and Tallerk sills.	133
Figure 4.5	Chondrite-normalized REE plot showing REE patterns of oceanic tholeiites and a typical continental tholeiite.	135
Figure 4.6	Alkali-silica diagram for the Ipiutak and Nasittok Subgroup basalts and the Tallerk sills.	139
Figure 4.7	Plot of Y/Nb ratios for Akaitcho Group lavas.	139
Figure 4.8	Y versus Zr plot for Ipiutak Subgroup basalts, Belleau volcanic complex basalts, and Sitiyok Complex amphibolite.	148
Figure 4.9	Chondrite-normalized REE plot for Ipiutak Subgroup basalts and Sitiyok Complex amphibolite dykes.	149

Figure 4.10	Y versus Zr plot showing Ipiutak Subgroup and Sityok Complex amphibolite dykes.	151
Figure 4.11	Y versus Zr plot showing Ipiutak Subgroup basalts, Sityok Complex amphibolite dykes, and Sityok Complex amphibolite.	151
Figure 4.12	Chondrite-normalized REE plot of Sityok Complex amphibolites	153
Figure 4.13	Geological map of the Tuertok volcanic complex	157
Figure 4.14	Chondrite-normalized REE plot of the lower basalts and the feldsparphyric gabbros of the Tuertok volcanic complex	159
Figure 4.15	Chondrite-normalized REE plot for the main basalt sequence of the Tuertok volcanic complex	161
Figure 4.16	Chondrite-normalized REE plot for the upper basalt unit of the Tuertok volcanic complex	163
Figure 4.17	Chondrite-normalized REE plot for Kapvik volcanic complex basalts and gabbros from the base of the complex .	166

Figure 4.18	Chondrite-normalized REE plot for basalts from the Kapvik volcanic complex and gabbros from the base of the complex.	168
Figure 4.19	Plot of Y versus Zr for the Kapvik volcanic complex basalts, gabbros from the base of the complex, and the Tallerk sills.	170
Figure 4.20	Plot of V versus Zr for the Kapvik volcanic complex basalts, gabbros from the base of the complex, and the Tallerk sills.	170
Figure 4.21	Chondrite-normalized REE plot for the Tallerk gabbro sills	173
Figure 4.22	Stratigraphic column for the Belleau volcanic complex and representative REE patterns?	175
Figure 4.23	Chondrite-normalized REE plot for the Belleau volcanic complex basalts .	177
Figure 4.24	Comparative stratigraphic section for the Grant Subgroup	179
Figure 4.25	Simplified stratigraphic column for the Akaitcho Group and representative REE patterns for each major basaltic horizon.	182

Figure 4.26	Y versus Zr plot for Vaillant Formation lavas.	193
Figure 4.27	Rb versus Sr plot for Vaillant Formation lavas.	193
Figure 4.28	Chondrite-normalized REE patterns for Vaillant Formation samples from Stanbridge Lake	195
Figure 4.29	Chondrite-normalized REE patterns for Vaillant Formation samples from the Coppermine River at 66°42'N.	195
Figure 4.30	Plot for several elements of log residence time in seawater versus log [concentration in seawater/concentration in upper continental crust]	199
Figure 4.31	Chondrite-normalized REE patterns of some post-Archean shales.	199
Figure 4.32	Chondrite-normalized REE plot for pelitic sedimentary rocks of the Ipiutak Subgroup	205
Figure 4.33	Chondrite-normalized REE plot for pelites of the Grant Subgroup, and Zephyr Formation arkoses	207
Figure 4.34	REE abundances in Akaitcho Group sedimentary rocks normalized to P.A.A.S.	209

Figure 4.35	Chondrite-normalized REE plot for eight Aglerok Formation pelites.	215
Figure 4.36	Chondrite-normalized REE plot showing range of five mafic tuffaceous pelites of the Aglerok Formation.	217
Figure 4.37	TiO ₂ versus Al ₂ O ₃ for Akaitcho Group sedimentary rocks.	219
Figure 4.38	Chondrite-normalized REE plot for felsic volcanoclastic pelites of the Aglerok Formation.	221
Figure 4.39	Chondrite-normalized REE plot of Odjick Formation pelites	223
Figure 4.40	a) Chondrite-normalized REE plot for three Aglerok Formation pelites sampled across closely spaced isograds b) Sample location map for Aglerok Formation pelites plotted in Figure a)	226 226
Figure 4.41	Chondrite-normalized REE plot for sedimentary rocks of the Wopmay Orogen.	228
Figure 5.1	Isochron plot for all analyzed samples of the Sityok Igneous Complex.	236

Figure 5.2	a) Plot of Sr versus model age for Sityok Complex rocks.	238
	b) Plot of Rb versus model age for Sityok Complex rocks.	238
Figure 5.3	Isochron plot for seven samples of the Vaillant Formation.	243
Figure 5.4	Isochron plot for five samples of the Belleau basalt complex.	246
Figure 5.5	Isochron plot for samples of the Edjuvit mylonite zone.	246
Figure 5.6	Isochron regression for the Okrark sills	251
Figure 5.7	Isochron regression for five samples of the Tuertok rhyolite.	251
Figure 5.8	Isochron regression for ten samples of the Rib Granite	253
Figure 5.9	Location and dates of other magmatic events related to the Akaitcho Group and development of the Coronation continental margin	258
Figure 5.10	Compilation of selected Rb-Sr and K-Ar dates from the Bear-Slave region	267

Figure 5.11	Radiometric age determinations in tectonic zones of the Wopmay Orogen, using information presented in Figure 5.10	269
Figure 5.12	Rb-Sr and K-Ar dates in the Basler-Mattberry Lake area in southern Zone 3	271
Figure 6.1	Spacing between volcanic complexes present in the Marceau Thrust Slice, crustal block B, northern Wopmay Orogen.	281
Figure 6.2	Plot of volcano spacing versus crustal/lithospheric thickness	283
Figure 6.3	Crustal sections based on p-wave seismic velocities for the Afar rift, ocean crust, Gulf of California, the Akaitcho Group estimate, and the present (and ancient) Slave Craton.	288
Figure 6.4	Inferred distribution of Nasittok Subgroup volcanic rocks and their correlatives and water depth during deposition.	291

Figure 6.5	Inferred depositional conditions for rhyolites in the upper Sinister and Tuertok volcanic complexes.	
	a) Plan view of Caribbean volcanic arc showing influence of current and wind directions, and water depth.	294
	b) Cross-section of Caribbean volcanic arc	294
	c) Cross-section of an Akaitcho Group rhyolite centre and related sedimentary rocks.	294
Figure 6.6	Conditions for the generation of basaltic and rhyolitic magmas.	298
Figure 6.7	Schematic diagram illustrating the preferred model for the development of the Akaitcho and Epworth Groups	310
Figure 6.8	Schematic diagram illustrating the evolution of the Coronation continental margin during the early Proterozoic.	315
Figure 7.1	Location of Proterozoic rifts of the Canadian Shield and adjacent areas	319

Figure 7.2	Stratigraphic sections for the Gulf of California and the Akaitcho Group	319
Figure 7.3	Reconstructed Proterozoic margins showing inferred setting of rift sequences	328
Figure A.1	Comparison of determinations of REE abundances in BHVO-1 by the author (MUN) and published values for the rock standard.	377
Figure A.2	Variation in analytical results for 4 separate determinations on sample F498A.80, a basalt	377
Figure A.3	Comparison of REE abundances in sample EH70-77, a hawaiian tholeiite as determined at MUN by XRF and at MIT by INAA.	379
Figure A.4	Comparison of REE abundances in SCO-1, a USGS rock standard as determined in this study, and the published values of McLennan and Taylor (1980c)	379
Figure B.1	Rb-Sr sample location map for the Okrark sills and the Belleau volcanic complex basalts	388

Figure B.2	Rb-Sr sample location map, Vaillant Formation basalts	388
Figure B.3	Geological sketch map showing the Edjuvit mylonite zone and Rb-Sr sample locations	390
Figure B.4	Rb-Sr sample location map, Sitiyok Igneous Complex.	390
Figure B.5	Rb-Sr sample location map for the Rib Pluton	391
Figure C.1	$\log_e a$ versus $\log_e b$ plot for conglomerate cobbles from the upper Tuertok volcanic complex	395

CHAPTER 1

INTRODUCTION

1.1 INTRODUCTION

The Akaitcho Group is a sequence of metasedimentary and metavolcanic rocks located in the Bear Structural Province, Northwest Territories, Canada (Figure 1.1). The Akaitcho Group is part of the Wopmay Orogen, an early Proterozoic mobile belt (Hoffman et al., 1970; Hoffman, 1980c). The stratigraphy, geochemistry, and geochronology of the Akaitcho Group were studied in order to understand the tectonic significance of the Akaitcho Group. This goal is of interest for the following reasons:

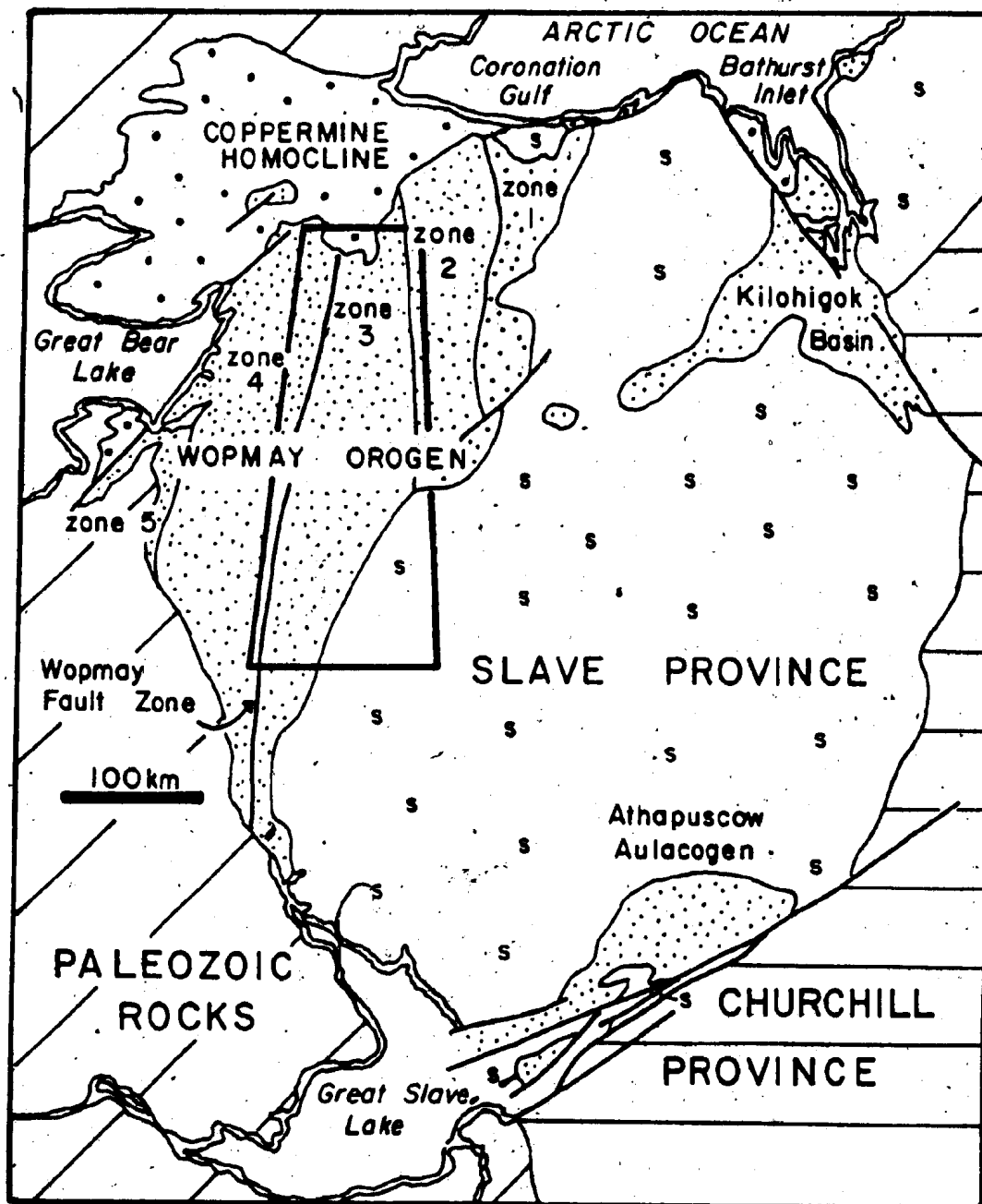
- i) Hoffman et al. (1978) and Hoffman (1979) have interpreted the Akaitcho Group as a sequence formed during initial rifting in the Wopmay Orogen. Hoffman (1980c) has suggested that the Wopmay Orogen preserves a complete Wilson Cycle. Testing of the hypothesis that the Akaitcho Group is an initial-rift sequence is critical, not only to the understanding of the geological development of the Wopmay Orogen, but also to the question of whether plate tectonic processes operated during this period in the Precambrian.
- ii) Present understanding of the early development of rifted continental margins is poor, because rift structures of modern continental margins are commonly covered by thick sedimentary sequences. This difficulty can be overcome by studying sediment-starved continental margins or very young

rifts. Alternatively, one can examine deformed continental margins, such as the one preserved in the Wopmay Orogen. If the Akaitcho Group is indeed an initial-rift sequence, then we have a unique opportunity to study the development of such a rifted margin in order to reach general (i.e. age-independent) conclusions.

1.2 PREVIOUS WORK

Most previous work in central Wopmay Orogen (Zone 3) (Figure 1.1) was done south of 65°N . The first systematic mapping was that of J.T. Wilson and C.S. Lord who mapped the Ingray Lake and the Snare River map areas at a scale of one inch to four miles (Lord, 1942). Lord (1942) introduced the term Snare Group for metasedimentary and metavolcanic rocks preserved west of the Bear-Slave boundary to the vicinity of Wopmay Fault Zone (Figure 1.1). The Snare Group did, however, include rocks on both sides of the Wopmay Fault Zone, because the Fault was not recognized at that time. Lord and Parsons (1952) mapped the Calder River map area (N.T.S. 86F), which includes the Calder River volcanic belt (Figure 1.2). The Calder River map area was remapped by J.C. McGlynn (1974, 1975, 1976). Frith et al. (1974, 1977) remapped the eastern half of the Ingray Lake area which straddles the Bear-Slave boundary, but focused on the geology of the Slave Province. In addition, 1:50,000 scale mapping was conducted in several areas in south-central Wopmay Orogen (Frith and Leatherbarrow, 1975; McGlynn, 1964; McGlynn and Ross, 1962, 1963; Ross, 1959, 1966; Smith, 1963).

Figure 1.1 Northwestern Canadian Shield. The Coppermine Homocline and the Wopmay Orogen constitute the Bear Province. Lower Proterozoic rocks are shown by the stippled pattern. The Kilohigok Basin and the Athapuscow Aulacogen are lithologically correlative with the Wopmay Orogen (Hoffman, 1981a). Akaitcho Group strata are present within Zone 3 of the Wopmay Orogen. Rectangle outlines area shown in Figure 1.2.



Several topical studies, mainly on metamorphic and structural themes, have also been undertaken in south-central Wopmay Orogen (Frith, 1978; Frith et al., 1974, 1975; Helmstaedt, unpublished ms.; Neilsen, 1978; Neilsen and Ghosh, 1981a, 1981b; Ross and McGlynn, 1965). The area between $64^{\circ}30'N$ and $66^{\circ}N$ was covered by a regional lake-sediment geochemistry survey of the Bear-Slave Province (Allan and Cameron, 1973; Allan et al., 1973).

The north-central part of the Wopmay Orogen, by contrast, was virtually unstudied. The Hepburn and Redrock Lake areas were first mapped at a scale of one inch to eight miles during the course of regional helicopter mapping of the northwest Canadian Shield (Fraser et al., 1960). Geologists of Eldorado Nuclear Limited mapped the Hepburn and Redrock Lake areas at a scale of one inch to four miles by helicopter (Mursky et al., 1970), in the early sixties, but did not improve greatly on earlier work. Fraser (1974) mapped the Epworth Group east of the Hepburn Batholith at a scale of one inch to four miles. Hoffman (1972, 1973) and Hoffman et al. (1971) mapped a cross-section across northern Wopmay Orogen. Hoffman (1972, 1973) spent a few weeks mapping volcanic rocks of what is now termed the Akaitcho Group near Kapvik and Belleau Lakes.

Systematic mapping of the Hepburn Lake area (N.T.S. 86J) was begun at 1:100,000 scale in 1977 by Dr. P.F. Hoffman of the Geological Survey of Canada (GSC) (Hoffman et al., 1978). During the course of the 1977 season it was recognized that

metavolcanic and metasedimentary rocks west of the Hepburn Batholith were not correlative with the Epworth Group, and the name "Akaitcho Group" was established for these rocks. The author began mapping the Akaitcho Group in June, 1978.

1.3 PRESENT STUDY

The most effective way to fully understand the tectonic significance of the Akaitcho Group is through an integrated approach - detailed mapping followed by geochemistry and geochronology on samples collected during mapping. Thus, the results of the laboratory studies can be directly related to the field work, and properly interpreted.

The Akaitcho Group was mapped at 1:50,000 scale by the author while employed as a senior assistant with the Geological Survey of Canada (GSC) during the summer of 1978, and under Energy Mines and Resources (EMR) research agreements during the summers of 1979 and 1980. Mapping of the Akaitcho Group was part of a GSC 1:100,000 scale mapping project in the Hepburn Lake area (N.T.S. 86J) under the supervision of Dr. Paul F. Hoffman. Dr. M.R. St-Onge conducted a metamorphic study of pelitic rocks in the Hepburn Lake map area, including the Akaitcho Group, as part of the GSC project and worked closely with the author. The author mapped 80 to 85% of all Akaitcho Group outcrops not affected by migmatization, and about 40 to 50% of all Akaitcho Group outcrops at higher metamorphic grade. Dr. Hoffman and Dr. St-Onge were responsible for most of the other mapping. Mapping was done on foot using 1:60,000

scale air photographs for navigation and plotting, and 1:20,000 scale enlargements of these photographs in areas of complex geology.

The author mapped the Akaitcho Group in three main areas of the Wopmay Orogen: the Hepburn Lake map area, parts of the Calder River Belt, and the Grant Lake area (Figure 1.2). The Akaitcho Group is best preserved in the Hepburn Lake area, which contains the most extensive exposures of low-grade Akaitcho Group rocks. For this reason, much of the stratigraphy of the Akaitcho Group was established in the Hepburn Lake area and extrapolated elsewhere. The Calder River Belt has a fairly monotonous, and continuous stratigraphy which can be traced to the Grant Lake area. Altogether, these three areas include about 60% of all low-grade Akaitcho Group outcrops.

Due to the contractual nature of the GSC field support, several papers concerning the Akaitcho Group have been published (Table 1.1). Although the thesis can be read without these papers, they do contain much field data. Many of these papers are preliminary reports. If any contradiction arises between the thesis and these reports, the thesis results should be regarded as more current.

The thesis is divided into two main parts. The first part (Chapters 2 to 6) presents the evidence that the Akaitcho Group is a probable initial-rift sequence in the Wopmay Orogen. The second part (Chapter 7) compares the Akaitcho Group with other rift sequences and draws general

Figure 1.2 Location of areas studied by the author in central Wopmay Orogen, May 1978 to September 1981. Akaitcho Group strata between the Four Corners and Grant Lake map areas are mainly preserved at upper amphibolite metamorphic grade, and are commonly migmatized. The Akaitcho Group is preserved at lower greenschist to upper amphibolite metamorphic grade in the areas studied by the author. More detailed maps showing the distribution of the Akaitcho Group are presented in Figures 2.3 and 2.4. Abbreviations: AL - Akaitcho Lake; BL - Belleau Lake; CR - Coppermine River; DL - Dumas Lake; HL - Hepburn Lake; IL - Ingray Lake; ML - Mattberry Lake; RD - Redrock Lake; RL - Rebesca Lake; SL - Stanbridge Lake; VL - Vaillant Lake.

LEGEND



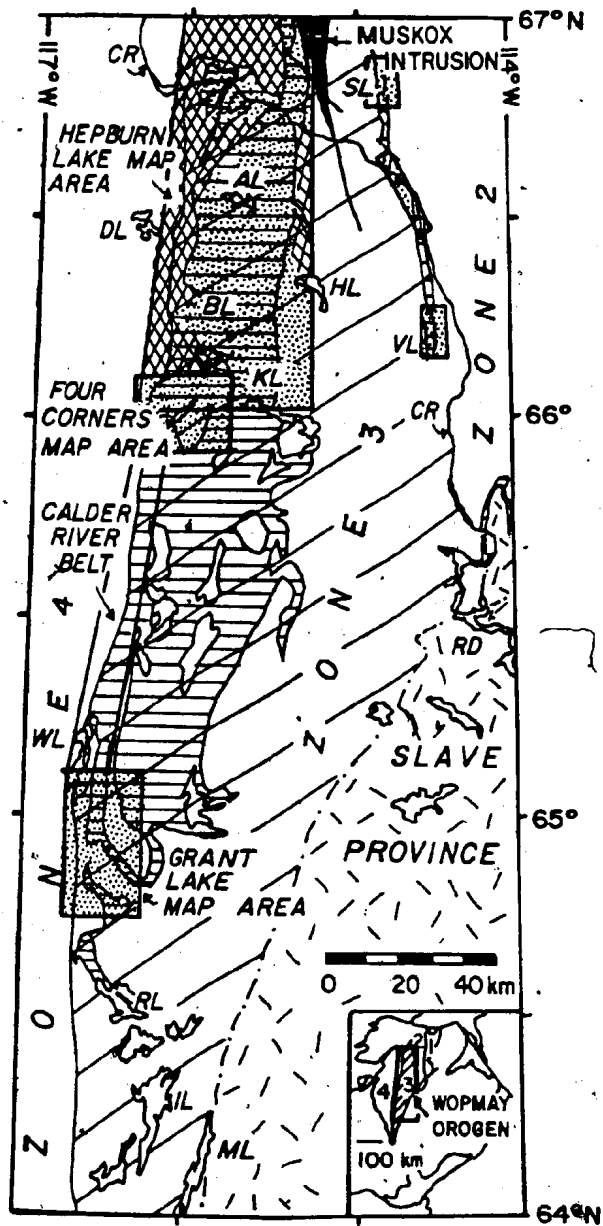
Akaitcho Group strata, all metamorphic grades



areas mapped solely by the author



areas mapped jointly by R.M. Easton, P.F. Hoffman, and M.R. St-Onge.



conclusions about the development of rifted continental margins.

1.4 NOMENCLATURE, METHODS AND MATERIALS

Nomenclature for sedimentary rocks follows Pettijohn (1975); for basaltic rocks, Basaltic Volcanism Study Project (1981); for rhyolites, Barker (1981); and for granitoid rocks, Streckeisen (1976). Metamorphic terminology follows the usage of St-Onge (1981). Analytical methods and precision for major, trace and RE (rare-earth) elements are given in Appendix A. Rubidium-strontium dating procedures and results are given in Appendix B. Unless indicated otherwise, diagrams using major-element analyses have been plotted using 100% anhydrous values. REE (rare-earth element) diagrams are normalized to the chondritic values of Masuda et al. (1973), unless indicated otherwise. References given in the Appendices are incorporated into the main reference list.

Table 1.1 Publications Related to Thesis

Easton, R.M. (1980a) Stratigraphy of the Akaitcho Group and Initiation of the Wopmay Orogen (Aphebian), Bear Province, N.W.T.; Geological Association of Canada, Abstracts with Programs, 5, 50.

Easton, R.M. (1980b) Stratigraphy and Geochemistry of the Akaitcho Group, Hepburn Lake Map Area, District of Mackenzie: An Initial Rift Succession in Wopmay Orogen (Early Proterozoic); in Current Research, Part. B, Geological Survey of Canada Paper 80-1B, 47-57.

Easton, R.M. (1981a) Stratigraphy of a Proterozoic Volcanic Complex at Tuertok Lake, Wopmay Orogen, District of Mackenzie; in Current Research, Part A, Geological Survey of Canada Paper 81-1A, 305-309.

Easton, R.M. (1981b) REE, U and Th contents of Proterozoic and Archaen sedimentary rocks from the Bear and Slave Structural Provinces, N.W.T., Canada; Geological Association of Canada, Abstracts with Programs, 6, A-16.

Easton, R.M. (1981c) Geology of the Four Corners and Grant Lake map areas, District of Mackenzie, N.W.T.; in Current Research, Part B, Geological Survey of Canada Paper 81-1B, 83-94.

Easton, R.M. (1981d) Stratigraphy of the Akaitcho Group and the development of an early Proterozoic continental margin, Wopmay, Orogen, N.W.T.; in Proterozoic Basins in Canada, F.H.A. Campbell, ed., Geological Survey of Canada Paper 81-10, 79-95.

Easton, R.M. (1981e) Crustal Structure of Rifted Continental Margins: Geological Constraints from the early Proterozoic (1.9 Ga) Akaitcho Group, Wopmay Orogen; N.W.T., Canada; in Papers Presented to the Conference on Processes of Planetary Rifting, p. 103-106, Lunar and Planetary Institute, Houston.

Easton, R.M. (1982) Crustal Structure of Rifted Continental Margins: Geological Constraints from the Proterozoic rocks of the Canadian Shield; Tectonophysics, in press.

Hoffman, P.F., St-Onge, M.R., Easton, R.M., Grotzinger, J. and Schulze, D. (1980) Syntectonic plutonism in north-central Wopmay Orogen (Early Proterozoic), Hepburn Lake map area, District of Mackenzie; in Current Research, Part A, Geological Survey of Canada Paper 80-1A, 171-177.

Hoffman, P.F., St-Onge, D.A., Easton, R.M. and St-Onge, M.R. (1981) Preliminary Geological Map of Hepburn Lake, District of Mackenzie; Geological Survey Open File 784, 1:100,000.

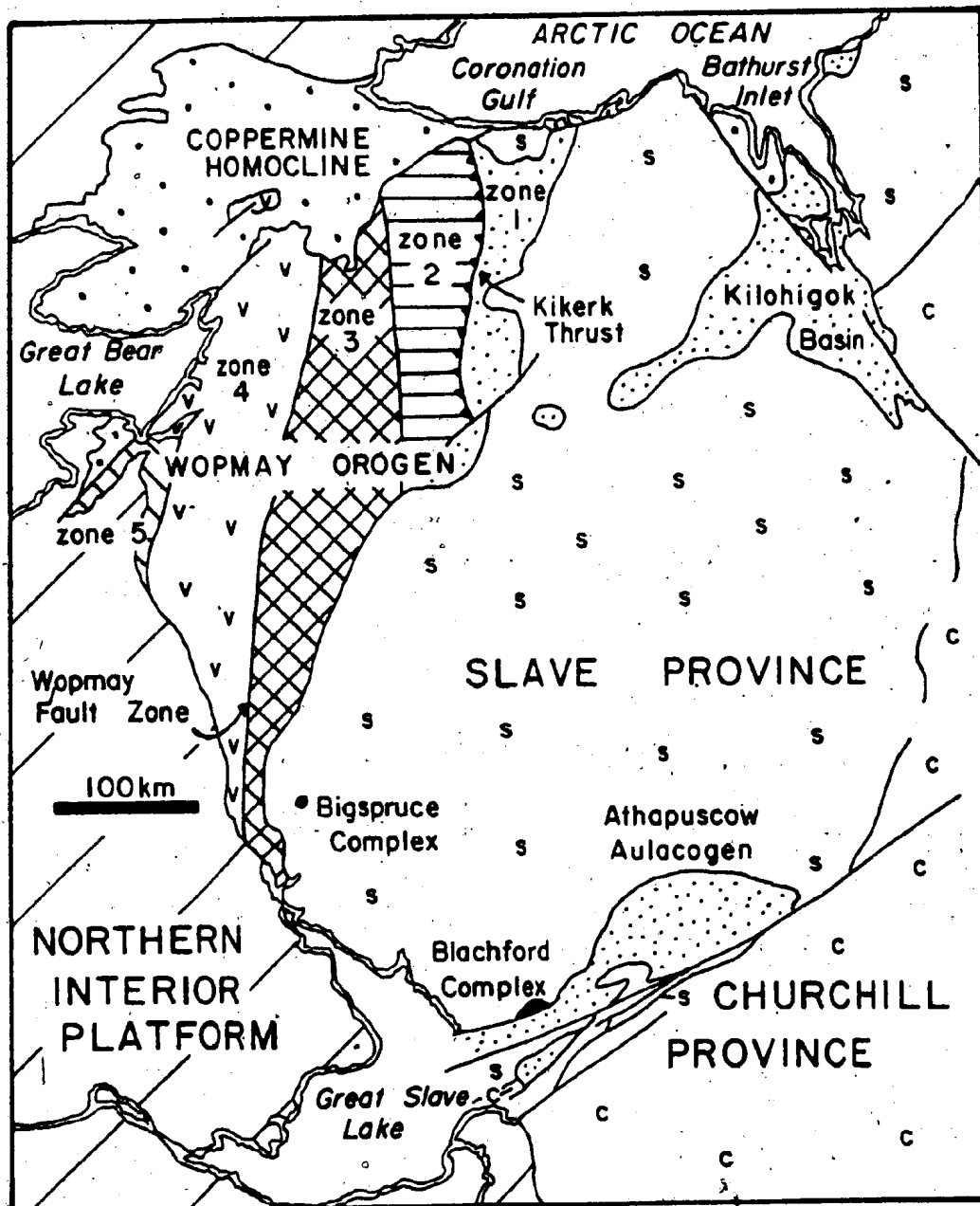
CHAPTER 2

GENERAL GEOLOGY2.1 WOPMAY OROGEN - REGIONAL GEOLOGY

The Wopmay Orogen (Fraser et al., 1972; Hoffman, 1980c) is a northerly-trending early Proterozoic orogenic belt in the northwestern Canadian Shield (Figure 2.1). The peak of orogenic activity, as determined by U-Pb zircon dates was between 1900 and 1860 Ma (Van Schmus and Bowring, 1980). The adjacent Slave Structural Province east of the Orogen is an Archean craton partly covered by a cratonic basin and an aulacogen correlative with the Wopmay Orogen - the Kilohigok Basin southwest of Bathurst Inlet (Campbell and Cecile, 1975, 1976, 1981) and the Athapuscow Aulacogen in the east arm of Great Slave Lake (Hoffman, 1968, 1969, 1981b; Hoffman et al., 1977). The Wopmay Orogen is covered in the north by post-orogenic Middle Proterozoic (1.6 to 0.9 Ga) rocks of the Coppermine Homocline (Baragar and Donaldson, 1973; Kearns et al., 1981). Flat-lying Phanerozoic sedimentary rocks cover the westward and southward extensions of the Wopmay Orogen.

The Wopmay Orogen can be divided into five tectonic zones (Figure 2.1) (Hoffman, 1980c; Hoffman and St-Onge, 1981). Zone 1 comprises thin, autochthonous platformal sedimentary rocks of the Epworth Group overlain by distal flysch and molasse of the Recluse Group and Takiyuak Formations respectively. The Kikerk Thrust Fault separates

Figure 2.1 Tectonic subdivisions of the Wopmay Orogen.
See text for details. The Akaitcho Group is
located mainly within western Zone 3 and along
the Zone 2/3 boundary. After Hoffman (1980c);
Hoffman and St-Onge (1981).



Zone 1 from Zone 2, and marks the eastern limit of thrusting. Zone 2 contains thicker, platformal (miogeoclinal) rocks of the Epworth Group, again overlain by flysch of the Recluse Group. Within Zones 2 and 3, both groups have been thrust towards the Slave Craton. The Cloos anticline or nappe separates Zone 3 from Zone 2, and roughly marks an important facies change in the Epworth Group between platformal rocks in the east (inferred outer continental shelf) and deeper water equivalents (inferred continental rise and slope deposits) to the west. Zone 3, also referred to as the internal zone, is a metamorphic and batholithic terrane. Supracrustal rocks in Zone 3 belong to the Akaitcho, Epworth, and Recluse Groups. The Akaitcho Group is present mainly in the western half of Zone 3. Peraluminous or S-type granitoids of the Hepburn and Wentzel Batholiths (Hoffman et al., 1980) intruded and metamorphosed the supracrustal rocks present within Zone 3. Together, Zones 1 through 3 comprise the classic "Coronation Geosyncline" (Hoffman, 1973; Hoffman et al., 1978). Supracrustal rocks in Zones 1 through 3 are assigned to the Coronation Supergroup (Hoffman, 1981a) and have been subdivided into a number of groups and formations as listed in Table 2.1.

The 'Wopmay Fault Zone' (Easton, 1981c) separates Zone 3 from Zone 4. Zone 4 contains weakly metamorphosed calc-alkaline volcanic and sedimentary rocks and epizonal granitoid plutons of the Great Bear volcano-plutonic belt (Hoffman and McGlynn, 1977; Hildebrand, 1981). Zone 5, also

Table 2.1 Stratigraphic nomenclature and regional correlation chart: Foreland Wopmay Orogen and associated basins (after Hoffman, 1981a). Correlations are based on lithology, and depositional and deformational history (Hoffman, 1973, 1981a; Fraser and Tremblay, 1969).

Foreland Wopmay Orogen.

CORONATION SUPERGROUP	RECLUSE GROUP	Takiyuak Fm.
		unnamed breccia
		Cowles Lake Fm.
		Asiak Fm.
	EPWORTH GROUP	Fontano Fm.
		Tree River Fm.
		Rocknest Fm.
	ODJICK GROUP	Odjick Fm.
	AKAITCHO GROUP	

Athapuscow Aulacogen

GREAT SLAVE SUPERGROUP	CHRISTIE BAY GROUP	unnamed fm.
		Pearson Fm.
		Portage Inlet Fm.
		Tochatwi Fm.
		Stark breccia
	PETHEI GROUP	
	KAHOCELLA GROUP	
	SOSAN GROUP	unnamed member
		Akaitcho River Fm.
		Kluziai Fm.
		Duhamel Fm.
		Hornby Channel Fm.
	UNION ISLAND GROUP	

Kilohigok Basin

GOULBURN GROUP	Amagok Fm.
	Brown Sound Fm.
	Omingmaktook breccia
	Kuuvik Fm.
	Peacock Hills Fm.
	Quadyuk Fm.
	Mara Fm.
	Burnside River Fm.
	Western River Fm.

known as the Hottah Terrane, consists of a metamorphic complex and a variety of foliated granitoids older than the epizonal plutons of Zone 4 (McGlynn, 1976, Hildebrand, 1981). Zone 5 has not yet been mapped in detail.

All five tectonic zones, and to a limited extent the Slave Craton, are affected by a system of conjugate transcurrent faults (Hoffman, 1980c; Hoffman and St-Onge, 1981). These faults are interpreted by Hoffman and St-Onge (1981) to be the last compressional event in the Wopmay Orogen. These transcurrent faults are also believed to have evolved into thrust faults during rotation, producing hexagonal-shaped, fault-bounded, 'crustal blocks' in the central part of the Orogen (Hoffman and St-Onge, 1981).

There are three significant features of the Wopmay Orogen. First, a complete section across the orogen is present in the well-exposed northern half of the orogen. This section has now been mapped at 1:100,000 scale. Second, Zones 1 to 3 preserve a sedimentary prism, the classic "Coronation Geosyncline", that has many features in common with sedimentary prisms associated with recent "Atlantic-type" continental margins (Hoffman, 1973, 1980c). Third, the Great Bear volcano-plutonic belt (Zone 4) has many features in common with recent continental magmatic arcs (Hildebrand, 1981). The combination of these features has allowed a convincing case to be made that plate-tectonic processes were instrumental in the formation of the Wopmay Orogen (Badham, 1978; Hoffman, 1973, 1980c).

2.1.1 Sedimentary Prism

The first plate tectonic model for the development of the Wopmay Orogen (Hoffman, 1973) was based on the study of the sedimentary prism present in Zones 1 to 3, and the aulacogen. The argument made in favour of the operation of plate tectonics during the development of the Wopmay Orogen was, and is, the similarity between the Wopmay Orogen, and Phanerozoic orogens and modern continental margins. (Hoffman, 1973, 1980c; Hoffman et al., 1970).

The lower Coronation Supergroup contains the Epworth Group (Table 2.1), which contains a lower, mature ortho-quartzite sequence that thickens to the west and is overlain by an upper, carbonate sequence (Hoffman, 1973; Grotzinger, 1982). Paleocurrent studies (Hoffman, 1973) indicate that the orthoquartzite was derived from the Archean Craton to the east. Near the boundary between Zones 2 and 3 a marked facies change occurs. The orthoquartzite sequence becomes more pelitic, and the carbonate platform sequence thins abruptly and disappears to the west (Grotzinger, 1982). This facies change is interpreted to mark the edge of a continental shelf (Hoffman, 1973, 1980c; Hoffman et al., 1978). A marked change also occurs between the Epworth Group and the overlying Recluse Group and Takiyuak Formation. Recluse Group deposition began with deposition of a black shale, which grades upward into a thick sequence of grey-wacke turbidites derived from the north and the west (Hoffman, 1973, 1980c). The source terrane for the grey-

wackes was of metamorphic and plutonic character (Jeletzky, 1974; Hoffman, 1973). Molasse (Takiyuak Formation) was also derived from a westerly source region (Hoffman, 1973), and may be related to unroofing of the Great Bear volcano-plutonic belt (Zone 4) (Hoffman, 1973). The sudden reversal of sediment transport, from early oceanward transport to later cratonward transport is common in many Phanerozoic orogens and usually reflects uplift in the core of the orogen.

In addition to the similarity of sedimentary facies and history of sedimentation to that found in many modern orogens, the deformational history of Zones 1 to 3 is also similar to that found in more recent orogens. In particular, folding and thrusting within Zones 2 and 3 is very similar in style to the fold and thrust belt in the Canadian Rockies, part of the Cordilleran Orogen (Hoffman, 1980c; Tirrul, 1982).

The Kilohigok Basin and the Athapuscow Aulacogen record the same sedimentological and deformational history as the orogen (Hoffman, 1973, 1981b; Campbell and Cecile, 1981). The Kilohigok Basin is an intracratonic basin related to the westerly-trending Taktu aulacogen, or failed arm, believed to underlie the Coronation Gulf (Campbell and Cecile, 1981). The Athapuscow Aulacogen has been interpreted to represent a failed arm of a triple junction related to continental separation (Hoffman, 1973, 1980c; Hoffman et al., 1974). Features similar to the Kilohigok

Basin and Athapuscow Aulacogen are present in Phanerozoic orogens (for example, the southern Oklahoma aulacogen in the Ouachita Orogen).

2.1.2 Great Bear Arc

Since 1973, it has been recognized that Zones 4 and 5 play an important role in any model of the development of the Wopmay Orogen. Zone 4 has similarities to modern continental magmatic arcs. The volcanic history, physical volcanology and chemistry of Zone 4 volcanic rocks (Hildebrand, 1981) are similar to those found in recent arcs. In addition, conglomerate in easternmost Zone 4 contains clasts apparently derived from the Wentzel Batholith, and, locally, sedimentary and volcanic rocks of Zone 4 lie unconformably on metamorphosed Akaitcho Group rocks and the Wentzel Batholith (Hoffman and Bell, 1975; Hoffman and McGlynn, 1977). Thus, at least by the later stages of volcanism in eastern Zone 4, Zone 3 rocks had been deformed, metamorphosed, uplifted, and exposed.

2.1.3 Development of the Wopmay Orogen - The Two Collision Model of Hoffman

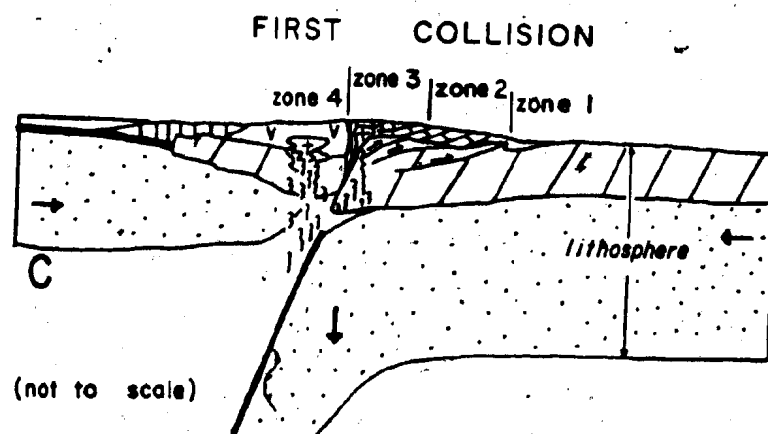
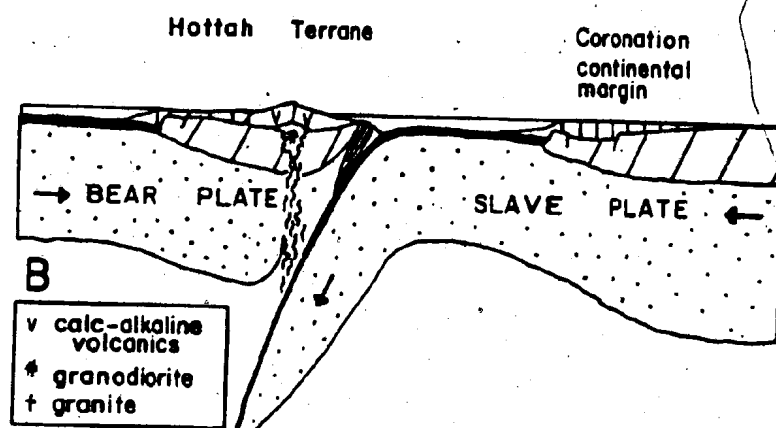
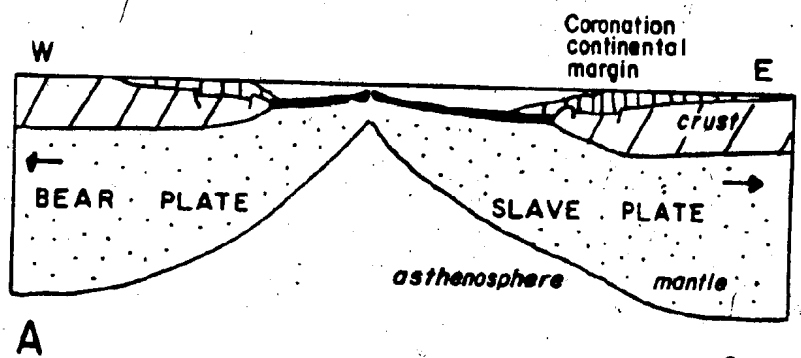
The current model for the development of the Wopmay Orogen (Hoffman, 1980c) is illustrated in Figures 2.2a, b, c, d, and e. This model is an amended version of an earlier model (Hoffman, 1973) and is based on detailed mapping across all of northern Wopmay Orogen. Mapping in Zones 3 and 4 has required many modifications to the 1973 model. The model of Badham (1978) is not considered here, because

it does not take into account the recent work performed in Zones 3 and 4 of the Wopmay Orogen, and is thus, at best, incomplete.

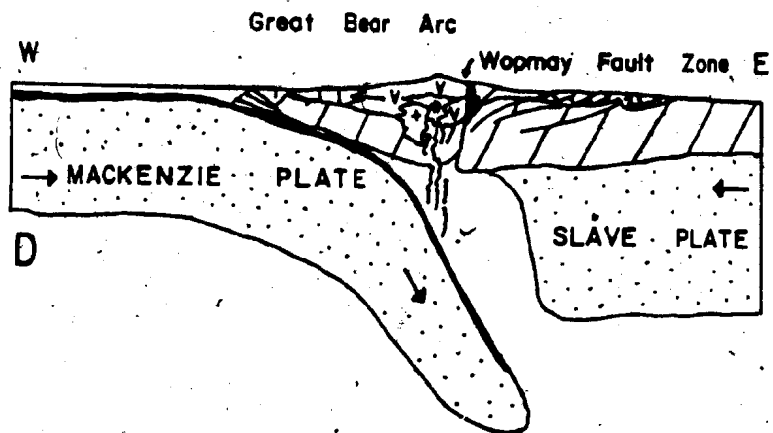
The essence of the current model is that two continent-continent collisions occurred, and that a complete Wilson Cycle is preserved in the first cycle. The Epworth Group was deposited on the edge of the Slave Craton following a rifting event which led to the generation of an ocean basin (Figure 2.2a), and two plates - the Bear Plate and the Slave Plate. The Hottah Terrane may represent the other margin of the originally rifted continent. It is not known if the Bear Plate was large, or if it was a micro-plate. Rifting was followed by west-dipping subduction under the Hottah Terrane (Bear Plate) resulting in closure of the ocean between the Bear and Slave Plates (Figure 2.2b) and continent-continent collision (Figure 2.2c). Folding and thrusting of the Coronation Supergroup, Recluse Group sedimentation, and intrusion and metamorphism of the Coronation Supergroup by the Hepburn Batholith resulted from this collisional event (Figure 2.2c). Following this collision, east-dipping subduction of oceanic crust west of the Hottah Terrane (Mackenzie Plate) began (Figure 2.2d). Subduction of the Mackenzie Plate resulted in the formation of the Great Bear continental arc (Zone 4). A second collisional event occurred at some later time, terminating magmatism in the Great Bear terrane, and forming the conjugate transcurrent faults present in the Bear Province.

Figure 2.2 Model for the development of the Wopmay Orogen.
Modified from Hoffman (1980c).

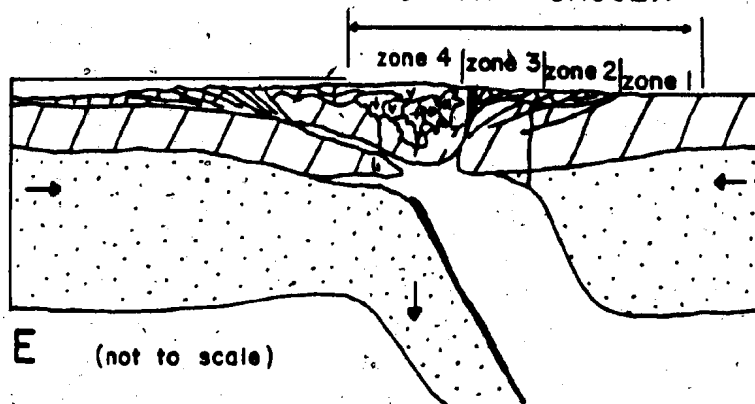
- A) Rifting leads to splitting of the Archean crust and the formation of two plates - the Bear and the Slave. The Odjick and Rocknest Formations are deposited on the Slave Plate as the ocean basin widens.
- B) Subduction of the Slave Plate beneath the Bear leads to the formation of the Hottah Terrane. Epworth Group deposition continues while the ocean basin decreases in size.
- C) Subduction results in continent-continent collision between the Bear and Slave Plates. The Coronation Supergroup is folded, thrust, intruded, and metamorphosed. The Bear Plate has been accreted to the Slave Plate.
- D) Subduction renews westward of the Bear Plate resulting in a continental magmatic arc (Great Bear arc). The Wopmay Fault Zone develops.
- E) Subduction again leads to continent-continent collision. The second collision results in the formation of NE-NW trending transcurrent fault systems and the crustal block structure in central Wopmay Orogen.



(not to scale)



SECOND COLLISION
WOPMAY OROGEN



Timing of these events is still not precisely known, but preliminary work by Van Schmus and Bowring (1980) indicate that the development of the Wopmay Orogen may have occurred within a span of fifty million years.

This thesis is concerned primarily with events occurring prior to the first collision event; i.e., the development of the continental margin and the relation to the Akaitcho Group to it. Later events, although important to the model as a whole, serve mainly to obscure relationships preserved by the earlier units.

Finally, it should be noted that the Wopmay Orogen could be divided into a north half and a south half at 65°N . North of 65°N , all tectonic zones are present. In Zones 3 and 4 we find the largest exposed areas of low-grade supracrustal rocks, and within Zones 3 and 4, granitic rocks, although abundant, are not dominant. South of 65°N , Zones 1 and 2 are absent, the proportion of low-grade metamorphic rocks in Zone 3 is small, and in Zones 3 and 4 granitic rocks predominate.

Whether the history of the Wopmay Orogen could have been elucidated without the critical preservation of Zones 1 and 2 (which serve to establish an autochthonous stratigraphy that can be carried westward, and which preserve the continental-shelf sequence) is problematic. It is possible, however, that many other Proterozoic Belts are similar to the southern Wopmay in their level of exposure, and this

may account, in part, for the difficulty in establishing the role of plate tectonics in their development.

2.2 GEOLOGY OF ZONE 3

2.2.1 Overview

Figures 2.3 and 2.4 are geological compilation maps for Zone 3 of the Wopmay Orogen. Figure 2.3 covers northern Wopmay Orogen (above 65°N) and Figure 2.4 covers southern Wopmay Orogen (below 65°N). The north half is better preserved, and has received greater study than the south, especially in the last decade. In addition, the author has conducted the majority of his study in the north half of the Wopmay Orogen. Thus, for ease of presentation, the geology of Zone 3 will be considered in two parts. Note that 65°N is not a fundamental geological boundary.

2.2.2 Northern Zone 3 (north of 65°N)

Hoffman and St-Onge (1981) recognized that northern Zone 3 can be divided into a series of hexagonal-shaped, fault-bounded, 'crustal blocks' or 'shingles' (Figure 2.5). These 'crustal blocks' are separated from each other by northeast-, northwest-trending transcurrent faults and north-trending reverse faults. Hoffman and St-Onge (1981) related the development of these 'crustal blocks' to the second collision in the Wopmay Orogen. The most important aspect of the blocks, to this study, is that the blocks have both distinctive stratigraphy, and metamorphic and structural characteristics. These are summarized below.

Block A - This block contains mostly shelf-facies Epworth

Figure 2.3 Geological map of the central metamorphic core zone (Zone 3) of northern Wopmay Orogen. Sources used in the compilation: Easton (1980, 1981a, 1981c); Fraser (1974); Fraser *et al.* (1960); Hoffman *et al.* (1978, 1980, 1981); Lord (1942); McGlynn (1964, 1974, 1975, 1976, 1977); Mursky *et al.* (1970). NOTE: A larger scale version of this figure is present in a pocket at the back of the thesis

LEGEND

- + granitic intrusions of the Hepburn and Wentzel Batholiths
- e EPWORTH and RECLUSE GROUPS
- s SNARE GROUP
- AKAITCHO GROUP
- a mainly sedimentary rocks
- △ mainly volcanic rocks
- ▼ low-grade rocks of the Grant Subgroup
- fault
- ma, me, m migmatite; derived from the Akaitcho Group; derived from the Epworth Group; parent undetermined
- • — BEAR-SLAVE Boundary
- ▲— thrust fault, teeth on the upper plate

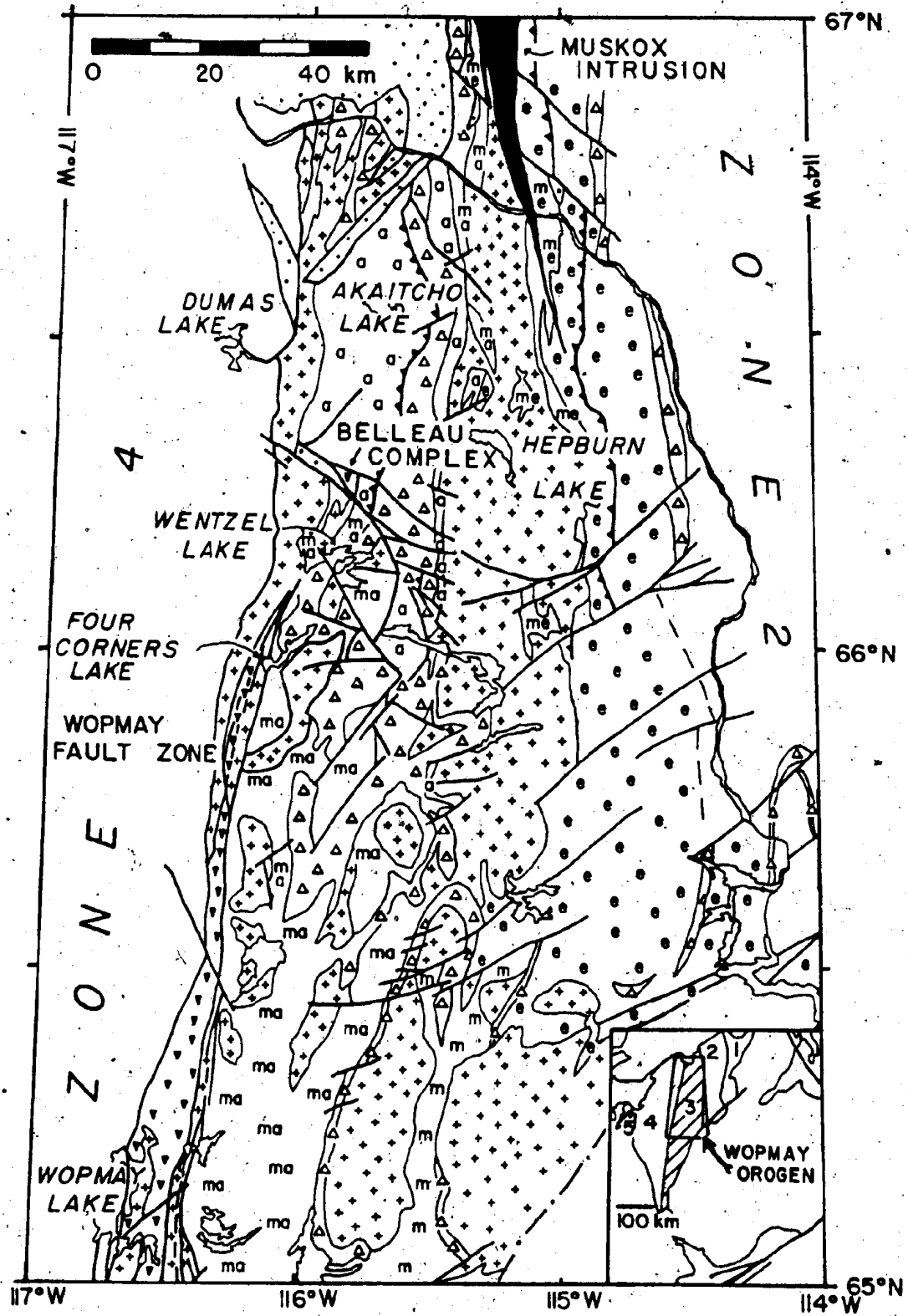




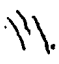

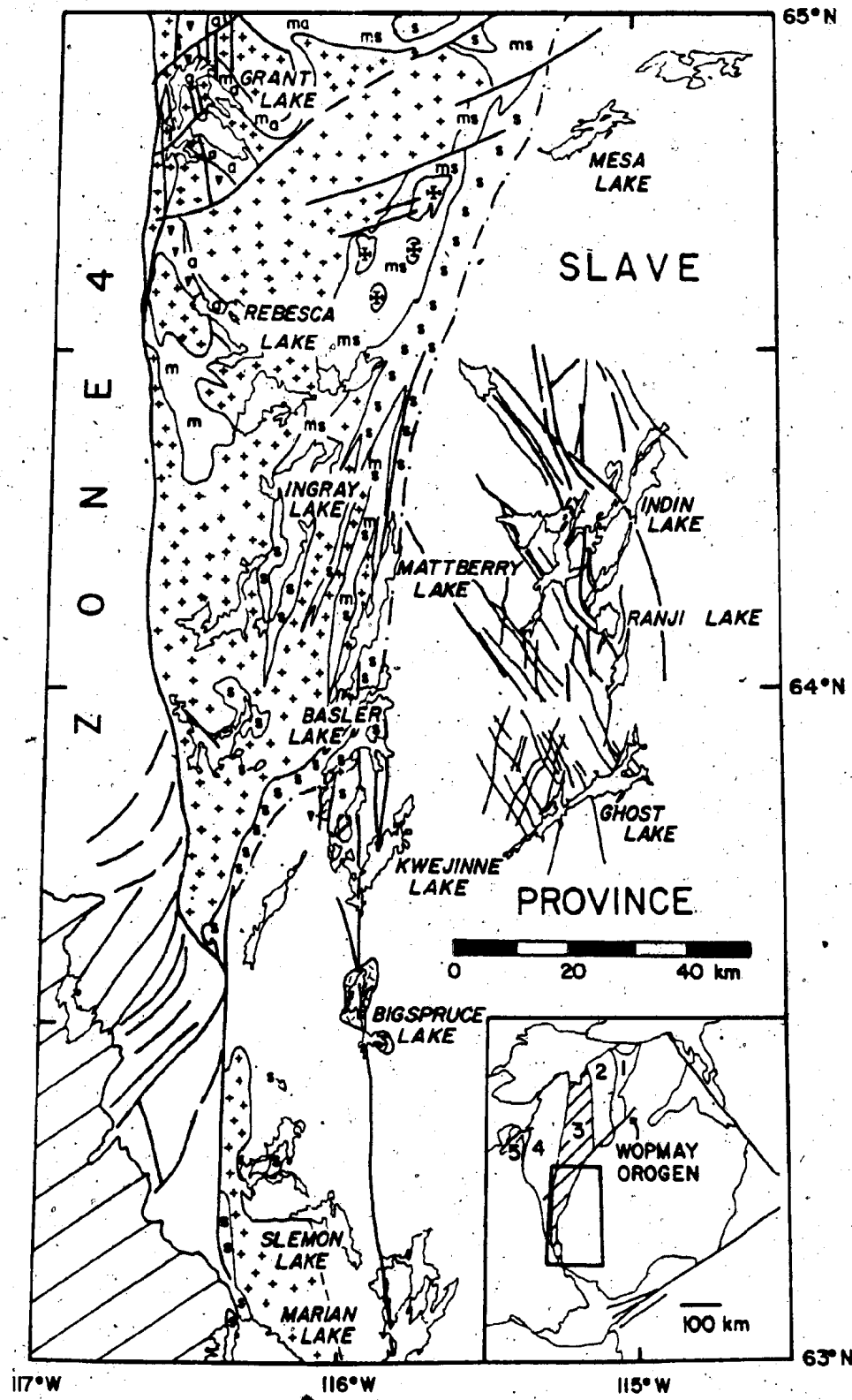


Figure 2.4 Geological compilation of Zone 3 in southern Wopmay Orogen. For detail of dykes in the Indin-Ghost Lake area consult Tremblay *et al.* (1953, 1954) and Wright (1954). Apparent absence of dykes in other areas of the Slave Province may reflect lack of detailed mapping. Sources: Douglas *et al.* (1974); Easton (1981c); Frith (1973, 1978); Frith and Leatherbarrow (1975); Frith *et al.* (1974); Lord (1942); McGlynn and Ross (1962, 1963); Ross (1959, 1966); Tremblay *et al.* (1953, 1954); Wright (1954). NOTE: A larger scale version of this figure is present in a pocket at the back of the thesis.

LEGEND

-  Paleozoic rocks
-  granitic rocks of the Hepburn Batholith, may include some remobilized Archean crust
-  gneiss domes, with Archean age cores, remobilized during the Proterozoic
- s Snare Group
mainly metasediments, minor dolomite, gabbro
- a Akaitcho Group
mainly metasediments, minor basaltic flows
- ▼ volcanic rocks, mainly pillowed basalt flows;
at Grant Lake, these rocks are assigned to the Grant Subgroup
- ma, ms, m migmatite; derived from the Akaitcho Group;
derived from the Snare Group; parent undetermined
-  alkaline igneous complex, nephelinite,
carbonatite
-  Indin diabase dykes
-  fault



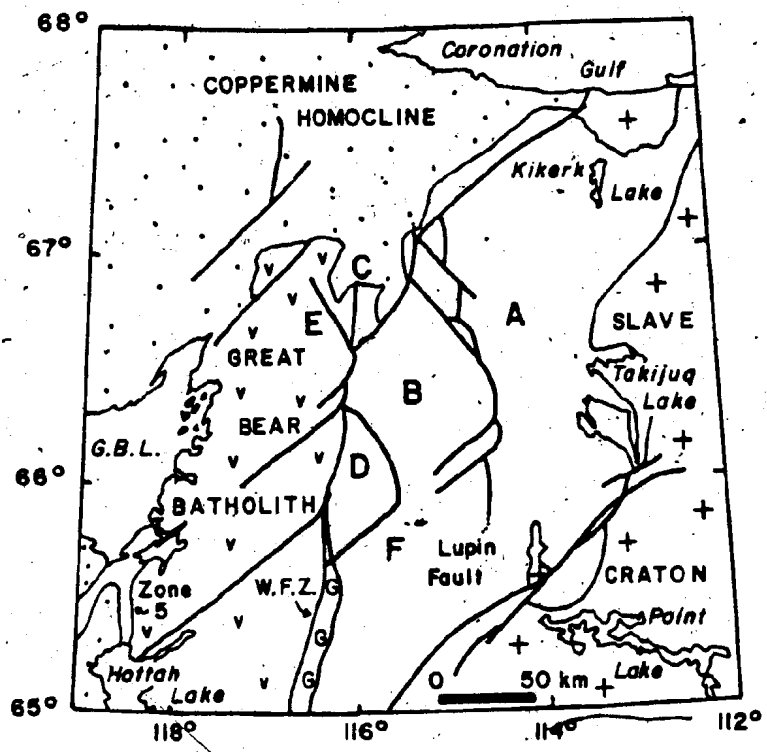
and Recluse Group rocks exposed at chlorite metamorphic grade. In northern block A, Akaitcho Group rocks are found in Cloos Nappe. In northern Cloos Nappe a broad recumbent fold is present. The remainder of the block appears to be dominated by upright-folds related to the first episode of thrusting.

Block B - This block underlies much of the Hepburn Lake area, and most of the Akaitcho Group stratigraphy was developed within this block. Stratigraphy is continuous within this block. Metamorphic grade ranges from chlorite to biotite grade, except near the Hepburn and Wentzel Batholiths, where it increases to sillimanite-microcline assemblages. North-trending upright folds are dominant, and no recumbent folds have yet been found.

Block C - This block is mainly covered by Hornby Bay sandstone. The Akaitcho Group rocks in this block are generally at high metamorphic grade (upper amphibolite), and no recumbent structures have been reported. An outlier of Dumas Group rocks rests unconformably on rocks of the Wentzel Batholith and metamorphosed Akaitcho Group rocks.

Block D - This block consists mainly of upper amphibolite grade metamorphic rocks. Kyanite-bearing rocks are present in the southern part of the block (St-Onge et al., 1982). Many recumbent folds of foliation and nappe structures are present (St-Onge et al., 1982). The recumbent folds have been refolded about northerly-trending axes. Stratigraphy is distinctive within this block, and complicated by the two

Figure 2.5 Major faults and structural blocks (A-G) in the northern part of the Wopmay Orogen. Coppermine Homocline consists of Helikian post-orogenic cover. Abbreviations: G.B.L. - Great Bear Lake; W.F.Z. - Wopmay Fault Zone; G - Grant Block. Modified from Hoffman and St-Onge (1981).



sets of folds and the high metamorphic grade.

Block F - Block F is located mainly in the Redrock Lake area. It may not be completely separated from block C, and its boundaries are poorly known at this time.

Grant Block - This block is entirely fault bounded, and contains the low-grade metamorphic rocks of the Grant Subgroup. In part, the boundary faults may be vertical, but at Grant Lake, one of the boundary faults dips shallowly (Easton, 1981c). This block may not have formed in the same manner as the others, but it does contain a continuous, fault-bounded distinctive stratigraphic sequence.

The areas mapped by the author include the Akaitcho Group rocks in block B and C, the northern part of block D, and the north and south ends of the Grant block. In addition, Akaitcho Group rocks near the boundary between blocks A and B were also studied (Figure 1.2). An outline of the geology of these areas follows. Emphasis is placed on the Hepburn Lake area because the Akaitcho Group is best exposed in this block. The other areas are referred to briefly.

Hepburn Lake map area (N.T.S. 86J)

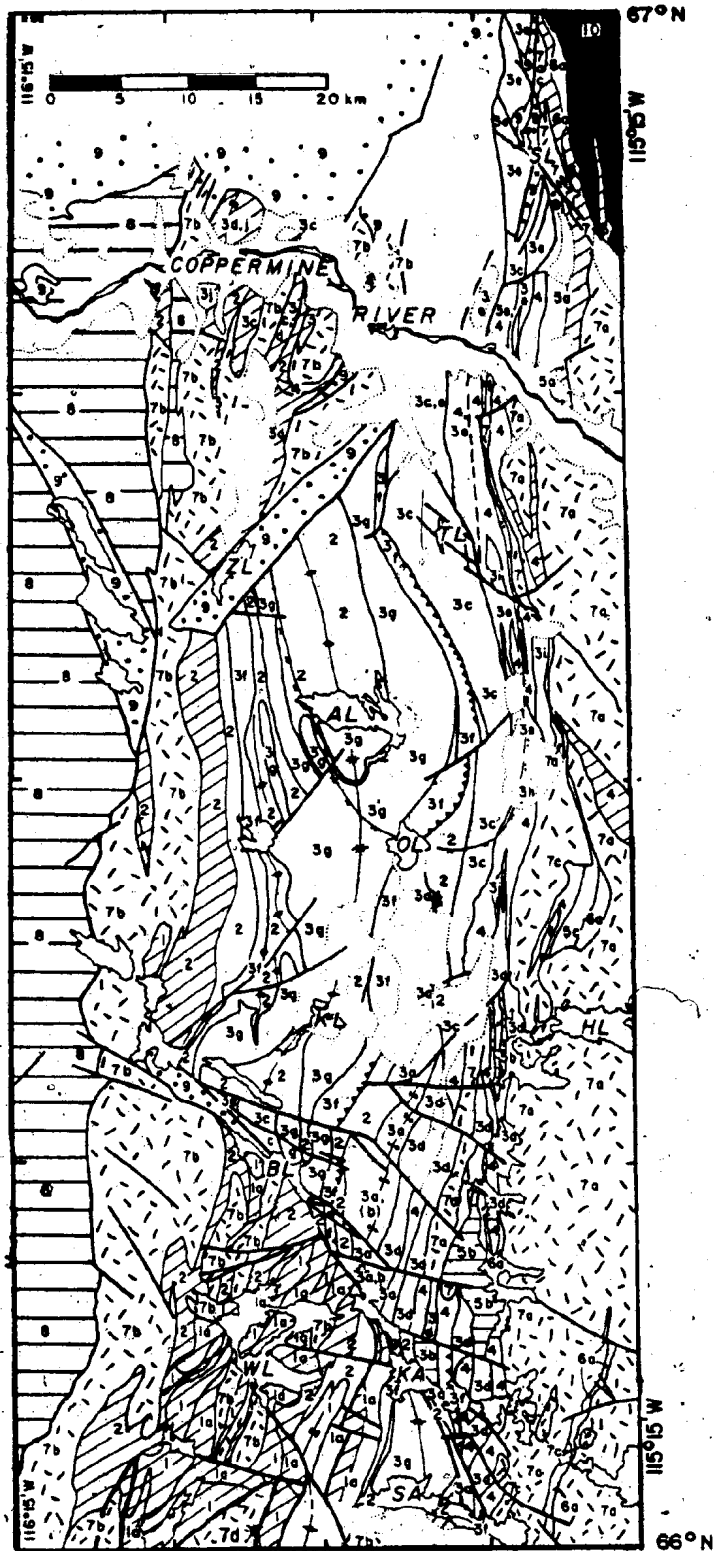
The geology of the Hepburn Lake map area has been described by Hoffman *et al.* (1978, 1980, 1981) and Easton (1980). Figure 2.6 is a geological map of the western half of the Hepburn Lake area showing the distribution of Akaitcho Group rocks.

The Hepburn Lake area straddles four crustal blocks - crustal blocks A, B, C and D. The characteristics of each

Figure 2.6 Simplified geological map of the Hepburn Lake map area (N.T.S. 86J/W $\frac{1}{2}$), showing distribution of the Akaitcho Group. This map is an updated version of Figure 6.1 of Easton (1980). The main modifications to the original figure are in the southwest corner of the map, and were based on mapping during the 1980 field season (Easton, 1981c). NOTE: A larger scale version of this figure is in a pocket at the back of the thesis.

LEGEND

- | | | |
|----|--|------------------|
| 10 | MUSKOX INTRUSION | |
| 9 | HORNBY BAY GROUP sandstone | |
| 8 | GREAT BEAR VOLCANO-PLUTONIC BELT (ZONE 4) | |
| 7 | a) granitoid intrusions of Hepburn Batholith;
b) syenogranite and garnet granite of Wentzel Batholith;
c) younger, mafic intrusions of Hepburn Batholith;
d) Sityok Igneous Complex, may be younger than Unit 1. | |
| 6 | EPWORTH GROUP a) Odjick Formation | |
| | AKAITCHO GROUP | |
| 5 | a) basalt flows; b) gabbro sills; c) siliceous siltstone | |
| 4 | olive pelites and volcanoclastic sediments - Aglerok Fm. | |
| 3 | Nasittok Subgroup volcanic complexes
a) aphanatic rhyolite; b) gabbro sills; c) massive and pillowed basalt; d) basalt tuff; e) porphyritic rhyolite flows; f) plagioclase-porphyritic rhyolite sills; g) orthoclase-porphyritic rhyolite sills; h) conglomerate; i) siliceous siltstone; j) marble, orthoquartzite | |
| 2 | subarkosic and arkosic turbidites of the Zephyr Fm. | |
| 1 | Ipiutak Subgroup amphibolite a) pelite | |
| */ | fold, of bedding, of foliation | AL Akaitcho Lake |
| — | fault | BL Belleau Lake |
| ↗ | Okrark Thrust Fault | HL Hepburn Lake |
| .. | biotite isograd,
mark on high T side | KA Kapvik Lake |
| ▨ | migmatite (over 30%
granitic material) | KL Kingarok Lake |
| | | OL Okrark Lake |
| | | SA Samandre Lake |
| | | SL Sinister Lake |
| | | TL Tuertok Lake |
| | | WL Wentzel Lake |
| | | ZL Zephyr Lake |



of these blocks have already been described. The Hepburn Lake area is dominated by crustal block B. Crustal block B can be divided into three subzones by the Marceau and Okrark Thrust Faults (Figure 2.7). A cross-section at 66°25' N across crustal block B also shows these structural subzones (Figure 2.8). The eastern subzone contains continental slope and rise deposits of the Epworth Group, and flysch and hemipelagic shales of the Recluse Group. The central subzone (Marceau Thrust Slice) contains intrusive rocks of the Hepburn Batholith (Hoffman et al., 1980), volcanic and sedimentary rocks of the upper Akaitcho Group, and continental rise pelites of the Epworth Group which conformably overlie the Akaitcho Group (Easton, 1980). Structure in the central subzone is dominated by a synclinatorium-anticlinorium pair (Figure 2.8). The anticlinorium is truncated against the Okrark Thrust, but exposes the upper Akaitcho Group. The synclinatorium served as the locus of intrusion of the Hepburn Batholith (Figure 2.7) (Hoffman et al., 1980). The western subzone (Okrark Thrust Slice) comprises sedimentary and volcanic rocks of the lower Akaitcho Group, and intrusive rocks of the Wentzel Batholith (Hoffman et al., 1980). The Okrark Thrust Slice also contains a synclinatorium-anticlinorium pair. In the Okrark Thrust Slice, the anticlinorium is truncated by the edge of crustal block E and served as the locus for intrusion of the Wentzel Batholith (Hoffman et al., 1980).

The synclinorium has a hinge roughly parallel to the Okrark Thrust, and exposes the lower Akaitcho Group.

Metamorphic grade in the three subzones of block B ranges from chlorite (lower greenschist facies) to above muscovite breakdown (upper amphibolite to granulite facies), and is spatially related to the Hepburn and Wentzel Batholiths (St-Onge, 1981; Hoffman *et al.*, 1980) (Figure 2.9). Folding and thrusting in the Wopmay Orogen occurred before metamorphism and batholith ~~intrusion~~ intrusion because metamorphic isograds transect Marceau Thrust (St-Onge, 1981). Folding also occurred during and after metamorphism because the isograds and thrusts are themselves folded (St-Onge, 1981).

Four Corners map area

The geology of this area is dominated by crustal block D (Figures 1.2, 2.4). The geology of the area has been outlined in Easton (1981c) and is not repeated here. The only significant change from the original report is that work to the south of the Four Corners map area by St-Onge *et al.* (1982) indicates that the Sityok Igneous Complex is part of a nappe.

Wopmay-Grant Lake map area

The geology of this area (Figures 1.2, 2.3, 2.4) is outlined in Easton (1981c).

2.2.3 Southern Zone 3 (south of 65°N)

The geology of southern Wopmay Orogen (Figure 2.4) is less well understood than the geology in the north, in part because mapping in southern Wopmay Orogen occurred sporad-

Figure 2.7 Major tectonic elements of the Hepburn Lake map area (N.T.S. 86J). Revised from Easton (1980).

Abbreviations: Ba - eastern subzone of crustal block B; Bb - central subzone (Marceau Thrust Slice) of crustal block B; Bc - western subzone (Okrark Thrust Slice) of crustal block B;

CN - Cloos Nappe; BF - Belleau Fault System;

OT - Okrark Thrust; MG - Mouse Valley Graben;

MT - Marceau Thrust; ZF - Zephyr Fault;

WF - Wopmay Fault Zone; -W- axis of Wentzel

Batholith; -H- axis of Hepburn Batholith.

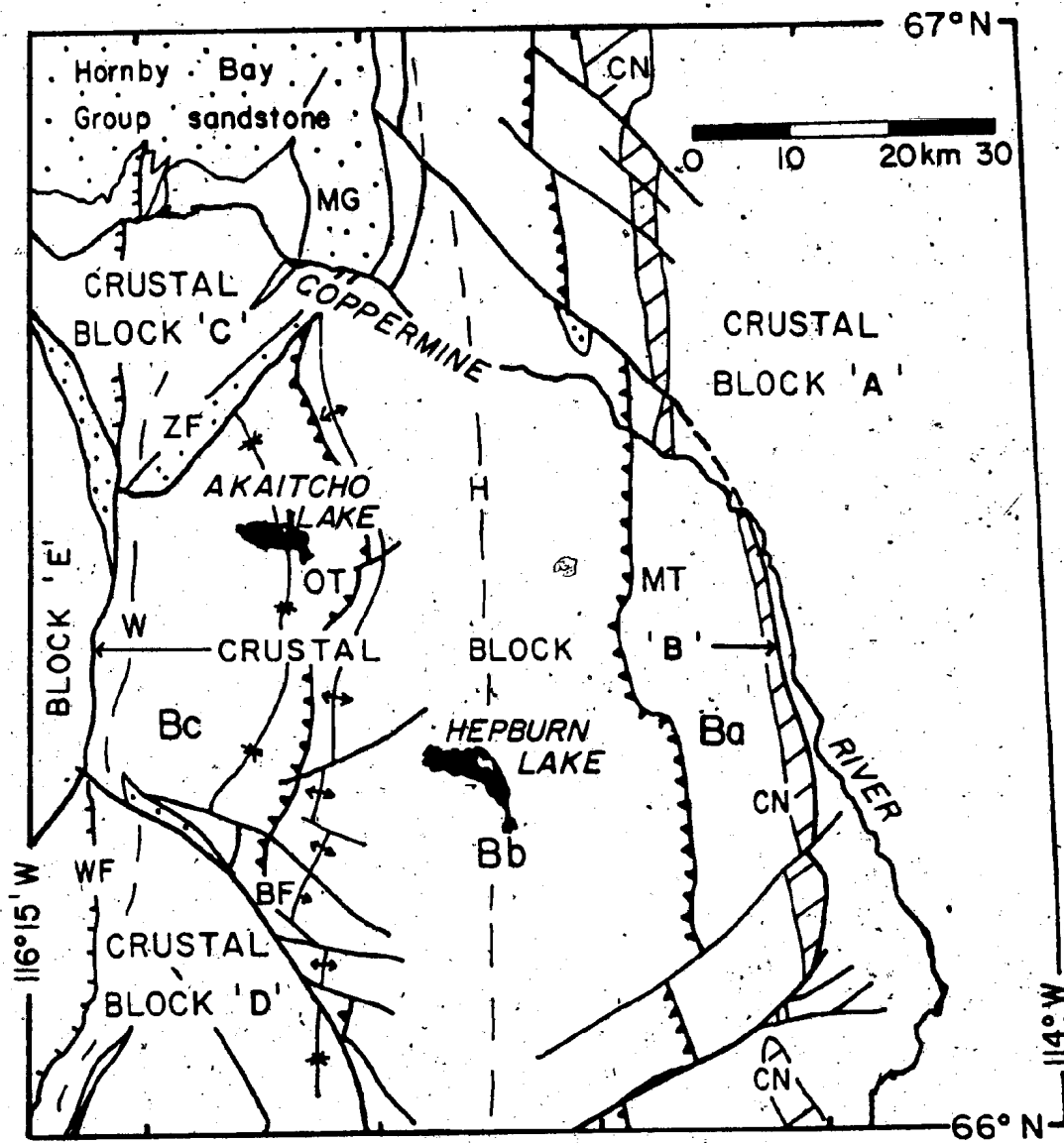
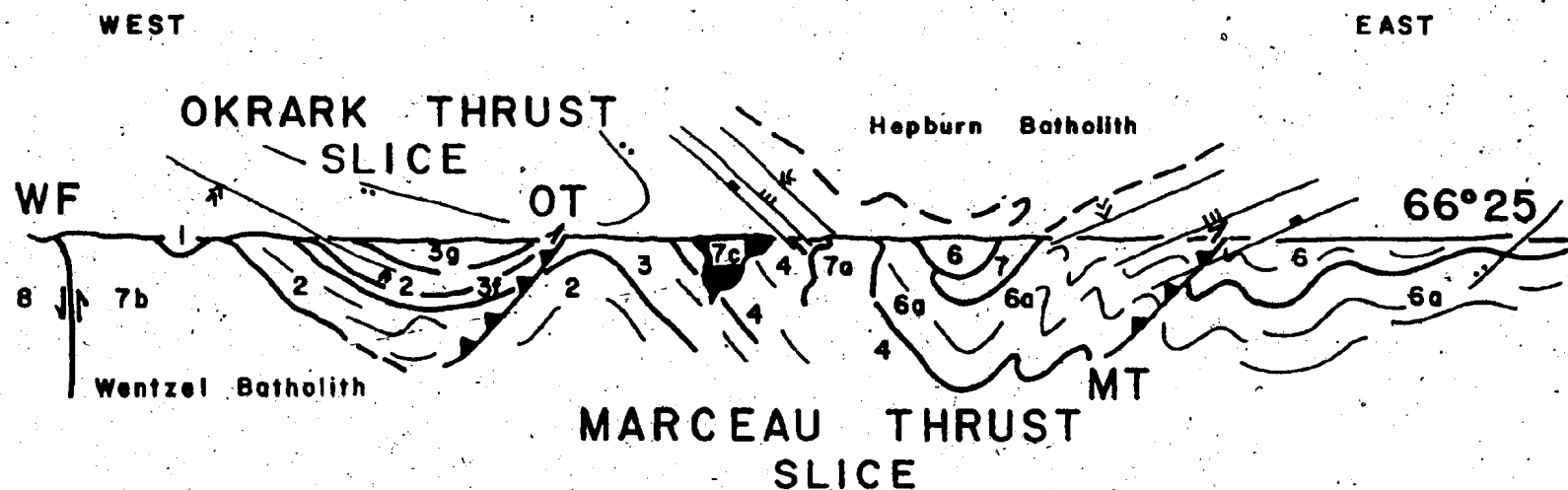
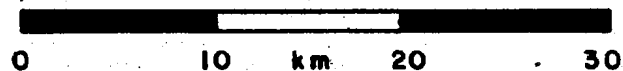


Figure 2.8 Generalized cross-section across the Hepburn Lake map area at $66^{\circ}25'N$, showing synclinoria-anticlinoria pairs and thrusts within the Akaitcho and Epworth Groups. Section lies within crustal block B. The Wopmay Fault in this area is faulted margin of crustal block E. Modified from Hoffman et al. (1980); Easton (1980). Legend as in Figure 2.6.



METAMORPHIC ISOGRAD
(mark on high T side)

- orthoclase
- sillimanite
- andalusite
- biotite



- WF Wopmay Fault
- OT Okrark Thrust
- MT Marceau Thrust

Figure 2.9 Metamorphic mineral assemblages and distribution of isograds in the Hepburn Lake map area (N.T.S. 86J/W $\frac{1}{2}$). Figure covers the same area as Figure 2.6. Modified from St-Onge (1981).

LEGEND



Muskox Intrusion



Hornby Bay Group sandstone



intrusive rocks of the Hepburn and Wentzel Batholiths

Mineral Assemblages



chlorite-plagioclase-quartz



muscovite-biotite-chlorite-plagioclase-quartz



staurolite-muscovite-biotite-plagioclase-quartz ~~± cordierite~~ andalusite



sillimanite-muscovite-biotite-plagioclase-quartz-liquid



sillimanite-K-feldspar-biotite-plagioclase-quartz-liquid

Mineral Isograds
(first appearance, mark on high T side)



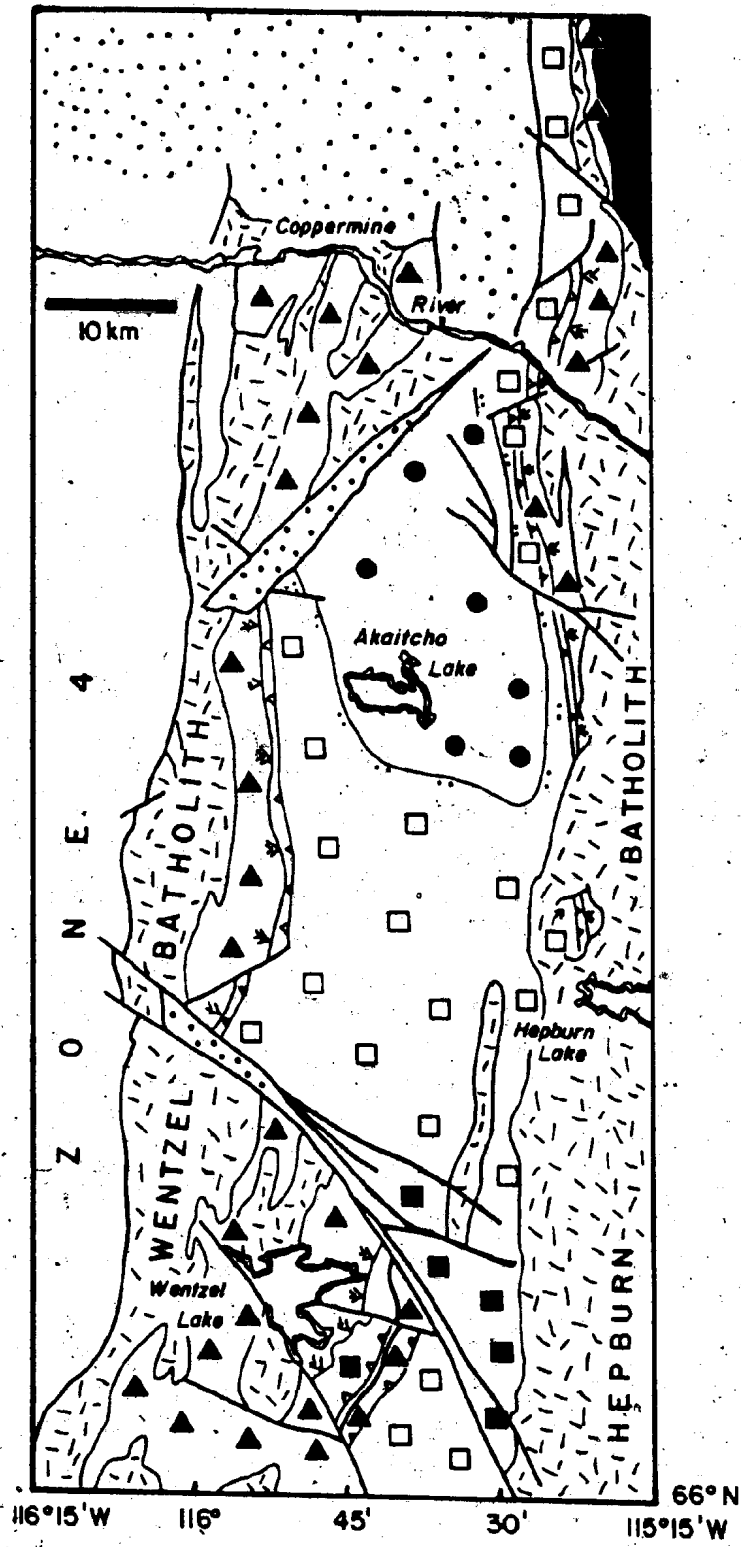
biotite



staurolite



sillimanite-K-feldspar



ically, and was performed by several workers from the mid-thirties to the early seventies. In contrast, most work in northern Wopmay Orogen has been done by a close-knit group since the early seventies. One result has been the establishment of two systems of stratigraphic nomenclature (Table 2.2). In northern Zone 3, rocks of the Akaitcho Group, Epworth, and Recluse Groups are present. In southern Wopmay Orogen, the Snare Group (Lord, 1942) consists of three lithologies: volcanics, clastic sediments, and dolomite. The relationship between the Snare Group and the other groups of the Coronation Supergroup is not well known, and will not be unravelled until mapping links the north and south parts of Zone 3. As an example of the problem, dolomite in the Mattberry Lake area could belong either to the Stanbridge Formation (Akaitcho Group), or the Rocknest Formation (Epworth Group), or to a unit not present in the north. Any attempted correlation of the Snare Group and other groups to the north is suspect. For the purpose of this report, the Snare Group is defined as metasedimentary and metavolcanic rocks west of the Bear-Slave boundary, and east of the Wopmay Fault Zone, which cannot, or have not, been assigned to the Akaitcho or Epworth Groups. This usage differs from Lord's (1942) usage in that it excludes rocks west of the Wopmay Fault Zone.

Southern Zone 3 differs from northern Wopmay Orogen in three major respects. First, the zone is much thinner to the south; second, areas of low-grade supracrustal rocks are

Table 2.2 Comparison between stratigraphic nomenclature in northern (above 65°N) and southern (below 65°N) Wopmay Orogen. The Snare Group may include elements of the Akaitcho, Epworth, and Recluse Groups. No correlation of units is implied.

NORTHERN WOPMAY OROGEN

CORONATION SUPERGROUP		Taklyuak Fm.
		Cowles Lake Fm.
	RECLUSE GROUP	Aslak Fm.
		Fontano Fm.
		Tree River Fm.
	EPWORTH GROUP	Rocknest Fm.
		Odjick Fm.
	AKAITCHO GROUP	

SOUTHERN WOPMAY OROGEN

SNARE GROUP	volcanic member
	dolomite
	clastic member

less common, and areally restricted; and third, granitic rocks and high-grade metamorphic rocks are areally more extensive. There are, however, several important aspects of southern Zone 3 geology relevant to this thesis.

First, recumbent folds are present in moderate- to high-grade metamorphosed Snare Group strata in the Ingray-Arseno Lake area (Helmstaedt, unpublished). The recumbent folds pre-date later upright folds. Thus, the structures observed in crustal block D in northern Zone 3 are not unique to that block. The recumbent folds are only observed in high-grade metamorphic rocks; and similar observations have been made at Grant Lake (Easton, 1981c). The relation of metamorphic grade to the recumbent folds is not known.

Second, several gneiss domes with Archean cores are present in southern Zone 3 (Frith et al., 1974, 1977) (Figure 2.4). The presence of these gneiss domes suggests that we see a change in structural style from north to south in Zone 3. Granitoid rocks in southern Zone 3 also show more involvement of Archean basement (Frith et al., 1977; Frith, 1978), perhaps indicative of a deeper level of exposure in the south.

Third, several north trending faults parallel the Bear-Slave boundary near the Basler-Mattberry Lake area in southern Zone 3 (Figure 2.4). One of these north-trending faults extends south of Basler Lake and is cut by the Bigspruce alkaline complex. The Bigspruce complex may be related to rifting of the Slave Craton prior to, or during,

Akaiŕcho Group deposition (Frith, 1978; Hoffman, 1980c). North- and northwesterly-trending faults near Indin Lake, about 40 km east of Zone 3 (Figure 2.4), were the loci of emplacement of many dykes of the Indin dyke swarm (McGlynn and Irving, 1975). The Indin, olivine-tholeiite, diabase dykes may be related to rifting associated with Akaiŕcho Group deposition (Hoffman, 1980c).

Fourth, amygdaloidal, mafic volcanic rocks (McGlynn and Ross, 1962) and gabbro sills and dykes (McGlynn and Ross, 1963) are present along the Bear-Slave boundary in the Basler-Mattberry Lake areas. These mafic volcanic rocks may be associated with rifting of the Slave Craton, although, as stated previously, correlations between these rocks and the Akaiŕcho Group are equivocal at this time.

CHAPTER 3

STRATIGRAPHY

3.1 INTRODUCTION

The distribution of the main groups of supracrustal rocks in Zones 2 and 3 of the Wopmay Orogen are shown in Figures 2.3 and 2.4. The Akaitcho Group is preserved at upper greenschist to lower amphibolite metamorphic grade in six main areas in the Wopmay Orogen: the Hepburn Lake area; the Calder River belt, Cloos Nappe, the Grant Lake area, the Rebesca Lake area and the Redrock Lake area (Figures 1.2). The author has mapped in the first four belts. The Akaitcho Group is best preserved in the Hepburn Lake area, and the stratigraphy presented here was originally established for that area (Easton, 1980). The Calder River Belt (Lord and Parsons, 1952; McGlynn, 1974, 1975, 1976; Easton, 1981c), the Grant Lake area (McGlynn, 1964; Easton, 1981c), and the Rebesca Lake area (Lord, 1942) are a continuation of the Hepburn Lake area (Easton, 1981d). Preliminary mapping in the Redrock Lake area (St-Onge *et al.*, 1982) indicates that the Akaitcho Group stratigraphy can be continued southward into the Redrock Lake sheet.

This chapter is concerned with the following supracrustal units: those units which possibly underlie the Akaitcho Group, the Akaitcho Group, and the Epworth Group. The Epworth Group constitutes the inferred passive continental-margin sequence of the Wopmay Orogen. Hence, the relationship of the Akaitcho Group to the Epworth Group has

important implications regarding the tectonic setting of the Akaitcho Group. The other supracrustal units of Zones 1, 2, and 3 of the Wopmay Orogen (Table 2.1) are not described. Descriptions of these units can be found in Hoffman (1973), Fraser (1974), and Hoffman (1981a).

This chapter briefly describes the Sityok Igneous Complex which may be older than the Akaitcho Group. It also briefly describes the various rock units the author has recognized and mapped within the Akaitcho Group and the stratigraphic relationships between these units. It also describes the Epworth Group rocks, and discusses the nature of the Akaitcho/Epworth Group contacts in several areas. Finally, this chapter describes rocks elsewhere in the Wopmay Orogen that may be lithologically correlative with the Akaitcho Group. It concludes with a brief statement on the stratigraphic constraints on the development of the Akaitcho Group. Much of the material on the Akaitcho Group in this chapter has already been published by the author (Easton, 1980, 1981a, 1981c, 1981d).

3.2 SITYOK COMPLEX

The Sityok Igneous-Metamorphic Complex (Easton, 1981c) is located near 66°N, 116°W (Figure 3.1). It consists of a tonalite gneiss (Unit 1); with enclaves of garnetiferous amphibolite, anthophyllite schist, and pelitic and quartzitic metasediments. The garnetiferous amphibolite is geochemically distinct from Akaitcho Group metavolcanic rocks (Chapter 4). The tonalite gneiss is cut by pink,

protomylonitic biotite monzogranite (Unit 2). The monzogranite is cut by dykes of basalt, 30 to 100 m wide, now amphibolite (Unit 3). All three units are cut by late granitic pegmatite veins, are foliated, and have undergone two stages of folding. Outcrop-scale recumbent folds with east-west trending axes have been refolded about north- to northwest-trending regional fold axes. The later folding affects amphibolite dykes in the northern part of the Sityok Complex (Figure 3.1).

The Sityok Complex may represent basement to the Akaitcho Group. The granite was emplaced into gneiss, and then cut by basalt dykes prior to metamorphism and deformation of the Sityok Complex and the Akaitcho Group. The basalt dykes have similar geochemistry to the basalts of the lower Akaitcho Group (Chapter 4). The Sityok Complex is in fault contact with all adjacent units. St-Onge *et al.* (1982) have interpreted the Sityok Complex as a nappe based on mapping south of the area mapped by the author. St-Onge *et al.* (1982) confirmed the observation of Easton (1981c) that the Sityok Complex is pre-metamorphic, and, in addition, they suggest that the Sityok Nappe was emplaced prior to the metamorphic culmination. However, simply because the Sityok Complex is allochthonous and pre-metamorphic does not establish the Complex as basement. Geochronology of the Sityok Complex (Chapter 5) is inconclusive regarding its age. Thus, although the Sityok Complex appears to be basement to the Akaitcho Group on the

Figure 3.1 Geology of the northern half of the Sityok Igneous Complex. The Sityok Complex consists of Units 1, 2, and 3. See text for further details.

LEGEND

- 12 granites near faults, felsite dykes
- 11 a) 'younger granite'; b) porphyritic syenogranite
- 10 DUMAS GROUP
- 9 granodiorite with patches of syenogranite
WENTZEL BATHOLITH
- 8 amphibolite syenogranite gneiss
- 7 garnet granite
AKAITCHO GROUP
GRANT SUBGROUP
- 5 a) siltstone and pelite; b) gabbro sills;
c) basalt; d) conglomerate; e) orthoquartzite and
siltstone
IPIUTAK SUBGROUP
- 4 a) pelite; b) arkose; c) amphibolite; d) basalt
tuff; e) basalt flows; f) orthoquartzite,
siltstone, and pelite
SITYOK IGNEOUS COMPLEX
- 3 amphibolite dykes
- 2 pink protomylonitic monzogranite
- 1 grey tonalite gneiss



basis of field relations, this interpretation has not yet been independently verified.

3.3 AKAITCHO GROUP

The term Akaitcho Group was introduced by Hoffman et al. (1978) for metavolcanic and metasedimentary rocks east of the Wopmay Fault Zone and west of the Hepburn Batholith which could not be correlated with Epworth or Recluse Group strata. The Akaitcho Group can be regarded most simply as consisting of lower, middle, and upper volcanic sequences separated by a lower coarse clastic and an upper pelite unit (Figure 3.2).

The Akaitcho Group presently is divided into three subgroups and seven formations (Easton, 1980, 1981c, 1981d; Hoffman and Pelletier, 1982). The subgroups can be divided into several formations, but formal subdivision is not yet warranted. These stratigraphic units are described briefly below. A generalized stratigraphic column for the Akaitcho Group, which also shows the lithological types and the facies relations between the main Akaitcho Group units, is presented in Figure 3.3. The central stratigraphic column in Figure 3.3 is based mainly on observations within crustal block B, which contains the most continuous, least deformed, and least metamorphosed stratigraphic section of the Akaitcho Group.

3.3.1 Ipiutak Subgroup

The oldest exposed rocks of the Akaitcho Group belong to the Ipiutak Subgroup (Easton, 1981c, 1981d), a diverse

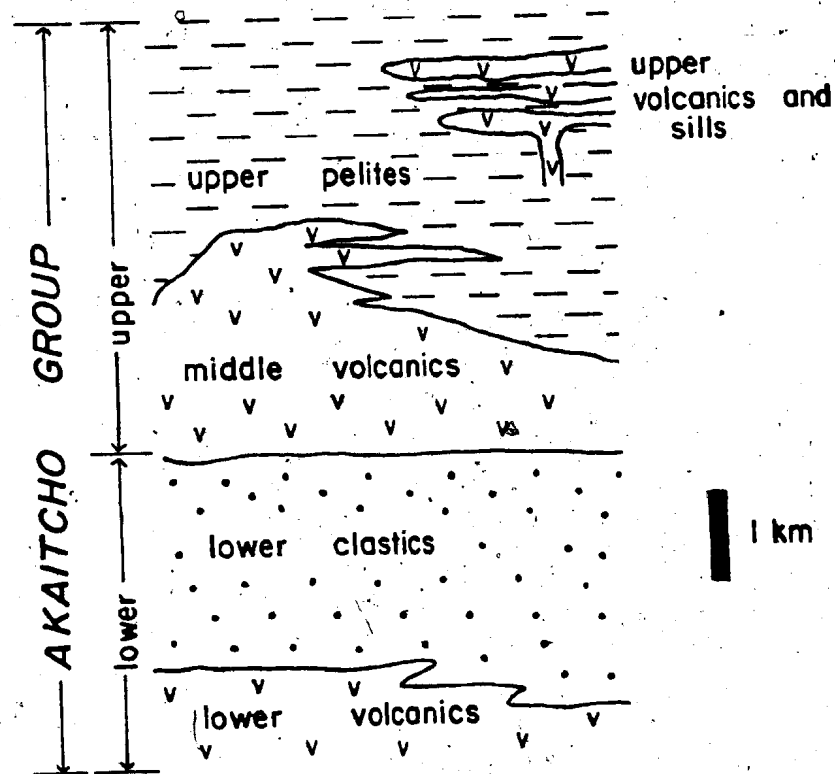







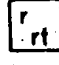

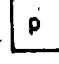

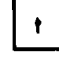

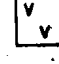

Figure 3.2 Generalized stratigraphic column for the Akaitcho Group.

Figure 3.3 Stratigraphic column for the Akaitcho Group in block B and suggested lithological correlations with the volcanic and sedimentary rocks in Cloos Nappe and the Grant block. The Akaitcho Group in block D consists of Units 1 and 2.

Key to Akaitcho Group Formations
(not in stratigraphic sequence)

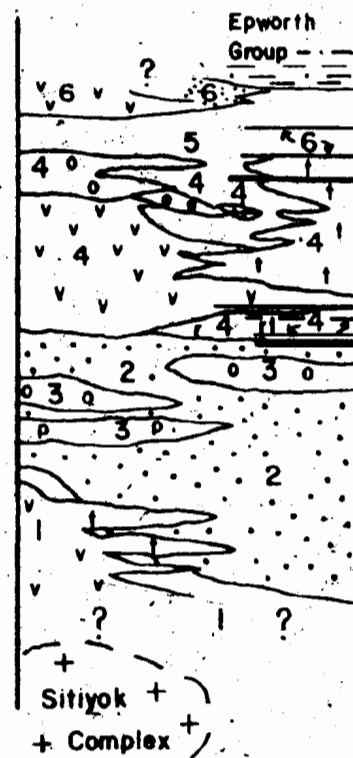
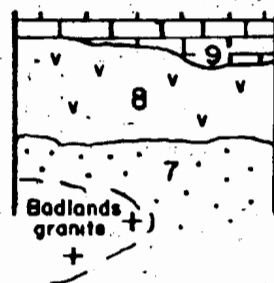
- 10 Grant Subgroup
- 9 Stanbridge Formation
- 8 Vaillant Formation
- 7 Drill Formation
- 6 Teller Sills and McGregor amphibolite
- 5 Aglerok Formation
- 4 Nasittok Subgroup
- 3 Okerok Sills
- 2 Zephyr Formation
- 1 Ipiutak Subgroup

LITHOLOGIES

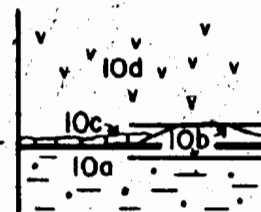
	pelite with quartzite interbeds		gabbro sills
	siliceous siltstone		porphyritic rhyolite flows and sills
	olive pelite and volcanoclastic sediments		high-Zr rhyolite flows and tuffs
	marble		plagioclase porphyritic rhyolite sills
	conglomerate		basaltic tuffs
	arkosic turbidites		pillowed and massive basalt flows
	pelite and siltstone		

BLOCK 'B'

CLOOS NAPPE (block 'A,B')



GRANT BLOCK



assemblage of metasedimentary and metavolcanic rocks preserved mainly at high metamorphic grade. The base of the Subgroup has not been observed.

Within crustal block B, about 300 to 500 m of locally pillowed amphibolite is present on the west limb of the major syncline that runs through Akaitcho Lake (Figure 2.7, 2.8, 3.4). The Wentzel Batholith has intruded the Ipiutak Subgroup in this area. Locally, a thin horizon of pelite is associated with the amphibolites. Both are overlain by arkosic turbidites of the Zephyr Formation.

The Ipiutak Subgroup is exposed mainly in crustal block D, a block with complex stratigraphic relationships due to the presence of recumbent folds of foliation which have been refolded about northerly axes (McGlynn, 1976, Easton, 1981c; St-Onge *et al.*, 1982) and thrust nappes (St-Onge *et al.*, 1982). As a result, although there is a lower volcanic sequence below and interfingering with the Zephyr Formation in crustal block D, the extent and significance of the stratigraphy of this terrane is poorly understood.

In spite of the complex geology, several stratigraphic units can be recognized within crustal block D. However, it is not always possible to relate these sequences to one another because of complications caused by the two phases of folding, the high metamorphic grade in the area, and the complex faulting present within the block (Figure 3.5, 3.6).

North and east of the Wentzel Fault (Figure 3.5) is a sequence of mainly arkosic turbidites, locally with some pelite and amphibolite horizons (Unit 2). Northeast of Wentzel Lake, these arkosic turbidites are intruded by garnet-bearing granites of the Wentzel Batholith (Unit 2b). A band of coarse- and fine-grained amphibolite, interbedded with pelite (Unit 4a), is present south of the Belleau Fault and runs through the centre of Wentzel Lake (Figure 3.5). Unit 4a is also present south of the Wentzel Fault.

Pillowed basalt and basaltic tuffs, preserved at greenschist to lower amphibolite grade, occur in two areas (Unit 3). North of Wentzel Fault, the basalts are interbedded with arkosic turbidites, and, based on facing directions, in the upper greenschist-grade turbidites, the basalts underlie the arkoses. South of Wentzel Fault, the basalts are more abundant, and are in fault contact with adjacent units. However, it is not known if the basalts south of Wentzel Fault are remnants of the Grant Subgroup preserved in a graben, or if they are a klippe or window of Nasittok Subgroup volcanic rocks.

South of Wentzel Lake, Unit 4a is the most common unit. It consists of 1 to 5 m thick bands of fine-grained amphibolite and garnet amphibolite interbedded with pelites. These amphibolites are interpreted to be mafic tuffs interbedded in a sedimentary sequence. West of Four Corners Lake, pelite becomes less abundant, and thicker, medium- to coarse-grained amphibolite units (possible flows or sills) become

Figure 3.4 Geological sketch map showing distribution of volcanic rocks interbedded with the lower Zephyr Formation in crustal block B. Amphibolite near the contact with the Wentzel Batholith may be part of the volcanic succession. Field relations between the volcanics and the sediments are similar to those present between Units 2 and 3 north of the Wentzel Fault in Figure 3.5.

LEGEND

WENTZEL BATHOLITH



garnet bearing granite (over 5% garnet) gneiss



granite gneiss

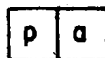
AKAITCHO GROUP



Okrark rhyolite sills; plagioclase-porphyritic; orthoclase porphyritic



Zephyr Formation; arkosic turbidites, minor pelite; pelite



Ipiutak Subgroup; pillowed basalt/amphibolite; amphibolite



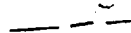
migmatite (over 30% granitic material)



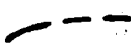
bedding; tops known, unknown



cleavage



geological contact; definite, approximate



fault; known, assumed

Mineral Isograds (mark on high T side)



staurolite



K-feldspar, sillimanite



granite pods

migmatite
(30% granitic material)

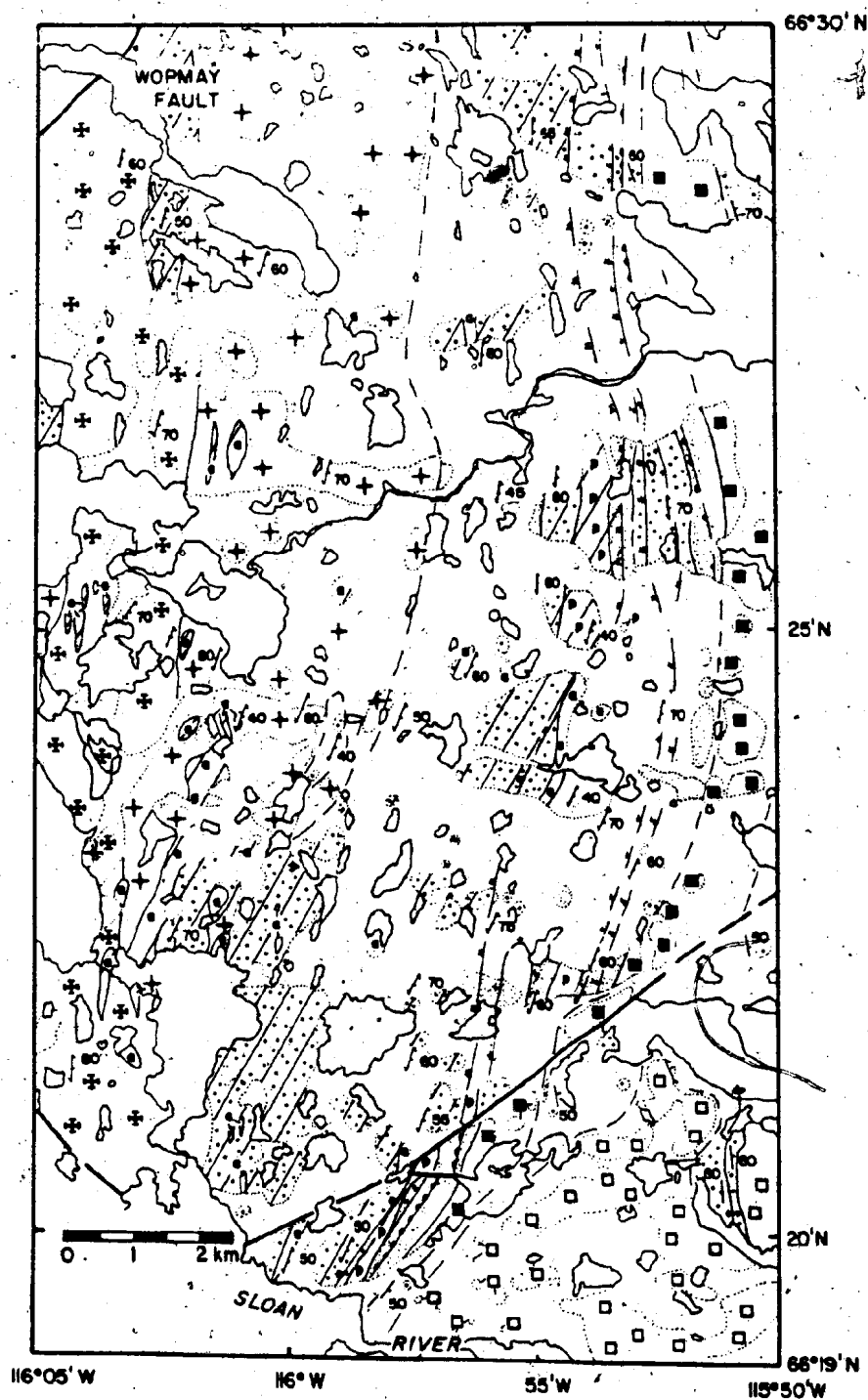


Figure 3.5 Stratigraphic sequences present in crustal block D. Data south of 65°50'N from St-Onge *et al.* (1982), Mursky *et al.* (1970), McGlynn (1976).

LEGEND



Hornby Bay sandstone

D Dumas Group



weakly foliated monzogranite,
some late granitoid plutons



garnet granite



Grant Subgroup

N felsic tuffs, pelites, volcanoclastic sediments,
gabbro sills of the Nasittok Subgroup

O Okrark rhyolite sills

Ipiutak Subgroup

5 5a amphibolite interbedded with orthoquartzite
5b amphibolite interbedded with pelite

4 4a amphibolite interbedded with pelite
4b amphibolite, medium and coarse grained
4c amphibolite interbedded with grey orthoquartzite

3 pillowed and massive basalt flows and tuffs,
low metamorphic grade

2 arkose and minor pelite, generally above migmatite
grade, probably correlative with the Zephyr
Formation, 2b arkoses, intruded by garnet granites

1? gneisses, migmatites, correlation unknown



Sitiyok Igneous Complex



fault



fold of foliation; synform, antiform



mylonite

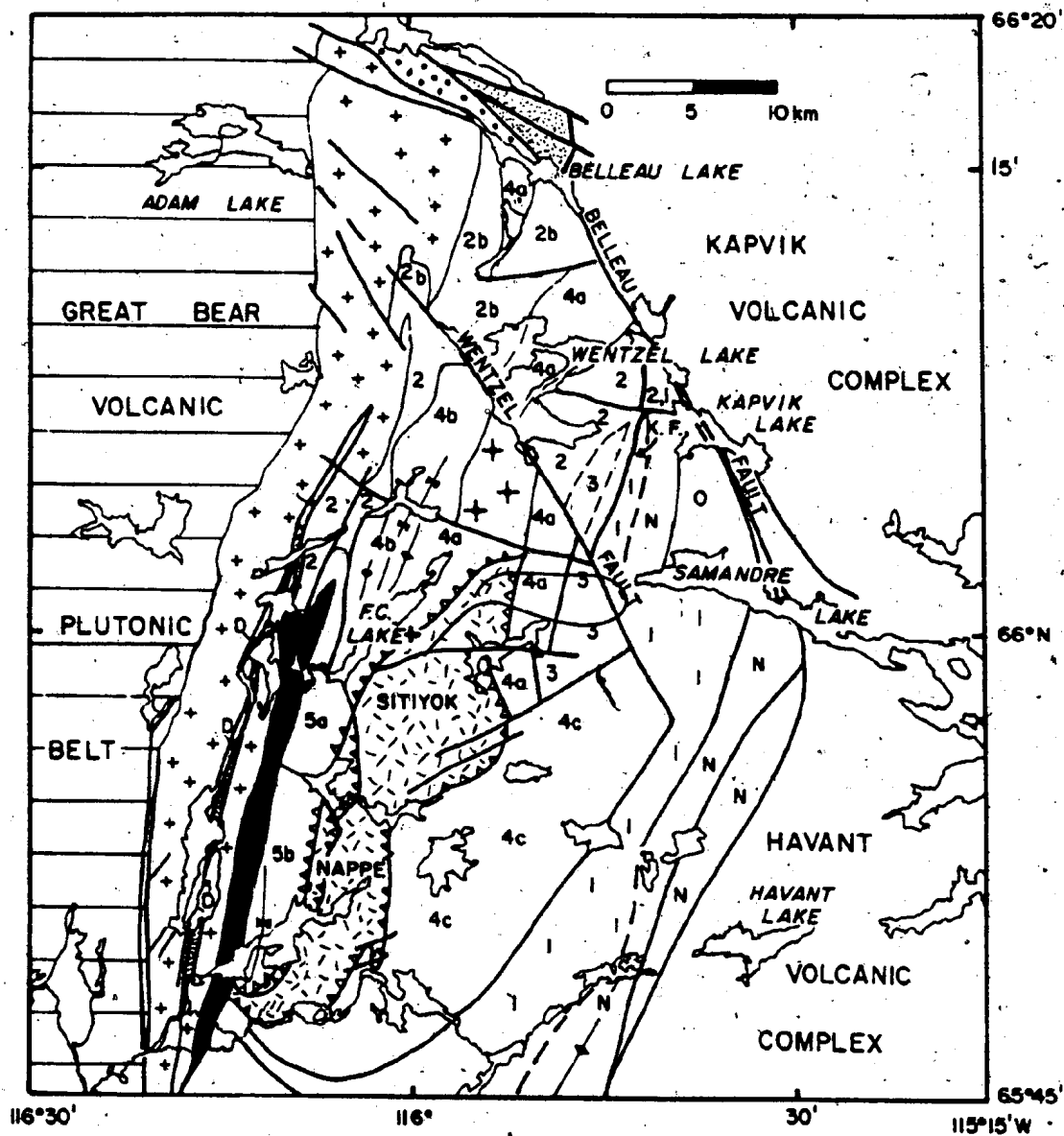




Figure 3.6 Distribution of metamorphic mineral assemblages in crustal block D. Data from Easton (1981c), St-Onge *et al.* (1982).

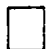
LEGEND


 granitoid rocks


 mylonite


 fault


Mineral assemblages


 muscovite-biotite-chlorite-plagioclase-quartz

 andalusite-muscovite-biotite-plagioclase-quartz


 sillimanite-muscovite-biotite-plagioclase-quartz-liquid


 sillimanite-K-feldspar-biotite-plagioclase-quartz-liquid

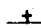
 kyanite-muscovite-biotite-plagioclase-quartz-liquid

 kyanite-K-feldspar-biotite-plagioclase-quartz-liquid


Mineral Isograd (mark on the high T side)

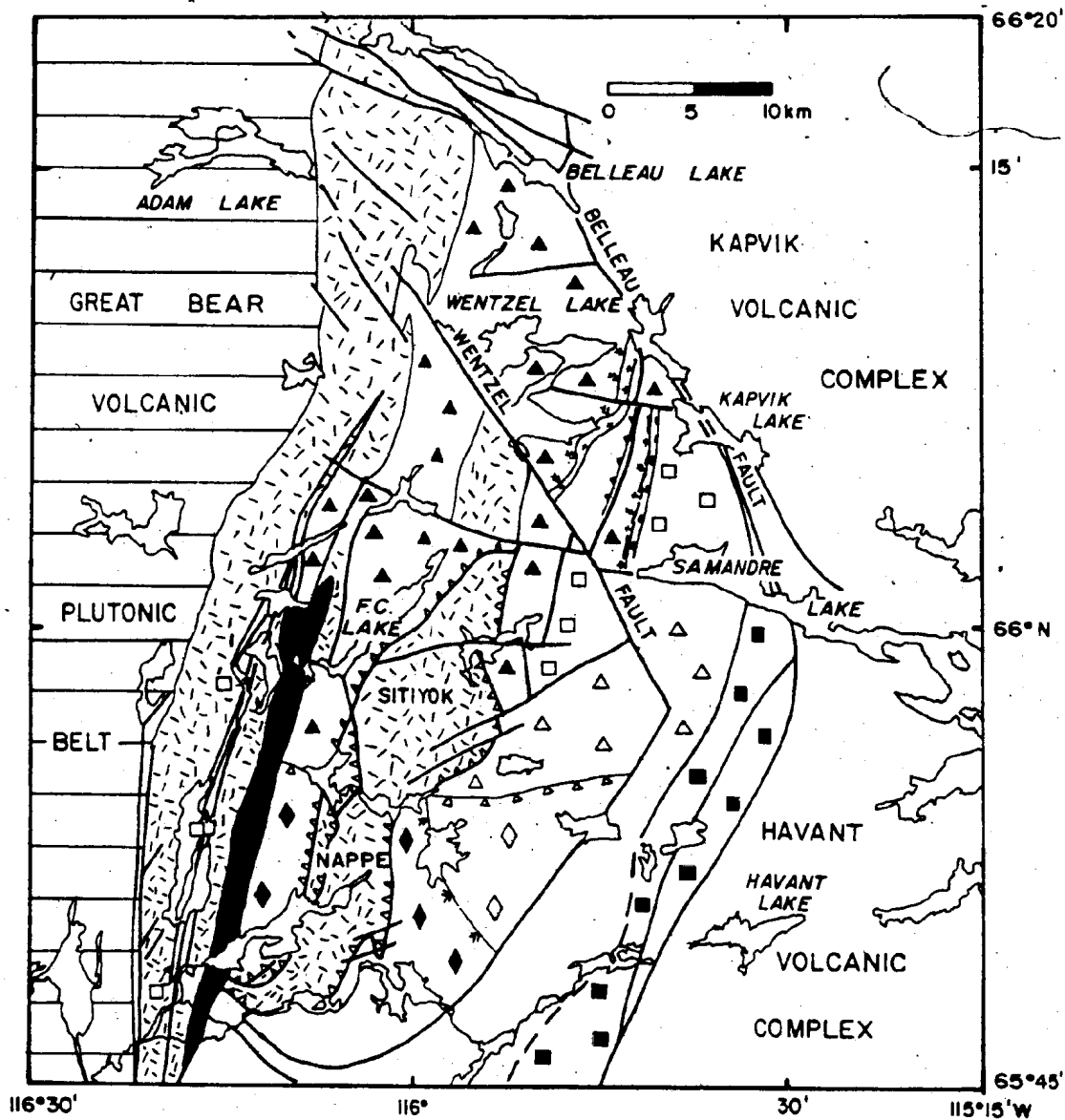
 staurolite

 andalusite

 granitic pods

 K-feldspar, Al_2O_5

 kyanite



more common (Unit 4b). Unit 4b may be a remnant of a volcanic edifice. If this is the case, then it is possible that the amphibolite layers in Unit 4a were tuffs deposited distal to the volcanic edifice. South of Four Corners Lake, 1 to 100 m thick bands of medium-grained amphibolite are found interbedded with grey orthoquartzite and siltstone (Unit 5a). These amphibolites could be flows or sills interbedded with clastic sediments. The orthoquartzites in Unit 5a are different in appearance from the arkosic turbidites (Unit 2) even at similar metamorphic grades. Similar lithologies (Unit 4c) are found east of the Sitiyok Igneous Complex (Nappe) and may be the same unit.

The problem in block D is that, because of recumbent folding and thrusting, there is no way to determine the importance of lateral facies variation (i.e. do Units 4a, 4b, and 5a represent a volcanic complex formed in a rift, with Units 4b and 5a representing sediments adjacent to the volcanic complex and the rift margin respectively) and vertical facies variation (i.e. is Unit 5a a southward facies of the Zephyr Formation that overlies a volcanic sequence (Units 4a and 4b)). Until the structural complexities within crustal block D can be unravelled, or until a less deformed section is observed at lower metamorphic grade, one can do little else except note that there are several lithological groupings within the Ipiutak Subgroup.

There are, however, three important characteristics of the Ipiutak Subgroup that have a bearing on the overall

development of the Akaitcho Group. First, there is a volcanic sequence beneath the Zephyr Formation, at least in crustal block B. Second, rhyolite has not been found in the Ipiutak Subgroup. Finally, as discussed in detail in Chapter 4, the Ipiutak Subgroup volcanic rocks are continental tholeiites; and the pelitic sediments have REE patterns indicating derivation from a continental, not a volcanic, source terrane.

3.3.2 Zephyr Formation

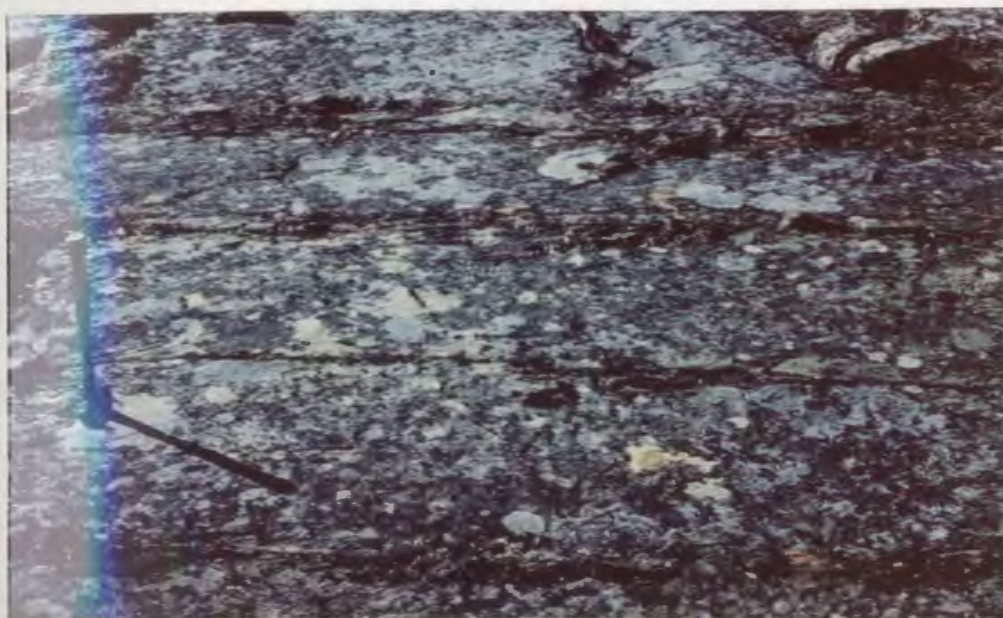
Up to three kilometres of subarkosic to arkosic flyschoid strata overlie the Ipiutak Subgroup. Turbidite beds typically range from 10 to 100 cm thick, and typically have arkosic, medium-sand bases with green or grey pelite tops (Figure 3.7, 3.8). Current structures are rarely observed in the turbidites. Complete Bouma sequences have been observed in Zephyr Formation turbidites in the vicinity of Akaitcho Lake. Rounded grains of epidote, tourmaline, and zircon are common in the basal turbidite beds. Upper and lower contacts of the formation are sharp. There is some regional variation in the Zephyr Formation. In the north, it consists of turbidite beds with well developed pelite layers. Near Kapvik Lake, pelite is a minor component of the Zephyr Formation. Pelite again becomes more abundant to the south.

3.3.3 Okrark Sills

Plagioclase-porphyrific and orthoclase- and plagioclase-porphyrific, 300 to 600m thick rhyolite-porphyry sills,

Figure 3.7 Bedding in typical Zephyr Formation turbidites north of Akaitcho Lake. Lichen cover is typical of the region.

Figure 3.8 Detail of base of a sandy turbidite bed. Note sharp contact between underlying pelite and overlying sand bed.



intrusive into the Zephyr Formation, are termed the Okrark sills (Figures 3.9, 3.10). The plagioclase-porphyritic and orthoclase-porphyritic sills are chemically indistinguishable (Chapter 4). Contacts between the sills and turbidites are generally sharp, and the sills have metamorphosed the adjacent sedimentary rocks near the intrusive contacts. The Okrark sills are geochemically correlative with low SiO_2 , high-Zr porphyritic rhyolite found in the upper parts of the Tuertok, Sinister, and Belleau volcanic complexes of the Nasittok Subgroup (Easton, 1980).

3.3.4 Nasittok Subgroup

The Nasittok Subgroup consists of three volcanic complexes: the Sinister, Tuertok, and Kapvik complexes (Figure 3.11). A fourth complex may be present in the vicinity of Havant Lake (Figure 3.11). The Sinister, Tuertok, Kapvik, and Havant volcanic complexes are correlated on the basis of marker horizons that can be traced between individual volcanic complexes. The Zephyr and Belleau volcanic complexes (Figure 3.11) are isolated from the other volcanic complexes, but are lithologically similar to the Sinister, Tuertok, Kapvik, and Havant volcanic complexes (Easton, 1980, 1981c). Both the Zephyr and Belleau volcanic complexes contain rhyolite, which is absent from the Ipiutak Subgroup.

The volcanic complexes typically have a 2 km thick basal basaltic unit containing pillowed flows (Figure 3.12) and varying amounts of basaltic tuffs (Figure 3.13), overlain by porphyritic rhyolite domes and flows (Figure 3.14).

Figure 3.9 Okrark sill overlying Zephyr Formation turbidites near Akaitcho Lake. Sill-Zephyr Formation contact is immediately above talus slope in centre of photograph.

Figure 3.10 Typical outcrop surface of a plagioclase-porphyrific sill showing strong deformation of grains. Sill located two km west of Kingarok Lake.

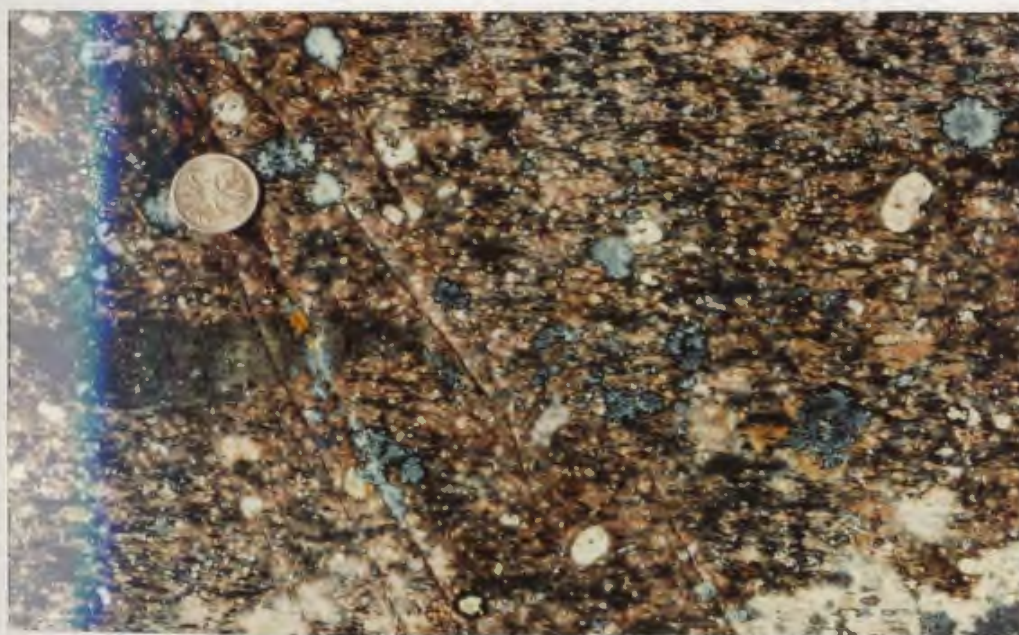


Figure 3.11 a) Distribution of volcanic rocks and location of volcanic complexes in the Hepburn Lake map area. Abbreviations: AG - Aglerok Lake; AL - Akaitcho Lake; HL - Hepburn Lake; HV - Havant Lake; KL - Kapvik Lake; OL - Okrark Lake; SL - Samandre Lake; ST - Stanbridge Lake; TL - Tallerk Lake; WL - Wentzel Lake; ZL - Zephyr Lake.

b) Distribution of volcanic facies within the Akaitcho Group volcanic complexes in the Hepburn Lake map area.

LEGEND (Figure b)

Rhyolites



mainly tuffs and bedded tuffs, locally lapilli tuffs and breccias



domes and flows, subaqueous



pyroclastic flows and ash-flows, probably subaerial

Basalts



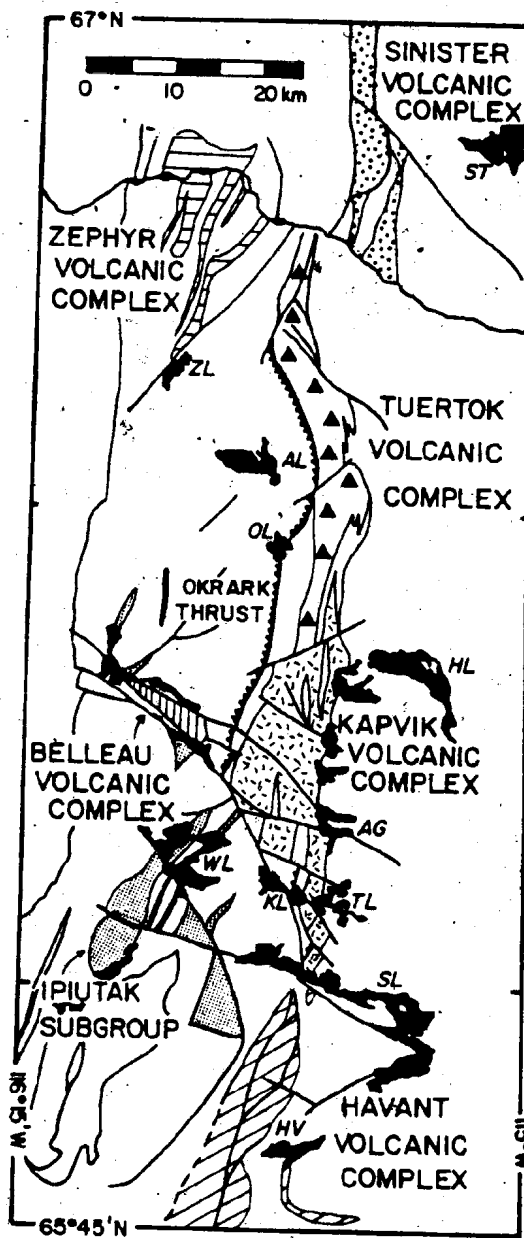
pillowed and massive flows



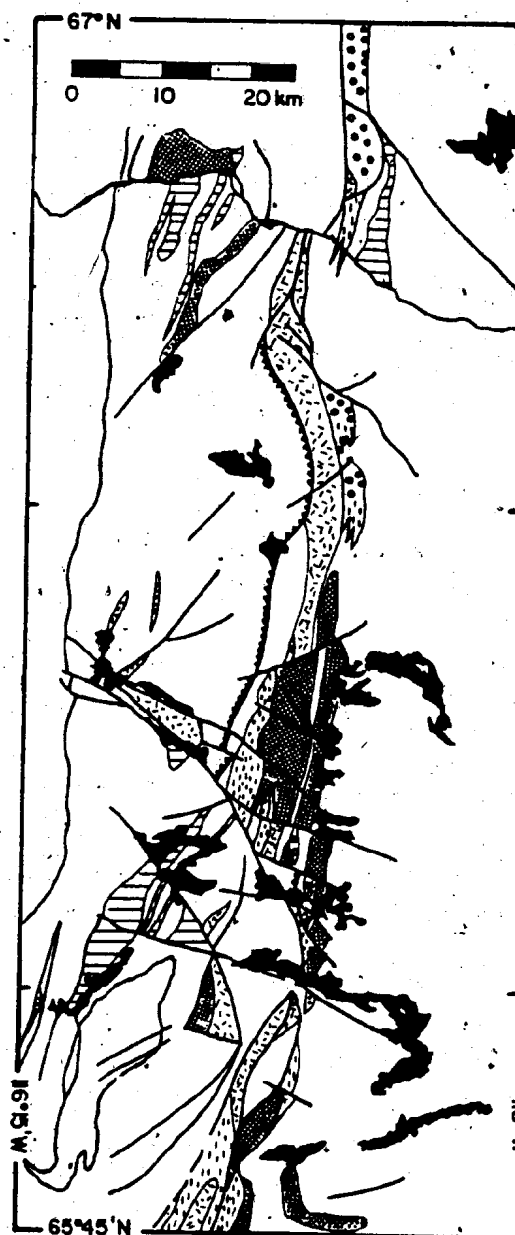
tuffs and lapilli tuffs, minor pillowed and massive flows



amphibolite



(a)



(b)

Figure 3.12 Pillowed basalt flows in the Nasittok Subgroup,
Tuertok volcanic complex.

Figure 3.13 Bedded mafic tuffs in the Nasittok Subgroup,
Kapvik volcanic complex.

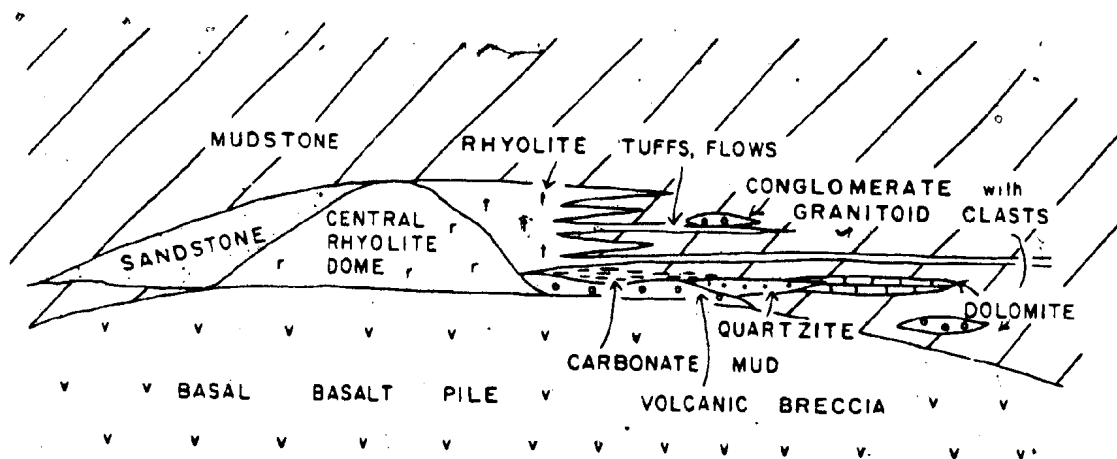
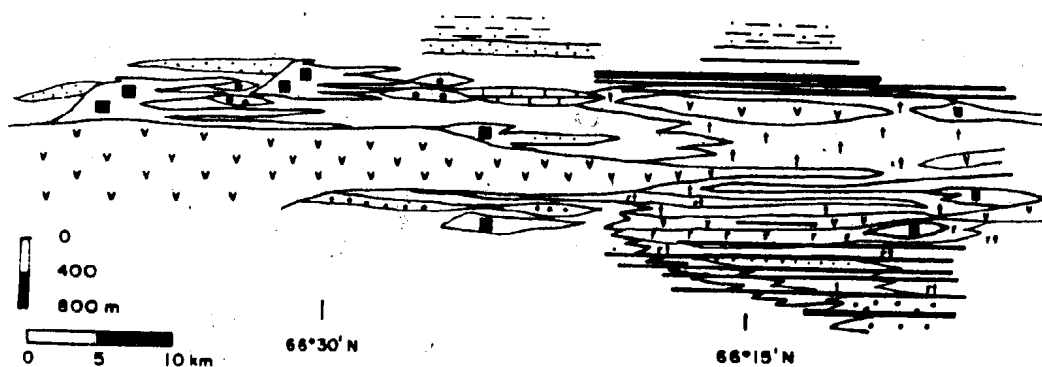


Figure 3.14 Generalized facies relationships between the Tuertok and Kapvik volcanic complexes.
Symbols as in Figure 3.3.

Figure 3.15 Generalized facies relationships in rhyolite centres overlying the Sinister, Tuertok, and Kapvik volcanic complexes.

TUERTOK

KAPVIK



Abundance ratios of felsic to mafic rocks are 0.2 to 0.3. The only exception to the typical stratigraphy (Figure 3.14) is the Kapvik volcanic complex where high-SiO₂, low-Zr rhyolite is present below the basal basalt sequence and which consists predominantly of basaltic tuff in the basalt unit (Figure 3.15). The Tuertok and Kapvik complexes are compared in Figure 3.14. The stratigraphy of individual volcanic complexes is given in more detail in Easton (1980, 1981a). The Tuertok volcanic complex (Easton, 1981a) is considered to be typical (Figures 3.14, 3.15).

The contact of the Tuertok volcanic complex with the Zephyr Formation is sharp, in the few places where it has been observed. The contact with the Kapvik volcanic complex is obscure, because a gabbro sill swarm intrusive into the Zephyr Formation underlies the basal rhyolites and basalts of the Kapvik complex (Figure 3.15). The bases of the other volcanic complexes are not exposed. The volcanic complexes are overlain, and interfinger with, the pelites of the overlying Aglerok Formation. Volcanism in the Nasittok Subgroup was mainly subaqueous, with pillowed basalt and basalt tuff being predominant. The rhyolites were deposited as water-lain tuffs, flows, and domes. A few possible welded ash-flow tuffs are present in the upper parts of the volcanic complexes indicating that, locally, volcanic complexes were subaerial. To the south, the proportion of tuff in the volcanic complexes increases (Figure 3.11b). One interpretation is that the change from pillowed to tuffaceous volcanism

reflects a decrease in water depth to the south. There is no evidence from the chemistry of the basalts to suggest that the change is due to differences in lava composition.

A recurring stratigraphic sequence occurs in the rhyolite volcanic domes that overlie the basalt centres (Figures 3.15). Sandstone wedges consisting of detritus shed from the domes are present on the north side of the domes. Volcanic breccias (Figure 3.16), conglomerates containing granite, granite gneiss, and orthoquartzite clasts (Figure 3.17), marbles (Figure 3.18), and orthoquartzites occur on the south side of the domes. Because these lithologies are closely related to the rhyolite domes, they are considered to be part of the Nasittok Subgroup.

3.3.5 Aglerok Formation

Olive pelites, 1 to 2 km thick, overlie and interfinger with the Nasittok Subgroup. Bedding in the pelites is on a millimetre to centimetre scale (Figures 3.19). Included with the pelites are volcanoclastic sedimentary rocks, minor basaltic and rhyolitic tuffs, and reworked basaltic and rhyolitic tuffs. In addition to the normal pelites (Figures 3.19), two other broad classes of sedimentary rocks can be distinguished in the Aglerok Formation. One type, the mafic tuffaceous pelites, is chlorite rich, and at appropriate metamorphic grade is garnet-bearing. The mafic tuffaceous pelites are distinct from the basalt tuffs in hand specimen, thin section, and major- and trace-element chemistry (Figures 3.20, 3.13) (Chapter 4). The second type is quartz

Figure 3.16 Volcanic breccia derived from a rhyolite dome
in the Tuertok volcanic complex.

Figure 3.17 Conglomerate. Note granite and orthoquartzite
clasts in the centre of the photograph. The
conglomerate is interbedded with pelite of the
Aglerok Formation above the Tuertok volcanic
complex.



Figure 3.18 Outcrop of marble, Tuertok volcanic complex.

Figure 3.19 Typical Aglerok Formation pelites, biotite
metamorphic grade.

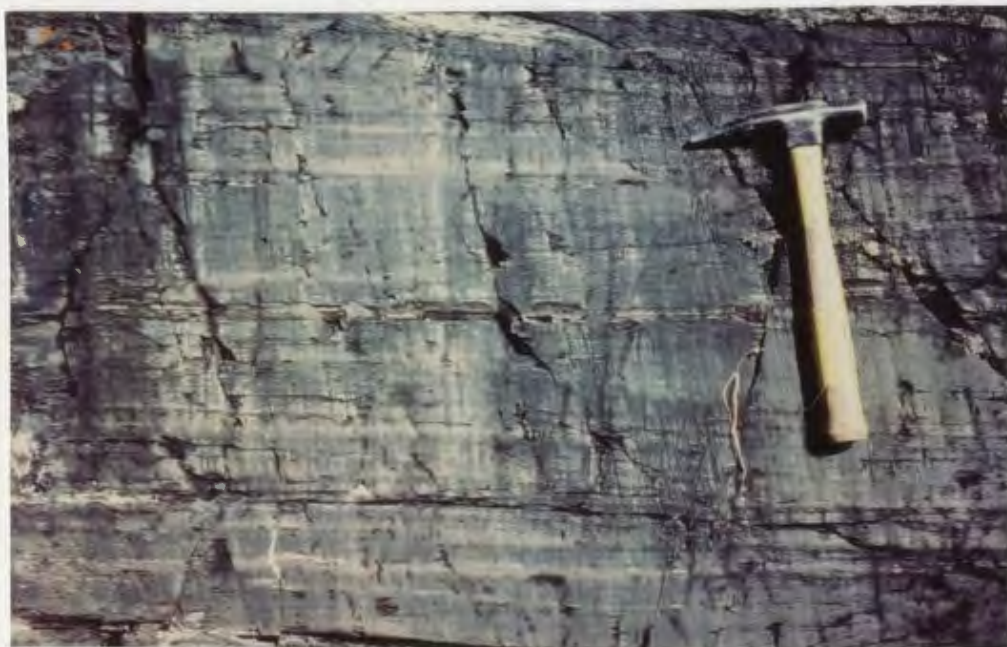


Figure 3.20 Mafic tuffaceous mudstone from the Kapvik
volcanic complex, biotite metamorphic grade.



and muscovite rich, and is closely associated with rhyolite eruptive centres (Figure 3.21). The felsic tuffaceous pelites are distinct from felsic tuffs in the Aglerok Formation (Figure 3.22).

The Aglerok Formation was derived primarily from erosion of volcanic rocks like the Nasittok Subgroup volcanic complexes, with a minor contribution from an adjacent source area (Easton, 1980, 1981b). Geochemical studies on the Aglerok Formation pelites (Chapter 4) support the above conclusion regarding source terrane. Contacts with the sills and volcanics of the overlying Tallerk Formation are sharp. A titaniferous siliceous siltstone underlies the Odjick Formation 8 km northwest of Hepburn Lake. This unusual member was previously included in the Tallerk Formation (Easton, 1981d). Because it is metasediment, and the rest of the Tallerk Formation is igneous, the siltstone is best included in the Aglerok Formation.

3.3.6 Tallerk Formation

McGregor Amphibolite Member

On the north shore of the Coppermine River, about 200 m of pillowed basalts, now amphibolite, overlie pelites of the Aglerok Formation. The thickness of these amphibolites is not known, because the upper part of the section is intruded by granitic plutons of the Hepburn Batholith (Figure 3.23).

Tallerk Sills

Fifty to two hundred metre thick gabbro sills intrude the upper part of the Aglerok Formation above the Kapvik and

Havant volcanic complexes. No extrusive volcanic rocks are associated with these sills, although the McGregor amphibolite member is probably contemporaneous.

The McGregor amphibolite and the Tallerk sills comprise the Tallerk Formation which includes the late igneous products of the Akaitcho Group. The extent of the Tallerk Formation is not known because, in many areas, the upper Aglerok and Tallerk Formations are intruded by tonalitic, granitic, and gabbroic intrusions of the Hepburn Batholith. Near Hepburn Lake, pelites of the Odjick Formation overlie the Aglerok Formation. Thus, in some areas, the Tallerk Formation is thin or absent. The absence of abundant amphibolite xenoliths or windows of Tallerk Formation rocks in the Hepburn Batholith, and the presence of many windows of Aglerok, Odjick, Fontano, and Asiatic Formation strata in the Hepburn Batholith indicates that the Tallerk Formation was not extensive.

3.3.7. Grant Subgroup

The Grant Subgroup (Figure 3.3) (Easton, 1981c) consists of 1000 m or more of metasiltstone, dolomite, and mafic volcanic rocks. The lowest part of the Grant Subgroup consists of 500 m or more of finely interbedded, grey- to buff-weathering metasiltstone and slate (Figures 3.24, 3.25). Beds of subarkosic to quartz arenite fine sand are rarely interbedded with the siltstones and slates. Locally, volcanoclastic sediments are present in the upper part of the sedimentary sequence. A 2 to 15 m dolo-

Figure. 3.21 Felsic tuffaceous mudstone, Kapvik volcanic complex.

Figure 3.22 Bedded rhyolite tuff, Kapvik volcanic complex.



Figure 3.23 Geological map of the southern half of the
McGregor Lake area (N.T.S. 86J/14).

LEGEND



Hornby Bay Group sandstone



Muskox Intrusion



biotite-orthopyroxene gabbro



leucogranite - Hepburn Batholith



granite - Hepburn Batholith

rf

pelites - Fontano Formation

eo

pelites with minor orthoquartzite -
Odjick Formation

Akaiitcho Group

M

McGregor amphibolite



olive pelite - Aglerok Formation

r

rhyolite flows and tuffs

p

pillowed and massive basalt flows

t

mafic tuffs



cleavage



lineation



fault



trace of outcrop



bedding, tops unknown



block C boundary fault

Mineral Isograds (mark on the high T side)



migmatite



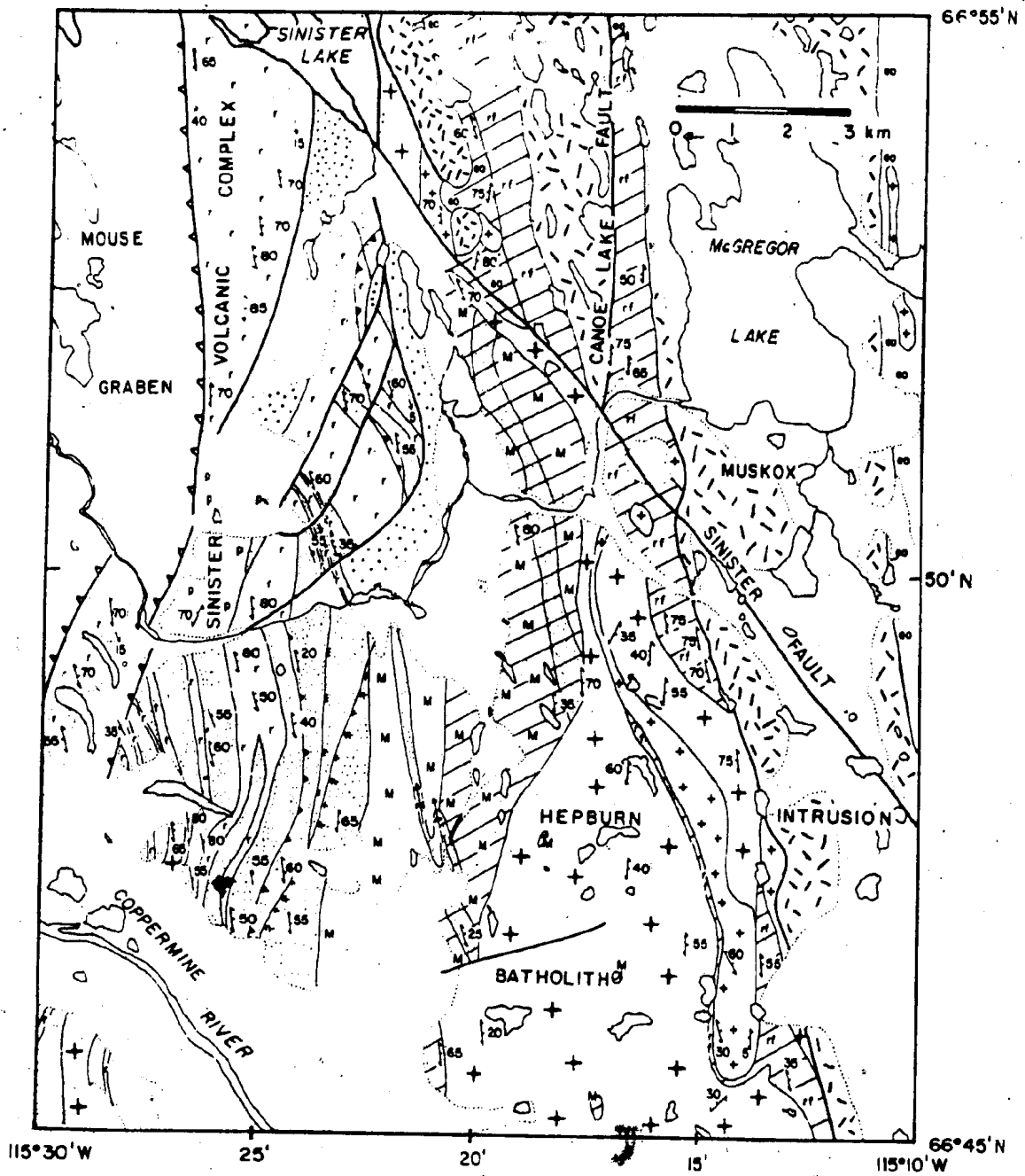
staurolite



sillimanite



granite pods, K-feldspar-sillimanite



mite horizon overlies the metasiltstones and slates in most areas (Figure 3.26). Metavolcanic rocks, mainly basalt flows and tuffs (Figure 3.27), overlie the sedimentary rocks. Rhyolite flows are interbedded with the mafic volcanics in a few areas. Gabbro sills are common along the dolomite-volcanic contact. The Grant Subgroup extends from the southern part of the Hepburn Lake area, through the Calder River belt, to Grant and Rebesca Lakes (Figure 3.28). It is always in fault contact with other rocks, has the monotonous stratigraphy outlined above, and is usually found at chlorite to andalusite grade. For these reasons, it was isolated as a separate subgroup. The metasedimentary rocks have been correlated with the upper Zephyr Formation, and the volcanic rocks with the lower Nasittok Subgroup (Easton, 1981c) on the basis of lithological and stratigraphic similarities (Figures 3.3, 3.29). Although correlative, the Grant Subgroup is distinctive. The metasedimentary rocks are generally finer grained than in the Zephyr Formation to the north. Hence, the Grant Subgroup metasedimentary rocks may be distal facies of the upper Zephyr Formation. The Grant Subgroup may be a more westerly derived thrust slice dissected by later faulting along the Wopmay Fault Zone.

3.3.8 Zone 2/3 Boundary

Three additional Akaitcho Group formations occur east of the Hepburn Batholith (Figure 3.30). The thickest accumulations of these formations are near Zone 2/3 boundary.

Figure 3.24 Finely laminated mudstone of the Grant Subgroup.

Figure 3.25 Siltstone interbed in Grant Subgroup mudstone. Andalusite is present in the mudstone beds.



Figure 3.26 Dolomite beneath volcanic rocks of the Grant Subgroup, Wopmay Lake.

Figure 3.27 Pillowed basalt in the Grant Subgroup.



Figure 3.28 Distribution of the Grant Subgroup in western Zone 3. Grant Subgroup rocks are commonly found adjacent to the Wopmay Fault Zone.

LEGEND

◇ granitoid and high-grade metamorphic rocks of Zone 3

≡ Grant Subgroup

⚡ Sityok Igneous Complex

+ weakly foliated monzogranites of uncertain age present along the Wopmay Fault Zone

— fault

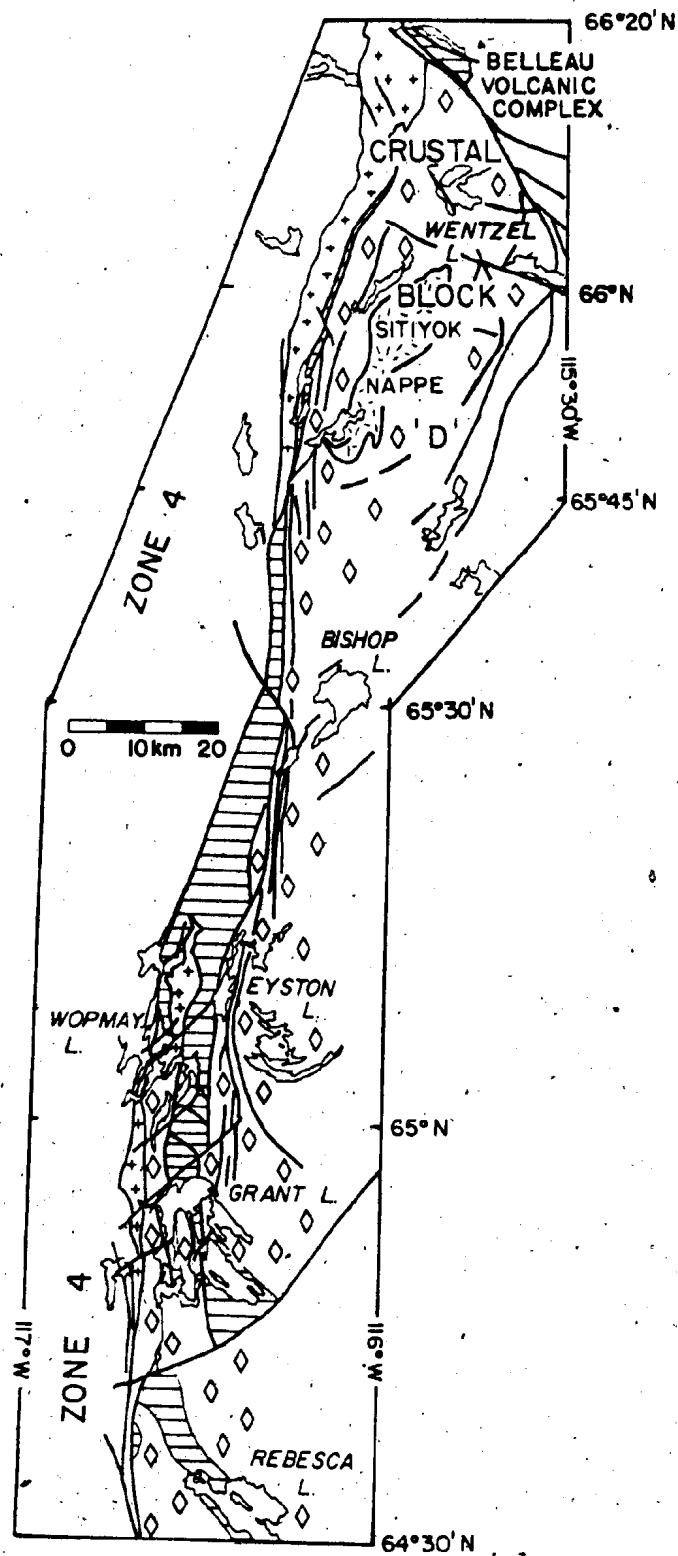
















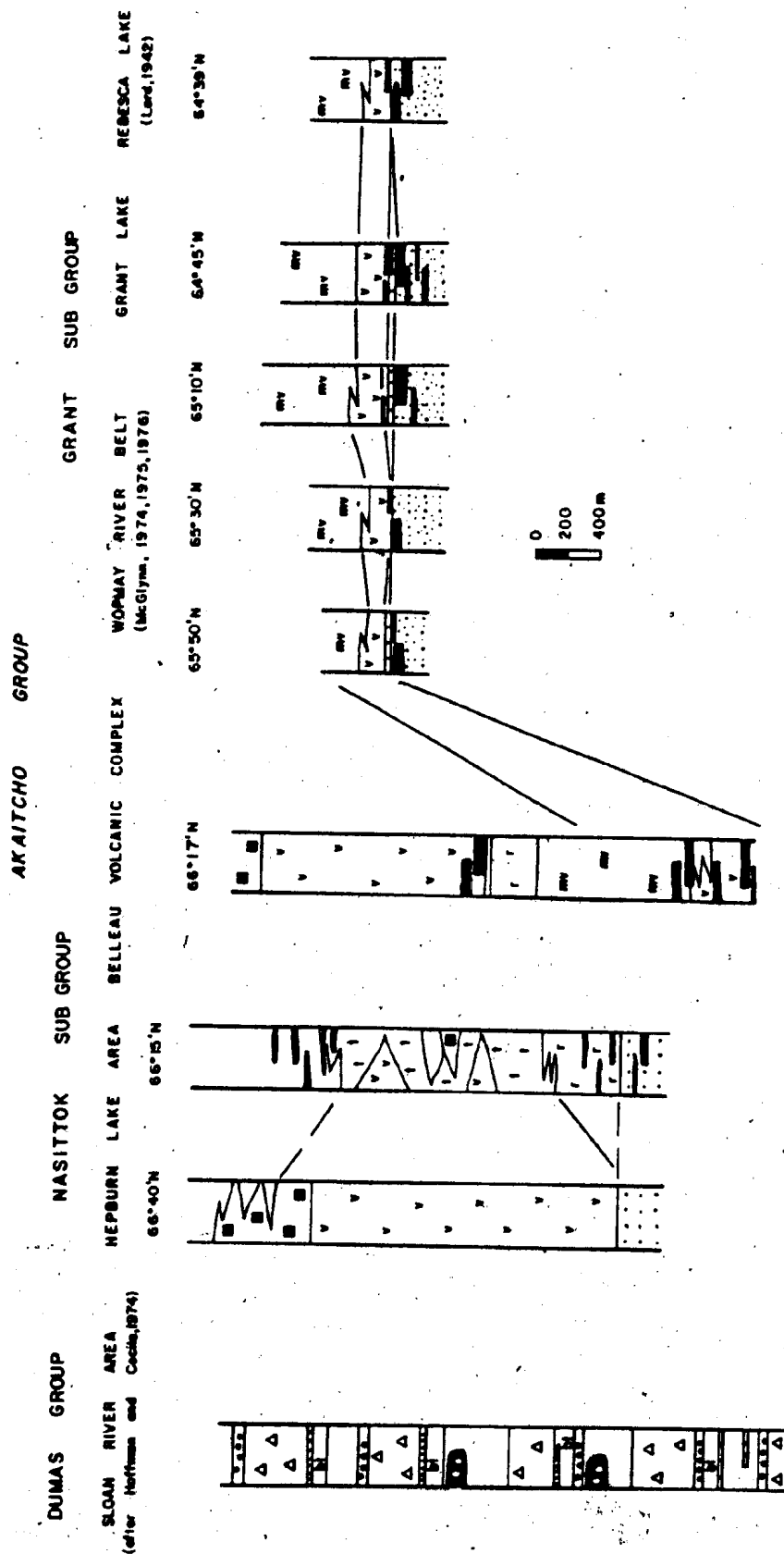
Figure 3.29 Comparative stratigraphic sections of the Grant Subgroup. Note the difference between the Dumas Group (Zone 4) and the Grant and Nasittok Subgroups. No correlation is implied between the Dumas Group and either the Grant or Nasittok Subgroups.

LEGEND

AKAITCHO GROUP LITHOLOGIES

DUMAS GROUP LITHOLOGIES
(absent from Akaitcho Group)

 rhyolite flows and tuffs	 trachybasalt
 basalt tuff	 'golf-ball' porphyry
 massive and pillowed basalt	 conglomerate
 pillowed basalt	 dacite to rhyolite ash-flow tuffs
 gabbro sills	
 porphyritic rhyolite flows and domes	
 dolomite	
 arkose and orthoquartzite	
 siltstone and slate	
 mudstone	



The units thin, and eventually die out to the east. The oldest of these formations is the Drill Formation. It is overlain by the Vaillant Formation, which in turn is overlain by the Stanbridge Formation (Figure 3.3).

Drill Formation

Medium- to thick-bedded, arkosic and pebbly sandstone turbidites interbedded with quartz- or granite-pebble conglomerates and minor black carbonaceous pelite are present in northern Cloos Nappe below volcanic rocks of the Vaillant Formation (Hoffman and Pelletier, 1982) (Figures 3.3, 3.30). Rhyolites and mafic tuffs, flows, and sills are locally interbedded with the sediments.

Mudstone and arkose in Zone 1 beneath the Odjick Formation (Hoffman, 1973) may be a distal facies of the Drill Formation. Hoffman and Pelletier (1982) have suggested that the Drill Formation is lithologically correlative with the Zephyr Formation.

Vaillant Formation

Metavolcanic rocks of the Vaillant Formation are found in Cloos Nappe and Carousel Massif (Hoffman et al., 1978). The Vaillant Formation between Vaillant Lake and 67°30'N consists mainly of calcite-filled amygdaloidal, pillowed basalt (Figure 3.31), pillow breccia, and monolithologic basalt lapilli tuff and breccia (Figure 3.32). Around Vaillant Lake, massive basalt flows are common, as are some probable subaerial flows. The probable subaerial flows have 3 to 6 m thick cores containing calcite-filled

vesicles (Figure 3.33), and 1 to 2 m thick breccia zones between adjacent cores. The breccia zones contain blocks and slightly rounded fragments of basalt similar to the underlying core, but more vesicular. The blocks are strongly hematized and more altered than the core zones. These core and breccia zones resemble typical aa flows (Macdonald and Wentworth, 1953). At Vaillant Lake, the sequence of massive (aa) flows is capped by 5 to 10 m of volcanic conglomerate containing clasts of basalt, siltstone, and sandstone. The conglomerate is overlain by dolomite of the Stanbridge Formation. Massive and pillowed basalt flows occur south of Vaillant Lake to 66°N where the volcanic rocks cease to crop out. Aphanatic rhyolite flows are present locally within the Vaillant Formation. In all outcrops, the Formation has a strong north-trending cleavage. Alteration of the basalts is extensive, even though adjacent and intercalated mudstones are at chlorite grade (lower greenschist). In thin section, the Vaillant basalts have a well-developed trachytic to ophitic texture, a texture observed by Fraser (1974) in Vaillant Formation basalts from Carousel Massif (Figure 3.30). The Vaillant Formation extends as far west as Kikerk Thrust. It thins abruptly east of Cloos Nappe and is present only as a thin layer of basaltic tuff to Kikerk Thrust (Hoffman, 1973). The Vaillant Formation has been correlated on the basis of lithology with the Nasittok Subgroup (Easton, 1981d; Hoffman and Pelletier, 1982) (Figure 3.3).

Stanbridge Formation











Massive to finely-laminated, cherty, commonly stromatolitic dolomite is intercalated with, and overlies, the Vaillant Formation (Figure 3.3). These dolomites are characterized by layers and lenses of quartz grit (Hoffman et al., 1978) (Figure 3.34). The Stanbridge dolomite does not resemble dolomites of Rocknest Formation. The Stanbridge dolomite is, however, lithologically identical to carbonate present in the Nasittok Subgroup, particularly in the Zephyr and the Tuertok volcanic complexes. The stratigraphic sequence of the Drill Formation arkoses, the Vaillant Formation basalts, and the Stanbridge Formation dolomite is similar to the sequence Zephyr Formation, Nasittok Subgroup, and local carbonates present in block B (Figure 3.3). The similarity of the lithologies, and the stratigraphic sequence makes the lithological correlation of the Stanbridge Formation with carbonates in the upper Nasittok Subgroup particularly probable.

3.4 EPWORTH GROUP

Two formations, the Odjick Formation and the Rocknest Formation, constitute the Epworth Group (Hoffman, 1981a). The Rocknest Formation is found only in Zones 1 and 2. The Epworth Group comprises the Coronation continental margin sequence (Hoffman, 1973, 1980c). Near Cloos Nappe, the approximate location of the ancient shelf-slope break, the Epworth Group is between and 2.5 km thick (Hoffman and Pelletier, 1982; Tirrul, 1982).

Figure 3.30. Distribution of the Drill, Vaillant, and Stanbridge Formations near the Zone 2/3 boundary. Data: North of 67°N from Hoffman and Pelletier (1982); 67° to 66°N from Hoffman *et al.* (1981); south of 66°N from St-Onge *et al.* (1982), Fraser (1974), Mursky *et al.* (1970).

LEGEND

-  Muskox Intrusion
-  Hepburn Batholith
-  Epworth and Recluse Groups
-  Akaitcho Group
-  Stanbridge Formation
-  Vaillant Formation
-  Drill Formation
-  reworked Archean granites
-  fault
-  thrust fault

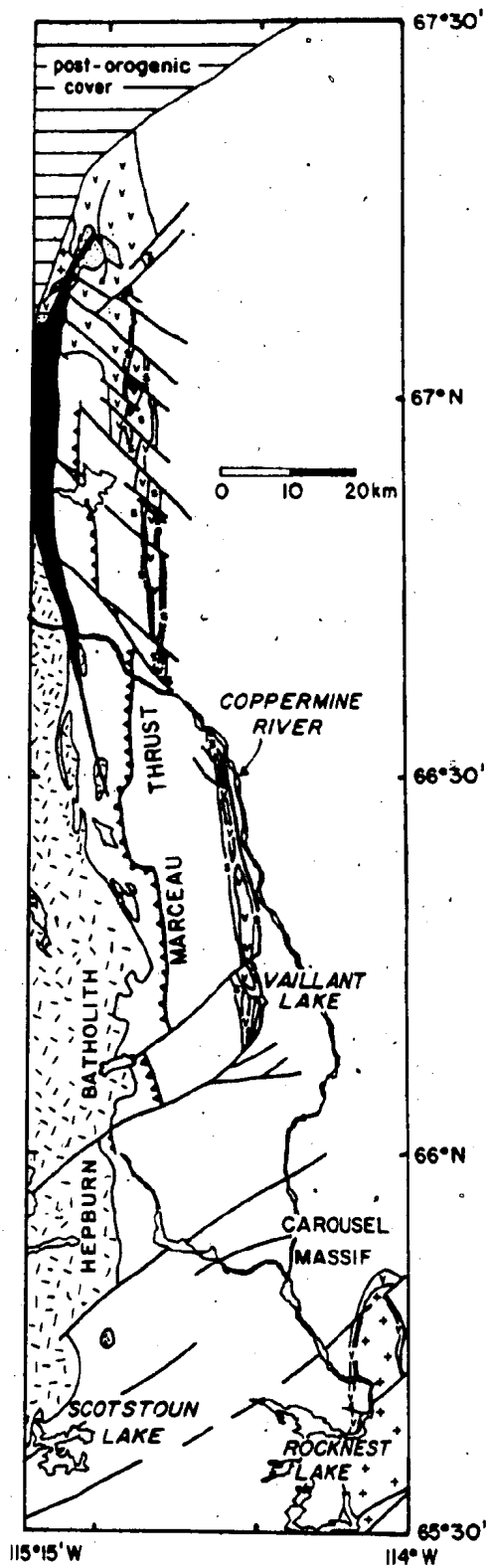


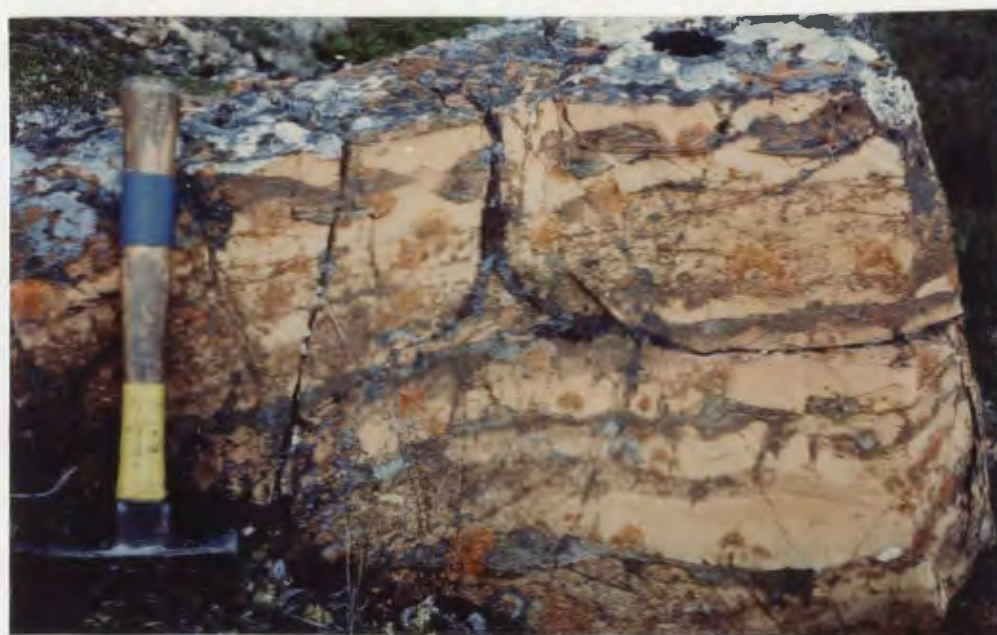
Figure 3.31 Pillowed basalt flow in the Vaillant Formation
near Stanbridge Lake.

Figure 3.32 Fragmental basalt, Vaillant Formation, near
Stanbridge Lake.



Figure 3.33 Vesicles in Vaillant Formation aa basalt flows,
Vaillant Lake.

Figure 3.34 Stanbridge Formation dolomite, Vaillant Lake.



3.4.1 Odjick Formation

External Zone

The Odjick Formation (Hoffman, 1973; Fraser, 1974; Hoffman *et al.*, 1981) in western Zone 2 consists of greenish argillite with thin (centimetre scale) graded beds of white orthoquartzite. A few quartz-pebble conglomerate beds occur at various horizons. Orthoquartzite and pebble-conglomerate beds become more abundant to the east. Paleocurrent studies indicate that the Odjick Formation was derived from the east; i.e. the Slave Province (Hoffman, 1970, 1973). The Odjick Formation is 1 km thick near Kikerk Thrust, and from 1 to 1.5 km thick near Cloos Nappe (Hoffman and Pelletier, 1982; Tirrul, 1982).

Internal Zone

West of Cloos Nappe, the Odjick Formation consists of pelite with occasional 2 to 5 cm thick orthoquartzite beds (Hoffman *et al.*, 1978).

3.4.2 Rocknest Formation

Argillaceous dolomite and stromatolitic dolomite, interpreted to be shallow-water tidal deposits (Hoffman, 1973, 1980; Grotzinger, 1982), form the bulk of the Rocknest Formation. The formation has a maximum thickness of 850 m near Cloos Nappe (the inferred ancient shelf edge) (Grotzinger, 1982).

3.5 AKAITCHO/EPWORTH GROUP RELATIONS

Knowledge of the Akaitcho-Epworth Group stratigraphic relations are critical in establishing the relative age of

the Akaitcho Group within the Wopmay Orogen. The relations are seen in four areas, and all areas indicate that the Akaitcho Group is older than the Epworth Group, and lies stratigraphically below it.

3.5.1 Area 1








Eight kilometres northwest of Hepburn Lake, metavolcanics of the Tuertok volcanic complex are overlain by 1 km of biotite-grade, east-facing Aglerok Formation metapelites (Figure 3.35). The metapelites grade upward into a 250 to 400 m thick unit of purple-tinged, massive, blocky-weathering siliceous siltstone. The metasiltstone changes upsection over 100 m into a greenish metapelite containing the distinctive 2 to 5 cm thick orthoquartzite beds diagnostic of the Odjick Formation west of Cloos Nappe (Hoffman et al., 1978). The presence of contorted fine-bedding, well-developed metamorphic minerals, and the distinctive cleavage/bedding pattern of the greenish metapelite all indicate that the pelite is Odjick Formation. The Odjick Formation pelites are east-facing, as are the underlying Aglerok Formation pelites. The staurolite and andalusite isograds transect the contact at a slight angle (Figure 3.35). Thus, any movement along this contact would of necessity be pre-metamorphic. The two formations appear to be concordant, if not conformable. However, a cryptic disconformity cannot be ruled out.

3.5.2 Area 2






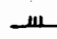
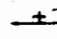
Similar relationships were also found 20 km south-

Figure 3.35 Geological sketch map showing Akaitcho/Epworth Group relationships 10 km NNE of Hepburn Lake.

LEGEND

-  Squatarola gabbro complex
-  Rib granite (post-metamorphic pluton)
-  Headnet granite (syn-metamorphic pluton)
-  Epworth Group - Odjick Formation
- pelite with orthoquartzite interbeds
Akaitcho Group
-  siliceous siltstone (Aglerok Formation)
-  olive pelite (Aglerok Formation)
-  marble, orthoquartzite
- | | | | |
|----------------------|---|---|-------------------|
| p
t
s

r | pillowed basalt
basaltic tuffs
gabbro sills

rhyolite | } | Nasittok Subgroup |
|----------------------|---|---|-------------------|
-  bedding, tops known, unknown  fault
- Metamorphic Isograds (mark on high T side)
-  staurolite-anthophyllite - in mafic units only
-  staurolite
-  andalusite
-  sillimanite
-  granitic pods

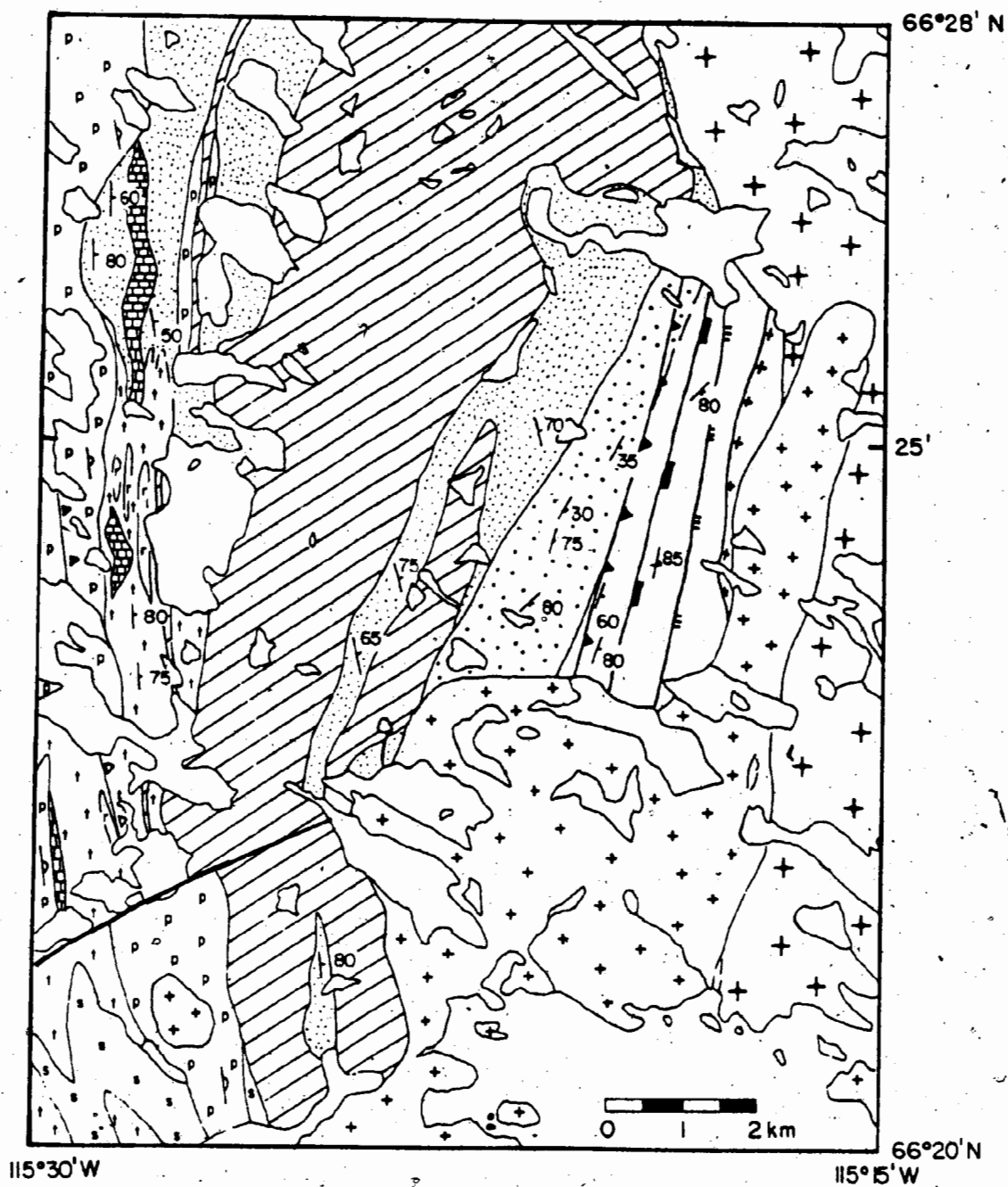


Figure 3.36 Geological sketch map showing Akaitcho/Epworth Group relationships 20 km SSE of Hepburn Lake. Contact indicated by A/E.

LEGEND



biotite-orthopyroxene gabbro sill



Rib granite (post-metamorphic pluton)



foliated Hepburn granodiorite dyke



Epworth Group (E) - Odjick Formation
- pelite with orthoquartzite interbeds

Akaitcho Group (A)



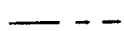
Tallerk gabbro sills



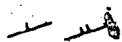
olive pelite (staurolite bearing
in map area)(Aglerek Formation)

p, t

basalt, pillowed, tuffs - Nasittok Subgroup



geological contact, known, approximate



bedding, tops known, unknown



fault



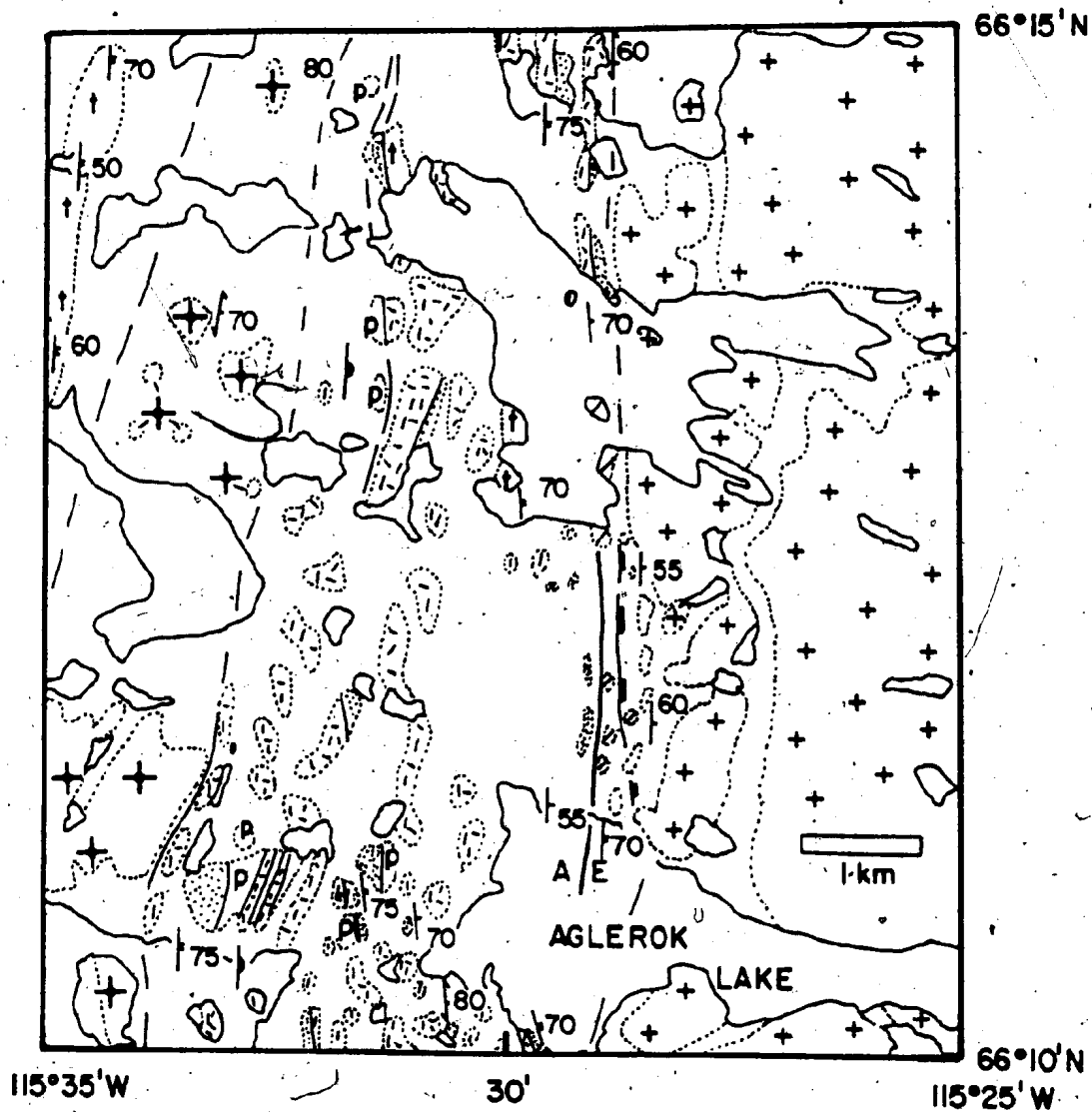
cleavage



pillow trend, with tops



andalusite isograd, mark on high T side



southwest of Hepburn Lake. East-facing metapelites of the Aglerok Formation, intruded by Tallerk gabbro sills, are overlain by east-facing metapelites of the Odjick Formation. Outcrop is poor in this area, the closest outcrops of Akaitcho and Epworth Groups being 300 m apart (Figure 3.36). The overall stratigraphy is similar to the sequence preserved northwest of Hepburn Lake.

In both Areas 1 and 2, it is thought that a thrust contact between the two groups is unlikely because:

- i) there is no discordance between any major structures along the contact; ii) the relationship in both areas is observed at the same stratigraphic horizon over several kilometres; and iii) both groups face in the same direction. None of these features are found associated with other thrusts in the area (block B).

3.5.3 Area 3

In northern Cloos Nappe, conglomerate and arkose of the Drill Formation underlie the Vaillant Formation basalts. Hoffman and Pelletier (1982) describe one area where the Odjick Formation disconformably overlies the Vaillant Formation.

3.5.4 Area 4

In Carousel Massif, metavolcanic rocks of the Vaillant Formation are interbedded with orthoquartzite of the lower Odjick Formation (Fraser, 1974; St-Onge et al., 1982).

3.5.5 Summary

The relationships observed in Areas 3 and 4 confirm the

observations made in Areas 1 and 2, but only if the lithological correlation of the Vaillant and Standbridge Formations with the Akaitcho Group is valid. At present, this correlation seems reasonable. In addition, there is some geochemical evidence (Chapter 4) that is consistent with the Akaitcho Group being overlain by the Epworth Group. Pelites from the upper Aglerok Formation have distinctive REE patterns. To date, this distinctive REE pattern has only been observed in one other unit, the lower Odjick Formation. The geochemical evidence is only consistent with the field observations, and does not prove them. Until evidence to the contrary is forthcoming, the Akaitcho Group is most reasonably interpreted to underlie the Epworth Group.

3.6 SNARE GROUP

The term Snare Group was introduced by Lord (1942) for metasedimentary and metavolcanic rocks preserved west of the Bear-Slave boundary, and includes rocks located on both sides of the Wopmay Fault. Although he did not designate a type area, it is evident that Lord (1942) considered metasedimentary rocks in the vicinity of Ingray and Mattberry Lakes to represent typical Snare Group lithologies.

As discussed in Chapter 2, the term Snare Group has been used mainly in southern Wopmay Orogen (Table 2.2). In the north, a different stratigraphic nomenclature has been used, with the terms Epworth, Recluse, Akaitcho, and Dumas Groups being applied to rocks west of the Bear-Slave boundary and adjacent to the Wopmay Fault Zone (Table 2.2). It

has been established that some rocks previously assigned to the Snare Group can be correlated with Dumas and Akaitcho Groups (Easton, 1981c, d). However, until the area between known Epworth Group strata and the type area of the Snare Group is mapped, correlations between the Akaitcho, Recluse, Epworth, and Dumas Groups and the Snare Group cannot be made.

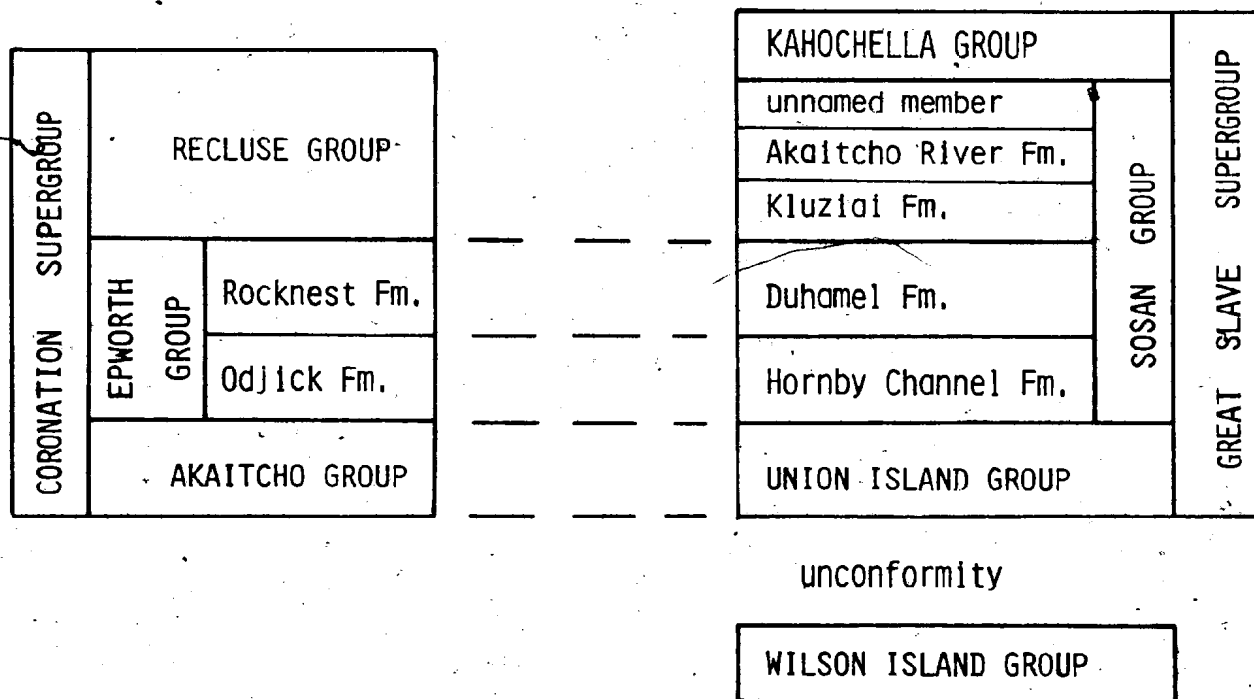
Near Basler Lake, andesites or basalts are present in association with conglomerate and quartzite in the Snare Group near the Snare/Archean unconformity (McGlynn, 1962). The overall stratigraphic sequence in this area is similar in some ways to the Vaillant Formation in the Carousel Massif and the Drill/Vaillant Formations at the northern end of Gloos Nappe. If these volcanic rocks are part of the Akaitcho Group, then they serve to emphasize the complex facies relationships likely to be present in the Snare Group.

3.7 REGIONAL CORRELATION

To date, the evidence indicates that the Akaitcho Group is older than the Epworth Group, and that the Akaitcho/Epworth contact is probably conformable. On this basis alone, the Akaitcho Group is part of the Coronation continental margin.

As mentioned in Chapter 2, the stratigraphic units in the Wopmay Orogen can be correlated with the stratigraphic sequences in the Athapuscow Aulacogen and the Kilohigok Basin (Tables 2.1, 3.1). Two periods of rift-related

Table 3.1 Lithological correlation of strata between the Wopmay Orogen and the Athapuscow Aulacogen. Only the lower Coronation and Great Slave Supergroups are illustrated. (after Hoffman, 1968, 1973, 1981a).



volcanism are preserved in the Athapuscow Aulacogen (Hoffman et al., 1977). The older, metamorphosed Wilson Island Group has been interpreted as an early, failed rifting event in the aulacogen (Hoffman et al., 1977). The Union Island Group forms the basal part of the Great Slave Supergroup and underlies the Sosan Group. The lower Sosan Group is correlative with the Epworth Group (Hoffman, 1973, 1981a) (Table 3.1). The Union Island Group is presumed to date from the initial formation of the aulacogen (Hoffman et al., 1977). The chemistry of the Union Island basalts differs from that of the Akaitcho Group (Easton, 1981d), but only limited data are available for the Union Island Group (Goff and Scarfe, 1978). Although the Union Island Group represents a rifting event in roughly the same stratigraphic position as the Akaitcho Group, the two groups may not be contemporaneous, and hence, not time-correlative. Nevertheless, it is significant that a rift-related sequence is present in both areas. No rifting sequence is present in the Kilohigok Basin.

3.8 SUMMARY: STRATIGRAPHIC CONSTRAINTS ON THE DEVELOPMENT OF THE AKAITCHO GROUP

The stratigraphy of the Akaitcho Group, and the facies relationships between the various lithologies present in the Akaitcho Group aid in the understanding of the depositional history and tectonic setting of the Akaitcho Group as outlined below.

First, there is the possibility that the Akaitcho Group was underlain by, and certainly was adjacent to, a continental terrane. This is indicated by the voluminous arkoses of the Zephyr Formation and the granite cobble-bearing conglomerates in the Aglerok Formation. The Sitiyok Complex may be a remnant of basement to the Akaitcho Group. In addition, the Vaillant Formation in northern Cloos Nappe and Carousel Massif were deposited on Archean granites.

Second, there is a lower volcanic sequence of uncertain thickness that lacks rhyolites or rocks of intermediate composition. Abundant garnet in these rocks suggests iron-rich compositions, possibly indicating fractionated basalts. This lower volcanic sequence is separated from the voluminous basalts of the Nasittok Subgroup by a thick sequence of arkoses. In addition, the Nasittok Subgroup volcanic complexes in block B (Sinister, Tuertok, Kapvik, and Havant) are oriented on a northerly trend. This linear trend is primary, because the facies can be traced out between complexes (Figures 3.11, 3.15). This linearity may be due to a rift-related fault or basin margin. The basalt edifices are capped by rhyolite volcanic centres; and the arkoses intruded by rhyolite sills. The rhyolites were erupted after the bulk of the basaltic volcanism, with no intermediate composition rocks being present, and with high felsic/mafic ratios. The rhyolites are too voluminous to be due to fractionation from the basalts, and can only be crustal melts. Volcanism waned in the upper Akaitcho Group, and is

represented by the Tallerk sills. The association of bimodal volcanics, which change in chemistry with time, and arkoses suggests a rift-setting (Basaltic Volcanism Study Project, 1981).

Third, the sedimentary rocks overlying the Nasittok Subgroup volcanic complexes consist of a pelite sequence. These pelites were derived from a source region similar to the volcanic rocks, but granite-cobble conglomerates intermixed with the pelites indicate a mixed, continental-volcanic, source terrane. The pelites, and the Tallerk sills, are overlain by pelites, interpreted to be continental-rise facies, of the Epworth Group indicating foundering of the area after, or during, Aglerok Formation deposition.

All of the above-mentioned relationships are consistent with the Akaitcho Group being deposited in a continental rift.

The lack of intermediate-composition volcanic rocks, and the paucity of pyroclastic rocks in the majority of the Akaitcho Group volcanic centres argues against the volcanic rocks being arc-related, either a continental or oceanic arc. Although the Nasittok Subgroup basalts could be flood basalts deposited in a continental basin, the basin was mainly subaqueous, and the basin foundered in order to accomodate strata of the Aglerok and Odjick Formations. Thus, the basin was getting deeper, if not larger, with time. Finally, the position of the Akaitcho Group beneath

the inferred passive-margin rocks of the Epworth Group suggests that the Akaitcho Group strata were deposited in a rift which preceeded development of an Atlantic-type continental margin.

CHAPTER 4

GEOCHEMISTRY

4.1 INTRODUCTION

Three important observations were made early in the study of the Akaitcho Group concerning the geochemistry of the extrusive rocks of the Group (Easton, 1980, 1981d). These observations still hold after further work.

1) The first observation was based originally on field work, and was later confirmed by major element analyses, namely that the Akaitcho Group extrusive rocks are bimodal (Figure 4.1). Figure 4.1 shows only flow rocks. Some tuffaceous rocks, which in part may be reworked or volcanoclastic sediments, do fall in the range of intermediate rocks, but these rocks are clearly recognizable in the field. No flow rock has been found with intermediate SiO_2 values.

2) The second observation is shown in Figure 4.2. Namely, two types of rhyolites are present in the Akaitcho Group: a high- SiO_2 , low-Zr type and a lower- SiO_2 , high-Zr type (Figure 4.2). Further work has shown that this subdivision is stratigraphic rather than a simple Si/Zr difference. Aphanitic, commonly tuffaceous rhyolites from the base of the Kapvik complex are high- SiO_2 , low-Zr rocks. Porphyritic rocks from the Okrark sills and the other volcanic complexes have lower SiO_2 and higher Zr contents. However, some sparsely-porphyritic rocks from these complexes do have high- SiO_2 and high-Zr contents. The lower Kapvik rhyolites

are tuffs or pyroclastic flows, whereas the other rhyolites are mainly domes and flows. With transport distance from a vent, tuffaceous volcanic rocks commonly show an increase in SiO_2 content because heavier, non-glassy material is lost by settling. If zircon is concentrated in a crystalline phase that settles, this mechanism would also produce lower Zr contents. Thus, it is suspected that the Kapvik rhyolites are chemically distinct in Si and Zr content because of their tuffaceous nature. REE patterns for both types of rhyolite are similar (Figure 4.3), suggesting a common origin.

3) The third observation is that there are two major basalt types. One type with affinities to recent continental tholeiites and a second type with affinities to type II ocean tholeiites (Figures 4.4a, 4.4b, 4.5). The basalts are distinguished by their major, trace, and REE characteristics. It was also observed that the oceanic tholeiites occur high in the stratigraphic section.

The important point to be made about these observations is that not only do they have a bearing on the tectonic setting of the Akaitcho Group - namely, they are consistent with the Akaitcho Group being a rift-related sequence - but that the geochemistry is corroborated by field data.

Bimodality was originally observed in the field (Hoffman et al., 1978; Easton, 1980). The two types of rhyolite occur at different stratigraphic horizons. And, although the two types of basalts cannot be distinguished by eye in

Figure 4.1 Plot of SiO_2 versus frequency for flow rocks of the Akaitcho Group (Ipiutak and Nasittok Subgroups). Note the composition gap between 56% and 67% SiO_2 .

Figure 4.2 Plot of Zr versus SiO_2 for Akaitcho Group rhyolites. Note the lower Zr and generally higher SiO_2 content of the lower Kapvik rhyolites. Low Zr values are also present in lower Kapvik rhyolites for which major element analyses are not available. Figure includes both Okrark sills and Nasittok Subgroup rhyolites.

- ◇ rhyolite flows and tuffs, lower Nasittok Subgroup (i.e. lower Kapvik rhyolites)
- △ porphyritic rhyolite flows, upper Nasittok Subgroup
- ▲ aphanatic rhyolite flows, upper Nasittok Subgroup
- Grant Subgroup
- ▽ Vaillant Formation

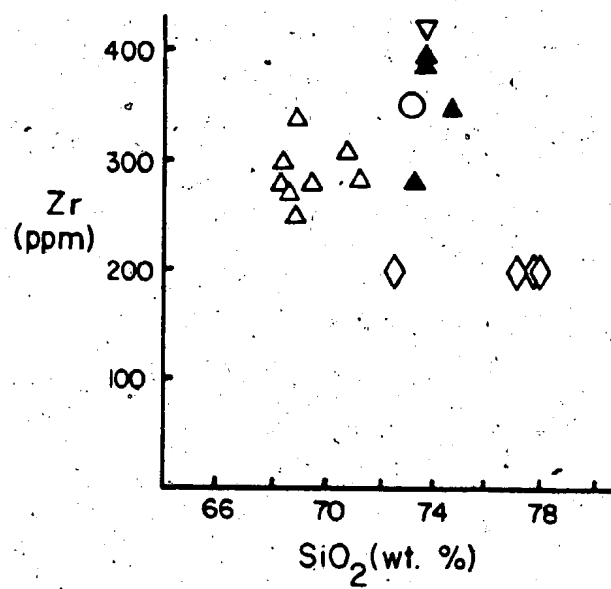
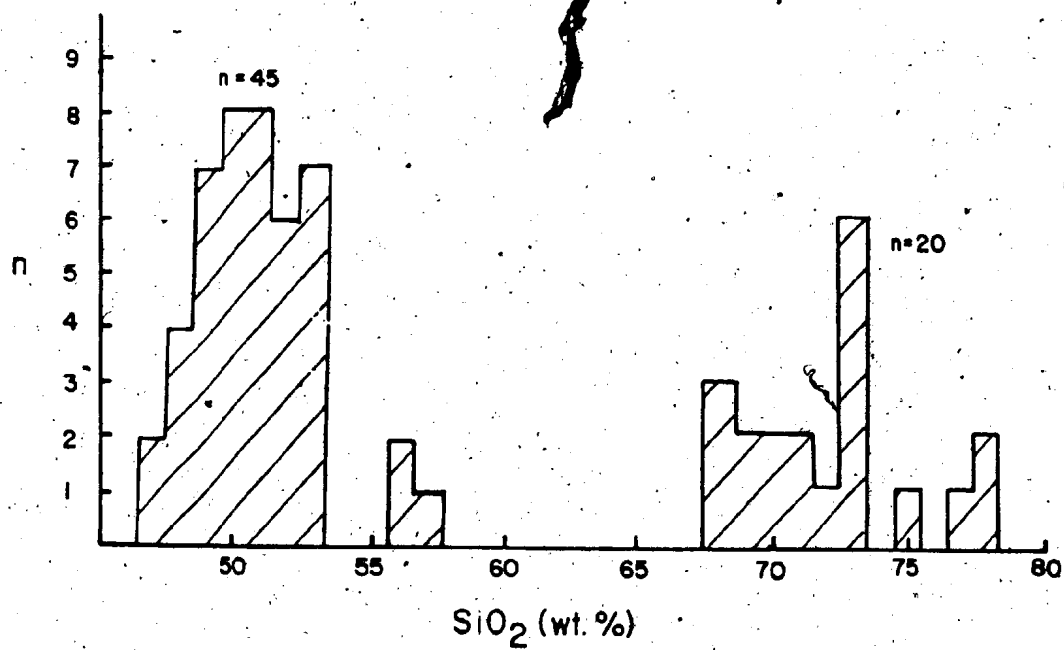


Figure 4.3 Chondrite-normalized plot of REE for lower Kapvik rhyolites. Note overlap with field of Nasittok Subgroup rhyolites and Okrark sills (8 porphyritic rhyolite flows and sills). Okrark sills and Nasittok Subgroup rhyolites cannot be distinguished on the basis of REE abundances.

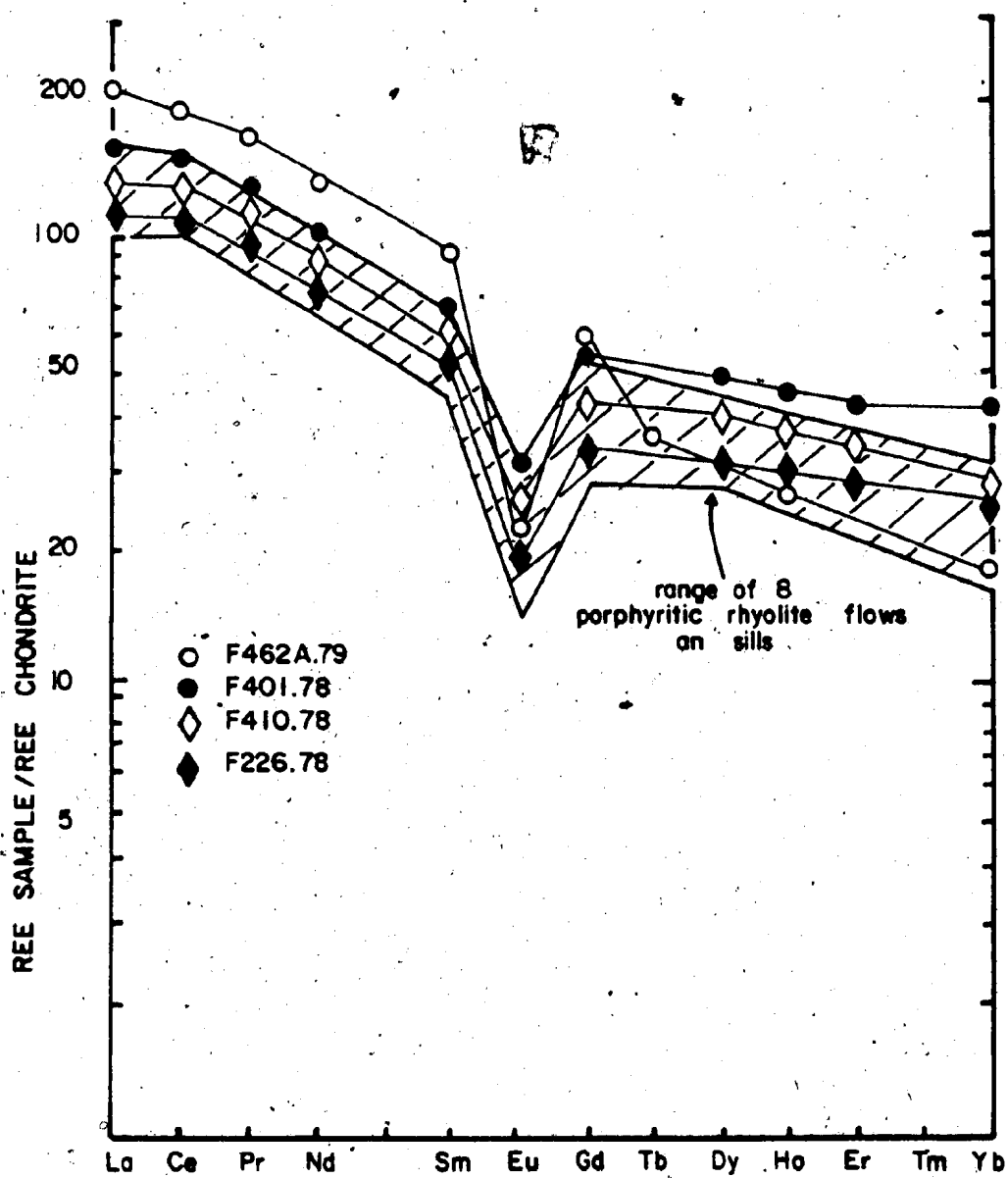


Figure 4.4 a) $\text{Ti-K}_2\text{O}_5\text{-P}_2\text{O}_5$ plot for Ipiutak and Nasittok Subgroup basalts (open triangles and crosses respectively), and Tallerk sills (x). Fifty-two (52) samples are represented. Fields after Pearce et al. (1975).

b) Ti/100-Zr-Yx3 plot for Ipiutak and Nasittok Subgroup basalts (open triangles and crosses respectively), and Tallerk sills (x). Fifty-two (52) samples are represented. Fields after Pearce and Cann (1973). Abbreviations: W.P.B.-within-plate basalts; O.F.B.-ocean-floor basalts. An additional 60 samples for which Ti, Y, and Zr values are available fall in the same area as the 52 samples shown.

◆ Archean mantle, bulk-earth values of Sun and Nesbitt (1977)

◇ Chondritic values, Sun and Nesbitt (1977)

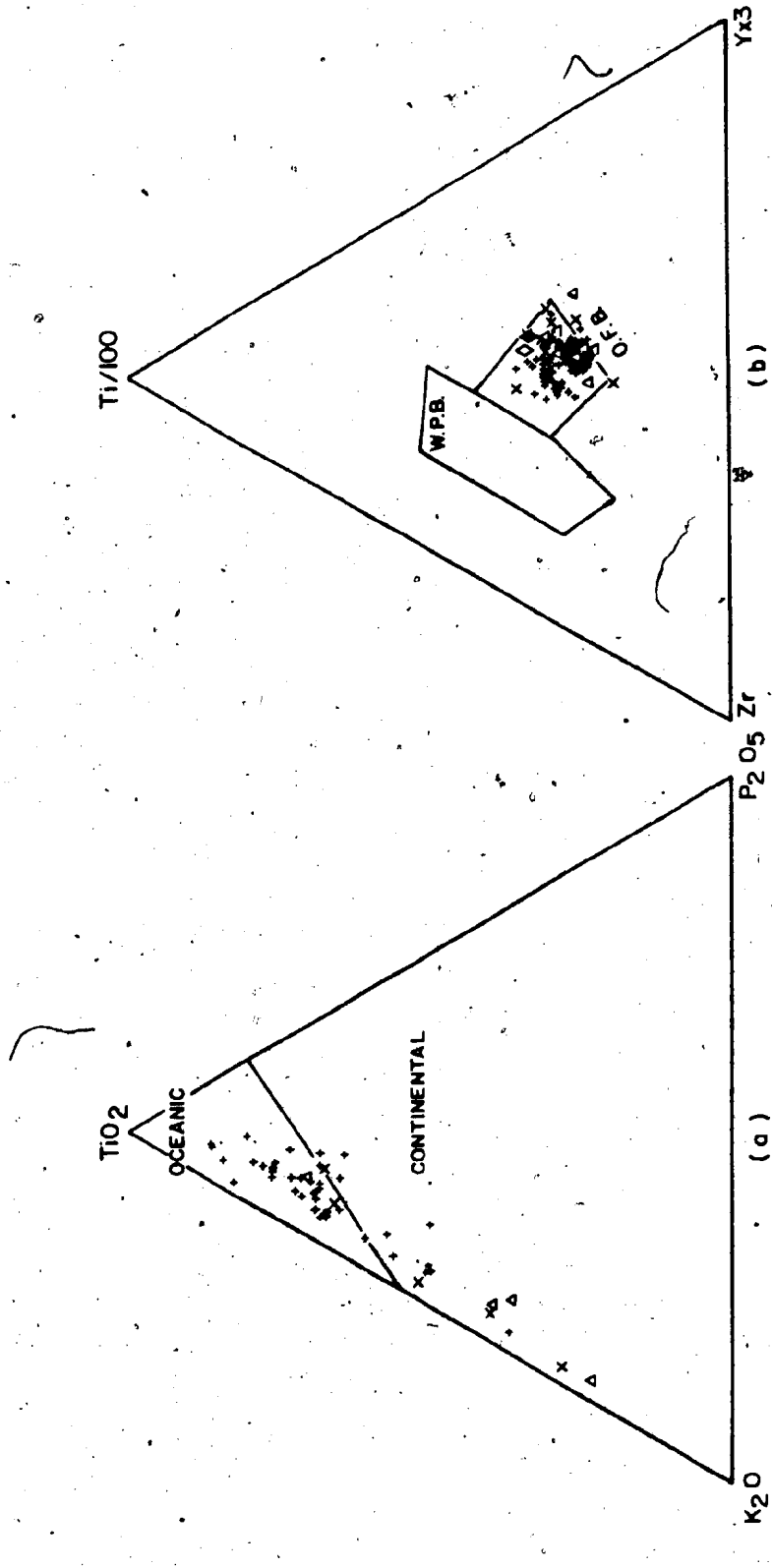
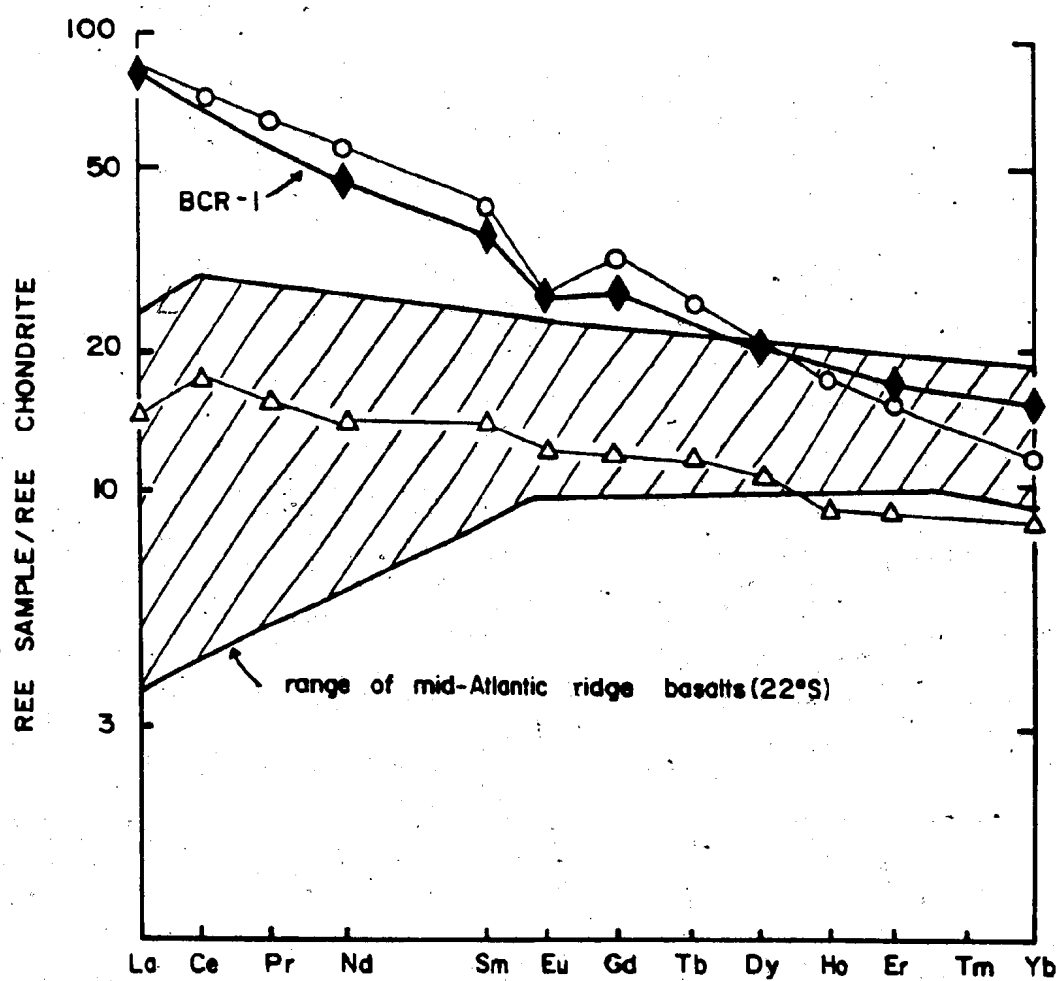


Figure 4.5 Chondrite-normalized REE plot showing REE patterns of oceanic tholeiites (range of mid-Atlantic ridge at 22°S; Bryan et al., 1976) and a typical continental tholeiite (BCR-1, Columbia River Basalt, recommended values of Abbey, 1980). An oceanic tholeiite from the Tuertok volcanic complex (F511.80, open triangles) and a continental tholeiite from the Tuertok volcanic complex (F484.80, open circles) are shown for comparison.



the field, the geochemical changes observed in the basalts are related to stratigraphic position. The above interpretations are supported by the correspondence between field observations and geochemical data.

The conclusions in this chapter are based on the results of analysis of 496 samples from Zone 3 for trace elements, of which 150 samples were analyzed for the major elements, and 175 samples were analyzed for the rare-earth elements. Of these, 94 major element, 336 trace element and 118 REE analyses are from volcanic and sedimentary rocks of the Akaitcho Group. These figures exclude duplicate and test analyses. The other rocks examined from Zone 3 were analyzed in order to characterize the geochemistry of the Akaitcho Group, although not all analyses of these other rocks are discussed in this chapter.

4.2 EXTRUSIVE ROCKS

4.2.1 Basalts

There are two basalt types present in the Akaitcho Group: one type with affinities to recent continental tholeiites and a second type with affinities to type II ocean tholeiites (herein referred to as oceanic tholeiites) (Basaltic Volcanism Study Project, 1981). The difference between these basalt types are seen in the major, trace, and rare earth elements (Table 4.1), but are best seen in the REE and some of the 'immobile' trace elements. Various trace element plots give varying results for the tectonic setting and discrimination of the Akaitcho Group basalts. For

example, in Figure 4.4a, the $\text{TiO}_2\text{-K}_2\text{O-P}_2\text{O}_5$ plot separates the Akaitcho Group basalts into continental and oceanic tholeiitic types. The results from this plot agree with the REE data.

However, in a Ti-Y-Zr plot (Figure 4.4b) all the Akaitcho Group basalts plot in the ocean floor basalt field. This can be explained by high degrees of partial melting in the source region for the continental and the type II ocean tholeiites. If pyroxene was a residual phase, or if pyroxene fractionation had occurred after melting, the continental tholeiites would plot in the within-plate basalt field. The Ti-Y-Zr abundances in the Akaitcho Group rocks are similar to those for modern oceanic tholeiites and chondrites (Sun and Nesbitt, 1977) and estimates for Archean mantle (Sun and Nesbitt, 1977) (Figure 4.4b), as would be expected if the basalts represented mantle-derived partial melts. The implication of this result is that the differences between the continental and oceanic tholeiites in the Akaitcho Group is not the result of different mantle source regions.

No alkaline rocks are present in the Akaitcho Group. On an alkali-silica diagram all Akaitcho Group basalts plot in the sub-alkaline field (Figure 4.6). Ratios of Y/Nb (Figure 4.7) for Akaitcho Group rocks are greater than 2, usually 5 to 7, again indicating a tholeiitic character.

In order to look at relations between stratigraphic position versus basalt composition, it is best to look at

Figure 4.6 Alkali-silica diagram for the Ipiutak and Nasittok Subgroup basalts (open triangles and crosses respectively), and Tellerk sills (x). Heavy diagonal line is the division between alkaline and tholeiitic rocks of Macdonald and Katsura (1964). The thin line is the dividing line of Irvine and Baragar (1971). Samples that lie between the two lines have either abnormally high Na, or high K contents.

Figure 4.7 Plot of Y/Nb ratios for Akaitcho Group lavas. Vaillant Formation lavas from Vaillant Lake (V.L.) are similar to other Akaitcho Group basalts. Vaillant Formation lavas from the Coppermine River (C.R.) may be hawaiites or basaltic andesites, hence their low Y/Nb ratios. Basaltic rocks from other areas are shown for comparison. Y/Nb for alkaline basalts is less than 1 for 'within-plate' basalts and less than 2 for ocean-floor basalts. Y/Nb ratios for tholeiitic rocks is greater than 2 for 'within-plate' basalts and greater than 3 for ocean-floor basalts. (OF - ocean-floor; OI - oceanic island; C - continental). Figure adapted from Pearce and Cann (1973).

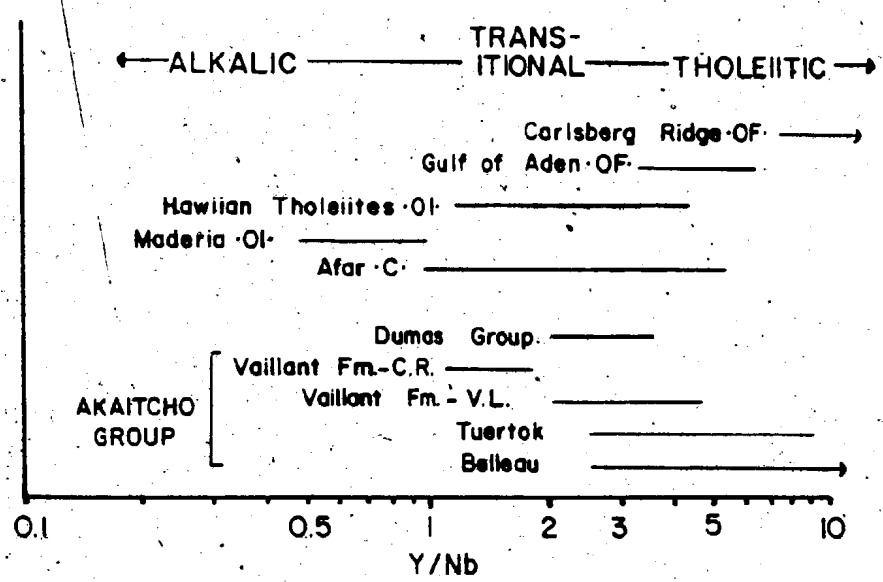
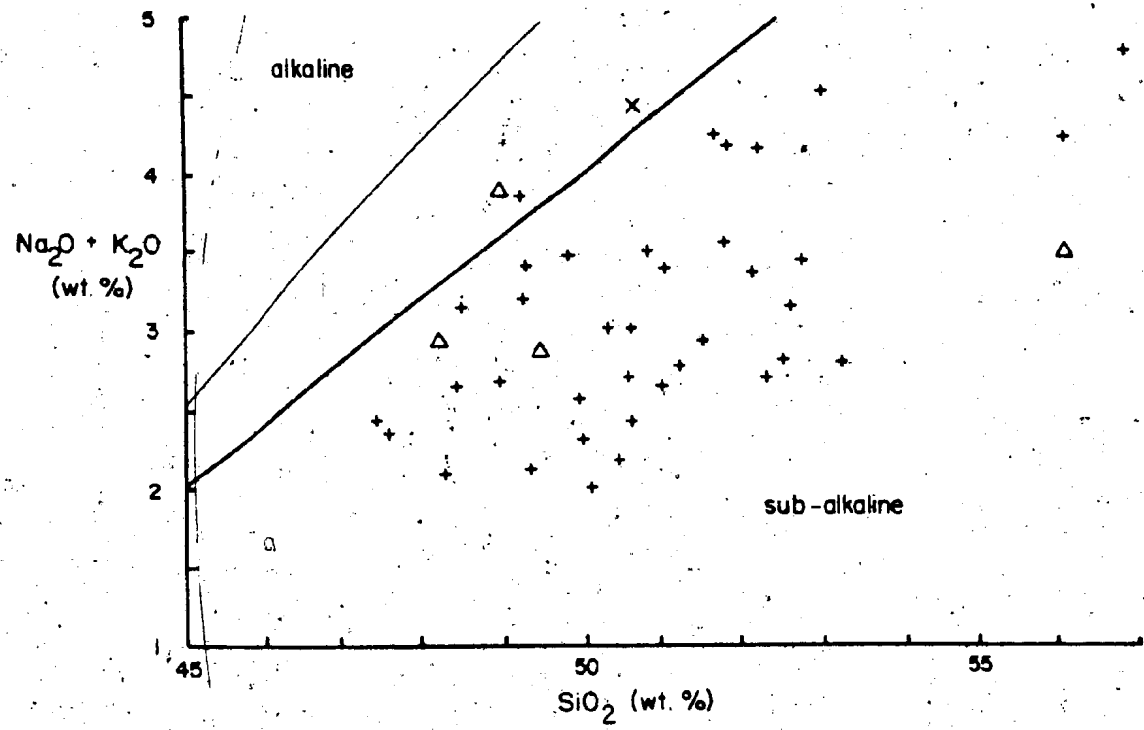


Table 4.1 Representative chemical analyses of Akaitcho Group basalts. Major elements in wt.%, trace and rare-earth elements in ppm.

Tuertok volcanic complex					
	Unit 3 F500.80	Unit 4 F498A.80	Unit 5 F450.80	Unit 6 F412B.80	Unit 8 F512.80
SiO ₂	46.8	46.2	50.4	49.7	49.6
TiO ₂	1.75	0.56	1.20	1.35	1.43
Al ₂ O ₃ ^t	15.6	20.6	13.2	14.2	13.2
Fe ₂ O ₃ ^t	10.34	8.49	12.54	12.69	13.62
MnO	0.18	0.12	0.19	0.20	0.22
MgO	8.69	6.17	7.06	6.84	6.65
CaO	10.00	10.59	9.05	11.22	8.95
Na ₂ O	2.76	2.16	3.17	1.65	2.30
K ₂ O	0.27	0.35	0.29	0.48	1.00
P ₂ O ₅	0.07	0.06	0.10	0.16	0.12
L.O.I.	3.33	3.45	2.18	2.00	1.86
Total	99.79	98.75	99.38	100.49	98.95
Nb	1	2	5	6	5
Zr	40	45	90	100	133
Y	20	17	32	36	46
Sr	129	235	194	159	108
Rb	5	6	4	15	8
Pb	7	0	5	9	9
Zn	98	52	98	104	76
Cr	407	95	79	94	42
V	251	186	336	310	333
Ba	69	59	68	100	237
Y/Nb	20	8.5	6.4	6	9.2
La	5.1	4.4	6.7	13.8	7.2
Ce	16.3	10.4	18.7	34.4	18.8
Pr	2	1.1	2.2	4.0	2.6
Nd	11.2	5.7	10.9	19.9	11.8
Sm	3.8	1.7	3.4	5.3	3.4
Eu	1.5	0.8	0.9	1.5	1.1
Gd	4.7	1.6	3.9	6.4	4.0
Dy	6.5	2.4	4.6	5.3	4.6
Ho	0.8	0.4	0.8	0.7	1.1
Er	2.4	1.0	2.5	2.9	2.8
Yb	2.4	0.9	2.4	2.1	3.5
ΣREE	57.7	31.3	58.0	97.0	61.6
La/Yb	2.1	4.9	2.8	6.6	2.1
Ce/Yb	6.8	11.6	7.8	16.4	5.4

Table 4.1 continued

	Tuertok volcanic complex			
	Unit 9	Unit 11	Unit 11	Sitiyok
	F528.80	F486.80	F488.80	Gneiss R117.79
SiO ₂	50.2	49.0	51.6	47.8
TiO ₂	1.54	2.51	1.57	3.14
Al ₂ O ₃	13.1	13.6	12.3	10.4
Fe ₂ O ₃ ^t	14.58	14.48	13.73	22.62
MnO	0.22	0.20	0.19	0.35
MgO	6.49	4.64	6.98	2.90
CaO	6.41	8.95	8.91	8.68
Na ₂ O	3.61	2.19	2.45	1.09
K ₂ O	0.43	0.71	0.30	0.60
P ₂ O ₅	0.14	0.45	0.15	1.40
L.O.I.	2.07	2.07	1.90	0.26
Total	98.79	98.80	100.00	99.24
Nb	8	10	8	25
Zr	122	216	130	440
Y	45	51	45	165
Sr	88	254	236	45
Rb	10	17	6	7
Pb	11	8	4	10
Zn	123	133	104	227
Cr	20	82	35	0
V	382	293	356	66
Ba	119	308	140	63
Y/Nb	5.6	5.1	5.6	6.6
La	9.0	23.0	10.6	59.90
Ce	22.9	56.6	29.0	150.60
Pr	3.0	6.6	3.5	19.9
Nd	13.2	29.2	17.0	94.2
Sm	4.0	7.1	4.9	26.8
Eu	1.05	2.3	1.7	7.5
Gd	4.8	7.1	5.7	30.8
Dy	4.9	6.6	6.3	29.7
Ho	1.0	1.4	1.2	5.9
Er	3.3	3.5	3.4	14.3
Yb	3.4	2.5	2.4	10.4
ΣREE	71.4	147.0	86.0	361.3
La/Yb	2.7	9.2	4.4	5.8
Ce/Yb	6.7	22.6	12.1	14.5

Table 4.1 continued

	Sitiyok Dyke F609A.80	Sitiyok Dyke R122.79	Ipiutak Subgroup →		
			F569.80	F697.79	F716.79
SiO ₂	47.2	47.8	49.1	50.6	
TiO ₂	0.93	0.64	0.99	2.12	
Al ₂ O ₃	13.7	15.0	13.6	12.6	
Fe ₂ O ₃ ^t	11.76	10.37	13.18	16.58	
MnO	0.18	0.17	0.21	0.26	
MgO	10.09	9.92	7.51	6.08	
CaO	10.95	9.79	11.75	8.89	
Na ₂ O	2.08	1.81	2.05	2.05	
K ₂ O	0.79	1.99	0.42	0.63	
P ₂ O ₅	0.16	0.06	0.10	0.24	
L.O.I.	1.59	2.91	0.77	0.46	
Total	99.43	100.46	99.68	100.51	
Nb	5	0	4	3	3
Zr	64	37	60	153	136
Y	25	21	27	63	56
Sr	105	72	132	150	132
Rb	45	197	10	10	5
Pb	9	8	37	7	85
Zn	87	100	104	117	158
Cr	93	357	88	23	51
V	262	239	294	482	424
Ba	318	103	92	136	107
Y/Nb	5	-	6.8	21	19
La		7.6			18.3
Ce		14.5			42.4
Pr		1.8			5.7
Nd		7.1			25.2
Sm		2.3			7.1
Eu		0.4			1.8
Gd		1.8			7.7
Dy		3.7			8.7
Ho		0.1			1.5
Er		1.7			4.4
Yb		1.8			3.6
ΣREE		43.2			127.4
La/Yb		4.2			5.1
Ce/Yb		8.1			11.8

Table 4.1 continued

	Belleau volcanic complex				
	Lower	Lower	Upper	Upper	Upper Gabbro
	F259.78	F262.78	F292C.78	F301.78	F289B.78
SiO ₂	50.0	51.3	45.7	48.86	46.71
TiO ₂	1.32	1.86	1.04	0.98	0.81
Al ₂ O ₃	13.8	13.1	16.4	15.85	16.7
Fe ₂ O ₃ ^t	12.83	14.99	11.63	10.78	10.27
MnO	0.23	0.22	0.14	0.17	0.14
MgO	6.90	5.29	8.06	7.39	7.94
CaO	9.57	7.97	10.89	9.98	10.26
Na ₂ O	2.24	2.65	2.0	2.0	2.2
K ₂ O	0.48	0.66	0.44	0.34	0.34
P ₂ O ₅	0.14	0.22	0.07	0.10	0.05
L.O.I.	2.10	1.65	2.59	3.44	3.29
Total	99.61	99.91	98.96	99.89	98.71
Nb	9	9	7	7	6
Zr	128	164	78	70	56
Y	37	45	18	22	24
Sr	202	176	269	228	166
Rb	18	18	17	10	10
Pb	2	6	2	28	0
Zn	113	123	128	280	101
Cr	37	19	11	130	283
V	282	339	84	218	206
Ba	109	170	210	75	56
Y/Nb	4.1	5	2.6	3.1	6
La	16.9	16.6	4.4	4.9	3.3
Ce	42.1	42.4	13.0	13.5	9.9
Pr	4.8	4.5	2.0	1.5	1.0
Nd	22.7	22.5	8.9	7.8	5.9
Sm	6.3	6.4	3.2	2.6	2.3
Eu	1.9	1.9	1.0	1.35	1.02
Gd	7.2	7.0	3.5	3.1	2.3
Dy	7.3	7.5	4.0	4.1	3.7
Ho	1.7	1.7	0.6	0.6	1.0
Er	3.6	4.1	2.0	1.9	1.5
Yb	3.2	4.0	1.9	2.6	1.3
ΣREE	119.6	119.7	45.2	44.5	33.9
La/Yb	5.3	4.2	2.3	1.9	2.5
Ce/Yb	13.2	10.6	6.8	5.2	7.6

Table 4.1 continued

← Kapvik volcanic complex →

	F397.78	F406.78	F405.78	F402.78	Lower Gabbro F432.78
SiO ₂			52.6	56.2	48.1
TiO ₂			2.26	2.06	0.94
Al ₂ O ₃			12.8	12.4	12.8
Fe ₂ O ₃ ^t			16.64	13.71	13.76
MnO			0.22	0.26	0.21
MgO			3.46	2.67	7.25
CaO			6.11	6.37	10.00
Na ₂ O			2.76	3.63	2.5
K ₂ O			1.72	0.76	0.84
P ₂ O ₅			0.56	0.35	0.05
L.O.I.			0.51	0.34	1.37
Total			99.64	98.75	97.82
Nb	6	7	12	12	7
Zr	82	97	184	187	65
Y	23	34	47	48	25
Sr	236	155	135	103	124
Rb	62	7	70	17	20
Pb	24	4	10	20	50
Zn	104	100	114	190	130
Cr	140	83	15	4	62
V	265	304	310	335	295
Ba	199	49	385	145	30
Y/Nb	13.8	4.9	3.9	4	3.6
La	2.3	6.2	15.4	23.7	3.5
Ce	7.1	16.3	40.8	53.8	10.3
Pr	0.9	2.0	4.9	6.2	0.8
Nd	6.4	9.8	21.5	26.4	5.6
Sm	2.3	3.3	5.4	6.4	1.9
Eu	1.2	1.1	1.7	1.7	0.92
Gd	2.8	3.7	5.9	6.5	2.7
Dy	3.3	4.5	6.4	6.7	3.6
Ho	0.6	0.7	1.4	1.4	0.9
Er	1.6	2.6	3.7	3.9	2.2
Yb	1.3	2.7	3.4	3.3	2.9
ΣREE	29.8	52.9	110.5	140	36.0
La/Yb	1.8	2.3	4.5	7.2	1.2
Ce/Yb	5.5	6.1	13.2	16.3	3.6

Table 4.1 continued

	Kapvik volcanic complex		Tallerk Sills		
	Lower Gabbros				
	F592.79	F464.79	F394.78	F336.79	F379.79
SiO ₂		48.2			49.5
TiO ₂		0.54			1.94
Al ₂ O ₃		16.9			12.7
Fe ₂ O ₃ ^t		10.54			16.54
MnO		0.18			0.21
MgO		9.71			5.23
CaO		10.29			7.00
Na ₂ O		1.82			3.58
K ₂ O		0.75			0.75
P ₂ O ₅		0.05			0.19
L.O.I.		1.55			0.57
Total		100.53			98.21
Nb	1	3	6		2
Zr	116	30	80		103
Y	50	21	27		44
Sr	175	135	207		169
Rb	31	18	15		23
Pb	38	8	4		9
Zn	171	78	81		126
Cr	44	0	220		0
V	374	0	223		821
Ba	128	0	41		149
Y/Nb	50	7	4.5		22
La	12.2	3.8	8.4	4.2	
Ce	30.0	7.6	23.8	12.4	
Pr	2.9	0.6	3.1	1.7	
Nd	16.5	4.0	14.4	8.8	
Sm	5.0	1.6	4.5	3.2	
Eu	1.8	0.82	1.7	1.2	
Gd	5.7	2.0	5.2	4.0	
Dy	7.0	3.1	6.6	4.8	
Ho	1.5	0.6	1.5	0.8	
Er	4.2	1.8	3.6	2.7	
Yb	4.2	2.5	5.1	2.8	
ZREE	85.0	26.8	72.3	48.0	
La/Yb	2.9	1.5	1.7	1.5	
Ce/Yb	7.1	3.0	4.7	4.4	

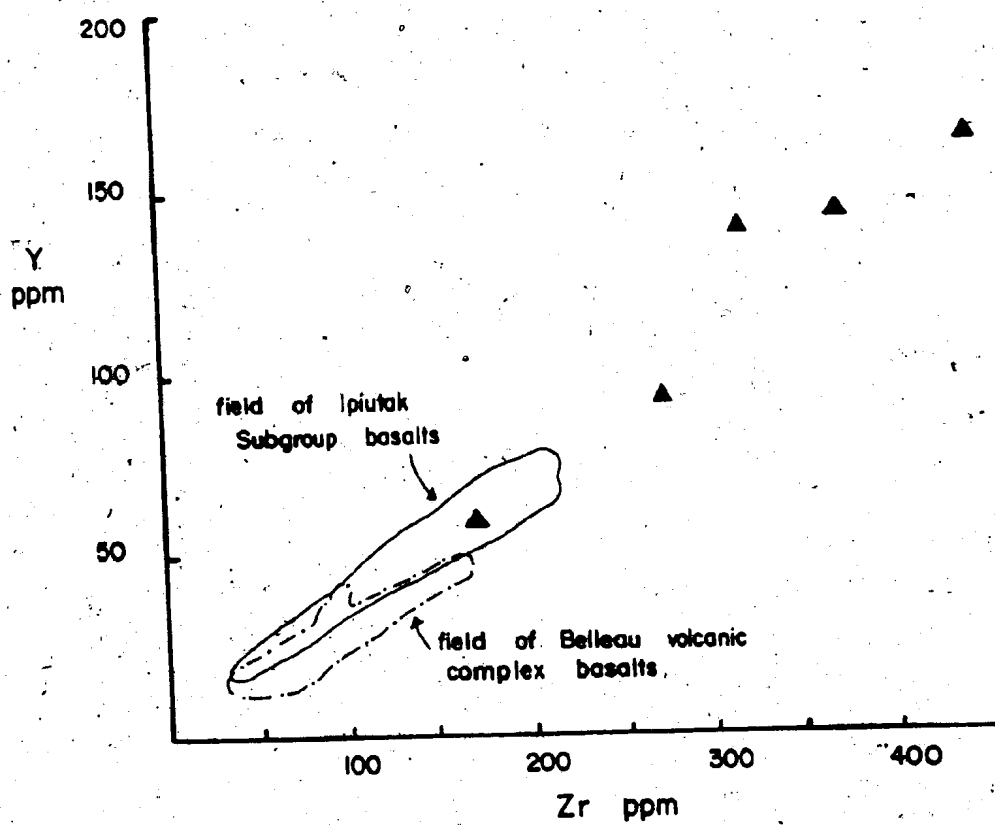
the individual volcanic complexes, and then draw general conclusions about the Akaitcho Group as a whole. The Sinister volcanic complex is not considered here, as its exposed area consists mainly of rhyolite, and only minor basalt. REE patterns are used chiefly in this section, because they clearly show the differences between the two basalt types, and show a group of elements at a glance.

4.2.2 Ipiutak Subgroup Basalts

No central volcanic complex is recognizable in the Ipiutak Subgroup because of the complex folding and thrusting present in the Subgroup (Chapter 3). Nevertheless, some generalizations can be made. First, the Ipiutak Subgroup basalts are continental tholeiites, and some are relatively evolved. For example, the fields of the Ipiutak Subgroup and the Belleau volcanic complex basalts are compared in Figure 4.8. The Belleau basalt field includes oceanic and continental tholeiites. Note the greater range of Y and Zr contents in the Ipiutak Subgroup basalts. The Ipiutak Subgroup basalts show the greatest range of Y and Zr in the Akaitcho Group. In Figure 4.9, the high REE abundances in some Ipiutak Subgroup basalts is apparent. Most continental tholeiites in the Nasittok Subgroup lie to the lower abundance side of the field. Although the Ipiutak Subgroup contains evolved continental tholeiites, the rocks are clearly not alkaline in character.

Second, the Ipiutak Subgroup basalts and the amphibolite dykes that cut the Sityok Complex granite (Unit 3,

Figure 4.8 Y versus Zr plot for Ipiutak Subgroup basalts (solid line), Belleau volcanic complex basalts (dot-dash line), and Sityok Complex amphibolite (Unit 1, filled triangles). Note high Zr and Y contents of Sityok Complex amphibolites, and clear separation from the Akaitcho Group basalts.



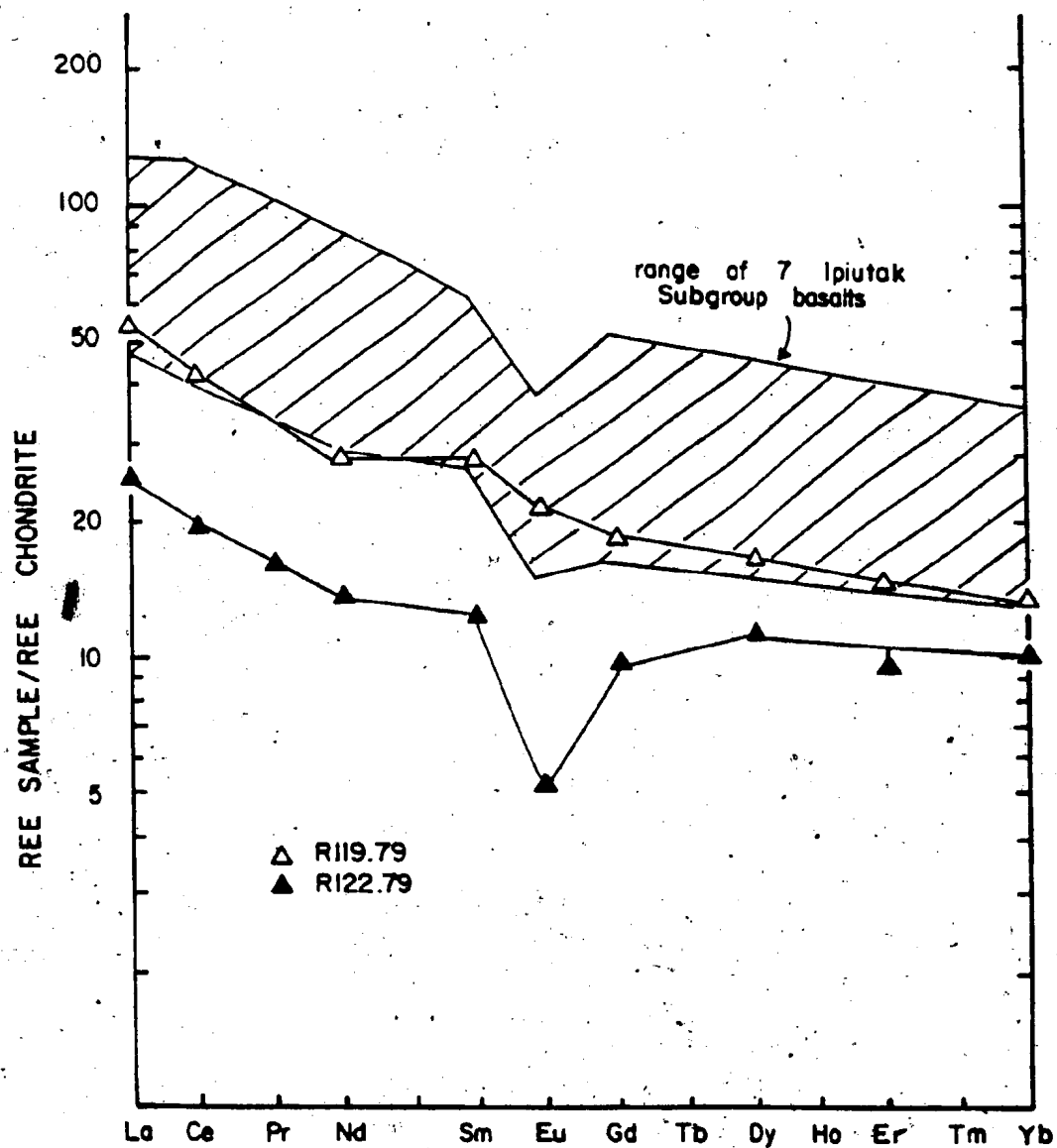


Figure 4.9 Chondrite-normalized REE plot for Ipiutak Subgroup basalts and Sityok Complex amphibolite dykes (Unit 3).

Figure 4.10 Y versus Zr plot showing Ipiutak Subgroup basalts (solid line) and Sityok Complex amphibolite dykes (Unit 3, open triangles). Note overlap of Ipiutak basalt field and the amphibolite dykes. Field of Belleau volcanic complex basalts (dot-dash line) is shown for comparison.

Figure 4.11 Y versus Zr plot showing Ipiutak Subgroup basalts (solid line), Sityok Complex amphibolite dykes (Unit 3, open triangles), and Sityok Complex amphibolite (Unit 1, filled triangles). Note clear separation of the Unit 1 amphibolites from the other units and the close correspondence of the amphibolite dykes (Unit 3) to the Ipiutak Subgroup basalts.

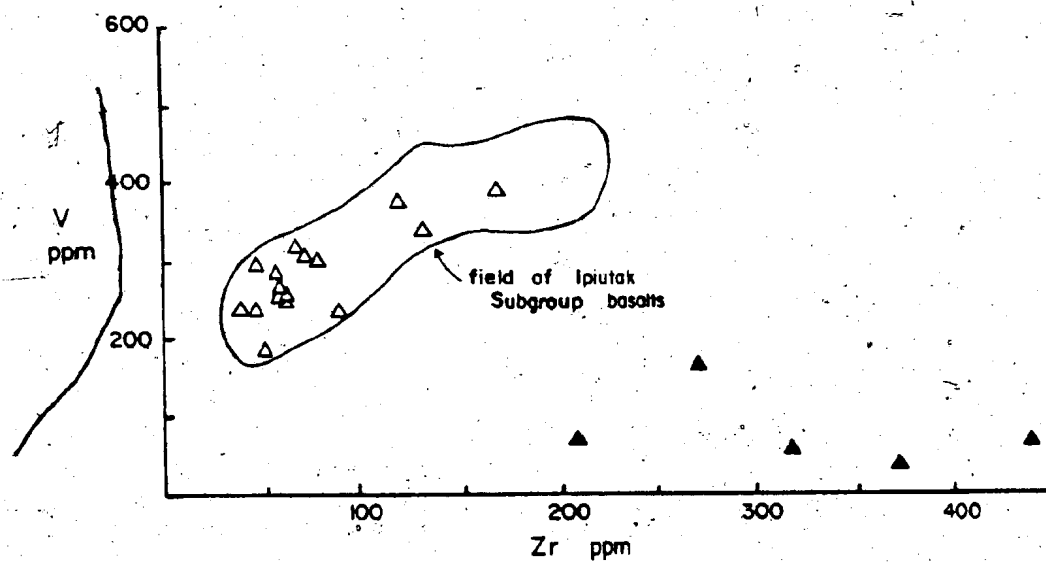
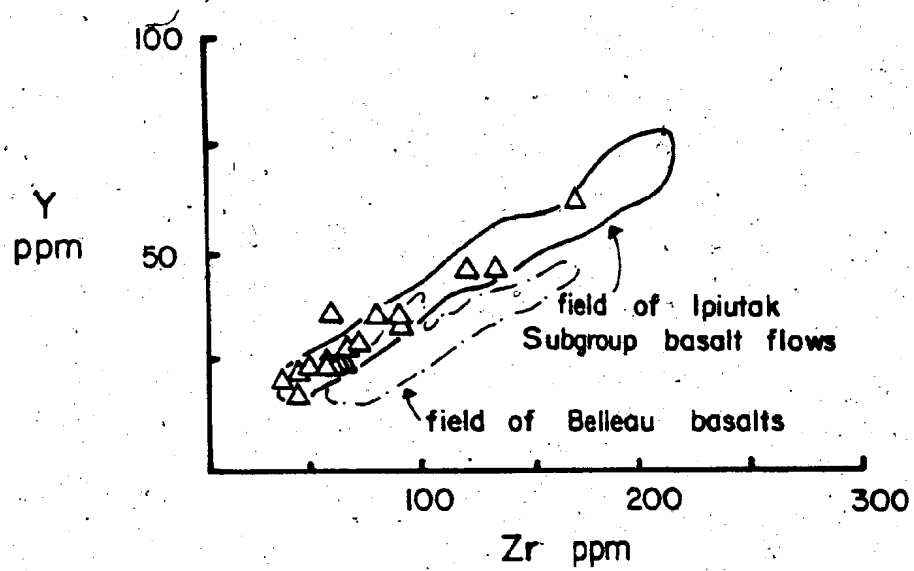
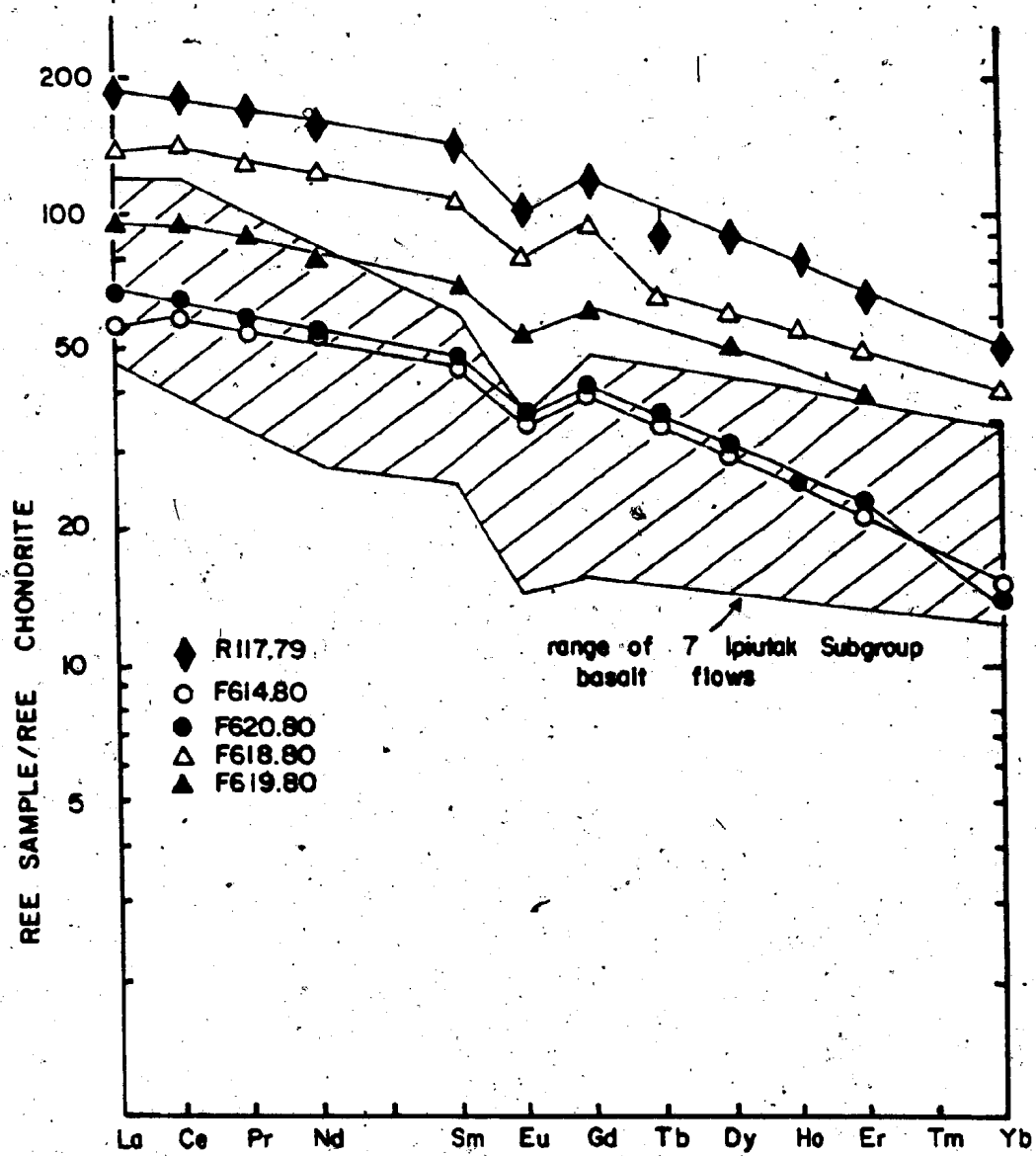


Figure 4.12. Chondrite-normalized REE plot of Sityok Complex amphibolites (Unit 1). Field of Ipiutak Subgroup basalts is shown for comparison. Note the small Eu anomaly in the Unit 1 amphibolites, and the high total REE abundances. Unit 1 amphibolites are also higher in TiO_2 and Fe than the Ipiutak Subgroup basalts.



Chapter 3.2) show close correspondence, suggesting that they may be cogenetic (Figure 4.9, 4.10, 4.11). The amphibolite dykes are somewhat more primitive in character than the lavas, suggesting that some shallow-level fractionation has occurred, or that the dykes sampled did not directly feed the lava sequence.

Third, the Ipiutak Subgroup basalts are clearly different from amphibolite (Unit 1, Chapter 3.2) present in gneisses of the Sityok Complex (Unit 1, Chapter 3.2) (Figure 4.10, 4.11, 4.12). The amphibolites present in the gneisses are clearly unrelated to any known Akaitcho Group rocks.

In summary, the Ipiutak Subgroup consists of continental tholeiites, some of which are more evolved than continental tholeiites higher in the Akaitcho Group, and these tholeiites were probably fed in part by amphibolite dykes (Unit 3) that cut the Sityok Complex. No rhyolites are present in the Ipiutak Subgroup.

4.2.3 Tuertok Volcanic Complex Basalts

The Tuertok volcanic complex is considered typical of the Nasittok Subgroup volcanic complexes. The Tuertok complex has been mapped and sampled in detail (Easton, 1981a).

The Tuertok volcanic complex (Figure 4.13) consists of a lower basalt sequence (Unit 3) (Figure 4.13) intruded by a feldspar-phyric gabbro (Unit 4). The gabbro unit has been interpreted to represent a sub-volcanic magma chamber (Easton, 1981a). A thick, mainly pillowed sequence of

basalts (Units 5 to 9) overlies the gabbro. Microporphyr-
itic and aphanatic rhyolite flows (Unit 10) occur as a 100
to 150 m thick unit overlying the main basalt section. A
mixed basalt-rhyolite unit (Unit 11) overlies the rhyolites.
Porphyritic rhyolite (Units 12 to 14) caps the Tuertok
volcanic complex.

REE patterns for the basaltic rocks are shown in
Figures 4.14, 4.15 and 4.16. The gabbros have relatively
flat REE patterns at ten time chondritic values, with no Eu
anomaly (Figure 4.14). This type of pattern is typical of
oceanic gabbros. The main part of the basalt pile (Units 5
to 9) consists dominantly of ocean tholeiites, a few of
which show slight LREE depletion (F511.80, F36.78, F38D.78)
(Figure 4.15). A few basalts have a more continental
tholeiite character, and occur in the upper part of the
sequence (F533.80) (Figure 4.15). The late basalts (Unit
11) which occur interbedded with thin rhyolite flows have
higher REE abundances than the main basalt sequence, and
resemble continental tholeiites (Figures 4.16, 4.5). These
late continental tholeiites may be the result of decreased
partial melting in the source region as volcanism waned.
Alternatively, they may be fractionated basalts produced
in a high level magma chamber.

In summary, the bulk of the Tuertok volcanic complex
consists mainly of ocean tholeiites, with minor continental
tholeiite and fractionated basalts being erupted during the
late stages of volcanism.

Figure 4.13 Geological map of the Tuertok volcanic complex

LEGEND

- 16 HORNBY BAY GROUP sandstone
 H tonalite and granite of HEPBURN BATHOLITH

AKAITCHO GROUP

- 15 AGLEROK FORMATION pelites, 15b sandstone

NASITTOK SUBGROUP

- 14 porphyritic rhyolite flows and tuffs,
 14b mainly bedded tuff, minor pelite
 13 pelite, carbonate, rhyolite tuffs
 12 crystal-rich porphyritic rhyolite
 11 pillowed, massive, tuffaceous dark green basalt,
 minor rhyolite, 11b much interbedded rhyolite
 10 dark, fine-grained rhyolite
 9 pillowed basalt
 8 pillowed basalt, thin selvages
 7 basalt breccia, tuffs thin flows
 6 as Unit 5, but with dark green basalt dykes
 5 pale green pillowed and massive basalts
 4 glomeroporphyritic feldspathic gabbro
 3 basalt, minor black shale
 2 OKRARK rhyolite sills, 2a plagioclase-porphyritic,
 2b orthoclase porphyritic
 1 ZEPHYR FORMATION arkosic turbidites
 AC Aklak rhyolite centre
 KC Kuno rhyolite centre

METAMORPHIC ISOGRADS

(mark on high T side,

data courtesy of M.R. St-Onge)

- | | | | |
|----|-------------------------|-----|------------------------------|
| •• | biotite | — — | fault, known, assumed |
| — | staurolite | ▲▲ | OKRARK thrust fault |
| — | sillimanite | — — | contact, known, approximate |
| — | K-feldspar, sillimanite | ▲ | bedding, tops known, unknown |
| + | granite pods | ▲ | pillow tops |
| — | migmatite | ▲ | foliation |

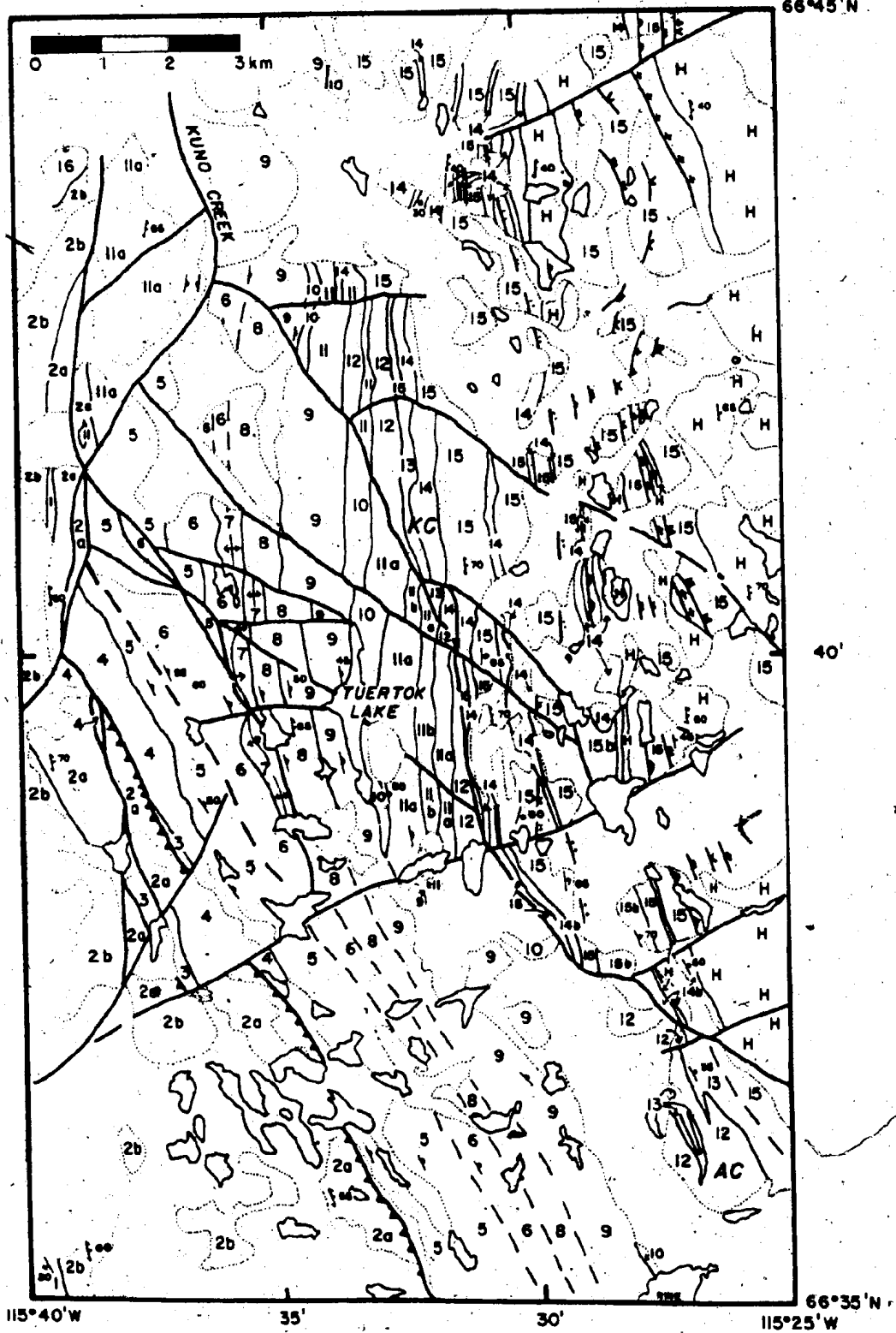


Figure 4.14 Chondrite-normalized REE plot of the lower basalts (Unit 3) and the feldspar-phyric gabbros (Unit 4) of the Tuertok volcanic complex.

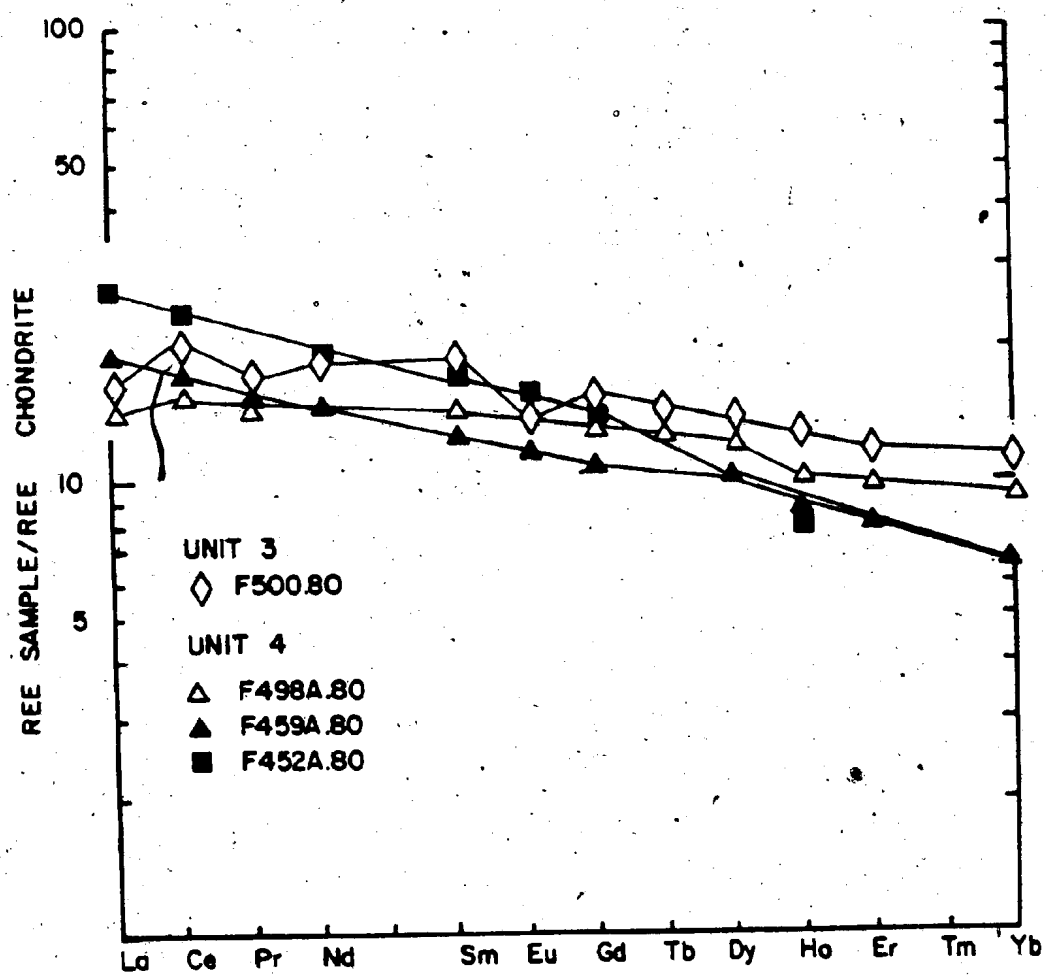


Figure 4.15 Chondrite-normalized REE plot for the main basalt sequence of the Tuertok volcanic complex (Units 5 to 9).

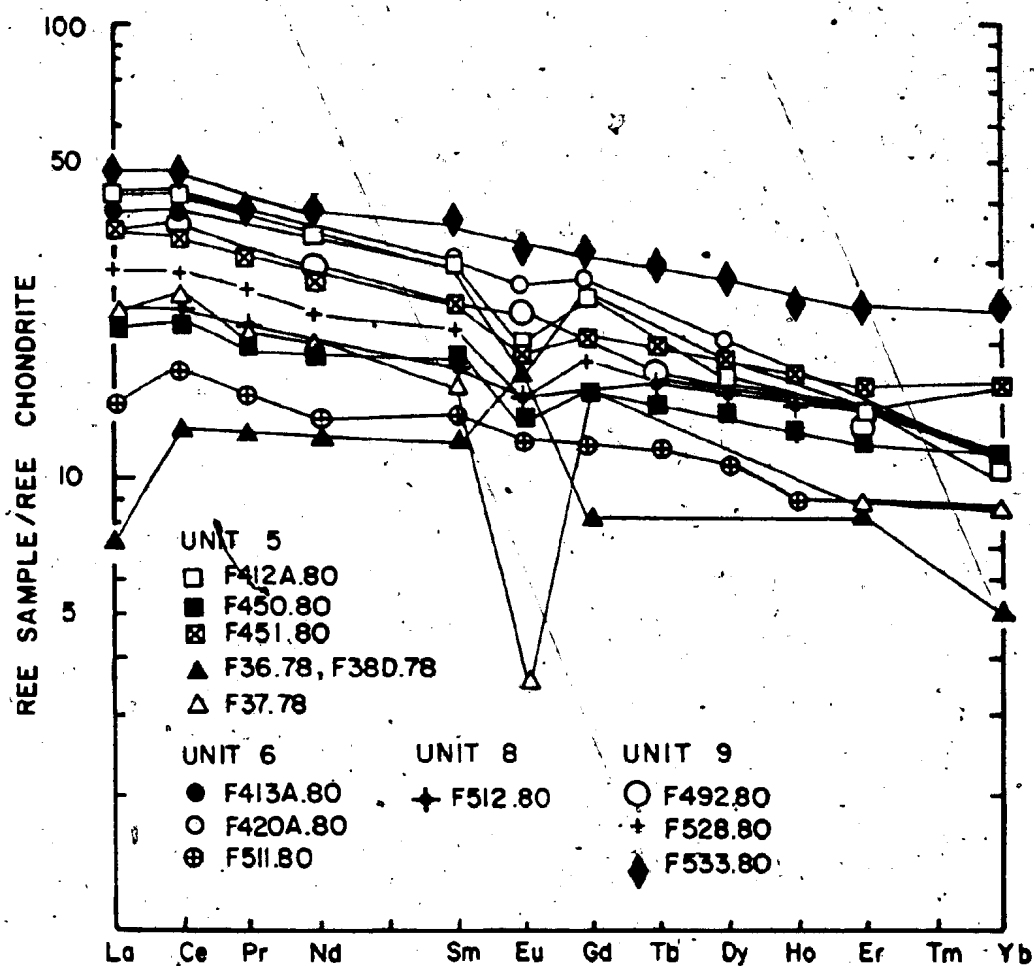
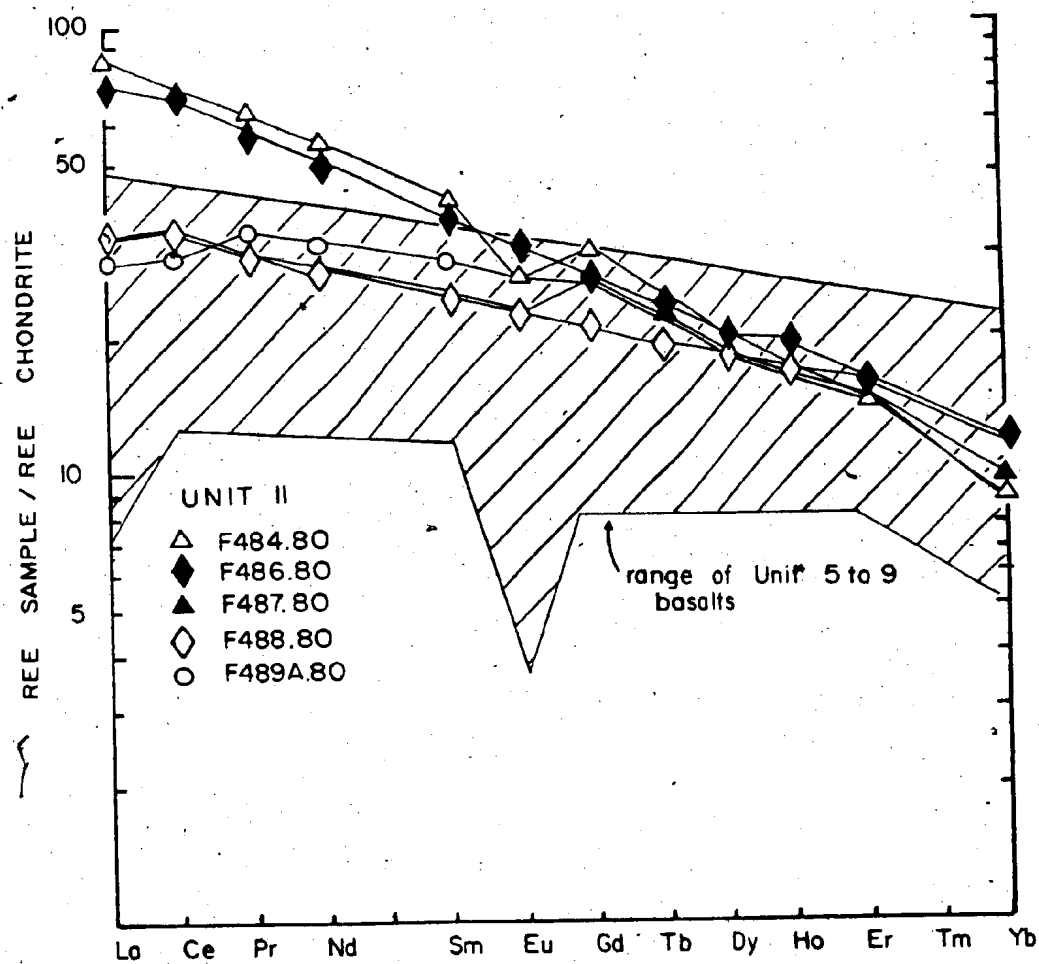


Figure 4.16 Chondrite-normalized REE plot for the upper basalt unit (Unit 11) of the Tuertok volcanic complex. Field of 13 main basalt lavas (Figure 4.15) is shown. Note greater total REE abundances in the Unit 11 lavas.



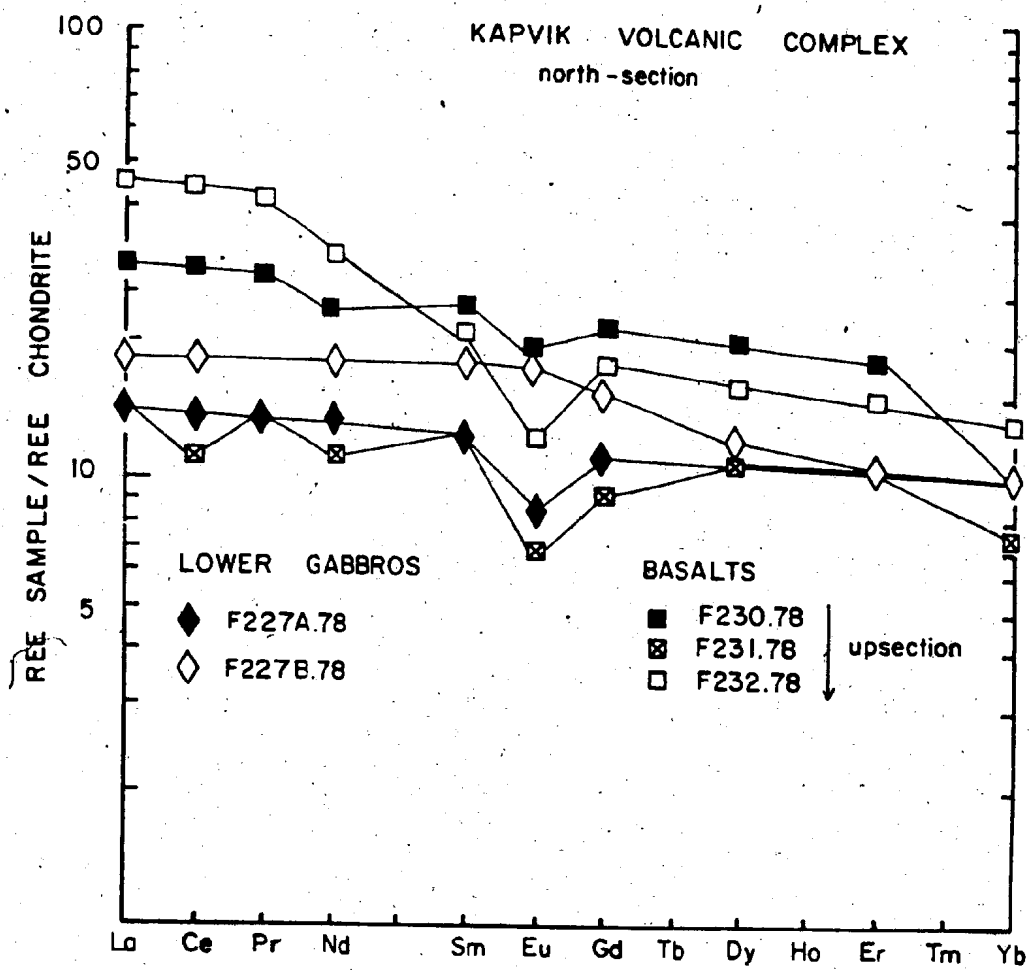
4.2.4 Kapvik Volcanic Complex Basalts

Samples from two traverse lines across the Kapvik volcanic complex were analyzed for REE (Figures 4.17, 4.18). Both continental and oceanic tholeiites are present in the north section (Figure 4.17), and there may be a trend from continental to oceanic basalts up-section. Gabbros at the base of the Kapvik volcanic complex are suspected to be feeders to the complex, and have oceanic compositions.

Samples from the south section of the Kapvik volcanic complex (Figure 4.18) show a definite trend from continental tholeiites to oceanic tholeiites up-section. Interfingering of the two basalt types does occur, and a continuum probably exists between the two basalt types. The gabbros at the base of the complex are both oceanic and continental tholeiites, as would be expected if the gabbros were cogenetic with the extrusive rocks.

A plot of Y versus Zr for all the Kapvik basalts (Figure 4.19) shows a clear separation between basalts which have oceanic REE patterns, and those with continental patterns. The continental basalts have higher Y and Zr contents than the oceanic basalts. The gabbros from the base of the complex lie in, and between, both fields. A plot of V versus Zr (Figure 4.20) shows less of a distinction between the two basalt types, although there is a tendency for the continental basalts to have higher V contents. Again, the gabbros overlap both fields.

Figure 4.17 Chondrite-normalized REE plot for Kapvik volcanic complex basalts and gabbros from the base of the complex. Traverse line across the north end of the complex ($66^{\circ}17'N$).



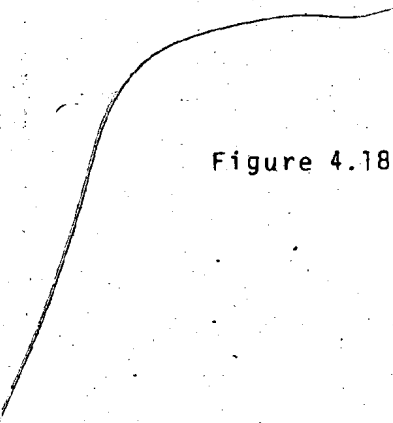


Figure 4.18 Chondrite-normalized REE plot for basalts from the Kapvik volcanic complex and gabbros from the base of the complex. Traverse line lies across the central part of the complex (66°15'N).

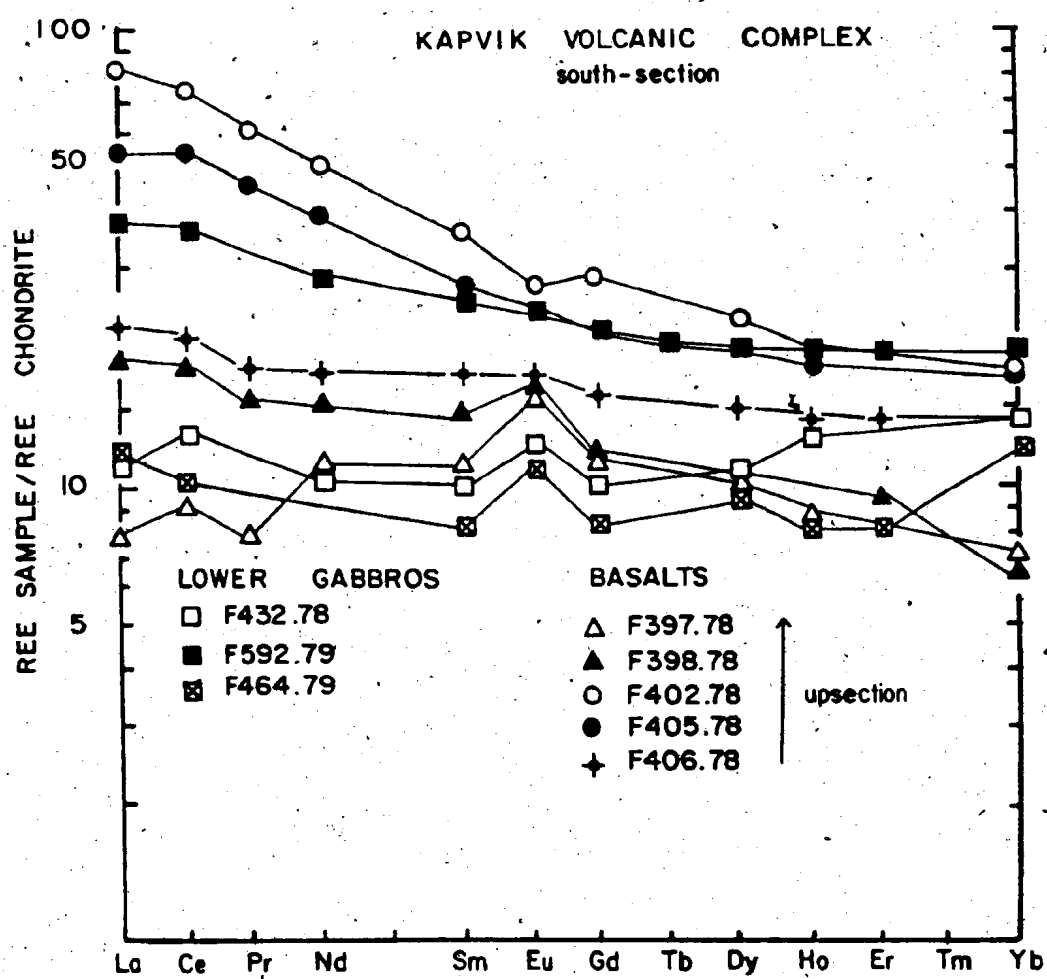
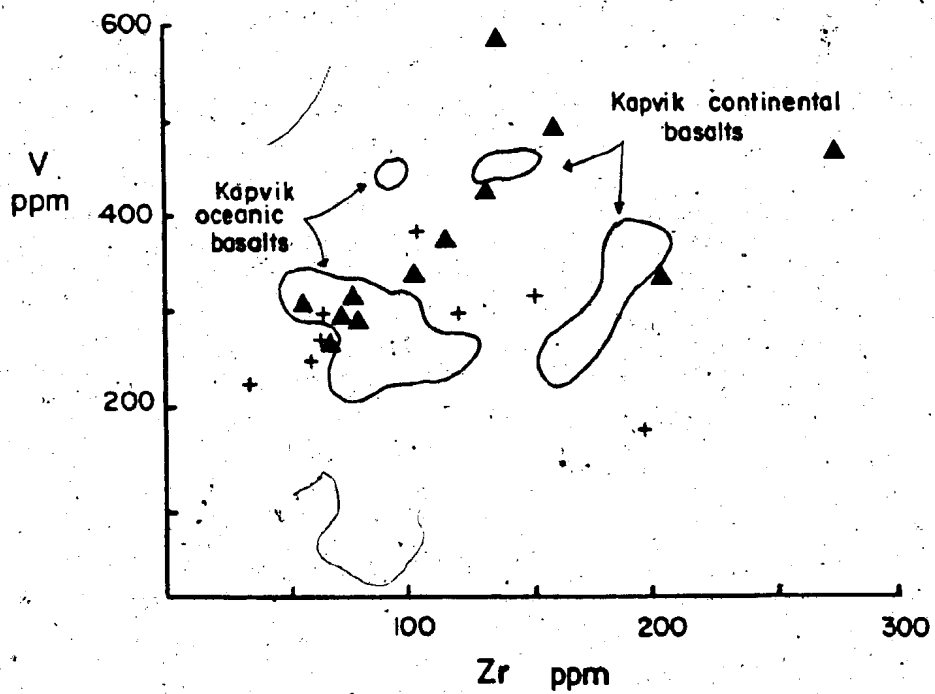
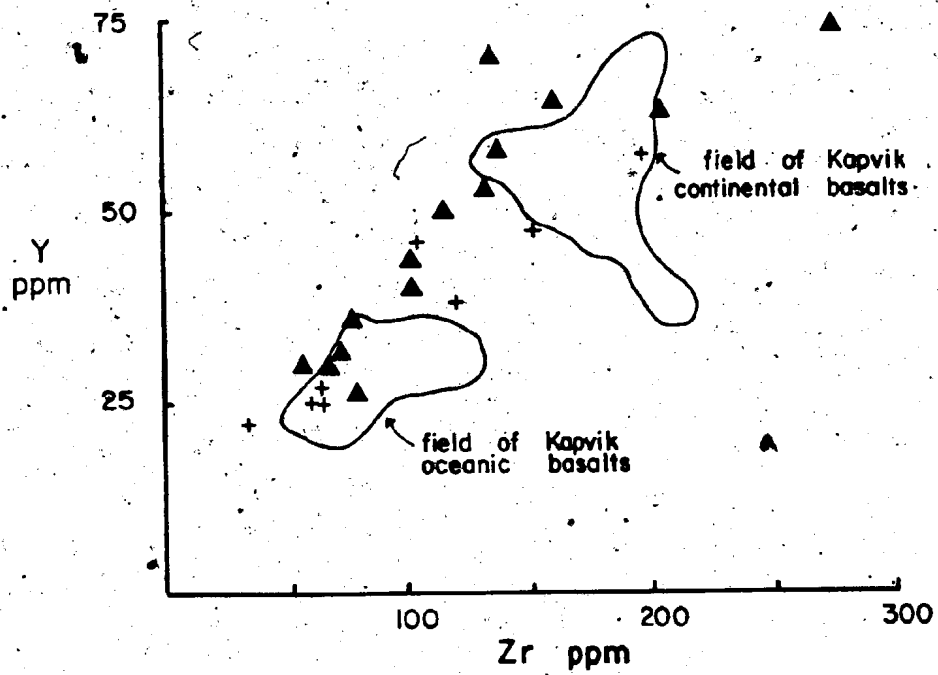


Figure 4.19 Plot of Y versus Zr for the Kapvik volcanic complex basalts (solid line, n=20), gabbros from the base of the complex (crosses, n=8), and the Tallerk sills (solid triangles, n=14). Distinction between oceanic and continental basalts is based on samples analyzed for REE.

Figure 4.20 Plot of V versus Zr for Kapvik volcanic complex basalts, gabbros from the base of the complex, and the Tallerk sills. Symbols as in Figure 4.19.



In summary, the Kapvik volcanic complex consists mainly of continental basalts, with some oceanic basalts occurring in the upper portion of the complex. The gabbros at the base of the complex are similar to the Kapvik basalts, and may have been feeders to the lavas.

4.2.5 Tallerk Sills

The Tallerk gabbro sills are found above the Kapvik and Havant volcanic complexes. As shown in Figures 4.19 and 4.20, the Tallerk sills overlap both the fields of the Kapvik basalts and the lower gabbros. REE results for two Tallerk sills overlying the Kapvik complex are shown in Figure 4.21. These two samples are oceanic tholeiites, although total REE abundances in F394.78 are relatively high (about twenty times chondrites). Based on the plots of V and Y versus Zr (Figures 4.19, 4.20), some of the Tallerk sills may have continental tholeiite compositions. In summary, the Tallerk gabbro sills show the overall trends present in the Kapvik volcanic complex.

4.2.6 Belleau Volcanic Complex Basalts and the Grant Subgroup Basalts

A stratigraphic column and the overall trends in REE for the Belleau volcanic complex are shown in Figure 4.22. The lower part of the complex consists of continental tholeiites (Figures 4.22, 4.23), with the upper part of the complex containing oceanic tholeiites (Figures 4.22, 4.23). There is a definite change from continental tholeiites to oceanic tholeiites up-section.

Figure 4.21. Chondrite-normalized REE plot for the Tallerk gabbro sills. Range of 13 Kapvik volcanic complex basalts and gabbros from the base of the complex is shown for comparison.

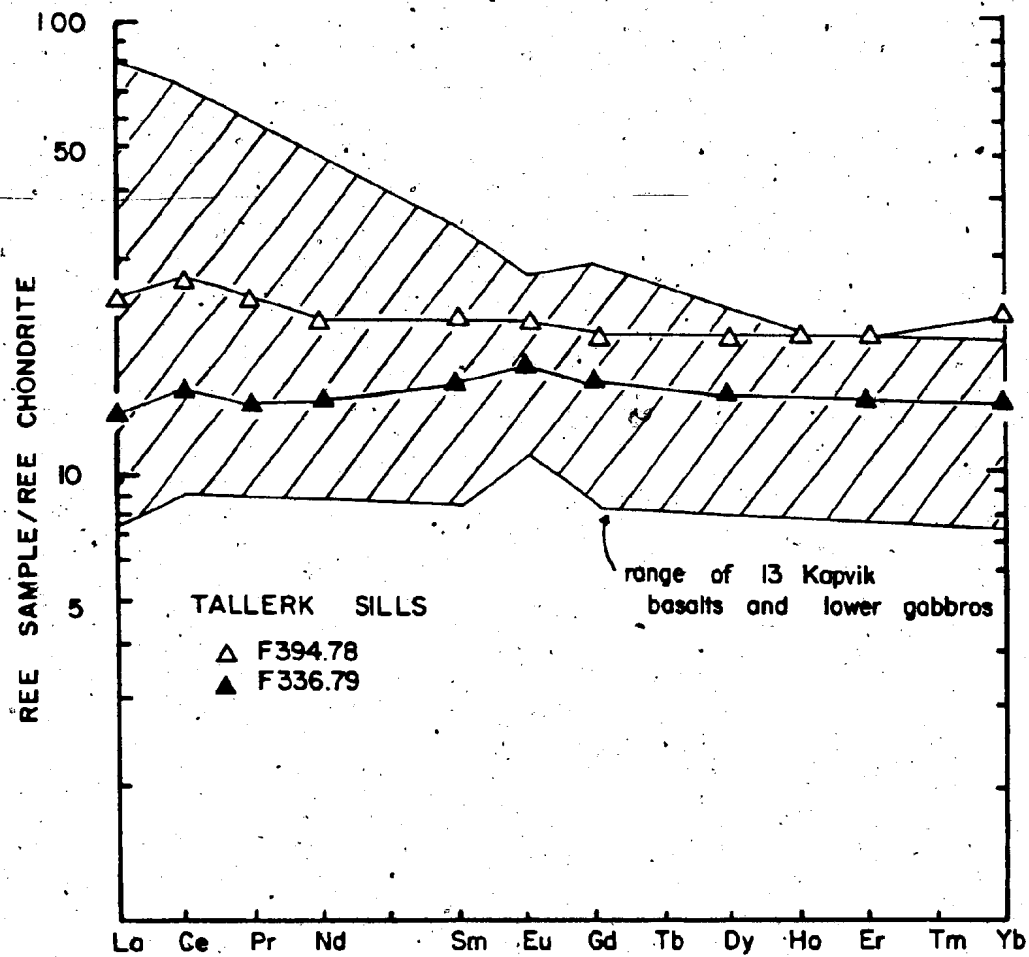







Figure 4.22 Stratigraphic column for the Belleau volcanic complex and representative REE patterns. The lower kilometre of the complex consists of continental tholeiites, the upper kilometre consists of oceanic tholeiites. REE symbols: open triangles - porphyritic rhyolite; filled circles - lower basalts; open circles - upper basalts; crosses - upper gabbro sills and dykes.

KEY TO LITHOLOGIES

-  rhyolite dome
-  rhyolite pyroclastic flow
-  basalt flows, pillowed and massive
-  gabbro sills and dykes
-  pelite, volcanic sandstones

BELLEAU VOLCANIC COMPLEX

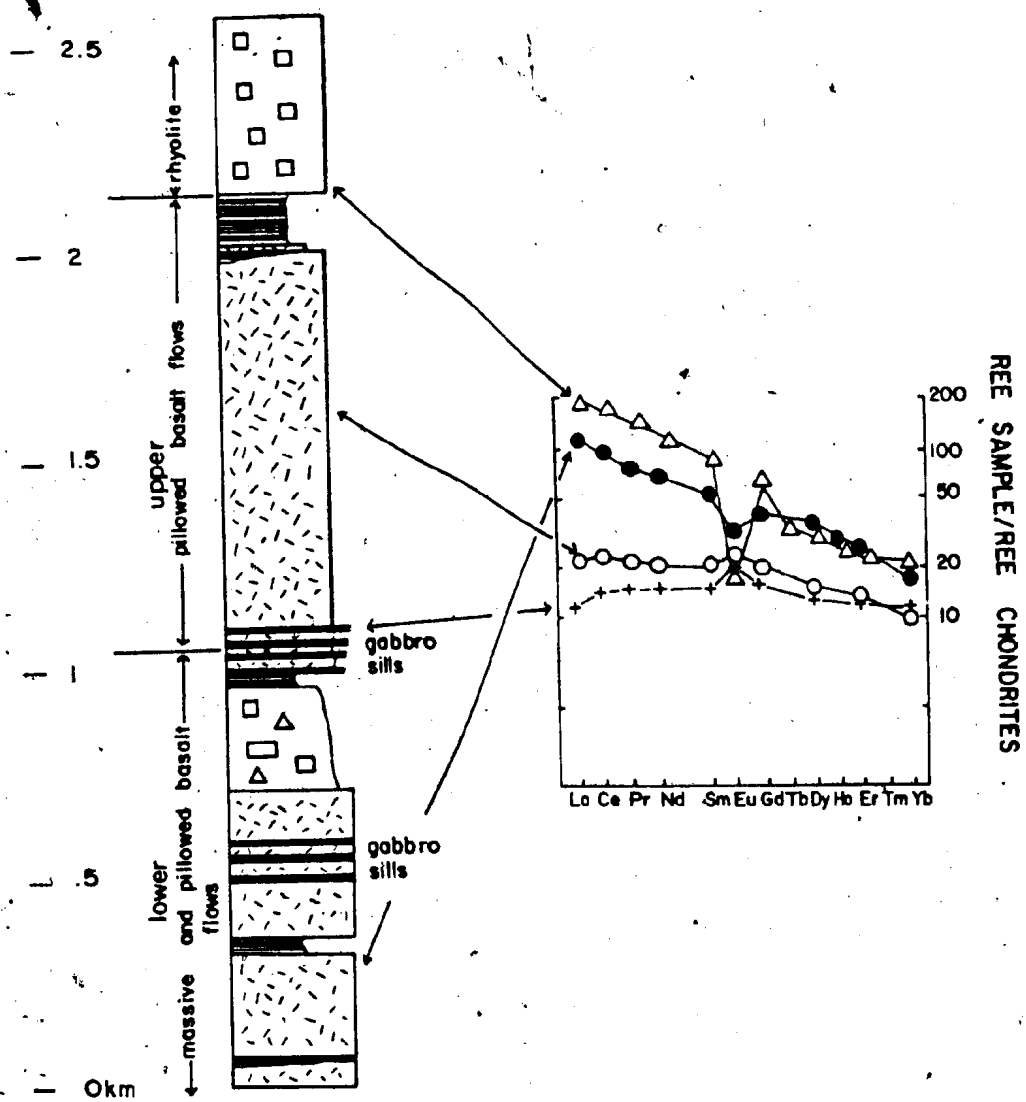


Figure 4.23 Chondrite-normalized REE plot for the Belleau volcanic complex basalts. Field of basalts from the lower part of the complex is shown - these rocks are continental tholeiites. Samples of oceanic tholeiites from the upper part of the complex are shown for comparison. Note the clear separation of the two groups of basalts.

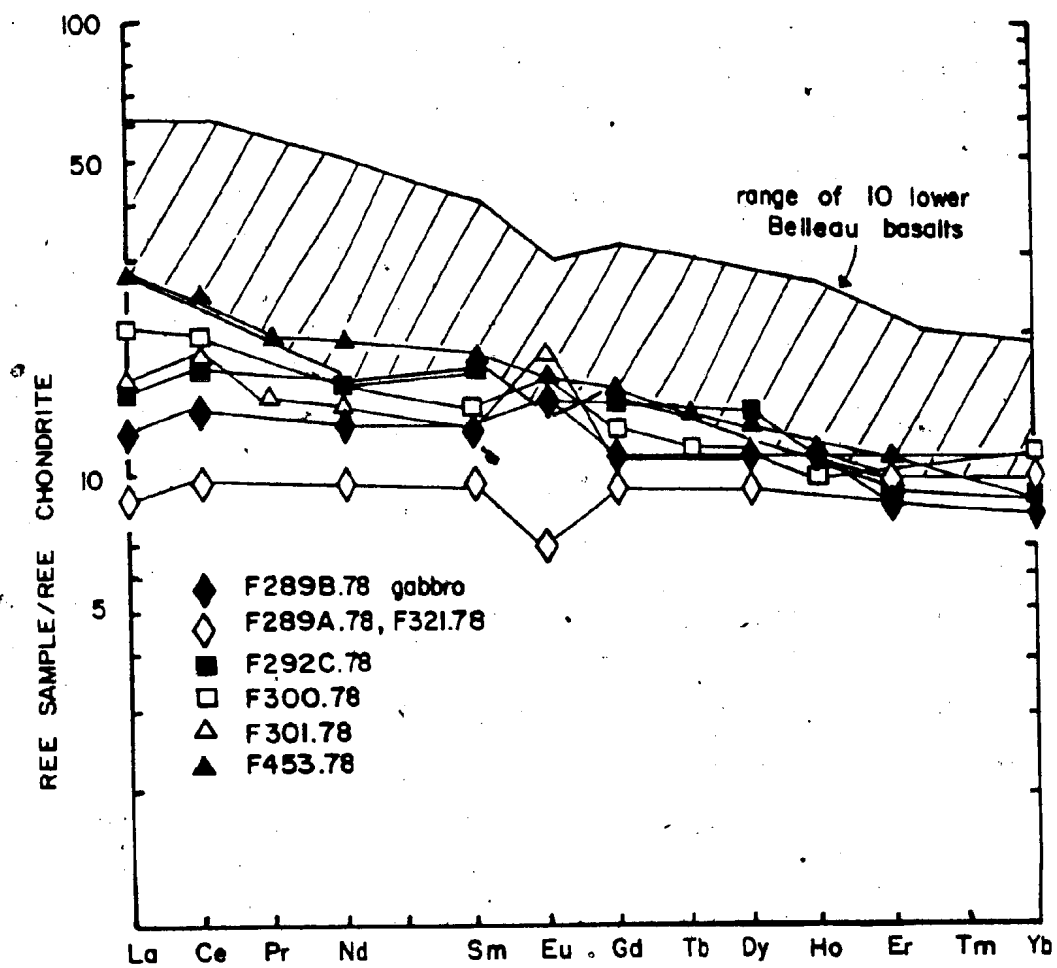









Figure 4.24 Comparative stratigraphic section for the Grant Subgroup. Note that to the south, only the lower, continental tholeiite part of the Belleau volcanic complex is likely to be exposed.

LEGEND

-  rhyolite flows and tuffs
-  gabbro sills
-  pillowed basalt
-  massive and pillowed basalt
-  dolomite
-  porphyritic rhyolite flows and domes
-  siltstone and slates

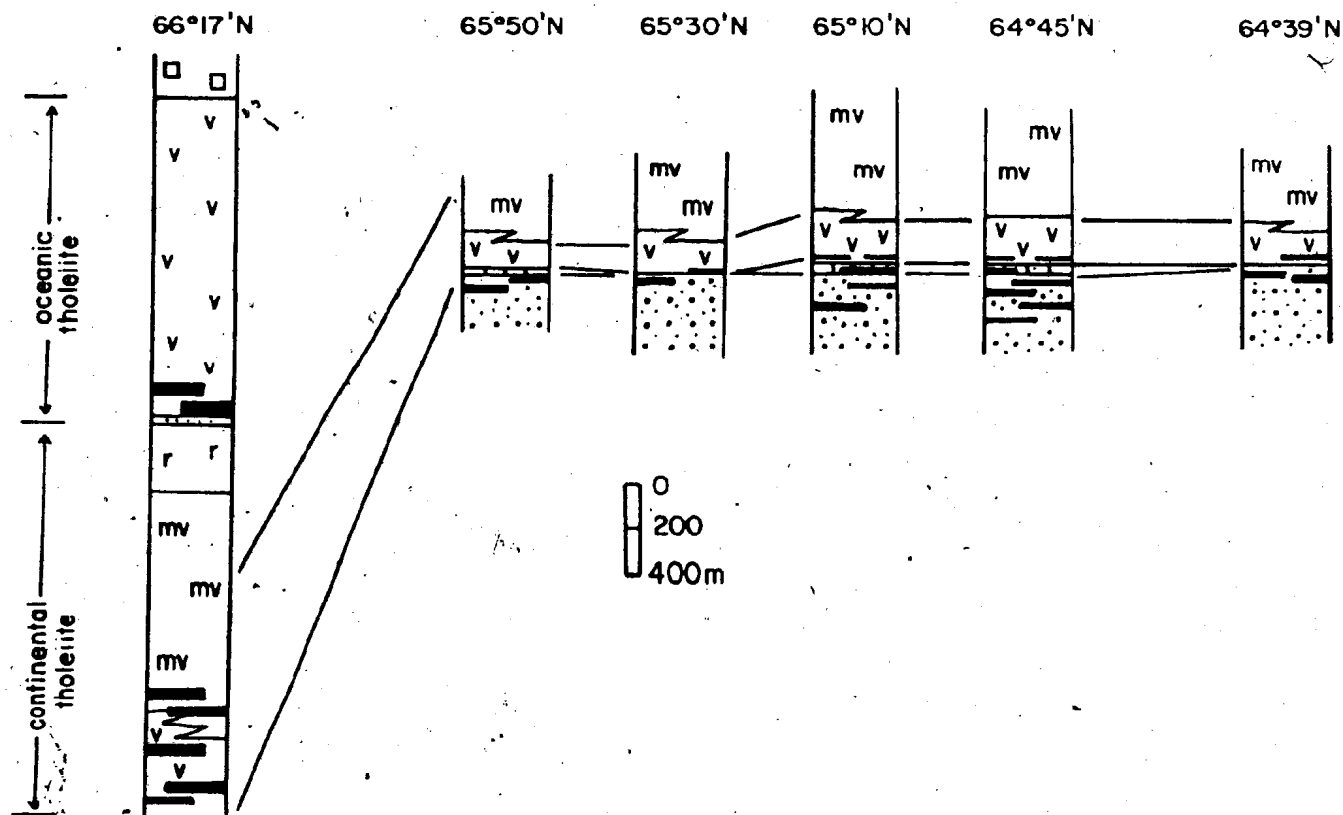
GRANT SUBGROUP

BELLEAU VOLCANIC
COMPLEX

CALDER RIVER BELT
(McGlynn, 1974, 1975, 1976)

GRANT LAKE

REBESCA LAKE
(Lord, 1942)



Data for the other Grant Subgroup basalts is sparse. Samples from Grant Lake are continental tholeiites. As shown in Figure 4.24, only the lower section represented by the lower part of the Belleau volcanic complex is present elsewhere in the Grant Subgroup. If oceanic tholeiites were present, they have probably been eroded.

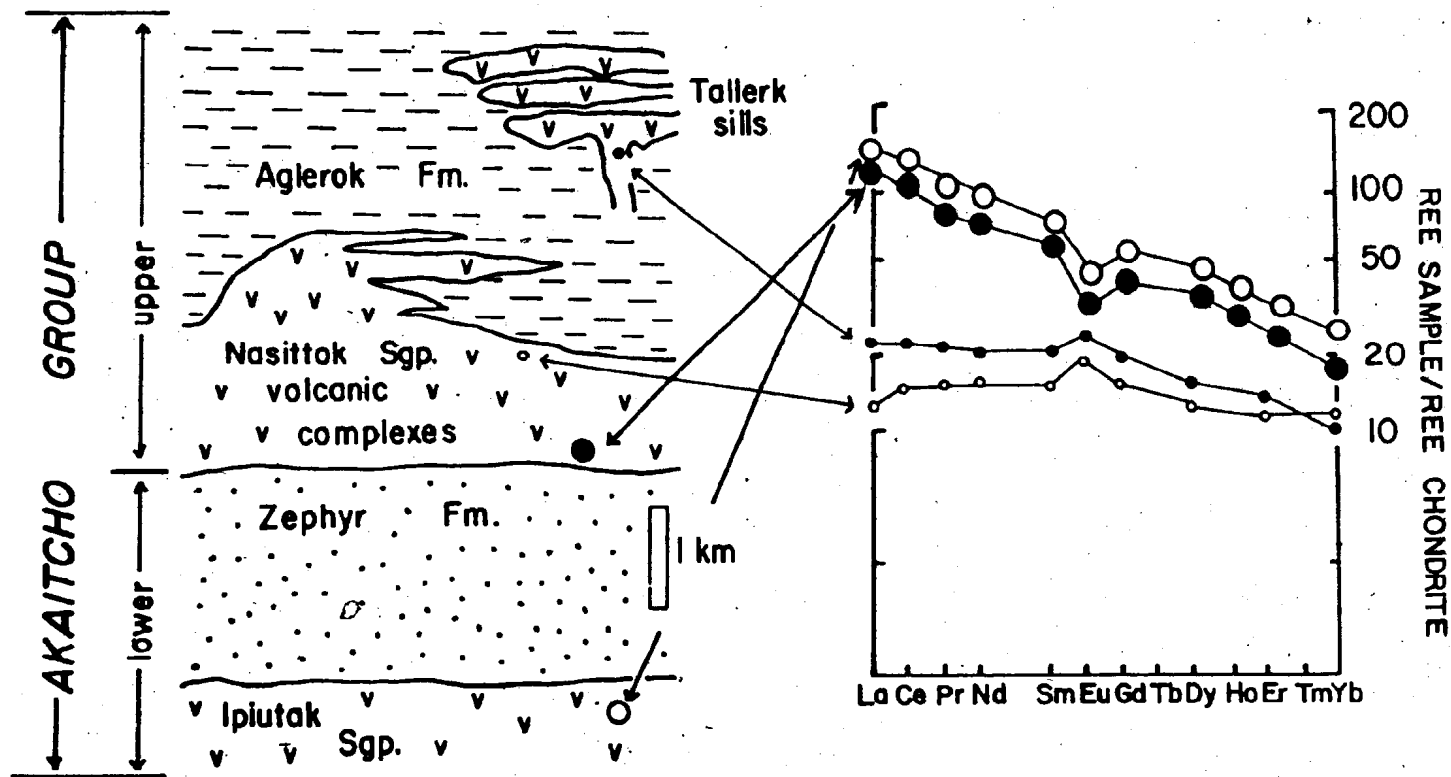
4.2.7 Akaiicho Group Basalts - Overall Trends

Figure 4.25 compares the REE patterns of several representative Akaiicho Group basalts to stratigraphic position. The overall trend is from continental and evolved continental tholeiites in the lower part of the Akaiicho Group to oceanic tholeiites in the upper part of the group. This evolution of basalt composition with time, from more evolved compositions to oceanic tholeiites, is present in many rifts that evolve into continental margins (e.g. Afar; Gass, 1970; Treuil and Joron, 1975; Barberi and Varet, 1977) and is consistent with the stratigraphic evidence (Chapter 3.8) that the Akaiicho Group is a rift sequence.

4.2.8 Rhyolites

The important question in regard to the Akaiicho Group rhyolites is the question of origin. Are they related to the basalts genetically?, or are they derived from crustal melting? Although two types of rhyolites may be recognized by stratigraphic position and Zr and SiO₂ values (Figure 4.2); all the rhyolites are sufficiently similar to be regarded as one group as far as source is concerned (Figure 4.3).

Figure 4.25 Simplified stratigraphic column for the Akaftcho Group and representative REE patterns for each major basaltic horizon. Symbols: large open circle - Ipiutak Subgroup (F718.79); large filled circle - lower Kapvik volcanic complex (F402.78); small open circle - upper Tuertok volcanic complex (F36.78); small filled circle - Tellerk sill (F336.79). Note that trend up section is from evolved continental tholeiites, through continental tholeiite to oceanic tholeiite.



The absolute abundances of REE in the rhyolites are approximately the same as REE abundances in the most fractionated Akaitcho Group basalts (Ipiutak Subgroup). More importantly, Ce/Yb ratios of the rhyolites (20 to 25) are different from the Ce/Yb ratios of the basalts (oceanic, 5 to 7; continental, 10 to 15). Although fractionation could produce the observed REE patterns in the rhyolites, the lack of any intermediate composition rocks, the abundance of rhyolite in the Akaitcho Group (felsic/mafic ratio of .2 to .3) and the absence of any sub-volcanic rhyolite plutons argues against the rhyolites being differentiates from the basalts. The rhyolites also have high Fe, Ti, Mn, K and Ba (Table 4.2) abundances, abundances that would not be expected if the rhyolites were derived from the basalts. The rhyolites also have high $^{87}\text{Sr}/^{86}\text{Sr}$ initial ratios (.704 to .709) (Chapter 5), although these ratios have probably been affected by a latter resetting event. In addition, granitoid xenoliths are present in Okrark sills near Belleau Lake, consistent with the rhyolites being crustally derived. The general occurrence of the rhyolites high in the Akaitcho Group stratigraphy is also consistent with the rhyolites being crustal melts; the rhyolites occurring late in the sequence because sufficient heat must be imparted to the crust by the basaltic magmas in order to form the rhyolites by partial melting.

In summary, it is most probable that the Akaitcho

Table 4.2 Representative chemical analyses of Akaitcho Group rhyolites. Major elements in wt.%, trace and rare-earth elements in ppm.

	aphanatic flows			
	Tuertok F504.80	Tuertok F466A.80	Grant Lake F361.80	Vaillant C217.77
SiO ₂	71.8	71.5	68.0	72.0
TiO ₂	0.43	0.38	0.10	0.99
Al ₂ O ₃	12.2	11.8	9.7	11.9
Fe ₂ O ₃ ^t	4.71	3.63	5.84	4.02
MnO	0.05	0.07	0.11	0.04
MgO	1.14	0.53	0.90	0.70
CaO	1.05	2.12	6.36	1.66
Na ₂ O	2.53	2.97	2.69	5.90
K ₂ O	3.72	4.35	2.40	0.54
P ₂ O ₅	0.16	0.05	0.05	0.12
L.O.I.	1.42	1.65	2.72	1.85
Total	99.21	99.05	98.87	99.72
Nb	15	18	27	51
Zr	279	398	357	424
Y	68	112	188	72
Sr	33	86	152	111
Rb	131	151	145	5
U	6	5	3	3
Th	21	28	13	15
Pb	41	26	12	14
Zn	68	77	119	27
Cr	2	0	0	0
V	26	6	6	50
Ba	745	735	377	162
La		25.3		34.4
Ce		70.9		76.4
Pr		9.4		7.8
Nd		40.2		31.9
Sm		10.3		6.9
Eu		1.6		1.1
Gd		11.4		7.3
Dy		12.2		8.1
Ho		2.5		1.9
Er		7.4		5.9
Yb		9.0		5.6
ΣREE		202.1		186.4
La/Yb		2.8		6.1
Ce/Yb		7.9		13.6

Table 4.2 continued

aphanatic flows and tuffs--lower Kapvik volcanic complex

	F410.78	F401.78	F228.78	F226.78	F462.78
SiO ₂	76.6	71.8	77.2	73.5	76.5
TiO ₂	0.22	0.45	0.21	0.40	0.18
Al ₂ O ₃	12.3	12.0	12.2	11.7	11.1
Fe ₂ O ₃ ^t	1.26	5.09	1.9	4.75	2.05
MnO	0.01	0.06	0	0.02	0.01
MgO	0.64	0.10	0.27	0.66	0.11
CaO	0.24	1.18	0.30	0.24	0.09
Na ₂ O	4.88	1.9	1.9	2.7	1.4
K ₂ O	2.28	5.70	6.53	4.50	6.89
P ₂ O ₅	0.02	0.03	0.01	0.03	0
L.O.I.	0.59	1.3	0.69	0.85	0.61
Total	99.04	99.61	101.22	99.35	98.85
Nb	20	30	21	19	24
Zr	198	448	196	353	205
Y	85	126	65	68	52
Sr	26	177	27	46	46
Rb	47	192	22	113	277
U		5			
Th		31			
Pb	24	31	10	10	311
Zn	29	99	44	84	36
Cr	9	0	7	5	6
V	11	3	12	14	6
Ba	311	1320	736	736	505
La	28.4	49.6		35.9	
Ce	70.8	122.3		90	
Pr	8.5	14.8		11.3	
Nd	29.3	60.3		46.3	
Sm	6.3	13.1		10.7	
Eu	0.7	2.3		1.3	
Gd	4.0	14		8.9	
Dy	4.4	16		6.8	
Ho	1.3	3.3		1.4	
Er	2.3	9.0		3.9	
Yb	3.7	9.0		4.2	
ΣREE	159.7	315.2		221	
La/Yb	7.7	5.5		8.6	
Ce/Yb	19.1	13.6		21.4	

Table 4.2 continued

	porphyritic flows and sills				
	Tuertok	Sinister	Okrark	Okrark	Okrark
	F40B.78	F203.78	orthoclase F420.78	orthoclase F248.78	plagioclase F107.78
SiO ₂	66.8	68.9	66.6	67.3	67.6
TiO ₂	0.75	0.75	0.68	0.65	0.64
Al ₂ O ₃	13.5	13.6	13.8	13.4	13.0
Fe ₂ O ₃ ^t	6.24	4.13	5.79	5.85	6.09
MnO	0.07	0.03	0.08	0.06	0.04
MgO	1.51	1.4	1.15	0.92	0.81
CaO	2.02	0.66	2.41	2.32	1.96
Na ₂ O	2.1	2.3	2.51	2.15	1.9
K ₂ O	4.53	4.95	4.38	5.01	5.19
P ₂ O ₅	0.14	0.09	0.16	0.12	0.14
L.O.I.	0.55	1.85	1.00	1.05	0.96
Total	98.19	98.66	98.56	98.83	98.32
Nb	15	18	22	16	16
Zr	271	281	302	276	280
Y	52	39	71	48	52
Sr	125	58	146	128	104
Rb	164	193	198	211	207
U			6		
Th			26		
Pb	40	12	34	35	23
Zn	94	64	85	105	79
Cr	24	16	8	12	10
V	60	54	54	50	41
Ba	760	830	828	805	797
La	44.5		44.7	31.7	35.3
Ce	114.9		111	85.7	91.5
Pr	14.7		13.2	9.2	11.4
Nd	56.6		53.1	40.8	46
Sm	12.8		10.3	8.7	10.2
Eu	2.2		1.5	1.7	1.2
Gd	11.5		9.7	8.1	9.5
Dy	13.1		10.1	9.7	10
Ho	2.3		1.7	2.4	1.4
Er	6.1		5.6	4.2	5.9
Yb	5.6		5.0	4.4	5.2
ΣREE	285.3		267.3	198.5	224
La/Yb	8		8.9	7.2	6.8
Ce/Yb	20.5		22.2	19.5	17.6

Group rhyolites are crustal-derived, and not differentiated from the basalts.

4.2.9 Vaillant Formation

The Vaillant Formation is considered separately for two reasons. First, it is separated from the rest of the Akaitcho Group by the Hepburn Batholith. Second, and more importantly, the Vaillant Formation lavas have some unusual chemical attributes, and may be much more severely altered than the Akaitcho Group lavas discussed so far.

The Vaillant Formation was sampled in three areas: at Stanbridge Lake; on the north and south shores of the Coppermine River at 66°32'N, 114°45'W; and at Vaillant Lake (Figure 1.2, 3.30). Most of the Vaillant Formation consists of mafic rocks, but rhyolites are present in a few localities.

The Vaillant and Stanbridge Lake samples are the most similar in trace element characteristics of the three areas (Table 4.3, Figure 4.26, 4.27). All samples have very low Sr values, much lower than is typical for the Akaitcho Group (Figure 4.27). In addition, there is more scatter in the data than is typical for samples from one geographic area in the Akaitcho Group (compare Vaillant Lake and Belleau samples, Figure 4.26, 4.27). Samples with the lowest Sr values have the highest Rb, Nb, Zr, Y and Ti contents, and contain abundant carbonate in hand specimen. Of the three samples from Stanbridge Lake, F142B.78 is extremely carbonatized and altered in hand specimen, much

more so than the other two 'fresher' samples. F142B.78 has the highest Sr value of any Vaillant sample, 570 ppm, as well as higher Nb, Y and Zr than the other two samples. REE data for the three samples from Stanbridge Lake (Figure 4.28) shows that the two 'fresher' samples have similar patterns, and they could be oceanic tholeiites. Sample F142B.78 is LREE-enriched, and probably had an original REE pattern similar to F138.78 and F139.78. The REE, and the 'immobile' trace elements are mobile in carbonate-rich fluids (Hynes, 1980; McLennan, 1981). The high LREE, Nb, Y and Zr values in sample F142B.78 which is also carbonate-rich strongly suggests that these elements have been affected during alteration. Similar trends in the Vaillant Lake samples indicates that these samples may be similarly altered. It should be noted that the Vaillant Formation is overlain by the Stanbridge Formation dolomite, and that carbonate-rich fluids may have percolated through the Vaillant Formation shortly after deposition, as well as during metamorphism. Thus, the Stanbridge Formation, as a nearby source of carbonate may be the major reason for the Vaillant Formation alteration.

The samples from the Coppermine River area are unusual compared with other Akaitcho and Vaillant rocks. All samples have high TiO_2 , Zr, Y and REE values (Table 4.2), and Y/Nb ratios cluster at 1.2, transitional between alkaline and tholeiitic rocks. Again, there is evidence of alteration in these samples. For example, F770.79 has very

low Na and K contents, as well as very high LOI. It also has the lowest Ti, Zr, Y and Nb values, and the highest Sr of all the Coppermine area samples. Carbonate is also abundant in this sample. The total REE abundances are lower in this sample than the others (Figure 4.29). The other samples also have unusual alkali contents, plus very low Ca and high LOI. Again, alteration of these samples is suspected, with F770.79 probably being the most altered sample. The effects of alteration are difficult to evaluate. Most of the Coppermine River area samples cluster together, and perhaps this cluster does reflect the original rock composition. If so, it is considerably different from the other Vaillant, and the Akaitcho Group lavas, and may be a hawaiite, or a basaltic andesite.

One rhyolite has been analyzed from the Vaillant Formation (Table 4.3). It is similar to the other Akaitcho Group rhyolites, and is intercalated with basalts at Vaillant Lake.

In summary, there may be two lava types present in the Vaillant Formation. One type is similar to the Akaitcho Group lavas and may be an oceanic basalt. The other type is unusual, and may be a basaltic andesite. All Vaillant Formation samples have been affected by some sort of carbonatization; and as a result, firm conclusions about the original chemistry of these rocks cannot be made. Correlation of the Akaitcho Group and the Vaillant Formation relies entirely on lithologic similarities. The lack of any

Table 4.3 Representative chemical analyses of Vaillant Formation mafic rocks. Major elements in wt.%, trace and rare-earth elements in ppm.

Coppermine River area

	F770.79	F771.79	F775.79	F777.79
SiO ₂	45.0	52.9	42.0	45.4
TiO ₂	2.42	3.38	3.74	3.55
Al ₂ O ₃	13.0	12.1	13.6	13.7
Fe ₂ O ₃ ^t	14.12	15.70	20.0	17.0
MnO	0.19	0.18	0.39	0.36
MgO	6.03	4.00	7.72	6.52
CaO	10.76	4.12	4.47	5.35
Na ₂ O	0.31	4.64	2.21	3.88
K ₂ O	0.47	0.09	1.42	0.86
P ₂ O ₅	0.22	0.33	0.46	0.35
L.O.I.	6.58	2.31	3.85	2.95
Total	99.10	99.75	99.86	99.96
Nb	38	60	67	60
Zr	184	283	304	271
Y	50	73	84	71
Sr	233	86	56	84
Rb	13	1	22	11
Pb	7	7	11	6
Zn	108	165	244	194
Cr	115	0	0	0
V	367	504	660	593
Ba	133	14	689	406
Y/Nb	1.3	1.2	1.3	1.2
La	24.2	38.9	31.2	32.9
Ce	61.6	95.8	85.8	88.2
Pr	7.6	10.2	10.8	10.9
Nd	32.6	45.9	48.6	50.6
Sm	8.0	10.4	11.6	12.2
Eu	2.0	3.5	2.8	3.4
Gd	7.8	10.6	12.5	12.1
Dy	8.0	10.9	12.8	12.0
Ho	1.1	2.3	2.4	2.5
Er	4.1	6.3	6.9	6.7
Yb	6.3	4.7	5.7	5.6
ΣREE	164	211.4	232	238
La/Yb	3.8	6.8	5.5	5.9
Ce/Yb	9.8	20.4	15.1	15.8

Table 4.3 continued

Stanbridge Lake area

	F138.78	F139.78	F142B.78
SiO ₂	48.9	45.6	52.1
TiO ₂	1.13	1.26	1.79
Al ₂ O ₃	13.15	14.09	13.10
Fe ₂ O ₃ ^t	10.38	13.91	10.38
MnO	0.17	0.19	0.12
MgO	6.51	7.27	1.39
CaO	11.08	11.82	17.50
Na ₂ O	2.6	1.7	0.0
K ₂ O	0.26	0.49	0.18
P ₂ O ₅	0.15	0.08	0.23
L.O.I.	4.18	3.28	3.4
Total	98.46	99.69	100.19
Nb	5	8	18
Zr	61	79	170
Y	30	26	36
Sr	139	165	570
Rb	7	10	5
Pb	4	4	6
Zn	90	109	43
Cr	110	100	65
V	307	336	290
Ba	177	350	70
Y/Nb	6	3.3	2.0
La	6.1	5.4	22.4
Ce	20.3	16.3	54.3
Pr	2.8	1.9	6.5
Nd	12.0	10.1	29
Sm	3.7	3.2	7.3
Eu	1.3	1.4	1.7
Gd	4.3	3.8	7.5
Dy	5.4	4.3	6.5
Ho	1.1	0.9	0.9
Er	2.7	2.3	3.3
Yb	3.4	1.6	1.4
ΣREE	63.4	51.6	141.2
La/Yb	1.8	3.4	16
Ce/Yb	6	10	39

Figure 4.26 Y versus Zr plot for Vaillant Formation lavas. Vaillant samples are from Stanbridge Lake (open boxes), Vaillant Lake (crosses), and the Coppermine River, at $66^{\circ}32'N$ (open triangles). Note difference between the Coppermine River and the other samples. Also note scatter compared to Belleau volcanic complex basalts.

Figure 4.27 Rb versus Sr plot for Vaillant Formation lavas. Symbols as in Figure 4.26. Note low Sr values of most Vaillant Formation samples. Field of Belleau basalts is shown for comparison.

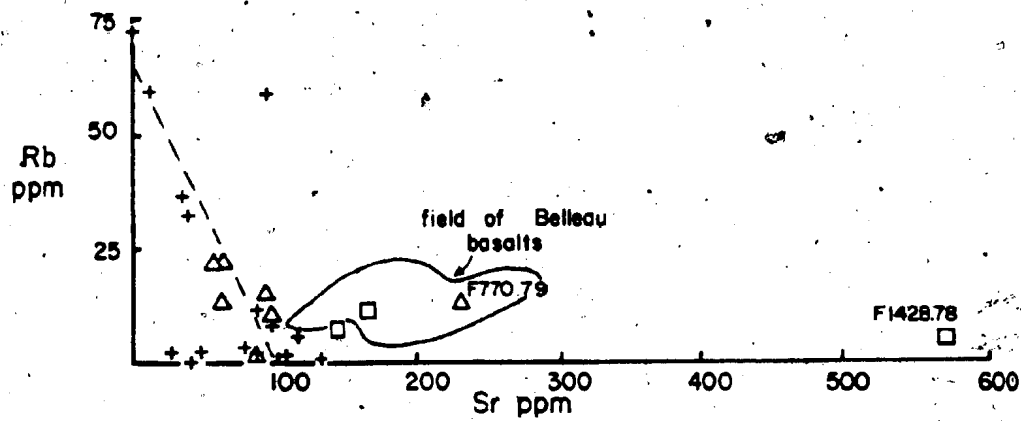
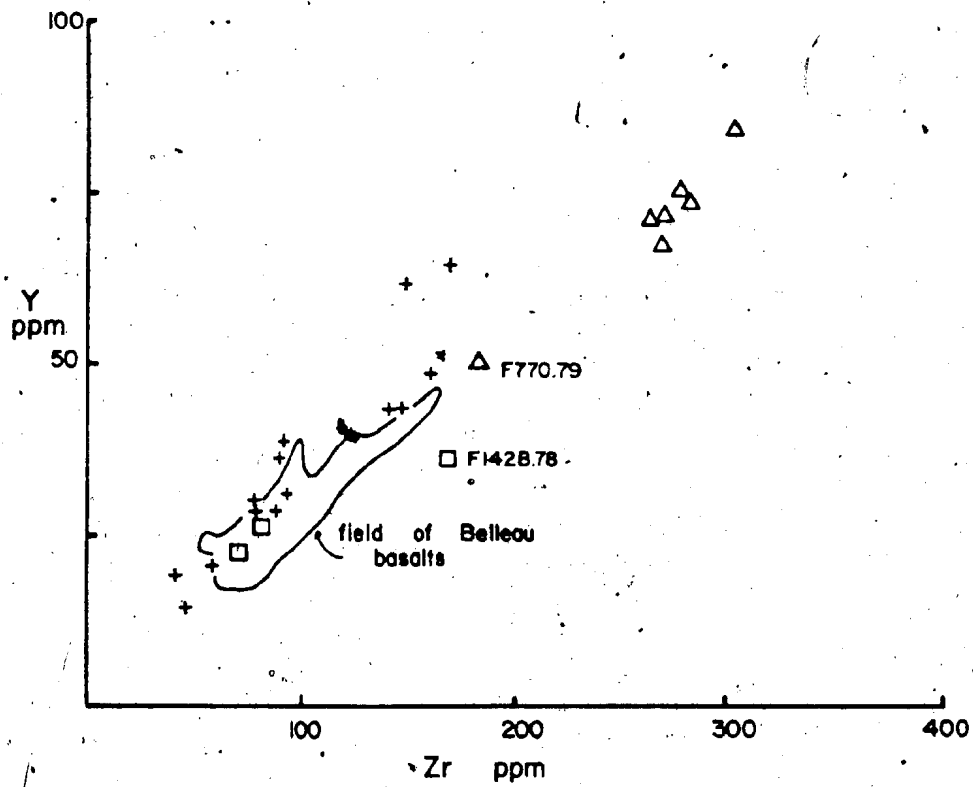
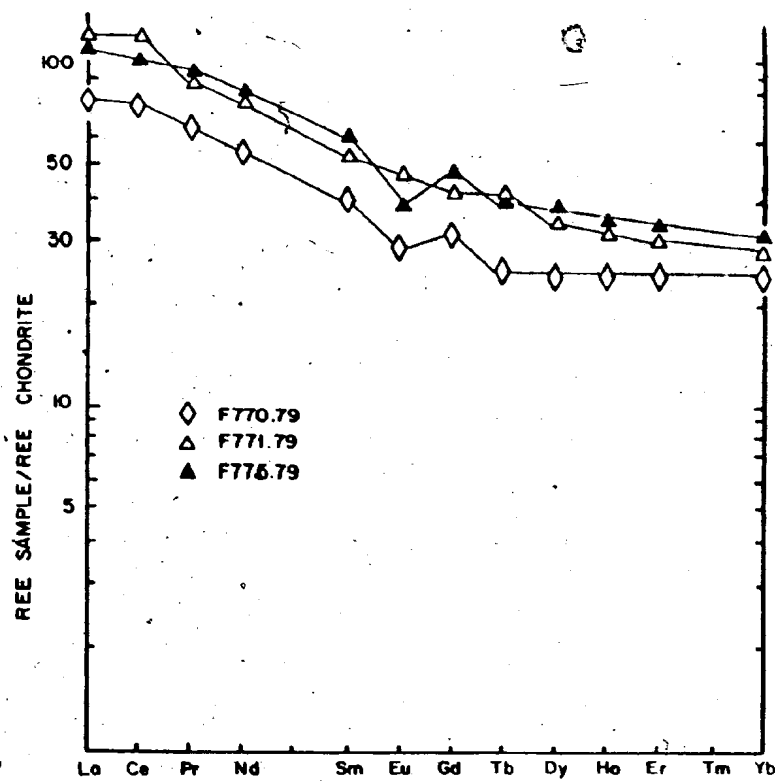
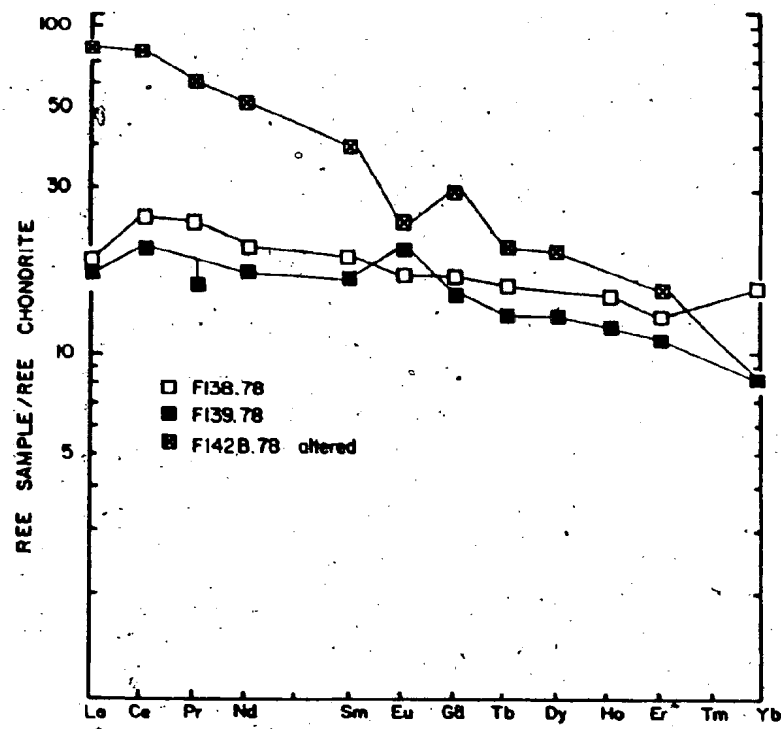


Figure 4.28 (Left) Chondrite-normalized REE patterns for Vaillant Formation samples from Stanbridge Lake. F142B.78 is severely altered in comparison to samples F138.78 and F139.78.

Figure 4.29 (Right) Chondrite-normalized REE patterns for Vaillant Formation samples from the Coppermine River at 66°42'N. Sample F770.79 is the most altered of the three samples. Samples F772.79, F776A.79, F776B.79, and F777.79 (not shown) have REE patterns and abundances similar to samples F771.79 and F775.79. Note that the REE patterns for the Vaillant Lake samples are different from those shown in Figure 4.28.



noticable alteration effects in the remainder of the Akaitcho Group indicates that the conclusions based on the geochemistry of the bulk of the Akaitcho Group samples are valid.

4.3 SEDIMENTARY ROCKS

4.3.1 Introduction

Fine grained sedimentary rocks are relatively abundant in the Akaitcho Group, mainly in the Ipiutak and Grant Subgroups, and the Aglerok Formation. These rocks are excellent indicators of metamorphic conditions, but provide little visible evidence of their source region. Knowledge of the source region for these sedimentary rocks would provide further constraints on the development of the Akaitcho Group.

One way of tackling the problem of source region for these rocks is to look at bulk rock geochemistry. Unfortunately, many factors affect the chemical composition of clastic sedimentary rocks. Some of these factors include:

- i) the average composition of the source rocks,
- ii) weathering processes,
- iii) transportation processes and sorting,
- iv) diagenesis, and
- v) metamorphism

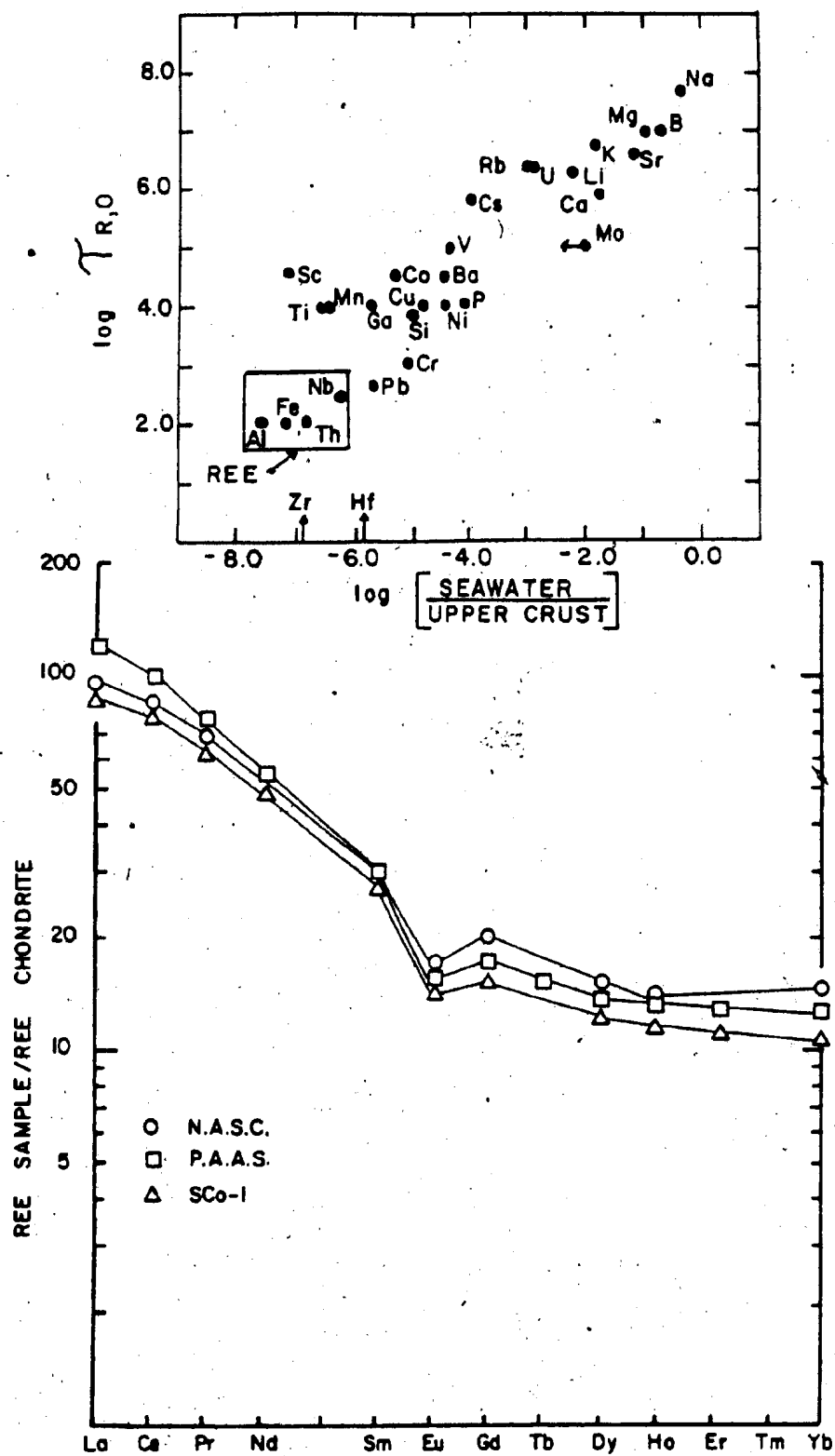
Some elements are affected by these processes more than others. For instance, elements such as the alkalies and the alkaline earths go easily into solution during weathering and diagenesis. Thus, their abundances in clastic sediment-

ary rocks do not reflect the composition of their source rocks in any simple manner. On the other hand, elements with the lowest concentrations in seawater relative to crustal abundances, such as REE, Th, Sn, Zr, Hf, Nb, Fe and Al are transferred more directly into clastic sediments and preserve a record of the source rock composition (McLennan, 1981) (Figure 4.30). Most common sedimentary and metamorphic processes do not affect the REE distribution in sedimentary rocks (McLennan, 1981). McLennan (1981) provides a detailed review of the behavior of the REE in the sedimentary cycle.

Mudstones are the best choice after tillites when attempting to estimate the chemical composition of the source region. This is due to the fine grain size and homogeneous condition of mudstones. The use of mudstones in examining the chemical composition of the source region has been well documented over the past several years (Haskin and Haskin, 1966; Haskin et al., 1966; McLennan, 1981; McLennan and Taylor, 1980a,b; McLennan et al., 1979, 1980; McLennan and Taylor, 1980a,b,c; Nance and Taylor, 1976, 1977; Taylor and McLennan, 1981b; Taylor, 1964, 1977, 1979; Wildeman and Haskin, 1973) and it has become widely accepted that the average REE pattern in sedimentary rocks reflects the REE abundances of the exposed continental crust (op. cit.). In addition, it has been recognized that post-Archean sedimentary rocks worldwide have similar REE patterns (McLennan, 1981) (Figure 4.31). In the light of

Figure 4.30 Plot for several elements of log residence time in seawater ($\log T_{R,0}$) versus log [concentration in seawater/concentration in upper continental crust]. Adapted from McLennan (1981). Elements with the lowest concentration in seawater, relative to their crustal abundances (REE, Th, Sn, Zr, Hf, Nb, Al, Fe, Ti) have the greatest potential for being transferred directly into clastic sediments and preserving a record of upper crustal composition.

Figure 4.31 Chondrite-normalized REE patterns of some post-Archean shales. N.A.S.C. - North American shale composite, Haskin *et al.* (1966); P.A.A.S. - Post-Archean Australian Shale, Nance and Taylor (1976), McLennan (1981); SCo-1, United States Geological Survey standard rock, Cody Formation shale (Cretaceous), McLennan and Taylor (1980).



these studies, sedimentary rocks from the Akaitcho Group were analyzed for REE concentrations in order to place further constraints on their provenance.

4.3.2 Lower Akaitcho Group Sedimentary Rocks

The sediments of the Ipiutak Subgroup and the Zephyr Formation and its correlative units constitute the lower sedimentary sequence of the Akaitcho Group. The arkosic sediments in the Zephyr Formation and orthoquartzite locally present in the Ipiutak and Grant Subgroups suggest derivation of the sedimentary rocks from an adjacent continental terrane.

The REE contents of the Ipiutak and Grant Subgroups, and the Zephyr Formation sedimentary rocks confirm what is known about the provenance of these rocks (Figure 4.32, 4.33, Table 4.4). Figure 4.32 shows pelitic rocks from the Ipiutak Subgroup and the lower Zephyr Formation. The patterns are typical of post-Archean sedimentary rocks (e.g. Figure 4.31, 4.34). Sample R90A.79 is a mafic tuff in the Ipiutak Subgroup, and although quartz-rich in thin-section it has distinctly different REE and other trace element abundances from the other samples (Table 4.4, Figure 4.34). Rocks of the Zephyr Formation are shown in Figure 4.33. Sample F28.78 is an arkosic turbidite. The high total REE abundances are consistent with the arkosic nature of this sample. Sample F319A.79 is an orthoquartzite from the Zephyr Formation near Kapvik Lake. The abundance of quartz in this sample lowers the total REE abundances, and apatite

Table 4.4 Representative chemical analyses of Akaitcho Group sedimentary rocks. Major elements in wt.%, trace and rare-earth elements in ppm.

	Zephyr Formation			Ipiutak Subgroup	
	arkose F443.80	arkose F28.78	arkose F521.79	pelite F709.79	mafic tuff R90A.79
SiO ₂	70.4	79.1	74.3	66.7	65.4
TiO ₂	0.77	0.50	0.18	0.66	0.69
Al ₂ O ₃	12.3	8.0	13.4	14.2	14.3
Fe ₂ O ₃ ^t	6.10	3.70	1.69	5.49	0.8
MnO	0.06	0.05	0.03	0.08	0.08
MgO	2.85	1.36	0.99	1.37	2.80
CaO	0.40	0.61	trace	1.66	0.38
Na ₂ O	1.49	1.59	1.98	2.16	1.96
K ₂ O	3.14	1.91	5.34	4.32	3.42
P ₂ O ₅	0.16	0.13	0.01	0.23	0.12
L.O.I.	2.72	1.46	1.50	2.04	3.01
Total	100.39	98.41	99.42	98.91	100.01
Nb	11	10	38	18	16
Zr	169	188	224	207	176
Y	33	30	119	46	37
Sr	6	121	34	106	63
Rb	140	130	236	190	172
U	7	4	6	8	4
Th	10	17	37	24	18
Pb	6	21	22	28	11
Zn	84	68	46	84	76
Cr	54	127	0	26	90
V	126	112	0	66	158
Ba	469	445	459	706	641
La		46.8		43.8	10.4
Ce		99.9		103.2	30
Pr		11.2		11.5	4
Nd		36.6		44.2	17.8
Sm		5.8		8.5	4.3
Eu		0.98		0.84	0.84
Gd		3.9		7.1	4.7
Dy		3.8		6.8	5.0
Ho		0.84		1.4	0.9
Er		1.9		3.3	2.4
Yb		2.5		2.6	1.9
ΣREE		214.9		233.9	82.9
La/Yb		18.7		16.9	5.5
Eu/Eu*		0.60		0.32	0.57

Table 4.4 continued

Aglerok Formation

	pelite F454.80	pelite F359.79	pelite F785.79	pelite F791.79	pelite F793.79
SiO ₂	74.1	61.2	60.8	61.9	62.2
TiO ₂	0.49	0.78	0.89	0.71	0.69
Al ₂ O ₃	12.7	19.0	17.0	17.4	18.0
Fe ₂ O ₃ ^t	2.11	6.86	6.79	7.16	7.24
MnO	0.05	0.12	0.16	0.10	0.10
MgO	2.24	2.45	3.23	3.14	2.64
CaO	0.34	0.43	1.71	0.80	0.53
Na ₂ O	2.61	1.55	1.31	2.00	1.98
K ₂ O	2.55	4.07	4.68	3.83	4.50
P ₂ O ₅	0.10	0.09	0.09	0.07	0.08
L.O.I.	2.38	2.87	2.59	2.61	2.57
Total	99.67	99.42	99.25	99.72	100.53
Nb	14	20	16	16	18
Zr	136	166	161	166	149
Y	33	43	37	27	44
Sr	22	67	62	51	92
Rb	118	165	232	134	207
U	0	7	12	3	4
Th	14	27	21	15	19
Pb	0	25	22	9	36
Zn	75	91	112	88	136
Cr	56	84	82	102	92
V	72	124	128	130	131
Ba	372	760	572	707	800
La	17.9	28.1	14.1	13.3	16.4
Ce	41.8	70.7	38.6	38.6	45.1
Pr	5.2	8.4	4.6	4.4	5.2
Nd	20.7	33.2	18.7	17.2	21.8
Sm	4.2	6.9	3.9	3.5	4.7
Eu	0.73	1.3	0.71	0.91	0.94
Gd	3.6	5.3	4.0	2.8	4.0
Dy	3.6	5.8	3.6	3.0	3.8
Ho	0.7	0.8	0.6	0.5	0.5
Er	1.9	2.1	2.4	1	1.4
Yb	1.7	1.7	1.8	1	1.7
ΣREE	101.7	165	93.5	87	106.2
La/Yb	10.5	16.5	7.8	10	9.7
Eu/Eu*	0.57	0.62	0.55	0.88	0.65

Table 4.4 continued

	Aglerok Formation			Grant Subgroup	
	siltstone F182.79	felsic pelites F408.78	F482.80	pelite F6.80	pelite F283.80
SiO ₂	66.2	76.1	61.3	57.9	62.1
TiO ₂	0.69	0.16	0.64	0.78	0.78
Al ₂ O ₃	15.2	11.2	14.9	18.7	18.1
Fe ₂ O ₃ ^t	5.66	2.54	9.21	8.86	7.08
MnO	0.05	0.02	0.16	0.09	0.06
MgO	2.49	3.22	3.53	3.05	2.34
CaO	1.42	0	0.45	0.91	0.57
Na ₂ O	2.73	0.20	1.22	1.85	2.00
K ₂ O	3.64	3.29	4.44	4.68	4.14
P ₂ O ₅	0.09	0.01	0.15	0.06	0.06
L.O.I.	1.81	24.71	3.12	2.20	2.34
Total	99.98	99.45	99.12	99.08	99.57
Nb	16	21	16	19	18
Zr	190	223	183	169	156
Y	23	67	44	41	34
Sr	90	181	25	96	112
Rb	152	11	196	239	202
U	5		10	2	3
Th	17		17	15	17
Pb	1022	29	15	13	17
Zn	1821	95	113	121	98
Cr	71	3	70	95	90
V	109	4	123	126	129
Ba	506	227	575	788	804
La	9.3	25.2		24.7	25.6
Ce	25.2	78.8		61.1	61.6
Pr	3.4	7.6		7.4	7.1
Nd	13.3	29.1		28.6	27.5
Sm	2.7	6.7		5.6	5.3
Eu	0.72	0.84		0.78	0.95
Gd	2.4	6.5		4.3	4.3
Dy	2.3	8.4		3.2	3.6
Ho	0.3	1.8		0.6	0.8
Er	1.5	4.3		1.7	2.3
Yb	1.1	5.1		1.1	1.9
ΣREE	62.5	175.1		140	142
La/Yb	8.5	4.9		22.5	13.5
Eu/Eu*	0.85	0.39		0.50	0.61

Figure 4.32 Chondrite-normalized REE plot for pelitic sedimentary rocks of the Ipiutak Subgroup. Except for R90A.79, a mafic tuff, the patterns are typical of post-Archean sedimentary rocks.

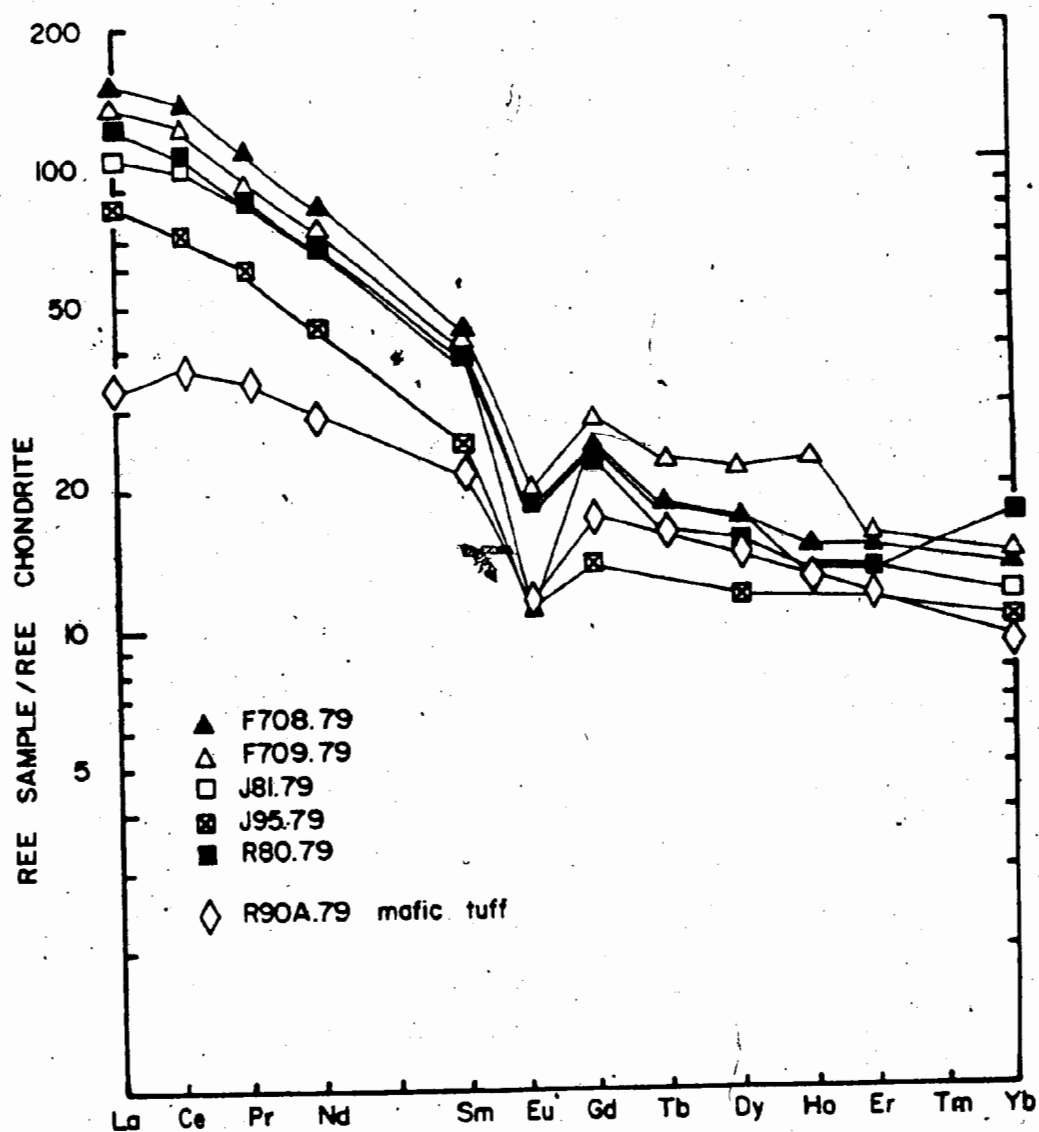


Figure 4.33 Chondrite-normalized REE plot for pelites of the Grant Subgroup, and Zephyr Formation arkoses.

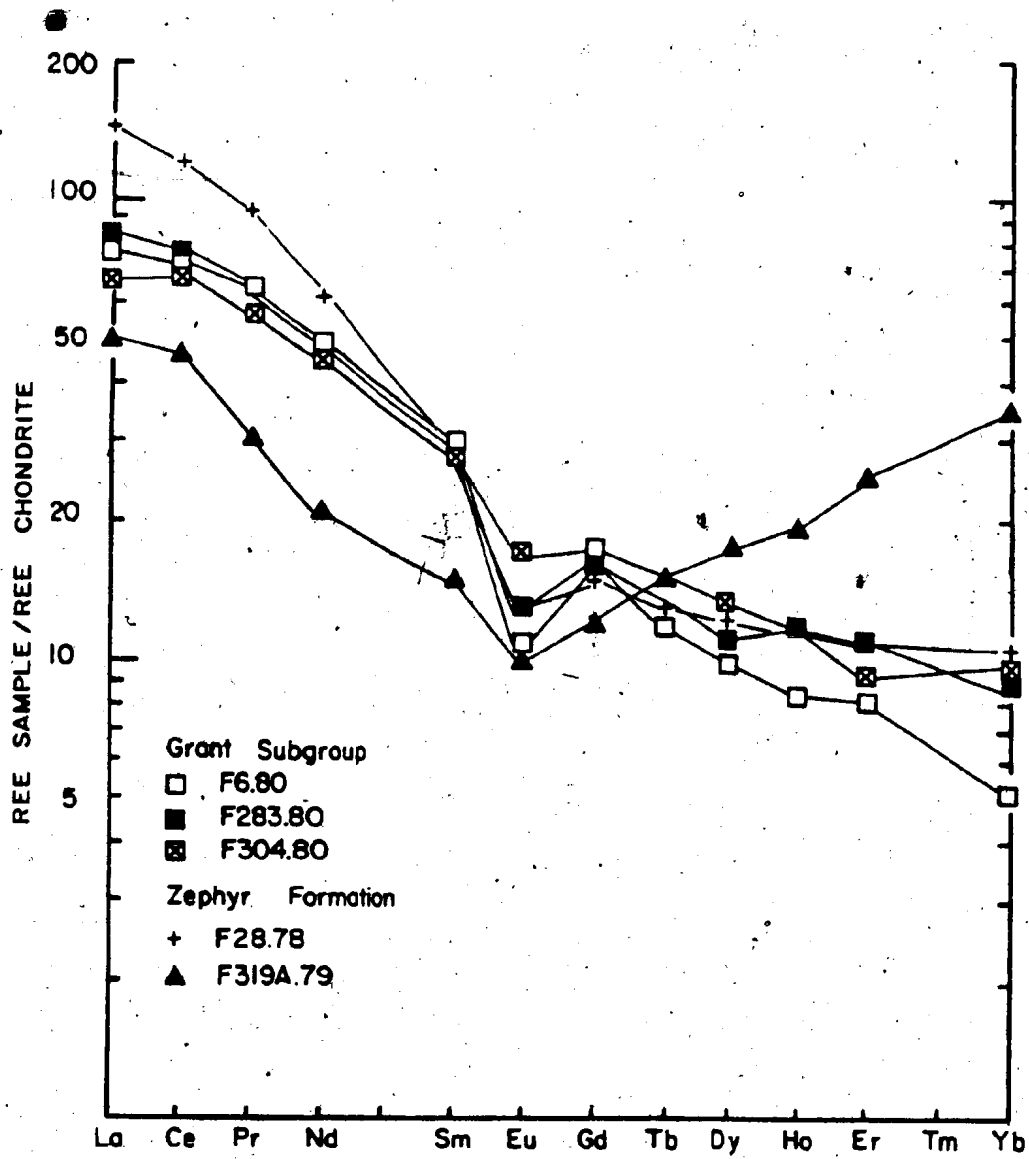
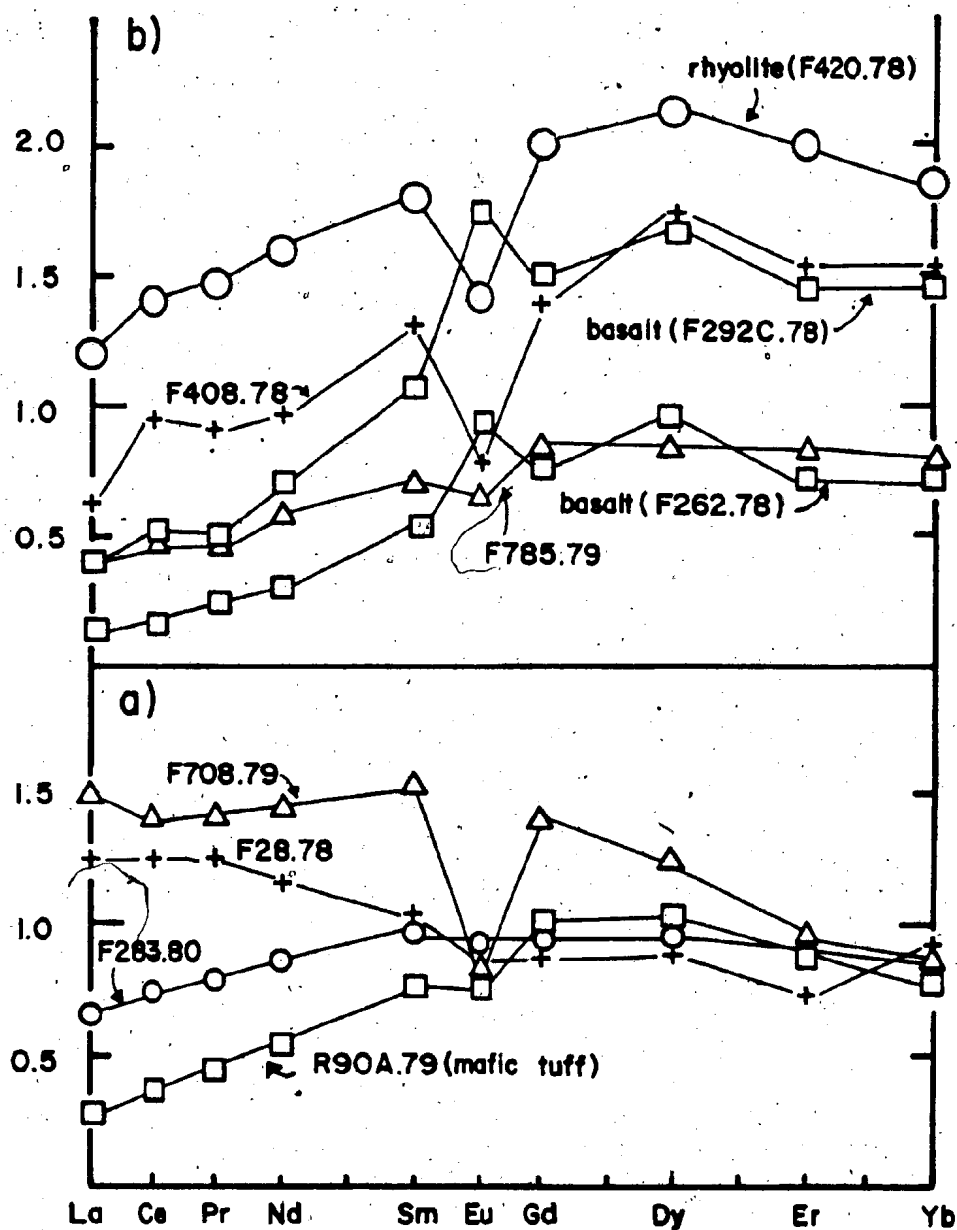


Figure 4.34 REE abundances in Akaitcho Group sedimentary rocks normalized to P.A.A.S. (post-Archean Australian Shale composite, Nance and Taylor, 1976; McLennan, 1981).

a) Representative Ipiutak Subgroup pelite

- (F708.79), Zephyr arkose (F28.78), and Grant Subgroup pelite (F283.80) normalized to PAAS. These samples illustrate the range in observed variation in lower Akaitcho Group sedimentary rocks. Note that R90A.79, a mafic tuff, has much lower LREE abundances than the sedimentary rocks.

b) Representative rhyolite (F420.78), continental basalt (F262.78), and oceanic basalt (F292C.78) normalized to PAAS. Sample F785.79 is a typical Aglerok Formation pelite. Note much lower abundances than PAAS and sedimentary rocks in the lower figure. Sample F408.78 is a felsic tuffaceous pelite. Note similarity in pattern to the rhyolite, and the high HREE abundances present in this sample. F408.78 is interpreted to have Akaitcho Group rhyolites as a major (40 to 50%) component of its source region.



and zircon in the sample account for the high HREE abundances in this sample. The Grant Subgroup is correlated with the Zephyr Formation (Figure 3.3). The REE patterns of siltstones and mudstones from the Grant Subgroup are also shown in Figure 4.33, and are typical of post-Archean sedimentary rocks (Figure 4.34), and indicative of a source terrane - the exposed continental crust - of overall granodioritic composition.

In summary, the REE data are consistent with the limited geological evidence (Chapter 3.3.2) that the lower sedimentary sequence was derived from an adjacent continental terrane. And, as we shall see, the REE content of the lower sedimentary sequence rocks are different from those observed in the upper sedimentary sequence.

4.3.3 Upper Akaitcho Group Sedimentary Rocks

In the upper Akaitcho Group, the majority of the sedimentary rocks are fine-grained, and there is little control on their provenance. Many of the sediments are found adjacent to volcanic complexes, and it is suspected that some of the sediments were derived from the volcanic complexes (Chapter 3.3.5). If the volcanoes made a significant contribution to these sediments, it should be observed in the REE abundances and patterns of the sedimentary rocks.

Figure 4.35 and Table 4.5 show the REE content of typical Aglerok Formation pelites. The patterns are typical of post-Archean sedimentary rocks, but total REE abundances

are variable, and in some samples, the Eu anomaly is less pronounced than in the sediments examined so far.

The range of mafic volcanoclastic pelites in the Aglerok Formation (Chapter 3.3.5) is shown in Figure 4.36. The range of the mafic pelites overlaps that of continental tholeiites of the Akaitcho Group. The close similarity suggests that the continental tholeiites may have made some contribution to the sedimentary rocks of the Aglerok Formation. There is a problem though. The continental tholeiites are lower in the stratigraphy than the oceanic tholeiites. If basalts made a contribution to the Aglerok Formation, the oceanic tholeiites would be a more likely source. However, a mixture of oceanic tholeiite and rhyolite would produce a pattern similar to that observed in the mafic tuffaceous pelites, and both are likely source rocks. Sediments derived from a source terrane of granodioritic composition, mixed with oceanic basalts would also produce the observed REE patterns in the mafic tuffaceous pelites. Ni and Cr contents of the Akaitcho Group basalts are low, and cannot be used to confirm a basaltic contribution. Ti/Al ratios are high in the Aglerok Formation pelites (Figure 4.37), and indicate that some contribution from the mafic volcanic centres has occurred. Thus, the geochemical results are consistent with the sedimentological evidence (Chapter 3.3.5) that basalts from the volcanic centres did contribute detritus to the Aglerok Formation, but were not the only source rock.

Data for felsic tuffaceous pelites is shown in Figure 4.38. They differ from the normal and mafic pelites in having slightly higher LREE abundances, and much higher HREE abundances. As shown in Figure 4.38, the upper range of the felsic tuffaceous pelites is similar to the REE pattern of the Akaitcho Group rhyolites. The high HREE content of the felsic tuffaceous pelites indicates that the rhyolites made a significant contribution to the felsic tuffaceous pelites, as there is no other known source rock containing high levels of HREE in the area. Again, the observed REE patterns in the felsic pelites could be mixtures of a) rhyolite and continental and oceanic basalts, b) rhyolite and continent-derived sediments, or c) a and b. Nevertheless, the Akaitcho Group rhyolites did contribute material to the Aglerok Formation.

In summary, the REE results for the Aglerok Formation indicate that volcanic rocks in the Akaitcho Group did contribute to the Aglerok Formation, although they were not the dominant source rock. The REE results are consistent with the field observations on the Aglerok Formation that indicate a similar conclusion (Chapter 3.8).

4.3.4 Upper Akaitcho/Lower Epworth Groups

Three samples obtained from the lower Odjick Formation and the uppermost Akaitcho Group have unusual REE patterns (Figure 4.39). The low total REE abundances of the rocks could be due to the silty nature of the samples, although samples S68.79 and F36.79 are not noticeably richer in

Table 4.5 Comparison of several post-Archean shale composites

UNIT	LREE/HREE	Eu/Eu*	ΣREE (in ppm)
ERTS (Odjick, Fontano, Asiak, Takiyuak)n=9	9.7 ± 2	0.63 ± 0.05	144 ± 32
UAS (Upper Akaitcho shale)n=8	8.5 ± 2	0.75 ± 0.05	120 ± 30
LAS (Lower Akaitcho shale)n=8	9.8 ± 2	0.66 ± 0.05	180 ± 45
PAAS (post-Archean Australian shales) (McLennan, 1981)	9.7 ± 2	0.67 ± 0.05	171 ± 41
NASC (North American shale composite) (Haskin <u>et al.</u> , 1966)	7.5 ± 2	0.66 ± 0.05	166 ± 38
SCo-1 (Cody shale, Cretaceous)	9.3 ± 2	0.88 ± 0.05	148 ± 33

Figure 4.35 Chondrite-normalized REE plot for eight
Aglerok Formation pelites.

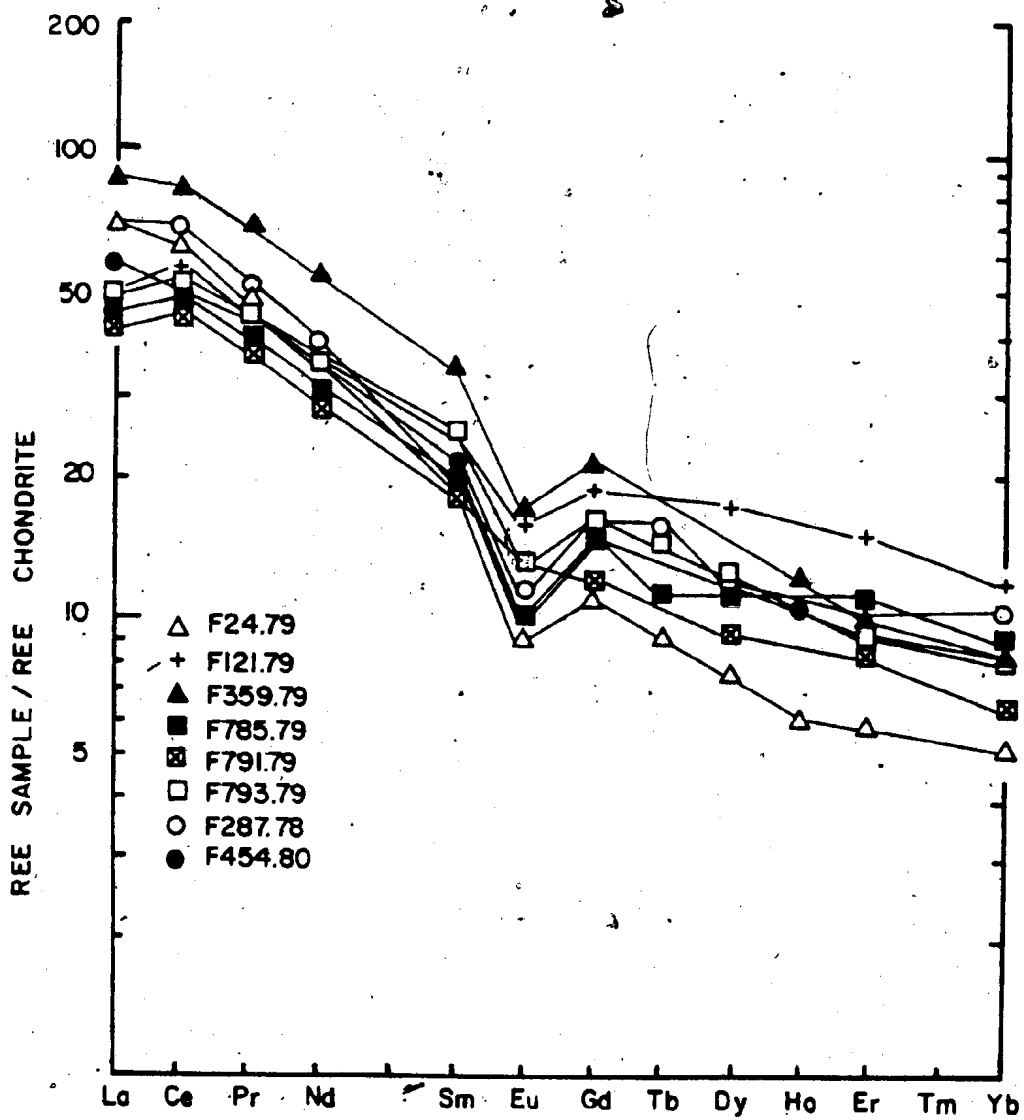


Figure 4.36 Chondrite-normalized REE plot showing range of five mafic tuffaceous pelites of the Aglerok Formation. Range of continental and oceanic basalts from the Kapvik volcanic complex are shown for comparison.

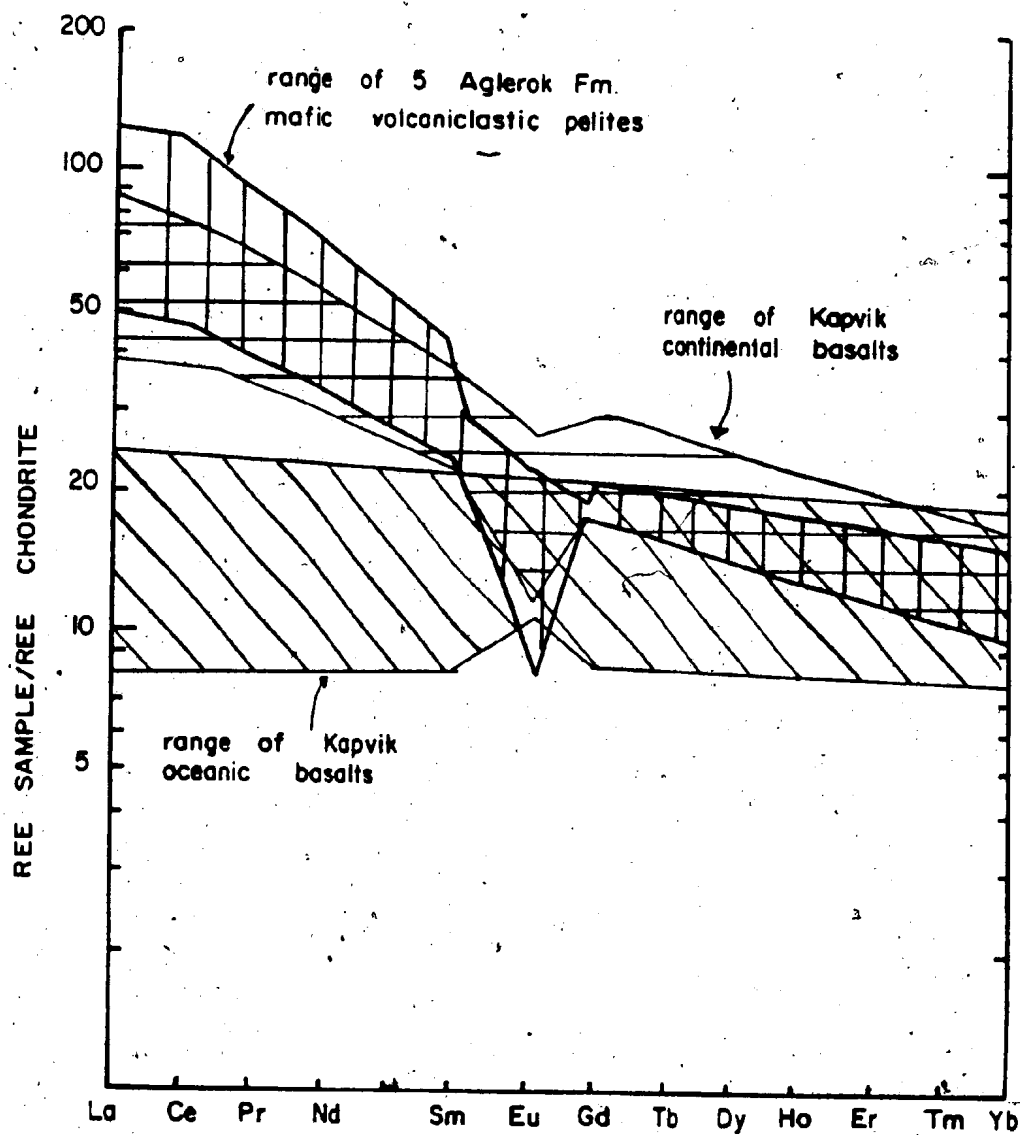


Figure 4.37 TiO_2 versus Al_2O_3 for Akaitcho Group sedimentary rocks. Symbols: Aglerok Formation pelites (+); Aglerok Formation felsic pelite (†); Zephyr Formation arkose (Δ); Zephyr Formation quartzite (\blacktriangle). Values for average basalt, granite, and continental crust from Taylor (1964). Note: felsic pelite has Ti/Al ratio similar to granitic rocks. Arkoses have Ti/Al ratios similar to average continental crust. Aglerok Formation pelites have Ti/Al ratios similar to a mixture of 3 parts granite to 1 part average Akaitcho continental basalt; or, to a mixture of 1 part granite and 1 part average Akaitcho oceanic basalt. The latter mixture is more likely because of the location of oceanic basalts high in the stratigraphic section.

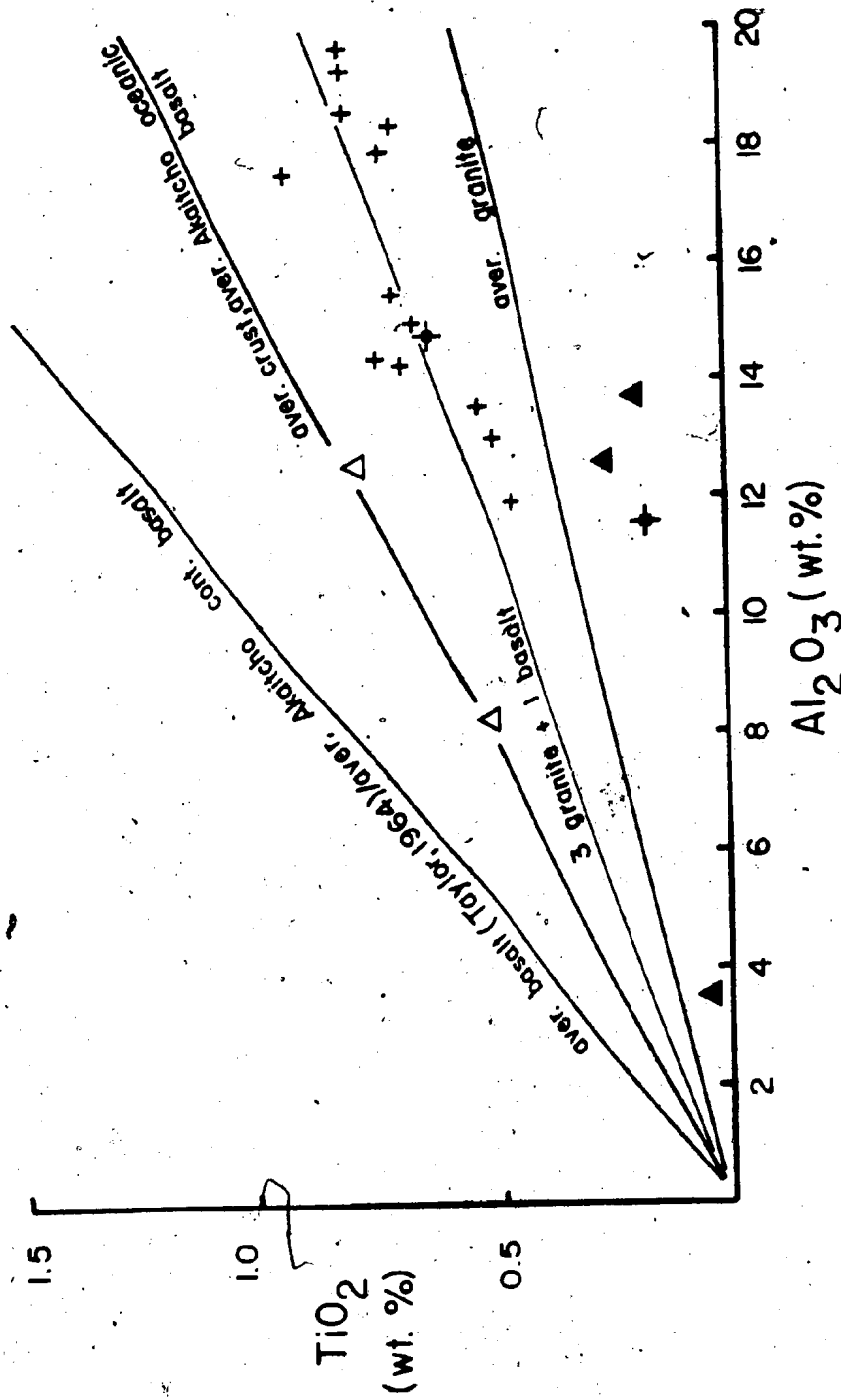


Figure 4.38 Chondrite-normalized REE plot for felsic
volcaniclastic pelites of the Aglerok Formation.
Note high HREE content of the felsic tuffaceous
pelites and the close correspondence of the
upper range of the felsic tuffaceous pelites
with the average Akaitcho Group rhyolite.

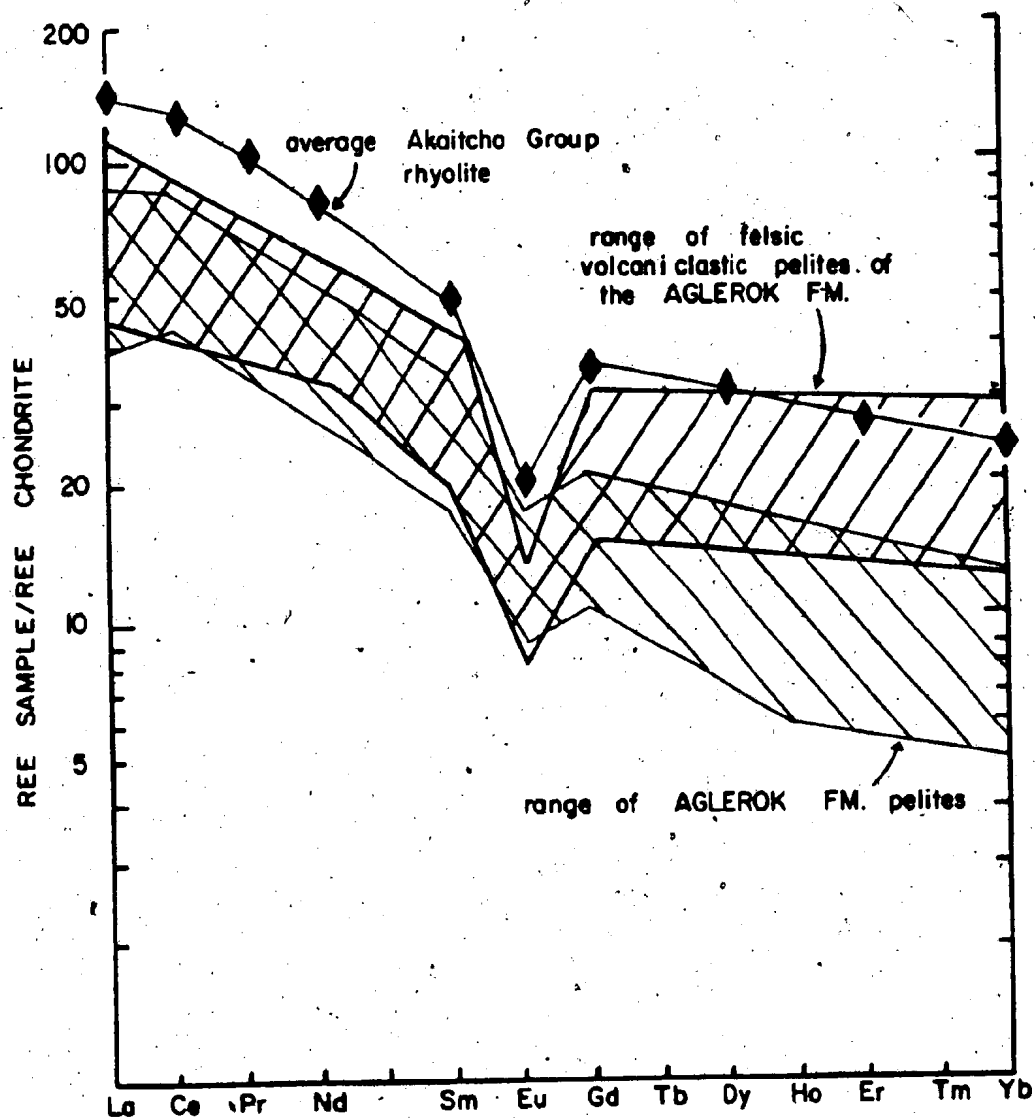
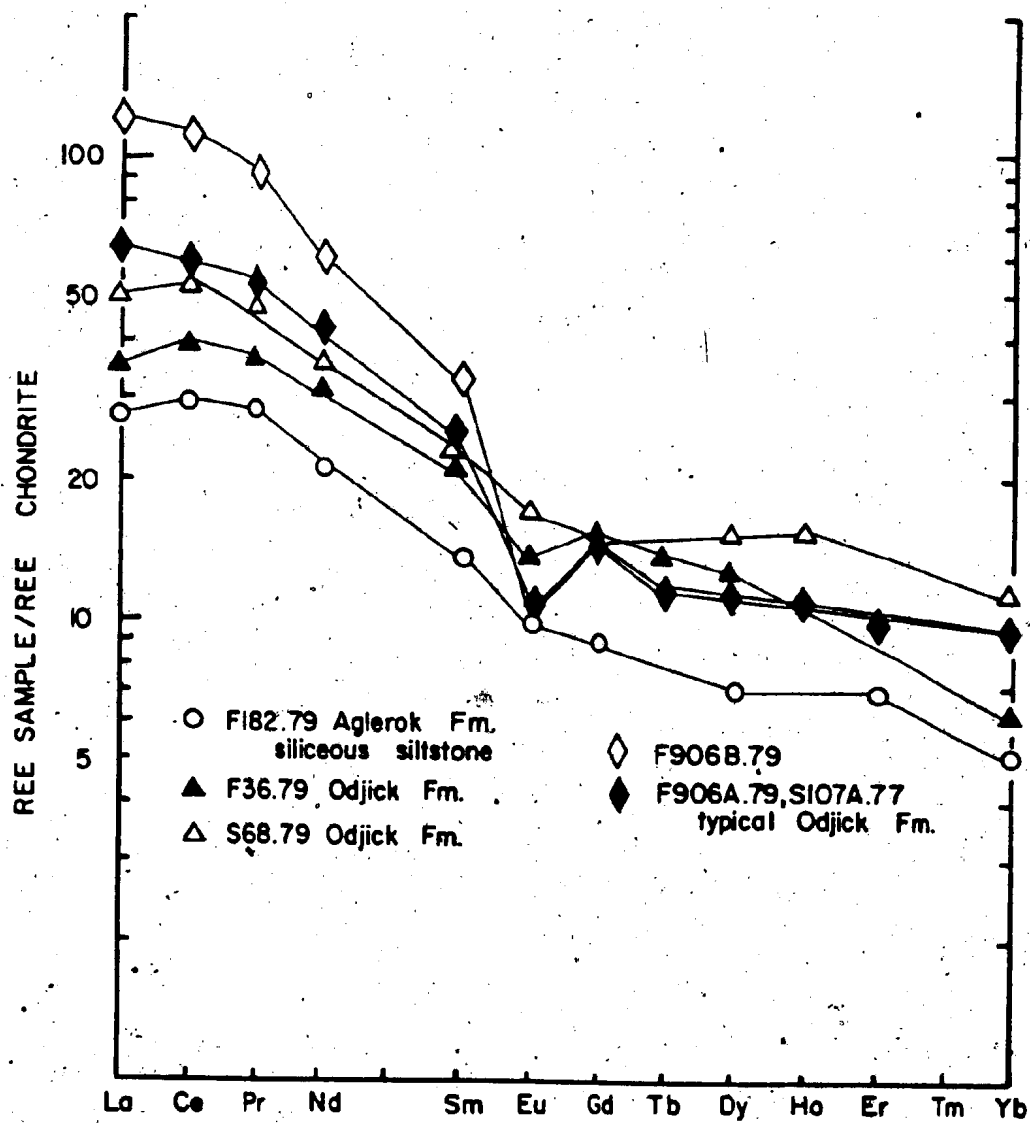


Figure 4.39 Chondrite-normalized REE plot of Odjick Formation pelites. Samples F182.79, F36.79, S68.79 are from the base of the lower Odjick Formation and the uppermost Akaitcho Group. They have only slight Eu anomalies and have relatively low total REE abundances. The two Odjick Formation samples (F36.79, S68.79) are more similar to the Aglerok Formation siliceous siltstone (F182.79) than the typical Odjick Formation samples. This may indicate that samples F36.79 and S68.79 had a source region somewhat in common with the upper Akaitcho Group.



quartz than F906A.79, which has a more typical post-Archean sedimentary rock REE pattern and abundances. Thus, these samples record some effect of the Akaitcho Group volcanic complexes which results in lower total REE abundances and lower Eu/Eu*. This effect may be localized, as the Odjick Formation typically has post-Archean sedimentary rock REE abundances consistent with derivation of this unit from the Slave Craton to the east (Figure 2.4).

4.3.5 Effects of Metamorphic Grade

No effect of metamorphic grade on the REE pattern or abundances could be observed in samples from a traverse across closely spaced isograds (Figure 4.40). Similar results were obtained by Cullers *et al.* (1974) and McLennan (1981).

4.3.6 Comparison with Other Post-Archean Sedimentary Rocks

Figure 4.41 compares the REE patterns and abundances of the lower Akaitcho Group sedimentary rocks, the upper Akaitcho Group sedimentary rocks, a composite of Epworth and Recluse Group and Takiyuak Formation shales, and the post-Archean Australian shale composite (PAAS - Nance and Taylor, 1976; McLennan, 1981). All four composites are similar, although the upper Akaitcho Group shales are distinctly lower in total REE. The latter, as discussed, indicates a contribution of the Nasittok Subgroup volcanic rocks to the Aglerok Formation.

4.4 SUMMARY

The geochemical studies reveal three main facts.

- Figure 4.40 a) Chondrite-normalized REE plot for three Aglerok Formation pelites sampled across closely spaced isograds. No noticeable effect of metamorphism can be observed in these samples.
- b) Sample location map for Aglerok Formation pelites plotted in Figure a).

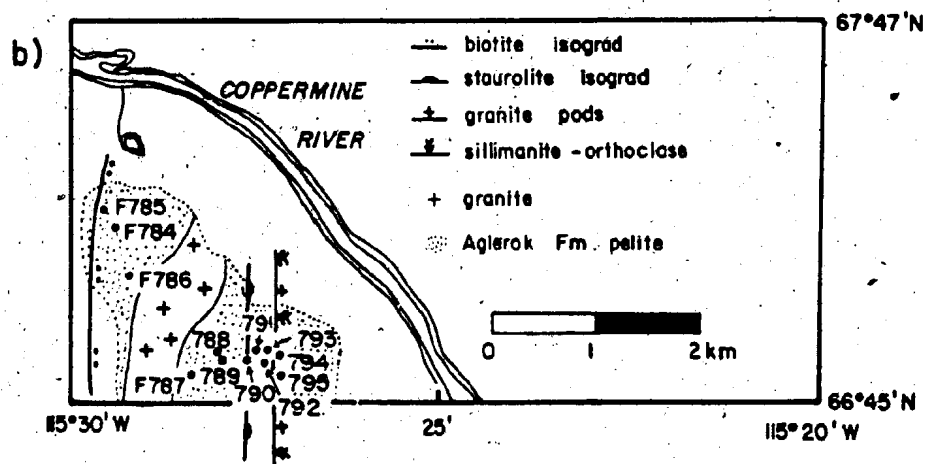
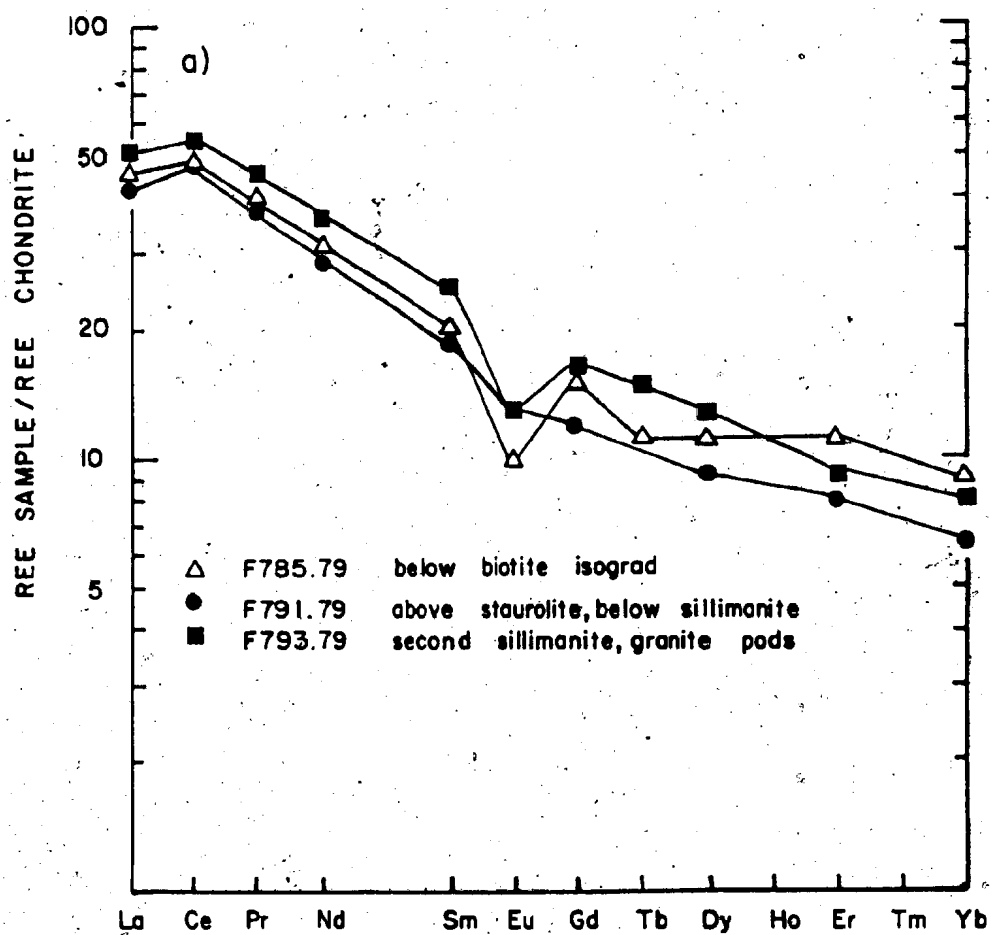
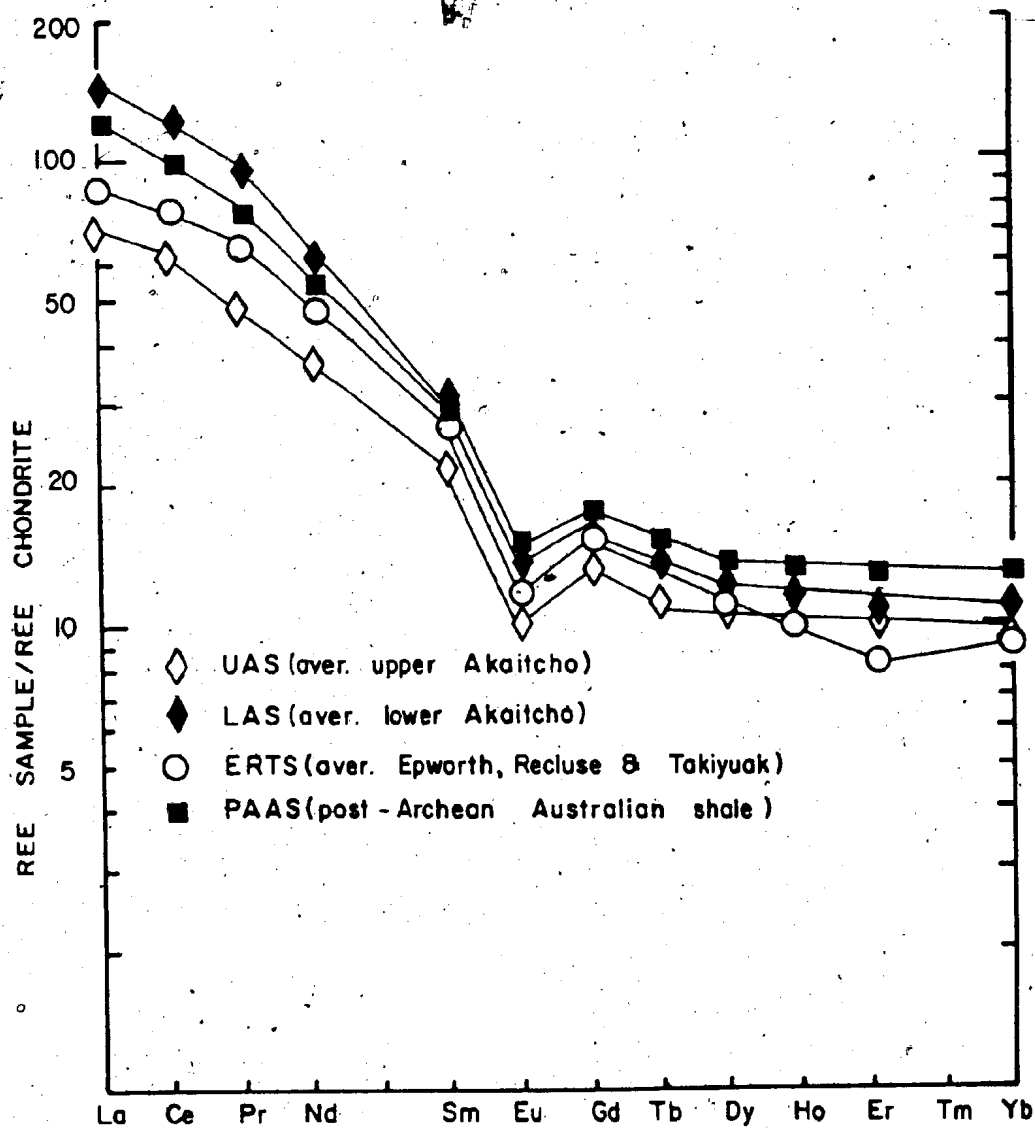


Figure 4.41 Chondrite-normalized REE plot for sedimentary rocks of the Wopmay Orogen. Abbreviations: UAS (average Aglerok Formation pelite - upper Akaitcho Group); LAS (average Ipiutak Subgroup and Zephyr Formation - lower Akaitcho Group); ERTS (average Odjick Formation, Recluse Group, and Takiyuak Formation shales); PAAS (average post-Archean Australian Shale, Nance and Taylor, 1976; McLennan, 1981).



First, the chemistry of the basaltic rocks evolves up-section from continental to type II ocean tholeiites. Second, the rhyolites are of crustal origin, and are high in the stratigraphic section. And, third, the sedimentary rocks indicate that a continental source area was present throughout Akaitcho Group deposition, although in the upper Akaitcho Group, the Nasittok Subgroup volcanoes were also an important sedimentary source. All of these observations are consistent with sedimentological and stratigraphic evidence indicating that the Akaitcho Group was deposited in a rift.

CHAPTER 5

ISOTOPE GEOCHEMISTRY AND THE AGE OF
THE AKAITCHO GROUP5.1 INTRODUCTION

The Sityok Igneous Complex, Vaillant Formation basalts, a Belleau volcanic complex basalt, a mylonite from the Wopmay Fault Zone, an Okrark rhyolite sill, a Tuertok volcanic complex rhyolite, and a post-metamorphic granite of the Hepburn Batholith were selected for Rb-Sr whole-rock dating. All of these units had good geological control, and reliable age determinations on these units would place constraints on the evolution of the Akaitcho Group. Except for the basaltic rocks and the mylonite zone, all units were also dated by the U-Pb zircon method by W.R. Van Schmus and S.A. Bowring at the University of Kansas. The U-Pb samples were collected by, or with, the author from the same outcrops as the Rb-Sr samples.

The Rb-Sr results from all the units indicate that a major disturbance of the Rb-Sr isotopic system occurred within Zone 3 of the Wopmay Orogen. The U-Pb results, presumably more reliable, indicate that the first Wilson cycle in the Wopmay Orogen occurred over a very short time interval - on the order of 10 Ma. This chapter discusses the Rb-Sr results, the distribution and significance of the isotopic disturbance, and the effect, if any, of this event on the geochemistry of the Akaitcho Group. Finally, the various age constraints on the Akaitcho Group

are reviewed, as are some of the implications arising from the U-Pb zircon dates.

5.2 Rb-Sr DATING

Details of the analytical procedures, sample locations, and analytical results are presented in Appendix B.

Isochrons are calculated using a slightly modified version of the program of Brooks et al. (1972). All errors are reported at 2 sigma (95% confidence level) unless otherwise indicated. Decay constants used are those recommended by Steiger and Jäger (1977). Rb-Sr dates from the literature have been recalculated to these constants, and K-Ar dates determined prior to 1977 have been corrected using the tables of Dalrymple (1979). The term errorchron is used in the sense of Brooks et al. (1972).

5.3 SITIYOK COMPLEX

All three units of the Sityok Complex - the tonalite gneiss, the monzogranite and the amphibolite dykes - were sampled and analyzed for Rb and Sr. Results of isochron regressions of the samples are given in Table 5.1 and Figure 5.1.

Gneiss

Ten samples of various phases of the gneiss were collected from one outcrop and analyzed for Rb and Sr. The six felsic phases define an errorchron date of 1880 ± 160 Ma (Table 5.1). Elimination of the high point (F610.80) and a slightly weathered sample (F612.80) gives an errorchron date of 1885 ± 34 Ma (Table 5.1). The four mafic samples of

the gneiss define an isochron date of 1597 ± 142 Ma (Table 5.1), which, although not statistically different from the errorchron date for the six felsic samples, does suggest some disturbance of the Sr isotopic system in the gneiss. Evidence for resetting of Sr isotopes is provided in the plots of Rb and Sr versus model age (Figure 5.2a, 5.2b). There is a positive correlation between Rb and Sr contents and model age. This is a common occurrence in reset isotopic systems (Bickford and Mose, 1975; Page, 1976). In addition, high Rb/Sr ratio samples such as F610.80 fall below the errorchron line, an indication of Sr loss (Page, 1976, 1978). The scatter of the samples on the isochron plot (Figure 5.1), the high C.S.D.F. (Chi squared/degrees of freedom = M.S.W.D. (mean square of the weighted deviates)), and the correlation between Rb and Sr and model age indicates that either there was incomplete homogenization of Sr isotopes during formation of the gneiss, or that the Sr isotopic system was reset by a later event. The latter interpretation is favoured because all the Sityok units show evidence for Sr isotopic disturbance.

Monzogranite

The monzogranite was sampled at two outcrops. Outcrop 1 is 100 m west of the outcrop from which the gneiss samples were collected, and is near the margin of the Complex. The six samples from outcrop 1 give an isochron date of 1716 ± 92 Ma (Table 5.1). Elimination of the high point which falls below the isochron has little effect, giving a date of

1745 \pm 106 Ma. These dates are close to the average K-Ar biotite dates of metamorphic and plutonic rocks in Zone 3, and does not agree with the field evidence (Chapter 3.2) indicating that the Sityok Complex is pre-metamorphic. Samples from outcrop 1 show a correlation between Sr and Rb and model age (Figure 5.2a, 5.2b), indicating that resetting of the isotopic system has probably occurred.

Samples from outcrop 2 show no correlation between Rb and Sr and model age, but when regressed give errorchron dates with Sr_i (Sr initial ratio) below 0.690, the value for BABI (basaltic achondrite at 4.6 Ga) (Basaltic Volcanism Study Project, 1981), clearly an unlikely result. Again, resetting of isotopic systems is suggested. The points do, however, fall on an 1840 Ma reference line with Sr_i of 0.700. A zircon sample collected by the author from the monzogranite at outcrop 2 gives a date of about 1885 Ma (W.R. Van Schmus and S.A. Bowring, personal communication, 1981).

All 10 monzogranite samples give an errorchron date of 1862 \pm 80 Ma (Table 5.1). The high Rb/Sr ratio samples plot below the errorchron. Although the samples from outcrop 2 give an Rb-Sr date close to the zircon date, both are anomalous. In addition, without knowledge of the geological relations in the area, or the zircon dates, it would be difficult to interpret the Rb-Sr data obtained from the monzogranite samples.

Amphibolite Dykes

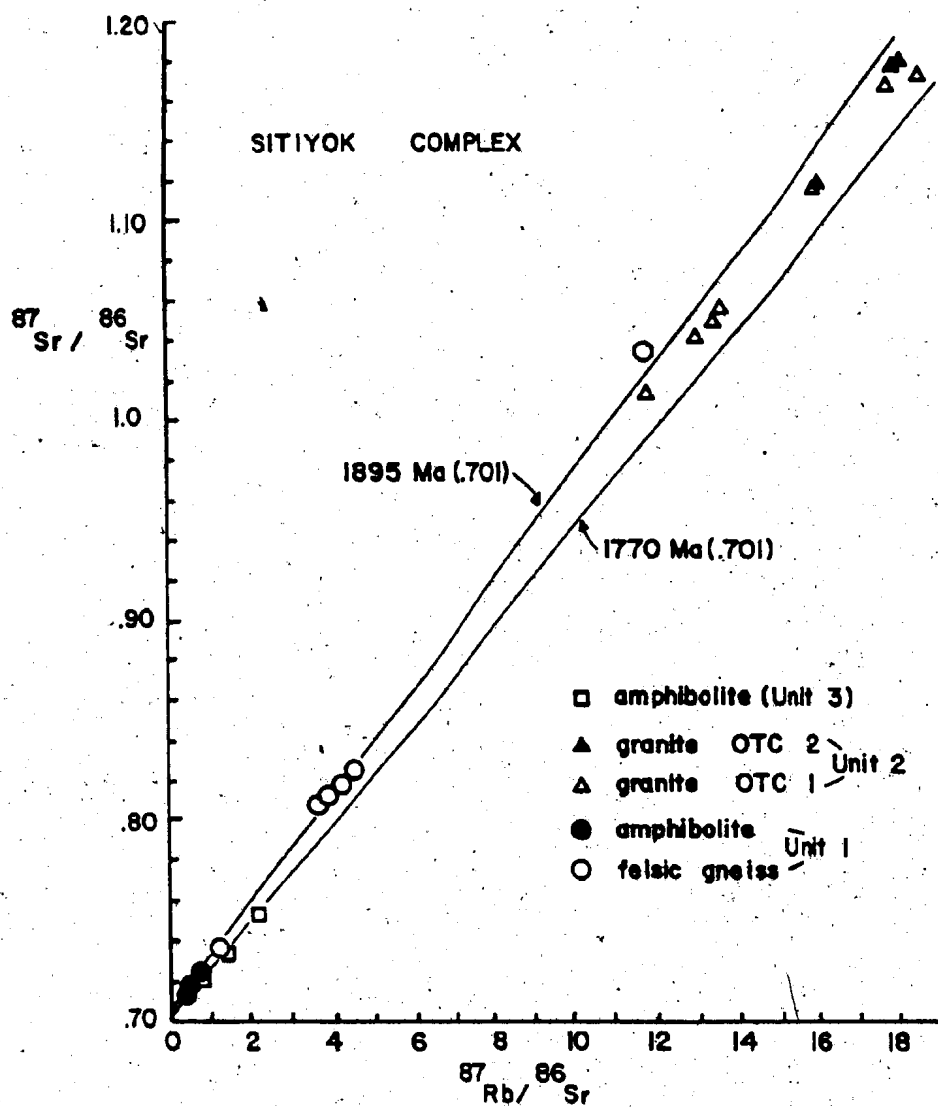
Only three samples of the amphibolite dykes were

Table 5.1 Isochron regressions for samples from the Sityok Igneous Complex. Data in Appendix B.

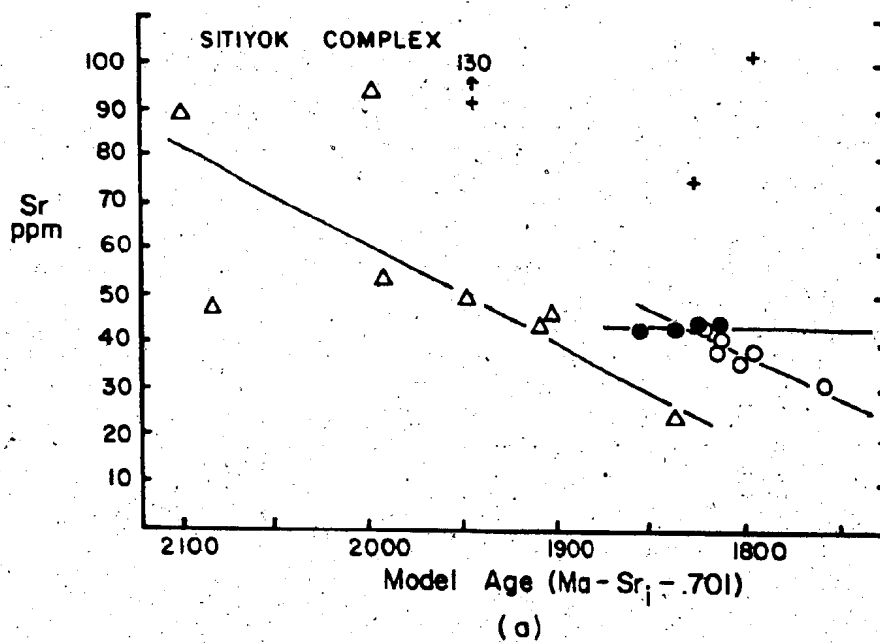
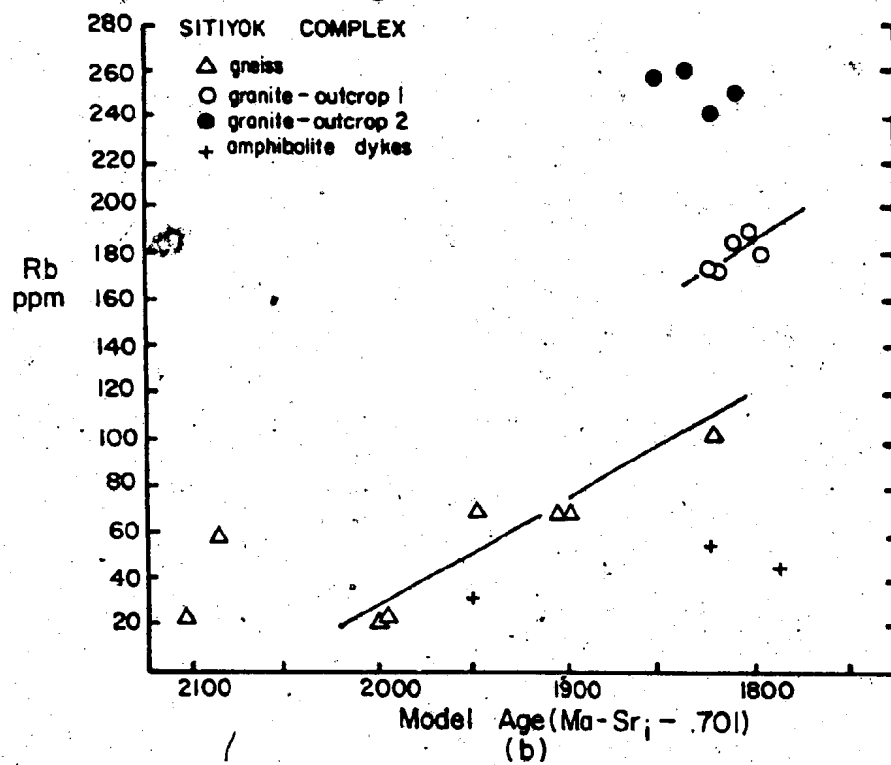
ISOCHRON REGRESSION					
	number of samples	CSDF*	Date (Ma)	Initial $^{87}\text{Sr}/^{86}\text{Sr}$	Comment
Sityok Gneiss (Unit 1)					
mafic	4	1.5	1597 ± 142	0.7066 ± 0.0014	- isochron
felsic	6	171	1880 ± 160	0.7050 ± 0.0080	- errorchron
felsic	4	5.2	1885 ± 34	0.7030 ± 0.0016	- errorchron; high point (F610.80) and weathered sample (F612.80) removed
Sityok Granite (Unit 2)					
OTC 1	6	3.6	1716 ± 92	0.7185 ± 0.018	- F608A.80 removed
	5	3.4	1745 ± 106	0.7130 ± 0.02	
OTC 2	4	4.0	1984 ± 132	0.6610 ± 0.032	
OTC 1 and 2	10	8.8	1862 ± 80	0.6900 ± 0.0180	- errorchron
	9	5.9	1883 ± 68	0.6860 ± 0.0150	- errorchron; F608A.80 removed
Gneiss and Granite	20	87	1825 ± 38	0.7048 ± 0.0009	- errorchron
Amphibolite Dykes (Unit 3)	3	19	1710 ± 200	0.7036 ± 0.0036	- errorchron

*Chi Squared/Degrees of Freedom = M.S.W.D.

Figure 5.1 Isochron plot for all analyzed samples of the Sityok Igneous Complex. Isochron regressions for the various phases of the Complex are listed in Table 5.1. The 1895 Ma reference line and the 1770 Ma reference line represent the zircon date of the older phases of the Hepburn Batholith and the mean K-Ar dates from Zone 3 respectively. Most Rb-Sr isotopic systems in Zone 3 have been reset to about 1770 Ma.



- Figure 5.2 a) Plot of Sr versus model age for Sityok
Complex rocks.
b) Plot of Rb versus model age for Sityok
Complex rocks.



analyzed because of the poor results obtained from the two older units of the Sityok Complex. The amphibolite dykes which were sampled cut the monzogranite at outcrop 1. The three samples define an errorchron of 1710 ± 200 Ma (Table 5.1).

In summary, it appears that the Sityok Complex has been disturbed by a later event, an event which has reset Sr isotopic systems to varying degrees in all units. In general, the mafic rocks have been affected to a greater extent than the granitoids. As shown in Figure 5.1, the Sityok samples generally fall between a 1900 Ma and a 1770 Ma reference line, with Sr_i of 0.701. The upper line is the average zircon date for the Hepburn Batholith (Van Schmus and Bowring, 1980), the lower line the average K-Ar biotite date in Zone 3.

5.4 VAILLANT BASALTS

Seven samples from two outcrop areas were chosen for Rb-Sr analysis. All seven points define an isochron of 1758 ± 46 Ma (Table 5.1; Figure 5.3). The four samples from outcrop 2 define an isochron of 1687 ± 52 Ma (Table 5.2). The three samples from outcrop 1 define an isochron of 1779 ± 30 Ma (Table 5.2), although this line is dependent on the high point (Figure 5.3). There is a correlation between Rb and model age for all the samples, and possibly for Sr and model age for the samples from outcrop 2 (inset in Figure 5.1). Carbonate, probably of secondary origin, is abundant in all samples, even in the fresher material

selected for dating. Sr contents in these rocks are low for rocks with the trace element characteristics of the Vaillant basalts, and Sr may have been leached from these basalts. Two samples of Vaillant basalt collected near the Carouse] Massif gave K-Ar biotite dates of 1700 ± 200 Ma (GSC-64-47, Wanless et al., 1965) and 1600 ± 135 Ma (CSC-65-67, Wanless et al., 1966). Archean basement in the Carouse] Massif adjacent to the Vaillant K-Ar samples gave a K-Ar biotite date 1770 ± 135 Ma (GSC-64-46, Wanless et al., 1965). The close correspondence of the Rb-Sr and the K-Ar dates, in addition to the correlation between Rb and model age and the presence of secondary carbonate in the samples indicates that the Rb-Sr isotopic system for the Vaillant basalts has been disturbed by a later event.

5.5 BELLEAU BASALTS

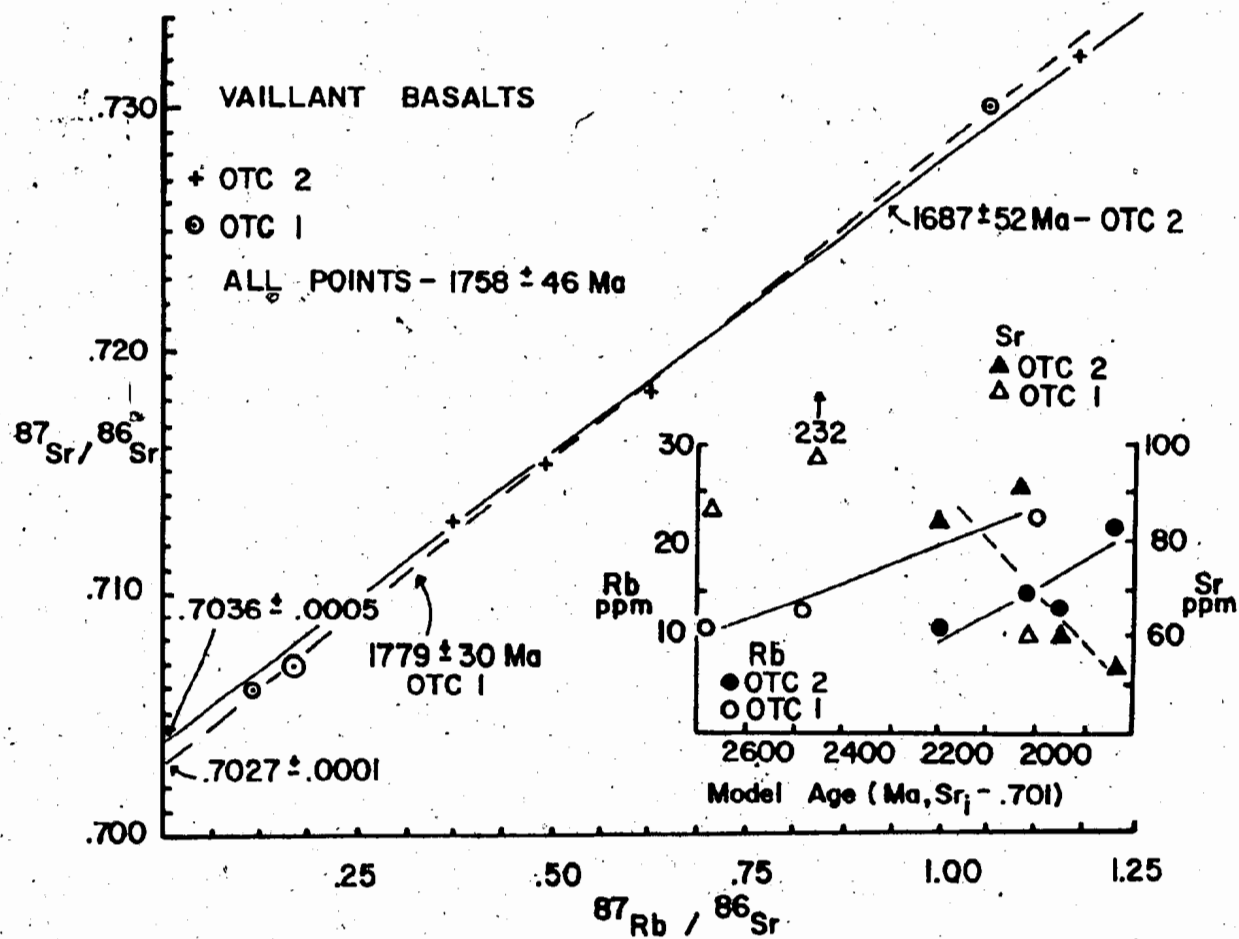
Five samples from one outcrop of the Belleau volcanic complex were selected for Rb-Sr dating. The five samples define an isochron date of 1378 ± 245 Ma (Table 5.2, Figure 5.4). The error is large because of the high analytical error in sample F448.78, and the small spread in the Rb/Sr ratio of the samples. However, the three best points give a similar result of 1390 ± 98 Ma (Table 5.2). There is a correlation between Rb and Sr and model age in the samples (inset in Figure 5.4). The isochron is clearly too young to be an age of emplacement or an age of metamorphism of the Akaitcho Group. The date may reflect late movement along the northwest-trending faults bounding the Belleau volcanic

Table 5.2 Isochron regressions for samples from the Vaillant Formation and the Belleau volcanic complex. Data in Appendix B.

ISOCHRON REGRESSION					
	number of samples	CSDF*	Date (Ma)	Initial $^{87}\text{Sr}/^{86}\text{Sr}$	Comment
Vaillant Formation					
All samples	7	2.2	1758 ± 46	0.7028 ± 0.0002	
OTC 2	4	0.89	1687 ± 52	0.7036 ± 0.0005	
OTC 1	3	1.0	1779 ± 30	0.7027 ± 0.0010	- line dependent on high point
Belleau Basalt					
All samples	5	0.3	1378 ± 245	0.7048 ± 0.0005	- high error in F448.78, small spread in Rb/Sr for 5 samples
Best samples	3	0.5	1390 ± 98	0.7047 ± 0.0002	- points F449, F450, F453

*Chi Squared/Degrees of Freedom = M.S.W.D.

Figure 5.3. Isochron plot for seven samples of the Vaillant Formation. Samples were obtained from two outcrop areas. Inset shows a plot of Rb and Sr versus model age. All samples show a correlation between Rb content and model age, although the two outcrops are distinct. Samples from outcrop 2 may show a correlation between Sr and model age.



complex (Figure 3.28). Late movement along these faults was associated with extension during deposition of the Hornby Bay sandstone (Hoffman, 1980a,b; Hoffman and St-Onge, 1981), and a Hornby Bay sandstone outlier is found adjacent to the Belleau volcanic complex. The age of Hornby Bay sandstone deposition has been estimated to be between 1600 and 1250 Ma (Hoffman, 1980c). The isochron obtained from the Belleau basalts is in rough agreement with this estimate.

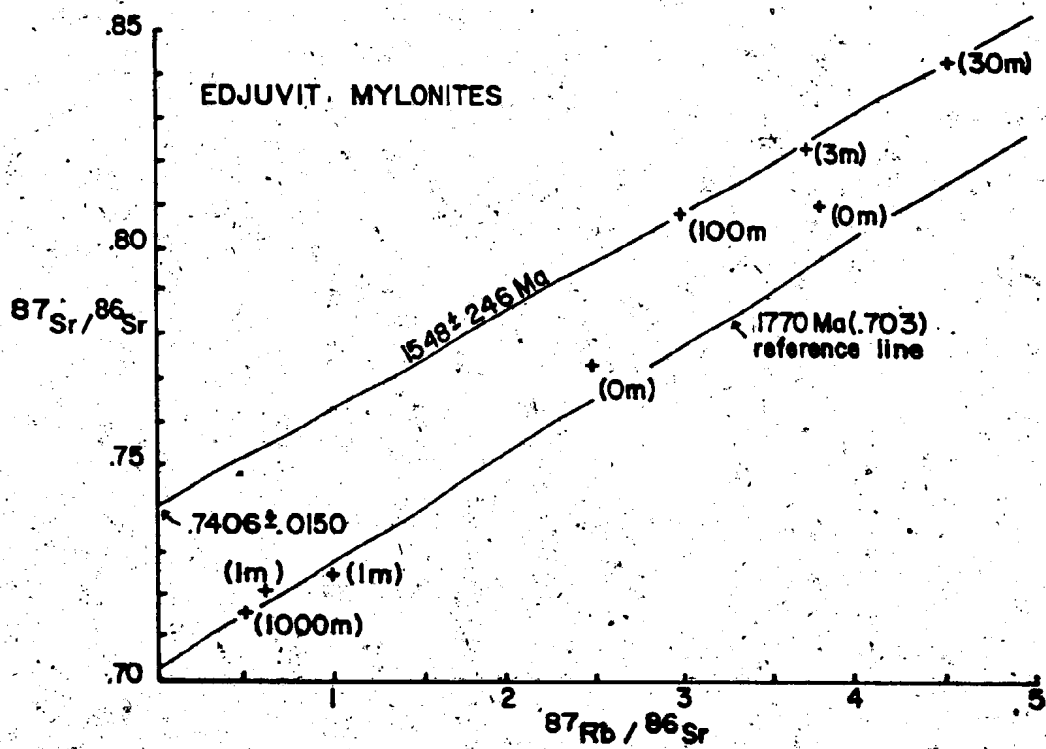
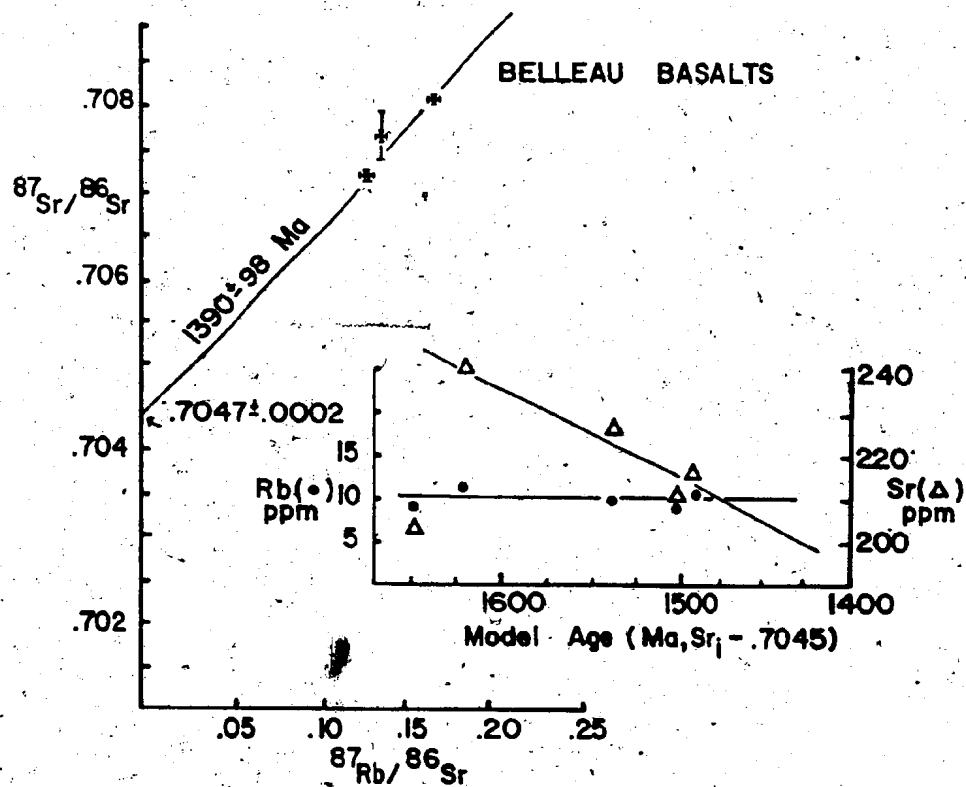
5.6 EDJUVIT MYLONITE ZONE

The date determined for the Belleau basalts indicated that it may be possible to date fault movement in the region. Resetting of Rb-Sr and K-Ar isotopic systems along major fault systems has been documented elsewhere (e.g. Scholz, 1980; Scholz et al., 1979).

Samples were collected from, and adjacent to, the Edjuvit mylonite zone between Grant and Wopmay Lakes. The mylonite zone is a branch of the Wopmay Fault System (Easton, 1981c). There is a wide spread in the data (Figure 5.5). Samples of granite gneiss collected between 3 and 100 m from the fault give a three-point errorchron of 1548 ± 246 Ma, C.S.D.F. = 21, $Sr_i = 0.7406 \pm 0.0150$. The other points are scattered. Rocks from the mylonite zone itself (2 only) define a line of 1952 Ma. No significance can be attached to either of these dates. The 1548 date is, however, close to K-Ar biotite, hornblende and whole-rock dates obtained from samples collected near other branches of the Wopmay

Figure 5.4 Isochron plot for five samples of the Belleau basalt complex. All samples were obtained from one outcrop. Isochron date is for the three best points. All five points give an isochron date of 1378 ± 245 Ma. Inset shows a plot of Rb and Sr versus model age. Both Rb and Sr show a correlation with model age.

Figure 5.5 Isochron plot for samples of the Edjuvit Mylonite Zone. Numbers in brackets beside the data point refer to the distance of the sample from the mylonite zone. A 1770 Ma reference line with Sr of 0.703 is shown.



Fault System in the area (Easton, 1981c). It is suspected that if the 1548 date is significant, then, it may record fluid movement along the fault system associated with extension related to Hornby Bay sandstone deposition.

5.7 OKRARK SILLS

A six-point isochron age of 1881 ± 120 Ma, from samples of the Okrark sills, was reported in Easton (1980). A typographical error resulted in the error being reported as 12 Ma, not 120 Ma. Redetermination of the original sample with improved precision gives an errorchron date of 1766 ± 105 Ma (Table 5.3, Figure 5.6). This errorchron includes three plagioclase- and three orthoclase-porphyritic sills from three outcrop areas. Addition of a sample of high-SiO₂ rhyolite from the lower Kapvik volcanic complex results in little change in the regression (Table 5.3). U-Pb zircon dates from the Okrark sills are in the range of 1900 Ma (W.R. Van Schmus and S.A. Bowring, personal communication, 1981). There is considerable scatter on the Rb and Sr versus model age plots. It is concluded that the errorchron date records a resetting event.

5.8 TUERTOK RHYOLITES

Five samples from a single outcrop define an errorchron of 1736 ± 62 Ma (Table 5.3, Figure 5.7). There is a probable correlation between Rb and Sr and model age. A U-Pb zircon date from the same outcrop is about 1900 Ma, similar to the Okrark sill zircon dates (W.R. Van Schmus and S.A. Bowring, personal communication, 1982). The Okrark sills

and the Tuertok rhyolite are suspected to be coeval (Easton, 1980), hence the correspondence of the zircon dates is not surprising. It is apparent that the Sr isotopic system has been reset, resulting in an Rb-Sr date about 100 Ma younger than the zircon date.

5.9 RIB GRANITE

The Rib Granite is a post-metamorphic pluton of the Hepburn Batholith (Hoffman et al., 1980). Samples were collected from three localities. A preliminary five-point isochron date was reported in Easton (1980) as 1750 ± 52 Ma. Five additional samples have been analyzed since. The ten samples give an isochron date of 1771 ± 36 Ma (Table 5.3, Figure 5.8), statistically indistinguishable from the earlier result. The ten-point isochron includes one slightly weathered sample (F88.79), which cannot be distinguished from the other samples. There is no correlation between Rb or Sr and model age (inset in Figure 5.8). The five samples from one outcrop do not define a line different from the ten-point isochron. The U-Pb zircon date of the Rib Granite is about 1885 Ma (W.R. Van Schmus and S.A. Bowring, personal communication, 1982), roughly 100 Ma older than the Rb-Sr date. The absence of any correlation between Rb and Sr and model age (inset in Figure 5.8) and the low analytical scatter compared with other dated units suggest that the Rib Granite date may be the age of emplacement. If so, then why is the zircon date 100 Ma older? Although the Rb-Sr date could be the age of emplacement of the Rib Granite, this is

Table 5.3 Isochron regressions for samples from the Okrark sills, the Tuertok Rhyolites, and the Rib Granite. Data in Appendix B.

ISOCHRON REGRESSION

	number of samples	CSDf*	Date (Ma)	Initial $^{87}\text{Sr}/^{86}\text{Sr}$	Comment
Okrark sills.	6	19	1766 ± 105	0.7043 ± 0.0070	- errorchron; 3 plagioclase porphyritic, 3 orthoclase porphyritic, from 3 outcrop areas
	7	16	1772 ± 102	0.7046 ± 0.0060	- errorchron; lower Kapvik volcanic complex rhyolite included
Tuertok Rhyolite	5	4.9	1736 ± 62	0.7090 ± 0.006	- errorchron; samples from one outcrop
Rib Granite	10	2.9	1771 ± 36	0.7074 ± 0.0018	- includes F88.79, a weathered sample
Rib and Tuertok	15	3.5	1750 ± 26	0.7083 ± 0.0016	
Rib, Tuertok, Okrark	21	0.9	1747 ± 38	0.7079 ± 0.0032	- errorchron

*Chi Squared/Degrees of Freedom = M.S.W.D.



Figure 5.6 Isochron regression for the Okrark sills.

Figure 5.7 Isochron regression for five samples of the
Tuertok Rhyolite.

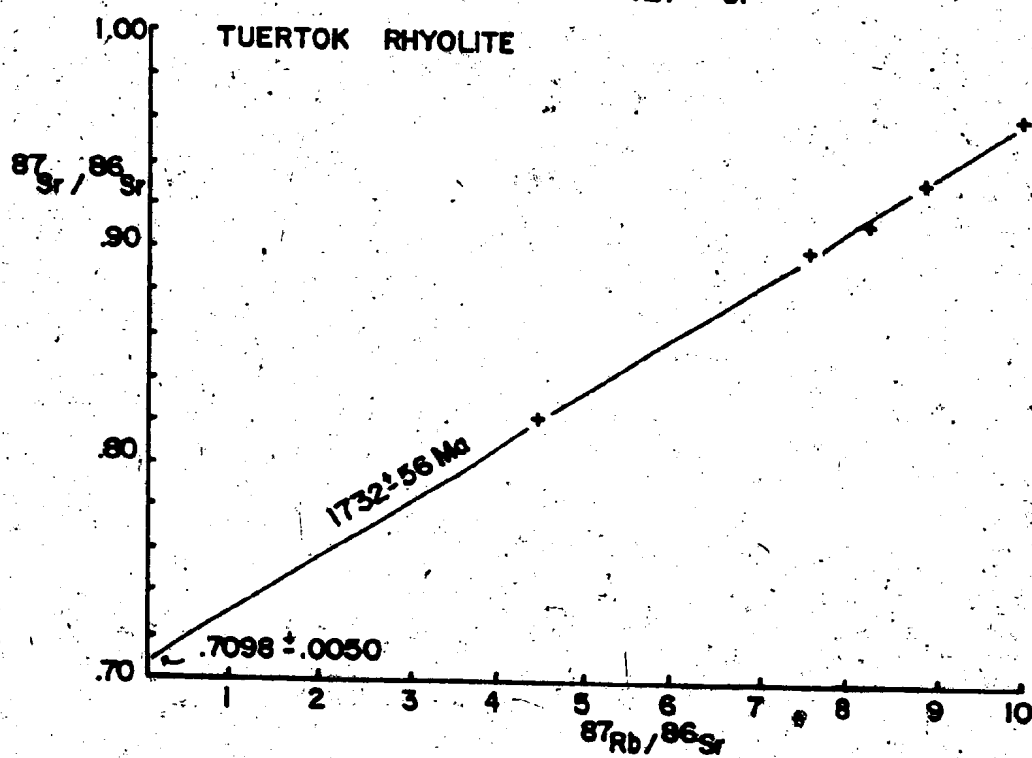
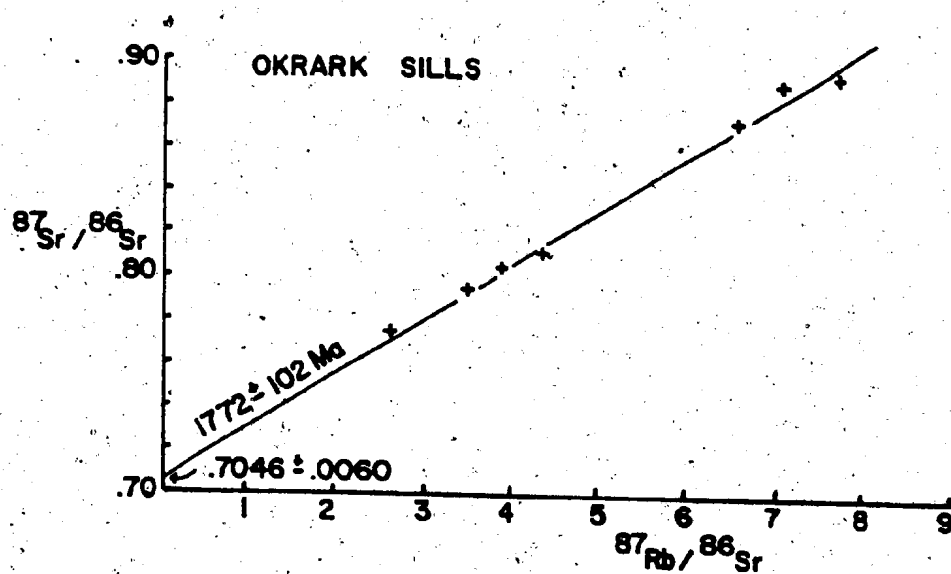
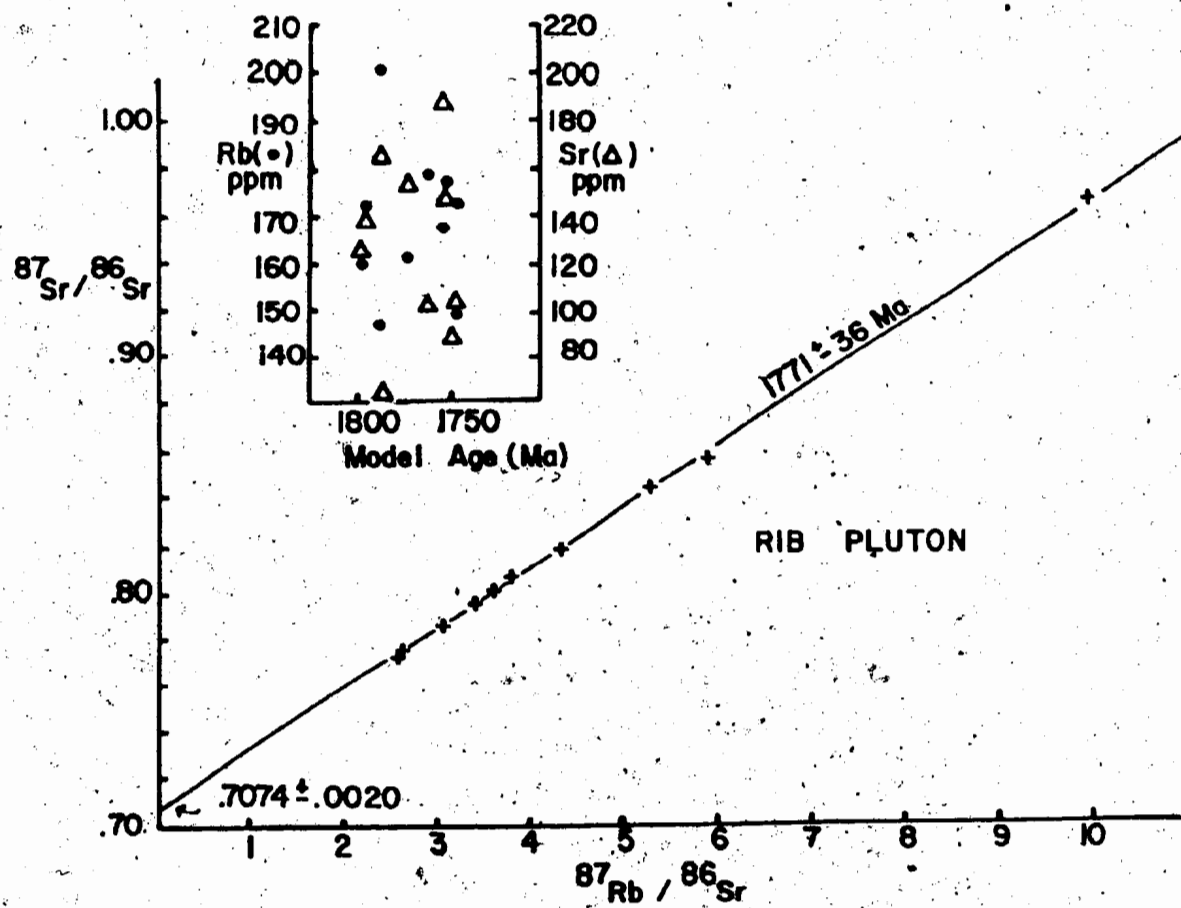


Figure 5.8 Isochron regression for ten samples of the Rib Granite. Inset shows a plot of Rb and Sr versus model age for the Rib Granite samples. There is no correlation between Sr or Rb and model age. This indicates that the Sr isotope system in the Rib has not been reset, or, that resetting resulted in complete homogenization of Sr isotopes in the pluton.



unlikely because of the large discrepancy between the Rb-Sr and the zircon dates of the Rib Granite.

5.10 OTHER AGE CONTROLS ON THE AKAITCHO GROUP

Table 5.4 is a summary of the relative age controls on the Akaitcho Group. The Akaitcho Group is pre-Epworth Group, and pre-orogenic. The minimum age of the Akaitcho Group is about 1900 Ma, the average zircon date of the Akaitcho Group rhyolites.

The maximum age of the Akaitcho Group is determined by several intrusions which may be associated with rifting along the Coronation margin (Figure 5.9). A Rb-Sr whole-rock isochron age on the Indin conjugate diabase dyke swarm is 2049 ± 86 Ma (Gates and Hurley, 1973, McGlynn and Irving, 1975). The Indin dyke swarm is associated with possible rift-related faulting (Frith, 1978; McGlynn and Irving, 1975). Two alkaline complexes possibly associated with rifting give similar ages. The Bigspruce Complex was emplaced at 2066 ± 40 Ma (Martineau and Lambert, 1975) and the Blachford Complex at 2081 ± 42 Ma (Wanless et al., 1979). All three dates represent a maximum age for the Akaitcho Group. If these rocks are related to the rifting event that produced the Coronation margin then these dates indicate protracted rifting, i.e. about 100 to 150 Ma. (Dates of rifting in the Appalachian Orogen in the late Proterozoic cover a time span of 200 Ma, Williams, 1979). Alternatively, the alkaline complexes and the Indin dyke swarm could be related to an earlier rifting event, possibly

Table 5.4 Age controls on the Akaitcho Group and related events and units in the Wopmay Orogen. All zircon dates reported in this table courtesy of S.A. Bowring, University of Kansas.

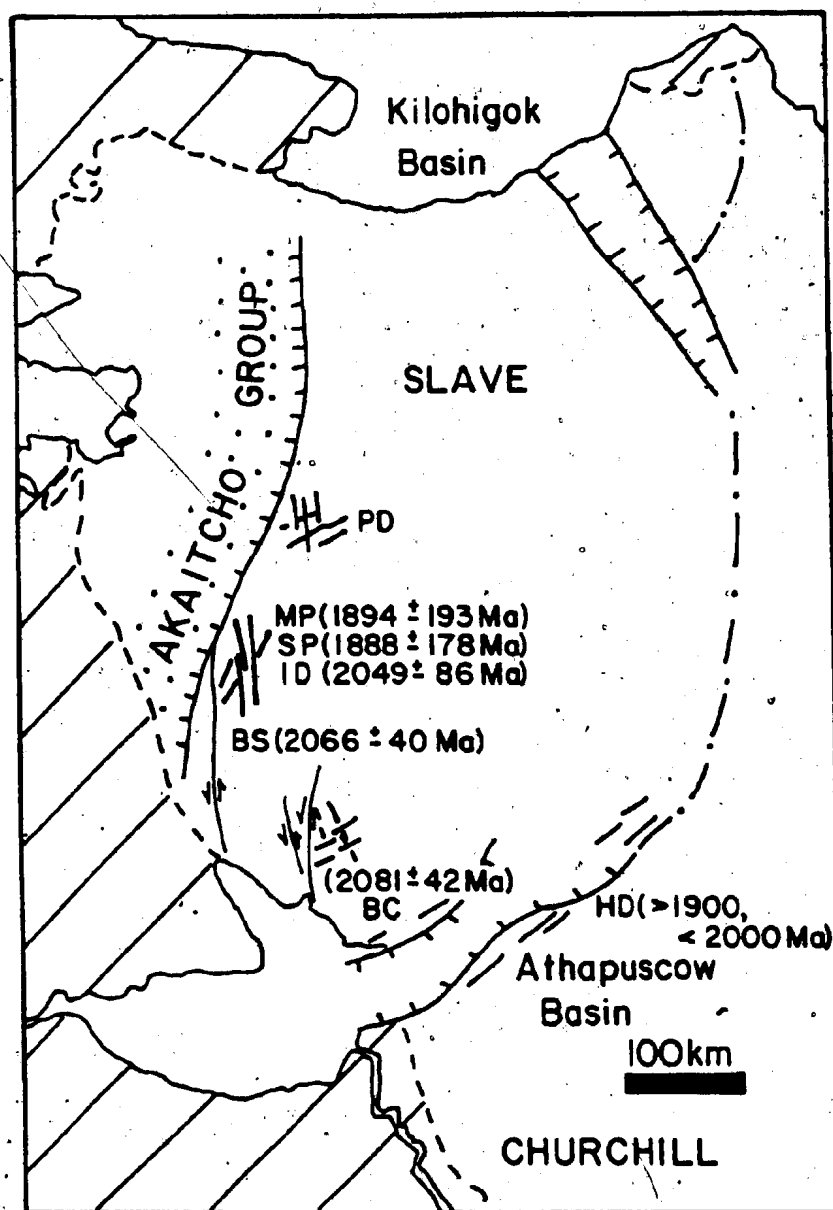
EVENT OR UNIT	AGE CONTROL	COMMENTS
AKAITCHO GROUP	<ul style="list-style-type: none"> - maximum age of 2050 to 2070 Ma - overlain by Odjick Formation, apparently conformably - rhyolite tuffs interbedded with Aglerok Formation pelites, pelites derived in part from Nasittok Subgroup volcanic complexes. Rhyolites dated at 1900 ± 24 Ma by zircon 	<ul style="list-style-type: none"> - based on Indin dyke swarm and alkaline complexes - could be disconformity
EPWORTH GROUP	<ul style="list-style-type: none"> - maximum age of 2350 Ma (late plutons at Point Lake) - minimum age of 1816 ± 144 Ma (Rb-Sr whole-rock on Takijuq Sill, McGlynn, 1980), K-Ar biotite ages of 1815 ± 70, 1835 ± 70 Ma (Wanless et al., 1965) 	<ul style="list-style-type: none"> - Rb-Sr whole-rock and mineral - Rb-Sr whole-rock, no correlation between Rb or Sr and model age
METAMORPHISM IN ZONE 3	<ul style="list-style-type: none"> - affects Akaitcho, Epworth, and Recluse Groups (St-Onge, 1981) - post-thrusting, isograds cut thrusts (St-Onge, 1981) - related to early phases of Hepburn Batholith (St-Onge, 1981) - P-T conditions indicate emplacement at 10 km depth (St-Onge, 1981) - Rib pluton cuts isograds, Rb-Sr whole-rock date of 1771 ± 36 Ma - minimum age same as Epworth Group, maximum age of 1895 ± 24 Ma (Hepburn Batholith zircon dates) 	

Table 5.4 continued

EVENT OR UNIT	AGE CONTROL	COMMENTS
DEFORMATION IN ZONE 3	- syn- to post-metamorphic, affects Akaitcho, Epworth, and Recluse Groups and early plutons of Hepburn Batholith, post-thrusting and folding	- Rib unaffected
HEPBURN AND WENTZEL BATHOLITHS	<ul style="list-style-type: none"> - intrude Akaitcho, Epworth, and Recluse Groups - emplaced at 10 km depth, source region about 25 km depth (Pattison, 1981; St-Onge, 1981) - minimum age of 1771 ± 36 Ma (Rb-Sr on Rib pluton) - zircon dates on all plutons cluster between 1880 and 1895 Ma - Dumas Group rocks rest conformably on Wentzel Batholith and metamorphosed Akaitcho Group rocks; allows about 10 Ma for batholith emplacement, cooling, uplift and erosion 	<ul style="list-style-type: none"> - includes Rib pluton - Dumas Group zircon dates about 1875 ± 10 Ma
UPLIFT OF GREAT BEAR TERRANE (ZONE 4)	- between 1875 to 1860 Ma, 1875 Ma zircon date on Dumas, Takiyuak Formation sediments 1860 to 1850 Ma (youngest Great Bear dates)	
HOTTAH TERRANE	- zircon date of 1920 Ma, basement to Zone 4?	
FAULTING	<ul style="list-style-type: none"> - Wopmay Fault Zone affects Dumas Group, hence younger than 1875 Ma, last movement could be about 1540 Ma (reset K-Ar and Rb-Sr systems adjacent the Fault Zone) - NE- and NW-trending faults cut the Wopmay - NE- and NW-trending faults predate the Western Channel diabase (Rb-Sr whole-rock date of 1392 ± 48 Ma (Wanless and Loveridge, 1977)). 	

Figure 5.9 Location and dates of other magmatic events related to the Akaitcho Group and development of the Coronation continental margin.

Abbreviations: PD - Point Lake Dykes (Easton et al., 1981); MP - muscovite pegmatite dyke, Hepburn Batholith intrusion in the Slave Province? (Frith et al., 1977); SP - Strachan granodiorite pluton (Frith et al., 1977), Hepburn Batholith intrusion in the Slave Province?; ID - Indin diabase dyke swarm (Gates and Hurley, 1973); BS - Bigspruce Alkaline Complex (Martineau and Lambert, 1975); BC - Blachford Alkaline Complex (Wanless et al., 1979); HD - Hearne Dykes, post-Butte Granite, post-Wilson Island, pre-Union Island Group, (Hoffman et al., 1977).



associated with the Wilson Island Group in the Athapuscow Aulacogen. In either case, these dates are a maximum age for the Akaitcho Group.

The tightest age control is provided by the Butte Island Granite in Athapuscow Aulacogen. The granite cuts the Wilson Island Group, is overlain by the Union Island Group, and cut by the Hearne dykes related to rifting in Athapuscow Aulacogen (Hoffman *et al.*, 1977). The Butte Granite has been dated at 2005 Ma by W.R. Van Schmus and S.A. Bowring of the University of Kansas. If the Union Island Group and the Akaitcho Group are lithologically correlative as suggested in Chapter 3, then the Akaitcho Group is between 2000 and 1900 Ma old.

5.11 U-Pb ZIRCON DATES FROM THE WOPMAY OROGEN

U-Pb zircon dates from various units from Zones 3 and 4 are presented in Table 5.5. Data is courtesy of W.R. Van Schmus and S.A. Bowring, both of University of Kansas. Zircons from Akaitcho Group rhyolites and the Okrark sills give dates of 1900 Ma. Most of the rhyolite samples were from porphyritic-rhyolite flows and domes overlying the Nasittok Subgroup volcanic complexes. Zircons from the majority of the syn-metamorphic plutons of the Hepburn and Wentzel Batholiths give dates of 1885 Ma. Zircon dates from Zone 4, the Great Bear magmatic arc, range from 1875 to 1850 Ma, only marginally older than those from Zone 3. In the 5 to 10 million year time span that may be

Table 5.5 U-Pb zircon dates from the Wopmay Orogen. Data courtesy of S.A. Bowring and W.R. Van Schmus, University of Kansas.

AKAITCHO GROUP

Okrark rhyolite sills, Nasittok	
Subgroup porphyritic rhyolite flows,	
Grant Subgroup rhyolite flows	circa 1900 Ma

HEPBURN BATHOLITH

Headnet Pluton (syn-metamorphic)	circa 1885 Ma
Rib Granite (post-metamorphic)	circa 1885 Ma

WENTZEL BATHOLITH

foliated granite phase	circa 1885 Ma
------------------------	---------------

GREAT BEAR MAGMATIC ARC

volcanic and plutonic rocks	range from circa 1850 to 1875 Ma
-----------------------------	-------------------------------------

BASEMENT TO DRILL FORMATION

circa 2585 Ma

SITIYOK IGNEOUS COMPLEX

monzogranite phase	circa 1885 Ma
--------------------	---------------

present between the Akaitcho Group rhyolites and the Hepburn Batholith, the Epworth Group must be deposited, folded and thrust, and intruded by S-type granitoids presumably derived from melting of sedimentary rocks or the lower crust (Hoffman *et al.*, 1980; Pattison, 1981; St-Onge, 1981). Clearly, the zircon ages impose severe time constraints on the development of the Wopmay Orogen.

5.12 DISCUSSION

5.12.1 Zircon Dates

There are three main explanations that can be considered regarding the zircon dates:

- i) the stratigraphy in the Akaitcho Group, and the Akaitcho/Epworth Group age relations have been interpreted correctly. The zircon dates are in error;
- ii) the stratigraphy in the Akaitcho Group, or the Akaitcho/Epworth Group age relations, or both, have not been interpreted correctly. The zircon dates are correct.
- iii) the stratigraphy is correct, as are the zircon dates.

The first explanation is not satisfactory. First, the zircon dates are in agreement with known geological relationships. Although errors overlap, the Akaitcho Group rhyolites are marginally older than the syn-metamorphic Hepburn plutons, and both are older than the Great Bear rocks present in Zone 4. Second, the reason for suggesting that the zircon ages are incorrect is the fact that they impose severe time constraints on the current model of the development of the Wopmay Orogen. (P.F. Hoffman, personal

communication, 1981). Another 10 to 20 Ma gap between the Akaitcho Group rhyolite and syn-metamorphic Hepburn pluton dates and the problem would not exist. Third, the zircons from the Akaitcho Group, the Hepburn and Wentzel Batholiths, and from the Great Bear magmatic arc show no features such as relict cores or high discordancy that would make the zircon dates suspect (W.R. Van Schmus and S.A. Bowring, personal communication, 1982). Until concrete evidence can be presented that all or some of the zircon dates are incorrect, this explanation is not tenable.

The second explanation is not entirely satisfactory either. First, the Akaitcho/Epworth Group relations have been established in several areas. Even if the relations in Areas 1 and 2 (Chapter 3) are not interpreted correctly; the presence of Vaillant Formation basalts interbedded with Odjick Formation orthoquartzites cannot be ignored, and indicate that a volcanic sequence was present beneath the Odjick Formation. Second, even if the Akaitcho Group was younger than the Odjick Formation, the Akaitcho Group would still be pre-metamorphic and pre-batholith intrusion. Third, if we assume that the Akaitcho/Epworth Group relations are correct, then the only way to make the Akaitcho Group older than 1900 Ma is to interpret the rhyolites and the Okrark sills as a magmatic episode later than the basaltic volcanism of the Akaitcho Group (P.F. Hoffman, personal communication, 1981). However, the rhyolites and Okrark sills are pre-metamorphic and pre-thrusting. If they

were younger than the other Akaitcho Group units, an explanation for their formation would still be needed. This explanation, as yet forthcoming, would have to explain the restriction of the sills to a specific stratigraphic horizon, and to crustal block B. In addition, the rhyolites present in the Kapvik and Havant volcanic complexes are bedded tuffs and crystal tuffs, clearly interbedded with the volcanic and sedimentary rocks of the Akaitcho Group. Thus, apart from the Okrark sills, and some of the porphyritic rhyolites overlying the Sinister and Tuertok volcanic complexes, the Akaitcho Group stratigraphy as outlined in Chapter 3 would remain much the same. In addition, rhyolites were present in the upper Tuertok volcanic complex as indicated by the REE evidence (Chapter 4). Thus, we can only separate from the Akaitcho Group those rhyolites that have been dated. The Tuertok rhyolite dated by Rb-Sr was also dated by U-Pb. This rhyolite is aphanatic, and clearly intercalated with Tuertok volcanic complex basalts. The zircon date of this rhyolite does not differ from the zircon dates of the Okrark sills or the porphyritic rhyolite domes. A rhyolite crystal tuff from the base of the Kapvik volcanic complex also has a zircon date similar to the other dated rhyolites (W.R. Van Schmus and S.A. Bowring, personal communication, 1982). Thus, until evidence can be presented that the bedded rhyolite tuffs at the base of the Kapvik and Havant volcanic complexes are significantly older than the porphyritic rhyolites, the suggestion that the stratigraphy

is in error and the zircon dates correct, is not entirely satisfactory.

The third explanation thus warrants, by default, further consideration. There is no evidence to suggest that the zircon dates are in error, or that the observed stratigraphic relationships are not interpreted correctly. The zircon dates have been questioned (P.F. Hoffman, personal communication, 1981, 1982) because they place severe constraints on the current collision model of the Wopmay Orogen (Hoffman, 1980c). Discussion of the third explanation will, however, be deferred until Chapter 6 - since such a discussion involves consideration of alternate models of the development of the Wopmay Orogen.

5.12.2 Regional Resetting of Rb-Sr Isotopic Systems

The Rb-Sr isochron dates for the analyzed units appear to have been reset. But what is the significance of this resetting? First, is it related to regional metamorphism, or to large-scale hydrothermal systems? Second, does the recurring date of roughly 1770 Ma have any geological significance.

Rb-Sr and K-Ar dates for the Wopmay Orogen and the adjacent Slave Craton are plotted in Figures 5.10 and 5.11. Rb-Sr and K-Ar dates from Zone 3 cluster at 1770 Ma (Figure 5.11). It is significant that the Rb-Sr and K-Ar dates are in rough agreement, indicating that both the Rb-Sr and K-Ar systems became closed to isotopic exchange at roughly the same time, i.e. about 1770 Ma in Zone 3.

Resetting of isotopic dates is not restricted to Zone 3 (Figure 5.11). For example, K-Ar dating has been extensive in the Basler Lake area near the Bear-Slave boundary (Figure 5.12). The Basler Lake granite has an Archean Rb-Sr whole-rock date of 2510 ± 106 Ma (McGlynn, 1972). A Rb-Sr mineral date from this granite is 1932 ± 24 Ma -- 600 Ma younger than the whole-rock date (McGlynn, 1972). K-Ar biotite dates from the Basler Lake granite range from 1743 to 1993 Ma, again about 600 Ma younger than the Rb-Sr whole-rock date. K-Ar muscovite dates range from 2101 to 2410 Ma, younger than the Rb-Sr whole-rock date but older than the biotite dates. It seems probable that the K-Ar and the Rb-Sr mineral dates are the result of resetting of these two isotopic systems by an event that occurred in the adjacent Bear Province; the difference between the K-Ar biotite and muscovite dates is due to the different response of these two minerals to resetting. Frith (1978) and Frith *et al.* (1977) interpreted the Rb-Sr and K-Ar dates in the region as indicating several thermal events, one at 2200 Ma, another at 1950 Ma, and a third at 1800 Ma. The existence of pervasive Rb-Sr isotopic disturbance in Zone 3 was not recognized at that time. Although it is conceivable that the K-Ar muscovite dates record a different event than the K-Ar biotite dates, it is more likely that they record different responses to a widespread alteration event.

Resetting of Rb-Sr systems on a regional scale by low-temperature hydrothermal systems has been documented in

Figure 5.10 Compilation of selected Rb-Sr and K-Ar dates from the Bear-Slave region. All dates in Map Inset shows the East Arm of Great Slave Lake (Athapuscow Aulacogen).

KEY TO ABBREVIATIONS

AB - Akaitcho Group, Belleau basalts	PEG - pegmatite
AG - Archean granites	PF - Pearson Formation
AR - Akaitcho Group, Tuertok rhyolite	RG - Rib granite
AV - Akaitcho Group, Vaillant basalt	RP - rhyolite porphyry
BS - Bigspruce alkaline complex	SC - Sitiyok Complex
BC - Blachford Lake alkaline complex	SG - Snare Group
DD - Diabase dykes	SP - Strachan pluton
EAL - East Arm Laccoliths	SV - Seton Formation
EG - Epworth Group	WI - Wilson Island Group
GBG - Great Bear granitoids	b - biotite
GBV - Great Bear volcanics	m - muscovite
HB - Hepburn Batholith	r - riebeckite
MS - Migration sills	h - hornblende
MYL - mylonite	w - whole-rock
OS - Akaitcho Group, Okrark sills	min - mineral

KEY TO SOURCES

- Rb-Sr, this study
- Rb-Sr, GSC, McGlynn (1972, 1980); Frith (1980)
- Rb-Sr, Frith et al. (1977)
- ⊕ Rb-Sr, Neilson and Ghosh (1981a, 1981b)
- Rb-Sr, Robinson and Morton (1972)
- Rb-Sr, Martineau and Lambert (1975)
- Rb-Sr, Baadsgaard et al. (1973); Pb-Pb, Cumming (1980)
- Rb-Sr, Góff et al. (1982)
- △ K-Ar, GSC, Lowdon (1960, 1961); Lowdon et al. (1963); Wanless et al. (1965, 1966, 1967, 1968, 1970, 1972, 1973, 1974, 1978, 1979).

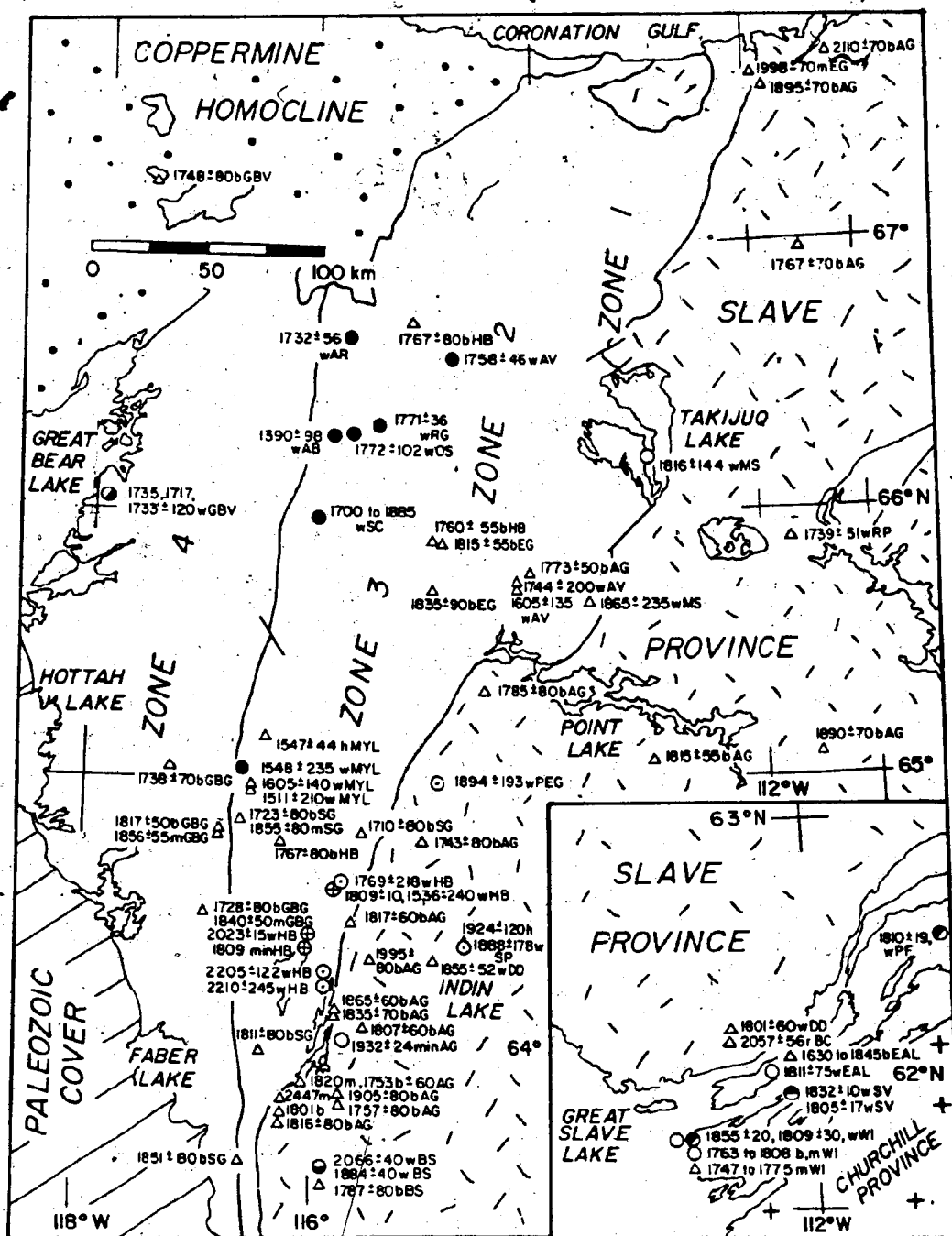


Figure 5.11 Radiometric age determinations in tectonic zones of the Wopmay Orogen, using information presented in Figure 5.10. Diagonal line is drawn through the Rb-Sr determinations from Zones 3 and 4 and the East Arm of Great Slave Lake. Rb-Sr dates have an average error of 30 Ma. K-Ar dates have an average error of 80 Ma, and show greater scatter than the Rb-Sr dates.

LEGEND

- △ K-Ar biotite dates, GSC, references as in Figure 5.10
- ▲ K-Ar muscovite dates, GSC, references as in Figure 5.10
- Rb-Sr whole-rock dates, this study, except Sitiyok Igneous Complex
- ◐ Rb-Sr whole-rock dates, this study, Sitiyok Igneous Complex
- Rb-Sr whole-rock dates, various laboratories, references as in Figure 5.10
- ◇ Rb-Sr mineral dates, various laboratories, references as in Figure 5.10
- ▨ range of zircon dates, as determined by W.R. Van Schmus and S.A. Bowring, University of Kansas

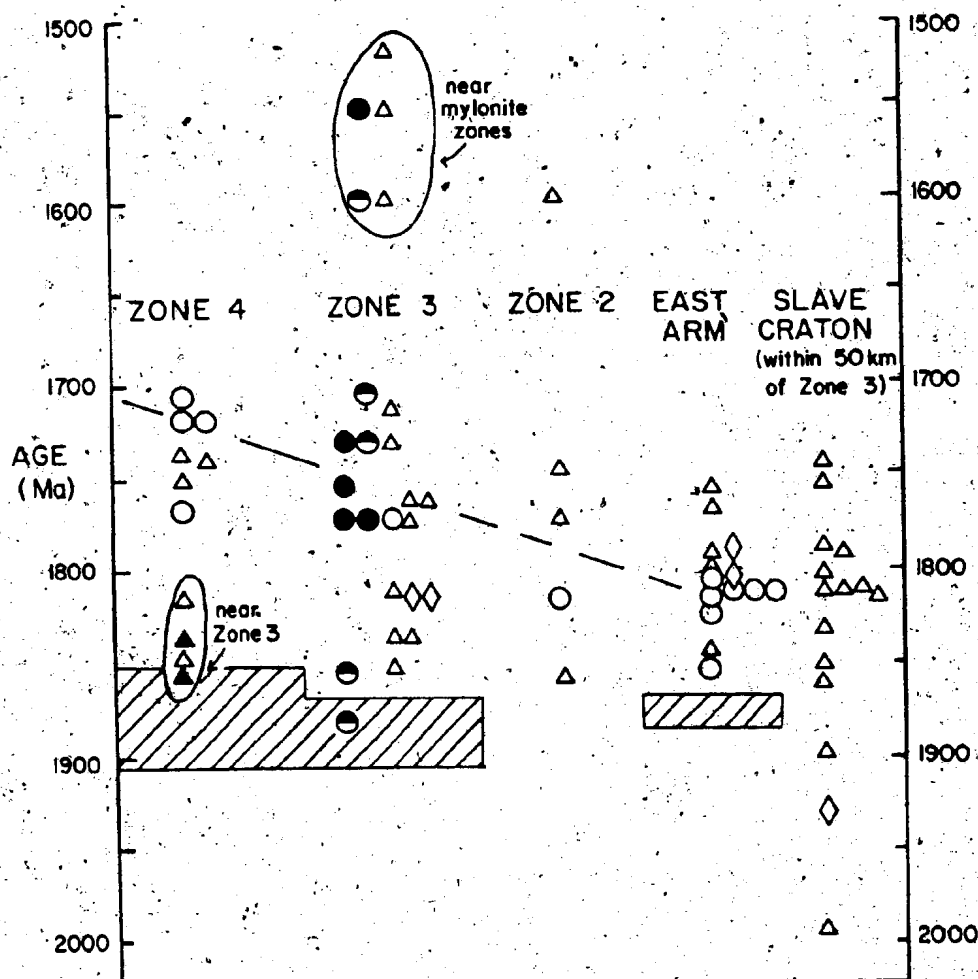
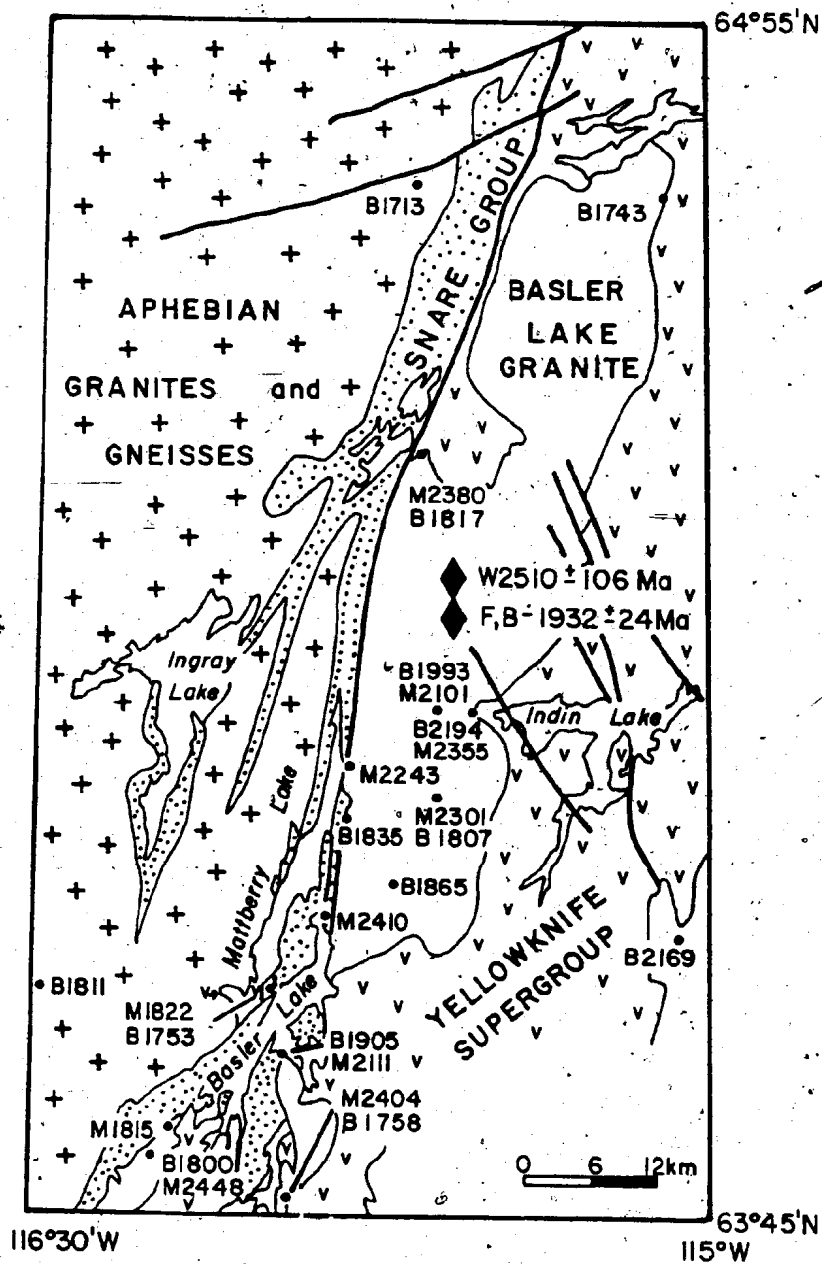


Figure 5.12 Rb-Sr and K-Ar dates in the Basler-Mattberry Lake area in southern Zone 3. Modified from McGlynn (1972). Data from McGlynn (1972) and Frith et al. (1977).



other Proterozoic orogens (Taylor, 1978; Page, 1976, 1978; Bickford and Mose, 1975). Taylor (1978) noted that resetting of Rb-Sr isotopic systems commonly occurs in two stages. First, a hydrothermal system is established and causes some alteration to the rocks, particularly the feldspar minerals. The second event causes further alteration, and is responsible for the major resetting of the Rb-Sr system. If the U-Pb zircon dates obtained by van Schmus and Bowring are reasonable indicators of the age of plutonism in Hepburn Batholith, then small-scale hydrothermal systems associated with batholithic emplacement could have made the rocks susceptible to later alteration. At some later time, a second period of hydrothermal alteration occurred, causing the pervasive isotopic resetting observed in Zone 3. It is not known to what tectonic event this second hydrothermal event is related, but it may be related to second collision.

Thus, the Rb-Sr dates probably record the cessation of a hydrothermal event (closure of Sr isotopes in feldspar, etc.), with the K-Ar dates recording cooling below the blocking temperature of Ar in micas. This event ended about 1770 Ma, about 100 Ma after the first collisional event in the Wopmay Orogen.

5.12.3. Rb-Sr Mobility - Implications for Other Elements?

In the preceeding chapter on geochemistry, definite conclusions are drawn about the development of the Akaitcho Group on the basis of the geochemistry of the Akaitcho Group

rocks. However, in this chapter, evidence is presented showing resetting of Rb-Sr and K-Ar isotopic systems by later regional events. One may rightfully ask that if Rb, Sr, and K have been mobile, what about other elements, particularly the "immobile" elements on which the conclusions in Chapter 4 weigh heavily upon. In this section, I will demonstrate that the "immobile" elements have remained immobile.

Belleau Basalt

The Belleau volcanic complex basalts were reset twice, once at about 1770 Ma, and a second resetting at about 1400 Ma. Thus, it might be expected that the Belleau basalts should show effects of one, or both, of the resetting events. The Belleau basalts show a change from continental tholeiites near the base of the complex to oceanic tholeiites in the upper part of the complex. These chemical changes can be related to changes within the stratigraphic section. Second, the change from continental to oceanic tholeiites is observed not only in the REE patterns, but also in the immobile trace elements and in the major elements. Although some, if not all, of the major element abundances are probably not the original abundances (e.g. K_2O), distinct differences between the two rock types do persist. The change from continental to oceanic tholeiites is also observed in other volcanic complexes, which were only reset at 1770 Ma. Thus, there is no evidence that the immobile element abundances within the Belleau basalts have been altered.

Tuertok Rhyolite

Eight samples of Tuertok rhyolite from one outcrop area 50 m by 100 m were analyzed for trace element abundances. Mobile elements such as Rb, Sr, Ba, Pb, and Zn show much variation on the outcrop scale. Immobile elements such as Ti, Zr, V, Y and Nb show almost no outcrop scale variation (Table 5.6). This could be due to the fact that these immobile elements have been immobile, or that they were very mobile and were completely homogenized. If the latter were the case, then the mobile elements might be expected to show closer coherence. Similar results have been found for other units where individual flows were sampled.

Vaillant Basalt

As discussed in Chapter 4, the Vaillant Formation basalts have undergone varying degrees of carbonate-related alteration. The effects of this alteration are shown by considerable scatter on trace element plots (e.g. Figure 4.26, 4.27). In addition, REE mobility can be documented between relatively 'fresh' and extremely altered samples from a single flow unit (Figure 4.28).

McLennan (1981) surveyed the literature pertaining to REE mobility. Only in cases where high water fluxes, and/or high CO_2 activity occurred were the REE demonstrably mobile. Hynes (1980) has reported evidence for mobility of Ti, Y and Zr during carbonate metasomatism. In the case of the Vaillant Formation basalts, Ti, Y, Zr and the REE can be shown to have been mobile, but the Vaillant basalts have

Table 5.6 Outcrop scale variation in eight samples of a Tuertok volcanic complex rhyolite flow. All units in ppm., except TiO_2 which is in weight percent.

Element	F466A.80	F466B.80	F466C.80	F466D.80	F466E.80	F466F.80	F466G.80	F466H.80	error*
Nb	18	20	19	21	20	22	20	20	1
Zr	398	400	395	400	399	389	405	398	12
Y	112	115	115	106	106	107	111	117	5
Sr	86	42	40	47	42	38	37	35	2
Rb	151	148	182	167	136	163	149	134	5
U	5	9	9	9	7	13	9	8	2
Th	28	29	27	24	23	21	28	24	2
Pb	26	27	32	29	36	27	21	19	1
Zn	77	87	97	82	80	87	84	95	4
Cu	14	9	16	11	13	11	8	11	1
V	6	3	10	8	3	1	6	7	1
La	50	48	60	62	61	61	61	60	3
Ce	111	102	106	102	114	115	102	106	5
Ba	735	705	801	816	684	777	717	715	30
TiO_2	0.38	0.41	0.42	0.41	0.40	0.38	0.40	0.41	0.02

*estimated analytical error, in ppm, 5% or 1 ppm, whichever is greater.
See Appendix A for further details.

undergone greater carbonatization than other Akaitcho Group basalts. The more important point is that the major and trace element contents of the Vaillant basalts indicates that they have undergone significant alteration. Significant alteration is not evident in the major and trace element contents of other Akaitcho Group rocks.

Summary

In the Akaitcho Group, there was mobility of isotopes, and the more mobile elements, but there is little evidence that the 'immobile' elements were mobile. The consistency of results obtained between different element groups, and the relation between these changes and stratigraphy suggests that the REE and other 'immobile' elements were essentially immobile, i.e. such effects were insignificant with respect to primary variations and/or analytical uncertainty. In the case where immobility of the trace and REE elements can be demonstrated, i.e. the Vaillant Formation, the rocks have undergone a unique alteration not observed in other Akaitcho Group units, and the rocks are easily recognized as altered.

In addition, it should be noted that sedimentary rocks in the Akaitcho, Epworth and Recluse Groups have REE patterns similar to post-Archean sedimentary rocks worldwide. If the REE were mobile in igneous systems, originally porous sediments would not be expected to retain their characteristic REE patterns, patterns that are not affected by metamorphic grade (Figure 4.39). Thus, REE mobility in the bulk of the Akaitcho Group strata is unlikely.

5.13 SUMMARY

Rb-Sr and K-Ar dates in the Wopmay Orogen were reset by a regional-scale hydrothermal alteration event. In Zone 3, Rb-Sr and K-Ar isotopic systems re-equilibrated about 1770 Ma. The K-Ar dates from central Wopmay Orogen cannot be regarded as ages of uplift, or of metamorphism, but rather are ages of closure of minerals to Ar loss following this alteration event. The alteration event ended about 100 to 150 Ma after the peak of orogenic activity as determined by U-Pb zircon dates (Van Schmus and Bowring, 1980). Although resetting of Rb-Sr and K-Ar isotopic systems occurred throughout Zone 3, there is no evidence indicating that the 'immobile' trace and rare-earth elements in the Akaitcho Group were significantly affected.

U-Pb zircon dates from the Akaitcho Group rhyolites are about 1900 Ma (W.R. Van Schmus and S.A. Bowring, personal communication, 1982). The zircon dates from Zone 3 of the Wopmay Orogen indicate that only a 5 to 10 Ma gap was present between extrusion of the Akaitcho Group rhyolites and the Hepburn Batholith plutons that metamorphosed and intruded the rhyolites.

CHAPTER 6

HISTORY AND TECTONIC SIGNIFICANCE OF THE
AKAITCHO GROUP6.1 INTRODUCTION

In the preceeding chapter, an overview of the geology, stratigraphy, geochemistry and geochronology of the Akaitcho Group has been given. All these aspects indicate, or are consistent with, the interpretation that the Akaitcho Group is a rift succession, and that the Akaitcho Group is in some way related to the development of the Coronation continental margin about 1.9 to 2.0 Ga ago.

This chapter has three main aspects. First, it presents additional material related to the Akaitcho rift. This material is 'derived' or 'interpreted' information, and is best separated from the descriptive evidence presented in the preceeding three chapters. Second, the tectonic setting of the Akaitcho rift is examined. Is the Akaitcho rift related to the initial development of the Coronation continental margin? Do the U-Pb zircon dates reported in Chapter 5 require modification of the current model (Hoffman, 1980c) for the development of the Wopmay Orogen? Finally, all the preceeding information is synthesized, and presented as a probable developmental history of the Akaitcho Group. This synthesis attests to the important role that the Akaitcho Group has in any model of the development of the Wopmay Orogen, and addresses the first aim of the thesis as stated on page 1; namely, is the

Akaiicho Group related to initial rifting of the Coronation continental margin in the early Proterozoic.

6.2 THICKNESS OF THE CRUST DURING NASITTOK SUBGROUP DEPOSITION

Mohr and Wood (1976) found that there is a relationship between crustal thickness, lithospheric thickness and volcano spacing along rift systems in East Africa. For older rift systems, if volcano spacing is known, then crustal thickness can be estimated (e.g., Windley and Davies, 1976).

The Kapvik, Sinister, Tuertok and Havant volcanic complexes, are all located in the Marceau Thrust Slice in crustal block B, have a linear trend (Figure 6.1) and are stratigraphically continuous. As shown in Figure 6.1, the spacing between the four volcanic complexes is regular, especially when compared to the variation noted by Mohr and Wood (1976). The spacings illustrated in Figure 6.1 are based on the sites of the major part of the volcanic edifices and represent maximum values.

The mean spacing between the volcanic complexes is 37.5 km, corresponding to a crustal thickness of 28 km and a lithospheric thickness of 41 km (Figure 6.2). Present crustal thickness of the Slave Craton is 33.9 ± 0.9 km (Barr, 1971), as determined by seismic refraction studies. This is 6 km thicker than the 28 km estimated for the crust underlying the Akaiicho Group about 1.9 Ga ago. Twenty-eight kilometres is a maximum estimate of crustal thickness

Figure 6.1 Spacing between volcanic complexes present in the Marceau Thrust Slice, crustal block β , northern Wopmay Orogen. Faulting has resulted in a slightly higher spacing between the Kapvik and Havant volcanic complexes.

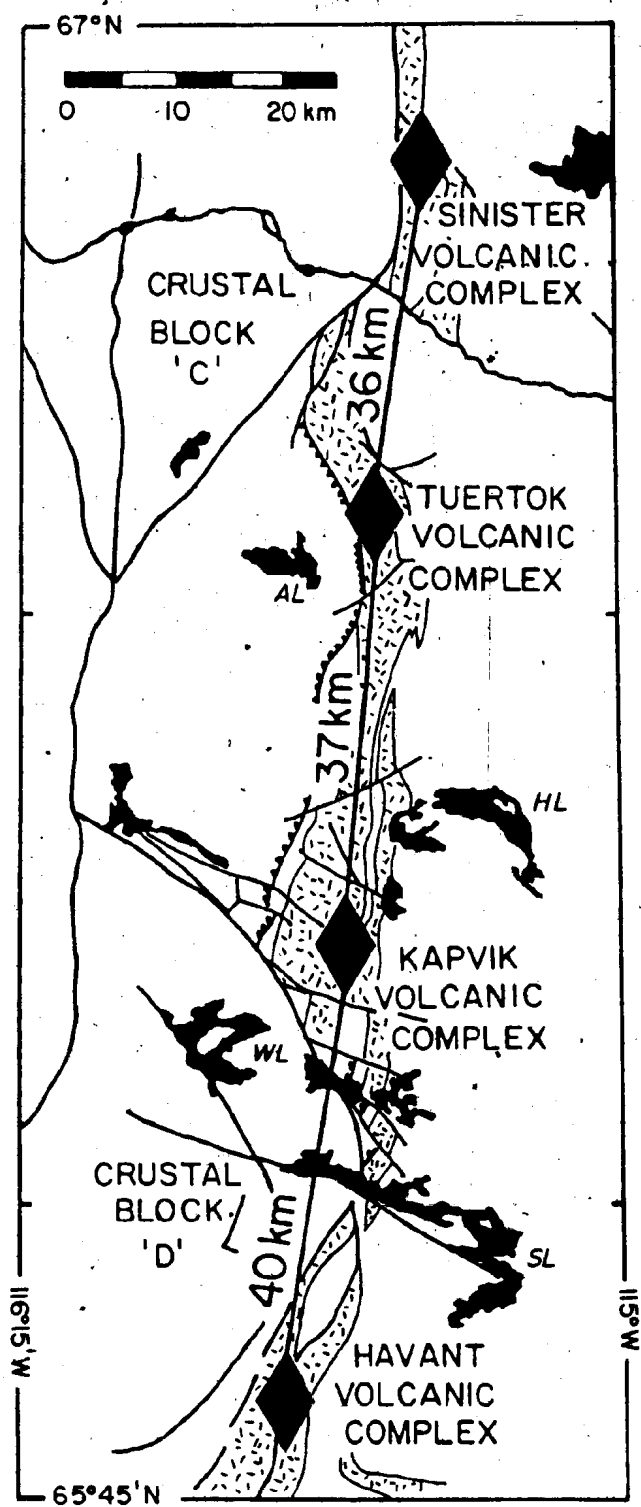
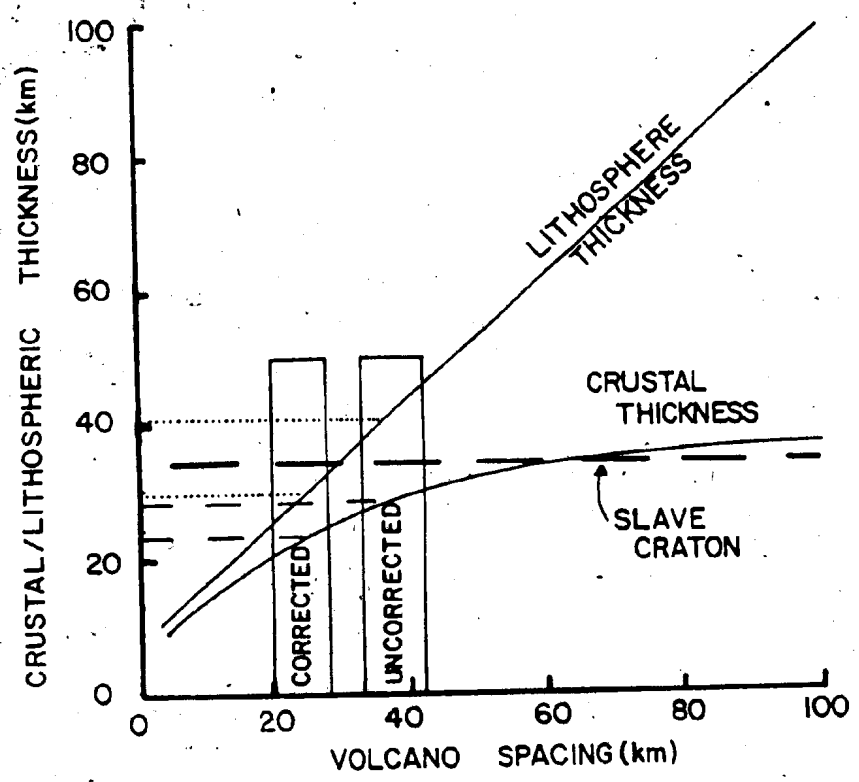


Figure 6.2 Plot of volcano spacing versus crustal/lithospheric thickness (after Mohr and Wood, 1976). Dotted lines (lithospheric thickness for corrected and uncorrected Akaitcho Group volcanoes); dashed lines (crustal thickness for corrected and uncorrected Akaitcho Group volcanoes); heavy dashed line (crustal thickness of Slave Craton (Barr, 1971)). Corrected column shown is for the first method discussed in the text. Width of bars indicates ± 2 km error in measured spacings. Height of bars has no significance.



during Akaitcho Group deposition, because it does not consider effects of deformation.

Two methods of correcting for deformation were attempted. Both methods use strain indicators of known original shape - granite and orthoquartzite cobbles in conglomerates - in the upper part of the Tuertok volcanic complex.

Measured ratios of axes, in now elliptical clasts, range from 1/1.2/1.7 to 1/1.1/2, averaging 1/1.15/1.7. These strain ratios are similar to those expected for simple or uniform extension (Hobbs *et al.*, 1976). In both calculations, it is assumed that deformation caused no volume change.

The first calculation is simplistic, but provides an estimate of the maximum change in volcano spacing. In the field, it was observed that the short axis (Z) is normal to the cleavage, and that the long (X) and intermediate (Y) axes are parallel to the cleavage. It is assumed that the clasts were originally spherical. Then, for a representative clast with measured axes of 4.5 cm x 4.5 cm x 7 cm, the originally spherical clast would have been shortened 0.7 cm normal to the cleavage, 0.7 cm along the Y axes, and lengthened by 1.8 cm (40%) (in this case, in a northerly direction) (Appendix C). This calculation is consistent with observations on deformed pillows in the Tuertok volcanic complex, which show stretching in a northerly direction. If lengthening of the volcanic complexes by 40% has occurred, then the original volcano spacing was 27 km.

This would give a crustal thickness of 24 km, and a lithospheric thickness of 30 km (Figure 6.2). This is a minimum value for crustal thickness, because the clasts probably were not originally spherical.

The second method does not assume that the cobbles were originally spherical. It was observed that the short axes (Z) are normal to the regional cleavage, and that the X and Y axes are parallel to the fold axes and are in the plane of the cleavage. The Y axes are assumed to be parallel to the strike of the regional cleavage. If we assume that the bulk of the observed strain is plane strain; not an unreasonable assumption in fold and thrust belts (Hobbs *et al.*, 1976; Reis and Shackleton, 1976; T.J. Calon, personal communication, 1981); then by definition, no extension has occurred along the Y axes. As the volcanic complexes are oriented parallel to the strike of the regional cleavage, then under the condition of plane strain, no extension has occurred in this direction, and no correction of the volcano spacings is required.

In any case, the estimated crustal thickness beneath the Nasittok Subgroup during deposition is 6 to 10 km thinner than the present Slave Craton. Windley and Davies (1976) estimated crustal thickness for the Archean Superior Province, using volcano spacings, at 35 to 40 km. Condie (1976) estimated that the crust underneath the Yellowknife greenstone belt (Slave Province) during the Archean was 31

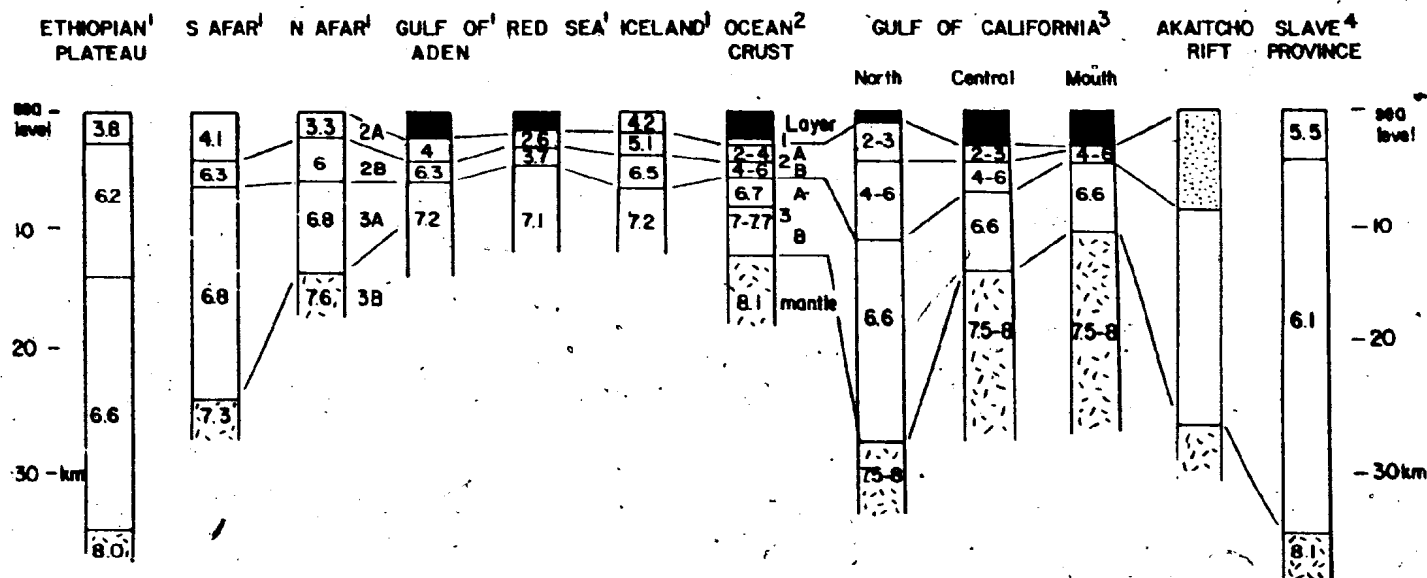
km. These estimates for crustal thickness in the Archean are similar to the present thickness of 33.9 ± 0.9 km (Barr, 1971). Hence, the estimates of crustal thickness beneath the Akaitcho Group during deposition indicate that the crust beneath the Akaitcho Group was probably thinner than that beneath the craton. Crustal thicknesses in the Gulf of California and beneath the stratoid series in southern Afar are both about 26 km (Moore, 1973; Mohr, 1978), including sedimentary and volcanic cover (Figure 6.3). These two modern rifts have several other similarities with the Akaitcho Group (Chapter 7).

6.3 PHYSICAL VOLCANOLOGY OF THE AKAITCHO GROUP

6.3.1 Basalts

This section is concerned with the Nasittok Subgroup volcanic complexes and lithologically correlative units (Figures 6.1 and 6.4). The basic shape of the Nasittok Subgroup volcanoes is shield-like (Figure 3.15). The lithologically correlative Tuertok and Grant Subgroup basalts consist mainly of massive and pillowed flows and show the same textures and features described by Dimroth et al. (1978) for Archean submarine lavas from Noranda, and modern submarine lavas (Ballard and Moore, 1977; Basaltic Volcanism Study Project, 1981). The lithologically correlative Kapvik and Havant basalts are mainly tuffaceous, although pillowed and massive flows are present locally (Figure 3.11). The mafic tuffs in the Havant and Kapvik

Figure 6.3 Crustal sections based on p-wave seismic velocities (km/sec) for the Afar rift, ocean crust, Gulf of California, the Akaitcho Group estimate, and the present (and ancient) Slave Craton. Note the greater thickness of oceanic crust in the developing rifts, particularly north and central Gulf of California and southern Afar. Layer with 4 to 6 km/sec velocities in the Gulf of California is a mixed layer of basalt and sediment (Moore, 1973; Einsele et al., 1980). Dotted pattern is estimated thickness of Akaitcho Group sedimentary and volcanic cover at the end of Nasittok Subgroup deposition. References:
1 - Mohr (1978); 2 - Salisbury et al. (1979);
3 - Moore (1973); 4 - Barr (1971).



volcanic complexes are associated with local basalt and rhyolite centres, and thin to the north and south between adjacent volcanic complexes. Thus, it is suspected that the tuffs are proximal, although many are probably water-lain air-fall tuffs.

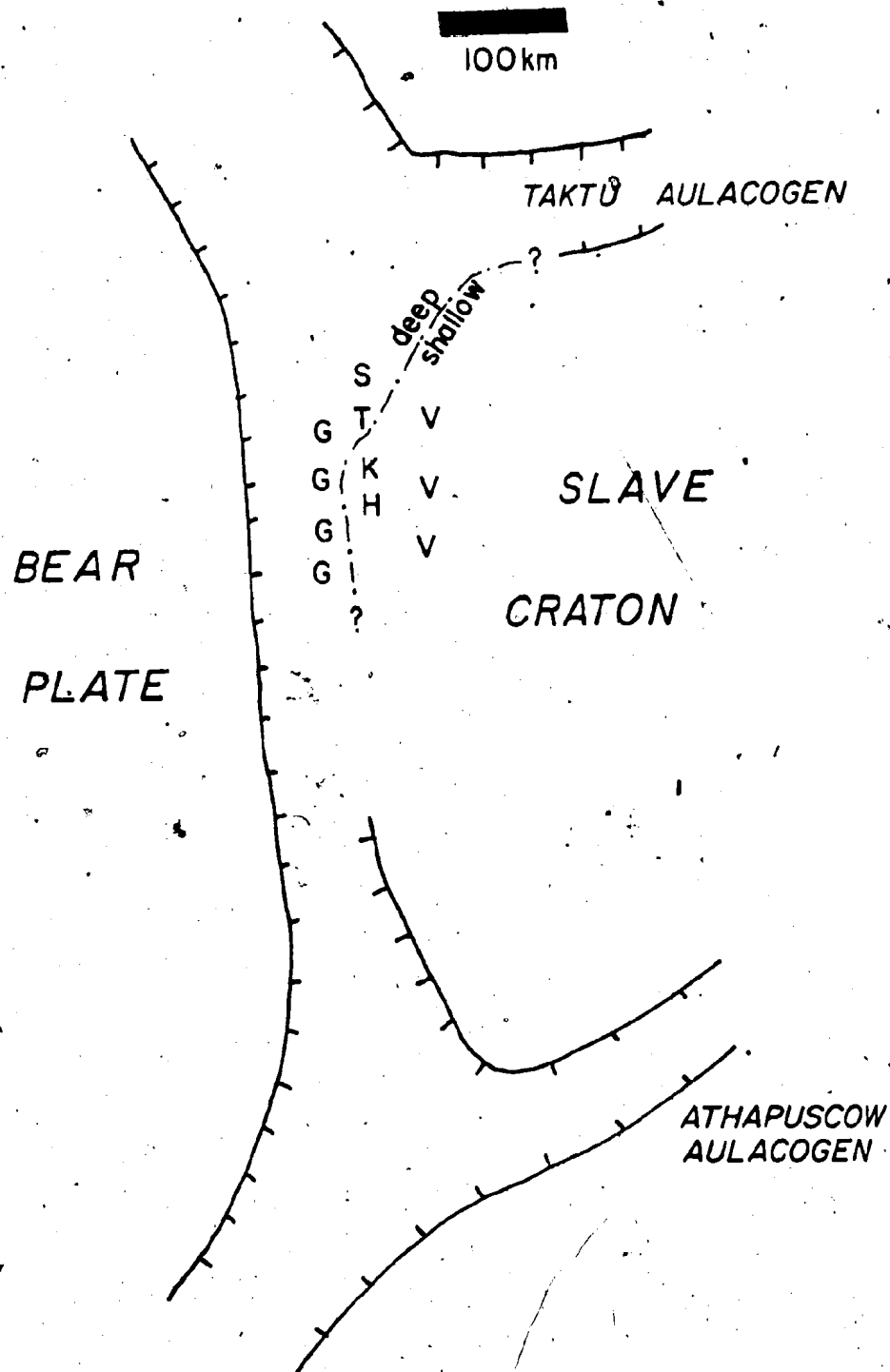
Water depth is a factor in controlling the nature of basaltic volcanism at the volcanic vent (McBirney, 1963; Moore, 1965; Moore and Fiske, 1969; Jones, 1969; McBirney and Williams, 1979). Submarine flows, usually pillowed, occur below 100 to 400 m depth, and pyroclastic volcanism occurs between 100 to 400 m depth and the surface. Because of the similarity in chemistry between the Nasittok Subgroup basalts, the change in style of volcanism from north to south in the Nasittok Subgroup is interpreted to indicate shallower water conditions to the south. The pillowed and massive Grant Subgroup rocks indicate that deeper water conditions existed to the west as well (Figure 6.4). The Vaillant Formation to the east contains subaerial, pillowed and tuffaceous basalts, and was probably deposited on land and in shallow water. Pillowed flows are more abundant to the north in the Vaillant Formation, possibly indicating deeper water conditions in the north. Figure 6.4 relates the location of the Nasittok volcanic centres and water depth, and how this information can be related to rifting of the Slave Craton in the Proterozoic.

6.3.2 Rhyolites

The rhyolites suggest the same water depth conditions

Figure 6.4 Inferred distribution of Nasittok Subgroup volcanic rocks and their correlatives and water depth during deposition. Some of the Vaillant Formation lavas (V) are subaerial. The shallow-deep water transition corresponds to a water depth of about 100 m. Below this depth tuffaceous volcanism is minor (McBirney, 1963; Fiske and Moore, 1969). Deeper water to the north may be the result of greater subsidence at the triple junction with the Taktu aulacogen. A recent analogy would be the Ethiopian Rift-Afar-Red Sea-Gulf of Aden region.

Abbreviations: S - Sinister Volcano; T - Tuertok Volcano; K - Kapvik Volcano; H - Havant Volcano; V - Vaillant Formation lavas (probably several centres); G - Grant Subgroup lavas (probably several centres).



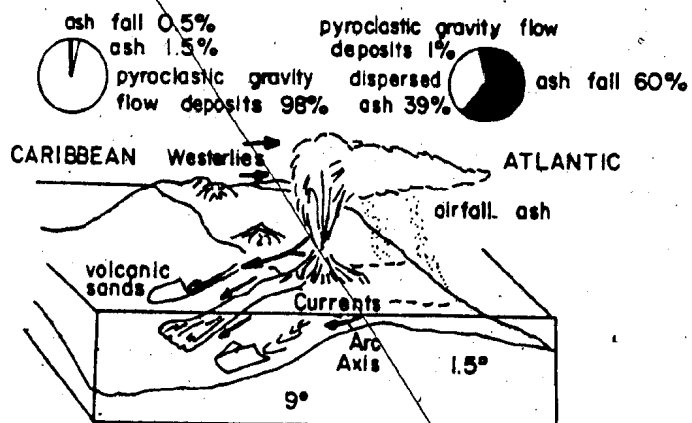
as the basalts. Figure 6.5 compares Akaitcho Group rhyolitic centres associated with the Tuertok and Sinister volcanic complexes with volcanic islands in the Caribbean. Although the scale of the volcanoes, and the tectonic setting are different, the same physical features are present. In the Caribbean, volcanic sands and debris flows accumulate on the deeper side of the islands, and air-fall tuffs, carbonates and volcanic conglomerates accumulating on the shallow side of the islands (Figure 6.5). In the Akaitcho Group, volcanic sands are present on the north side of the rhyolite centres, with quartzite, marble, conglomerate and air-fall tuff present on the south side. Because of the similarity between the Akaitcho and the Caribbean volcanoes, deeper water conditions are inferred to have been present on the north side of the Akaitcho Group rhyolite centres. In the Caribbean, the distribution of the air-fall tuffs is influenced by strong westerly winds. Air-fall tuffs are most abundant on the south side of the Akaitcho Group rhyolite centres; and a dominant wind direction may have been influential in controlling the distribution of the rhyolitic air-fall tuffs in the Akaitcho Group.

In the Kapvik and Havant volcanic complexes, rhyolites are mainly tuffaceous, and occur low in the stratigraphic section. Although the effect of water depth on rhyolitic magmas is less pronounced (McBirney, 1963; Williams and McBirney, 1979), the occurrence of more tuffaceous rocks to

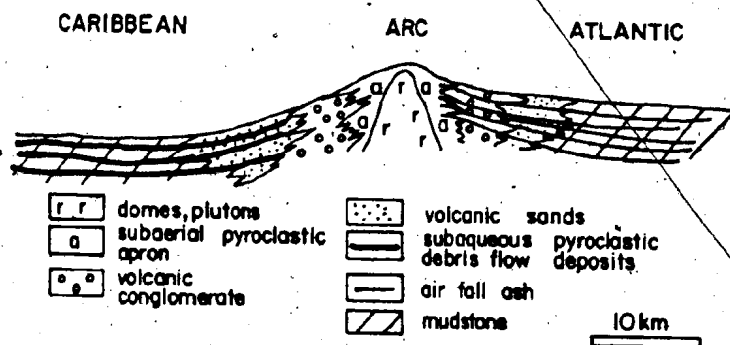
7

Figure 6.5 Inferred depositional conditions for rhyolites in the upper Sinister and Tuertok volcanic complexes.

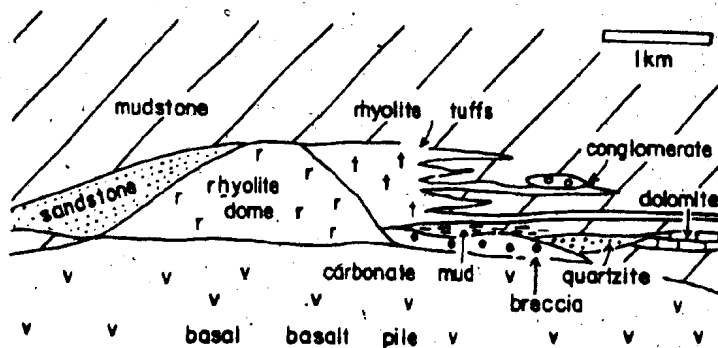
- a) Plan view of Caribbean volcanic arc showing influence of current and wind directions, and water depth (from Sigurdsson et al., 1980).
- b) Cross-section of Caribbean volcanic arc. Note air-fall tuffs to the east, and volcanic sands and debris flow deposits to the west (from Sigurdsson et al., 1980).
- c) Cross-section (left-north; right-south) of an Akaitcho Group rhyolite centre and related sedimentary rocks. Note similarity with Caribbean arc cross-section but also the difference in scale. These figures compare gross volcanic features, not chemical, composition or tectonic setting.



a)



b)



c)

the south is similar to the trend observed for the basaltic rocks.

Rhyolites in the Grant Subgroup consists of small flows and domes. The absence of tuffaceous rocks in the Grant Subgroup, either rhyolitic or basaltic, is interpreted to indicate that deeper water conditions existed west of the volcanic complexes presently exposed in crustal block B.

6.3.3 Tallerk Sills

The Nasittök Subgroup volcanic complexes are overlain by a thick pelite sequence (1 to 2 km) intruded by the Tallerk gabbro sills. Basaltic magma intruded into thick (over 500 m), fine-grained, water-saturated sedimentary sequences commonly forms sill complexes rather than erupting on the surface (McBirney, 1963; Fridleifsson, 1977; McBirney and Williams, 1979; Einsele *et al.*, 1980). Deep water conditions (over 400 m) are more prone to the formation of sill complexes (McBirney, 1963).

The Tallerk sills in the Aglerok Formation above the Kapvik and Havant volcanic complexes suggests that moderate water depths were present during accumulation of the pelite sequence. Water depth was also deep during accumulation of the Odjick Formation slope-facies deposits (Hoffman, 1980c). This sedimentation history is consistent with the interpretation that the Akaitcho rift deepened with time.

6.3.4 Summary

Aspects of the physical volcanology of the Akaitcho Group are consistent with the interpretation that the

Akaiitcho Group was deposited in a basin that deepened to the north and the west, and that deepened with time. As shown in Figure 6.4, the inferred distribution of water depth during volcanism can be accommodated by a rift model.






6.4 ORIGIN AND SIGNIFICANCE OF THE AKAITCHO GROUP RHYOLITES

As discussed in Chapter 4, the geochemical signature and volumes of the Akaiitcho Group rhyolites are consistent with the rhyolites being crustally-derived. Models of rifting such as those advocated by Burke and co-workers (Burke and Dewey, 1973; Basaltic Volcanism Study Project, 1981) generally assume only minor basaltic volcanism, usually of peralkaline affinities. Many older rift sequences such as the Pecos greenstone belt (Robertson and Moench, 1979; J.M. Robertson, written communication, 1981), the Oklahoma aulacogen (Hanson and Al-Shaieb, 1979), the Cape Smith Foldbelt (Hynes and Francis, 1982a, 1982b) and the Karoo (Tankard *et al.*, 1982) have abundant rhyolites of subalkaline affinity chemically similar to the Akaiitcho Group rhyolites. Many of these older rift sequences may have formed in settings different from the East African Rift, and hence may have different magmatic signatures. At present, there is no characteristic magma signature for rift sequences (Baldrige, 1981).

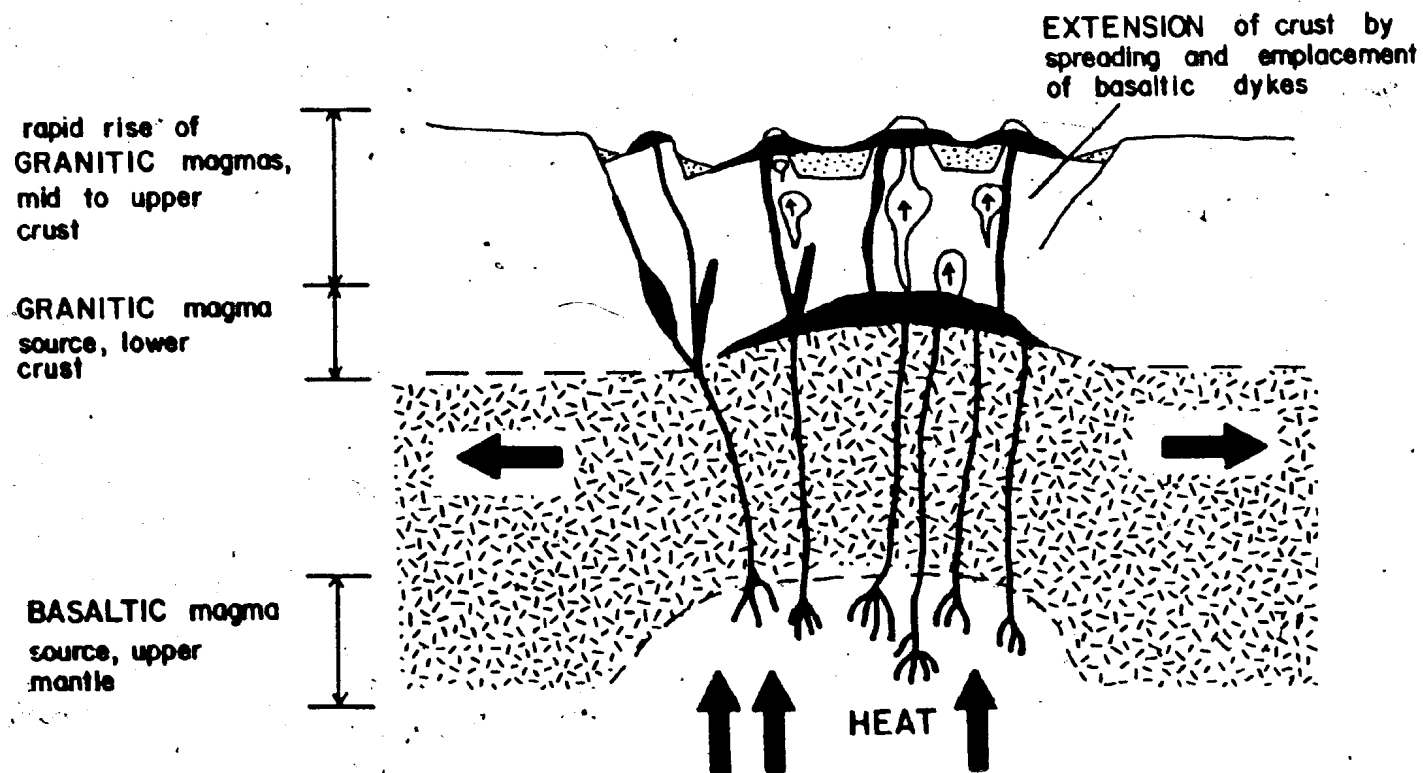
Recent models of rhyolitic magma genesis acknowledge the presence of crustally-derived magmas (Hildreth, 1981; Eichleberger, 1978) (Figure 6.6). These models require that sufficient amounts of heat be transferred to the lower crust

Figure 6.6 Conditions for the generation of basaltic and rhyolitic magmas. (After Hildreth, 1981; Eichleberger, 1978).

LEGEND

-  basaltic magma
-  granitic magma
-  sedimentary rocks
-  crust
-  mantle

BASALTIC and RHYOLITIC VOLCANISM



to induce melting (usually by intrusion of large volumes of basaltic magma), and that the granitic melts reach the surface, in order to get rhyolitic volcanism. Extensional regimes such as rifts are commonly associated with large volumes of basaltic magma, and the combination of extension, heating of the crust by the asthenosphere, and crustal thinning all aid in generating granitic magmas and allowing them to reach the surface. The above factors also influence the amount of rhyolitic volcanism (see Hildreth, 1981, his figure 15). Short-lived, basalt-poor rifts are unlikely to have significant rhyolitic volcanism. Longer-lived, rifts with abundant basaltic magmatism are likely to have abundant rhyolitic volcanism. A hotter lithosphere in the Proterozoic (e.g. Sleep, 1979; McKenzie and Weiss, 1980) would aid in transferring heat to the lower crust, and aid in crustal melting.

Several of the conditions for rhyolitic magma genesis and subsequent eruption are present in the Akaitcho Group. Basaltic volcanism is voluminous as indicated by the Ipiutak and Nasittok Subgroups. The amount of basaltic magma that did not reach the surface cannot be determined, but may have been significant. Estimates of crustal thickness indicate that crustal thinning had occurred, and that the lithosphere was relatively thin. The position of the Akaitcho Group rhyolites high in the stratigraphy is consistent with the rhyolites being crustal melts, and hence, requiring time to be generated and reach the surface. Thus, the models of

rhyolitic magma genesis suggested by Hildreth (1981) and Eichleberger (1978) are considered applicable to the Akaitcho Group rhyolites.

If the Akaitcho Group rhyolites were derived by the above means, then basaltic volcanism may have migrated westward by the time the rhyolites were erupted, as the inferred new plate boundary migrated away from the locus of initial rifting. Thus, sea-floor spreading may have been occurring contemporaneously with rhyolitic volcanism at the rift margin.

6.5 U-Pb ZIRCON DATES AND MODELS OF THE DEVELOPMENT OF THE WOPMAY OROGEN

6.5.1 Introduction

The U-Pb zircon dates indicate that about 10 Ma elapsed between extrusion of the Akaitcho Group rhyolites and intrusion of the oldest phases of the Hepburn Batholith (Table 5.5). The time interval between the rhyolites and the batholithic rocks may be as little as 1 Ma, or as great as 30 Ma on the basis of the analytical errors of the zircon dates. More precise zircon dates (i.e. with 2σ errors of ± 2 Ma) are needed to further constrain the time span involved. For the sake of discussion, it is assumed that the time gap between the rhyolites and the granitoids is 5 to 10 Ma.

The zircon dates place severe constraints on any model for the development of the Wopmay Orogen. Two important questions with respect to the zircon dates are: i) Can the

Akaitcho and Epworth Groups be deposited in 10 Ma or less? , and, ii) Can the Hepburn Batholith be emplaced in 5 Ma or less?. If the answers to either of these questions is no, then serious doubt is cast on either the zircon ages, or the stratigraphic relationships as interpreted herein. If both answers are yes, then the zircon dates, if we assume them to be valid, can be used to constrain models of the development of the Wopmay Orogen.

6.5.2 Subsidence Rates and the Deposition of the Akaitcho and Epworth Groups

About 3 km of sedimentary rock overlies the Akaitcho Group rhyolites [about 1 km of Aglerok Formation; about 1 km of Odjick Formation (Tirrul, 1982; Hoffman and Pelletier, 1982); and 850 m of Rocknest Formation (Grotzinger, 1982)]. Lithologically correlative units in the Athapuscow Aulacogen (Union Island and Sosa Groups) (Hoffman, 1981b) and the Kilohigok Basin (Western River Formation) (Campbell and Cecile, 1981) are of equivalent thickness, i.e. 2 to 3 km. The total Akaitcho and Epworth Group succession is about 8 km thick, half of which consists of volcanic rocks.

Long term rates of sediment deposition are controlled dominantly by the rate of subsidence (Blatt *et al.*, 1980). McKenzie (1978) has shown that the subsidence history of many sedimentary basins can be modelled in terms of an initial phase of stretching of the lithosphere, followed by a period of exponentially declining thermal subsidence. Royden and Keen (1980), Keen and Cordson (1981) and

LePichon and Sibuet (1981) have applied McKenzie's model to subsidence studies of passive margins.

In the model, the lithosphere is stretched and thinned by a factor β during rifting. Extension of the lithosphere may be uniform, where the crust and the subcrustal lithosphere are stretched equal amounts; or non-uniform, where the crust and the subcrustal lithosphere are stretched by different amounts. Extension in either case is accompanied by passive upwelling of hot material from the asthenosphere, which increases the geothermal gradient and heat flow. During extension, the crust subsides rapidly in response to changes in density which must be isostatically balanced (Keen and Cordsen, 1981). The initial stretching phase results in what is termed initial subsidence. The effects of extension terminate 10 to 15 Ma after rifting. Then the lithosphere cools and contracts, causing further subsidence (termed thermal subsidence).

Measured thermal subsidence rates along the North American, North Atlantic margin for the first 80 Ma following rifting fit a relationship $y = 300(\pm 80) t^{1/2}$ m (Keen, 1979) where y = thermal subsidence and t = time. Using this relationship, it would take about 100 Ma to deposit the Aglerok Formation and the Epworth Group. Even using subsidence rates from the Mississippi Embayment, which, at 200 m/Ma, are among the most rapid at present (Blatt *et al.*, 1980), it would require 15 Ma for deposition of the Aglerok Formation and the Epworth Group. A hotter lithosphere in

the Proterozoic (e.g. Sleep, 1979; McKenzie and Weiss, 1980) would result in lower thermal subsidence rates (McKenzie et al., 1980).

Thermal subsidence is however only part of the total subsidence. McKenzie's (1978) model predicts 2 to 3 km of initial subsidence (no sediment loading) in the first 10 Ma following rifting of the North American Atlantic margin (Royden and Keen, 1980) and the Galicia margin (LePichon and Sibuet, 1981). Keen and Cordser (1981) compared measured thermal subsidence rates and seismic refraction results from the Sauk well off of Nova Scotia with the extension model (McKenzie, 1978). The seismic results indicate that initial subsidence of 2.5 to 3 km occurred in the first 10 Ma after rifting. Thus, initial subsidence could account for deposition of the Aglerok Formation and the Epworth Group in a period of about 10 Ma after rifting began.

A hotter, and thinner lithosphere in the Proterozoic (e.g. Sleep, 1979; McKenzie and Weiss, 1980) results in more rapid, and greater subsidence (McKenzie et al., 1980). For example, using the equations and data of LePichon and Sibuet (1981), initial subsidence (unloaded) for the Galicia margin is 2.5 km with β of 3.24. However, if we only change the lithosphere thickness (from 125 km to 80 km), initial subsidence (unloaded) increases to 3.5 km with β of 3.24. Sediment loading commonly results in doubling of the total subsidence (e.g. McKenzie et al., 1980; Royden and Keen, 1980; Sclater et al., 1980, LePichon and Sibuet, 1981).

In fact, initial subsidence in the Vienna Basin of 6.5 km (sediment loaded) has occurred in less than 10 Ma (Sclater et al., 1980).

Subsidence of 7 to 8 km (sediment loaded) can occur in the initial subsidence phase following rifting, and does occur in some recent tectonic settings (e.g. the Vienna Basin, Sclater et al., 1980). A thinner lithosphere in the Proterozoic would result in greater initial subsidence than in the Recent. Thus, deposition of the 7 to 8 km of Akaitcho and Epworth Group strata could occur in 10 Ma or less. Rocknest Formation carbonate deposition causes no significant problems. Paleomagnetic results (McGlynn and Irving, 1978, 1981) indicate that Rocknest Formation deposition probably occurred at a paleolatitude of 15° to 25° S, presumably under semi-tropical conditions. Modern carbonate sedimentation rates are conservatively estimated at 1 km/Ma (Schlager, 1981). Using this estimate, Rocknest Formation deposition could have taken place in 850,000 years, or less, as long as subsidence was roughly equal to the rate of carbonate deposition.

It is difficult to estimate subsidence rates for periods less than 10 Ma - the length of the initial subsidence phase. Under such conditions, the length of the extension phase can no longer be regarded as roughly instantaneous (Jarvis and Mackenzie, 1980), and there is insufficient data from modern areas for comparison. Hence, 10 Ma for deposition of 8 km of Akaitcho and Epworth Group

strata may be close to a minimum period for Akaitcho/Epworth Group deposition.

6.5.3 Emplacement of the Hepburn Batholith

If about 10 Ma is a minimum time for Akaitcho and Epworth Group deposition, then, the Hepburn Batholith must be emplaced in only 1 or 2 Ma if the zircon dates are valid. Pitcher (1979) discusses the longevity of plutonism. In North American caldera complexes, which are regarded as the surficial expression of batholiths (Smith and Bailey, 1968; Christiansen and McKee, 1978; Hildreth, 1981), individual cycles of volcanism are interpreted to represent the time-spans of crystallization and differentiation in individual sub-volcanic plutons. Individual volcanic complexes range in age from 1.5 to 4 Ma (e.g. Steven and Lipman, 1976), and are inferred to represent nested plutonic complexes. Estimates of magma-rise range from 0.3 to 0.03 m per year in cool crust, to a hundred times this after heating of the crust (Pitcher, 1979).

The source region for the Hepburn Batholith is at about 25 km depth on the basis of geobarometry measurements on garnets in Hepburn Batholith intrusions (Pattison, 1980; Pattison et al., 1981). The Hepburn Batholith was emplaced at 10 km depth (St-Onge, 1981). Using the lower rate of magma rise of 0.03 m per year, it would take 500,000 years to emplace the batholith. In heated crust, magma generation and batholith emplacement could be more rapid (Pitcher, 1979), certainly on the scale of North American

caldera complexes. In the Archean, Davis et al. (1982) report time intervals of less than 5 Ma between cessation of volcanism and intrusion of post-orogenic granites. Thus, rapid formation and intrusion of granitic magmas is reasonable on the basis of studies of Recent and Archean terranes.

6.5.4 Discussion

It is possible to deposit the Akaitcho and Epworth Groups and intrude them with granitoids in a period of about 10 Ma using Phanerozoic and Recent sedimentation rates. The model for the development of the Wopmay Orogen proposed by Hoffman (1980c) assumed a significant time interval between the Akaitcho Group rift sequence and first collision. The zircon dates indicate that this is not the case, and requires a rethinking of the events which may have occurred prior to the first collision.

There are 3 tectonic regimes that may be applicable to Akaitcho Group deposition and models of the development of the Wopmay Orogen up to the first collision. These settings are discussed below.

Strike-Slip (Pull Apart) Basin

This tectonic regime is considered unlikely because of the abundance of volcanic rocks in the Akaitcho Group, and the absence of a homoclinal succession. Pull-apart basins such as the Carboniferous basins in the Appalachians (Bradley, 1982) are characterized by rapid subsidence, but are dominated by clastic sedimentation with minor volcanism. Volcanism can occur in pull-apart basins if significant

extension occurs (Crowell, 1974). However, it is difficult to resolve the geochemical trends observed in the Akaitcho Group with such a setting. In addition, the Athapuscow and the postulated Taktu Aulacogens are more consistent with an intracontinental rift setting than a strike-slip model.

Marginal Basin

The Akaitcho Group could be the result of back-arc spreading behind a continental magmatic arc that existed prior to the Great Bear magmatic arc. Back-arc spreading would have reached the marginal ocean-basin stage in order to account for the abundant ocean tholeiites in the Akaitcho Group, and the Epworth Group inferred passive-margin sequence. The arc would have to be west of the present Wopmay Fault Zone, and is no longer exposed.

This interpretation is considered unlikely because; i) there is no evidence of arc detritus in the Akaitcho Group; ii) there is no evidence of volcanic rocks, e.g. air-fall tuffs, which could have been derived from a volcanic arc west of the present Wopmay Fault Zone; iii) the Akaitcho Group volcanic rocks lack the high chondrite-normalized Ba to La ratios, high Al_2O_3 , and low TiO_2 , Ni and Cr values characteristic of island-arc tholeiites in marginal basins (Basaltic Volcanism Study Project, 1981). However, some recent marginal basin basalts cannot be distinguished from mid-ocean ridge basalts on the basis of chemistry (Basaltic Volcanism Study Project, 1981); iv) the Hepburn Batholith is granitic in overall composition; and it has been argued by

Hoffman et al. (1980) that the Hepburn intrusive suite is similar to batholiths found in continental collision zones, rather than subduction zones; v) rifting in marginal basins usually begins with rapid clastic sedimentation and rhyolitic ash-flow sheets (Karig and Jansky, 1972; Tarney et al., 1976). In the Akaitcho Group, rhyolitic volcanism is late, not early, in the development of the basin. Although possible, there is no evidence at present to support the marginal basin hypothesis.

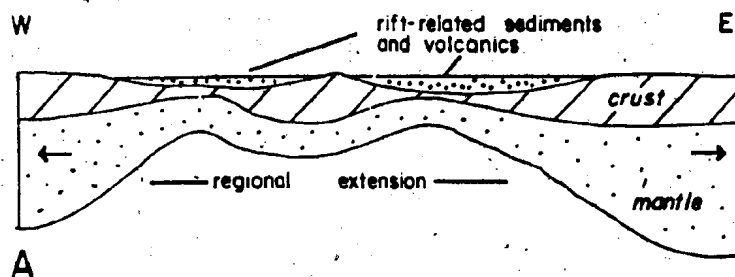
Continental Rifting Leading to Limited Sea-floor Spreading

This is the interpretation favoured by the author. Crustal extension causes formation of a rift, and rapid subsidence of the rift follows. Crustal extension with β greater than 3 is needed in order to get the tholeiitic volcanism observed in the Akaitcho Group (LePichon and Sibuet, 1981). Rifting probably led to the generation of some ocean-crust, e.g. a Red Sea size ocean, and a well-defined continental margin on which the Epworth Group was deposited. Sea-floor spreading was short-lived, possibly due to a spreading-ridge jump (e.g. Figure 6.7; National Research Council, 1979). Closure of the basin occurred due to compressive forces acting on both the Bear and Slave Plates (e.g. Figure 6.7); and resulted in folding and thrusting. Because the crust was thin, and still hot from rifting, granitic magmas formed quickly and rose to form the Wentzel and Hepburn Batholiths. No ophiolites are observed because of the lack of a sizable ocean. The model outlined

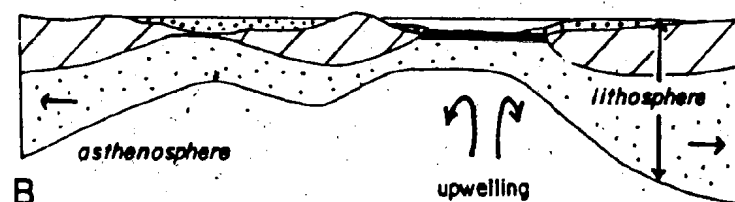
Figure 6.7 Schematic diagram illustrating the preferred model for the development of the Akaitcho and Epworth Groups. Time interval between Figures A and D is about 10 Ma.

- A - regional extension results in crustal thinning, subsidence and accumulation of volcanic and sedimentary rocks.
- B - limited sea-floor spreading (heavy black line) occurs in the eastern part of the zone of extension.
- C - spreading-ridge jumps to the western part of the zone of extension. Bear Plate is an isolated continental remnant.
- D - collision of Bear and Slave Plates causes deformation and intrusion in the Wopmay Orogen. Note that the Slave Plate is moving westward. Ocean-spreading continues west of the Bear Plate.

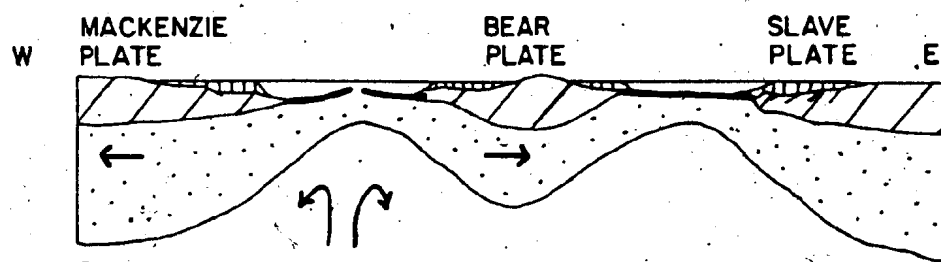
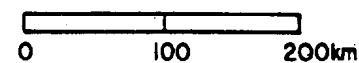
Figures A, B, and C are adapted from the National Research Council (1979; their Figure 5.3).



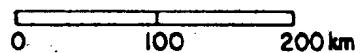
A



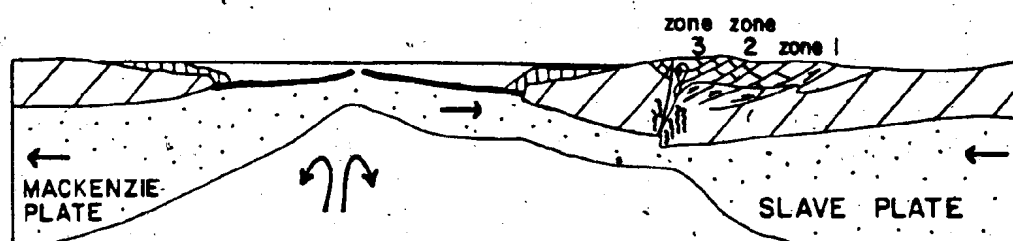
B



C



FIRST COLLISION



D

above resolves the geology and the zircon dates. This interpretation differs from that of Hoffman (1980c) in the size of the ocean formed after rifting. The only constraint on the size of the ocean is the zircon dates:

The presence of a small ocean basin does not repudiate the importance of plate interactions in the Proterozoic. Closure of the Akaitcho rift and ocean is the result of other forces acting on the Bear and Slave plates, presumably the result of other plate interactions. In addition, the Great Bear magmatic arc persisted for at least 15 Ma, and would require subduction of several hundred kilometres of ocean crust during its period of activity (Hildebrand, 1981).

6.6 DEPOSITIONAL HISTORY OF THE AKAITCHO GROUP

Between 1.9 and 2.05 Ga ago rifting began in the western part of the Slave Craton. Alkaline-peralkaline igneous complexes and tholeiitic dyke swarms were intruded into the Slave Craton starting about 2050 Ma. Block-faulting of the western margin of the present Bear-Slave boundary at about $115^{\circ}30'W$ also began at this time. The Sityok Igneous Complex and the crustally-derived rhyolites suggest that the Akaitcho Group was originally deposited on continental crust. This crust had thinned from about 34 km to 26 km by the time of Nasittok Subgroup deposition. By analogy with recent rifts, this crust probably thinned to the west towards the centre of the rift, either by rotation along fault blocks in the upper crust (Morton and Black,

1975; Zanettin and Justin-Visentin, 1975) or by ductile-spreading of the lower crust (Bott, 1976; Montadert et al. 1979). Again, by analogy to recent rifts, this period of crustal thinning may have lasted for 50 to 60 Ma (Cochran, 1981). Alternatively, the alkaline complexes could be related to an earlier period of rifting at 2.05 Ga, and the Akaitcho Group related to rifting that began between 1.9 and 1.95 Ga ago.

The oldest rocks observed in the Akaitcho Group in northern Wopmay Orogen are continental tholeiitic basalts, hence rifting may have been well advanced by the time of Ipiutak Subgroup deposition. Continental terranes were still near by, and shed arkose in large volumes into the Akaitcho rift. As rifting continued, large basalt volcanoes were constructed. The tholeiitic chemistry of the Akaitcho Group basalts in these volcanoes suggests significant degrees of partial melting in the mantle source area, and considerable crustal thinning. While ocean tholeiites were being erupted from these volcanoes, ocean-floor spreading may have started to the west. The onset of ocean-floor spreading is rapid once extensive crustal thinning has occurred (Cochran, 1981). The large volumes of basaltic magma injected into and through the crust caused crustal melting leading to eruption of the Akaitcho Group rhyolites. Water depth increased to the north and west as rifting progressed (Figure 6.4). The rift basin deepened with time and accomodated large volumes of sedimentary and volcanic

73

material. Volcanism waned with intrusion of the Tallerk sills, possibly due to westward migration of the rift axis, or termination of magmatism with the onset of sea-floor spreading.









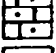



Continent-derived, westward prograding, clastic rocks of the Odjick Formation buried the Akaitcho Group (Campbell and Cecile, 1981) and formation of the Coronation passive continental-margin sequence began. The tectonic evolution of the Akaitcho Group is shown schematically in Figure 6.8.

The subsequent history of Epworth and Recluse Group deposition is unclear. If the zircon dates are valid, then ocean-floor spreading was limited, and deformation rapidly followed rifting (e.g. Figure 6.7). If the zircon dates are ignored, or are shown to be suspect, then the model of the development of the Wopmay Orogen proposed by Hoffman (1980c) may be a realistic explanation. In either case, Hoffman's (1980c) interpretation of events following the first collision in the Wopmay Orogen may be tenable.

Figure 6.8 Schematic diagram illustrating the evolution of the Coronation continental margin during the early Proterozoic. Diagram may represent a time span of as little as 10 Ma.

- I - post-Ipiutak Subgroup deposition and syn-Zephyr Formation deposition. Akaitcho Group units older than the Ipiutak Subgroup, if they exist, are considered as part of the basement.
- II - late Nasittok Subgroup deposition. Rift-type ocean crust, similar to that found in the Gulf of California and the Afar, has developed on the thinned continental crust underlying the Nasittok Subgroup.
- III - late Aglerok Formation deposition. The centre of volcanism has migrated westward, and development of normal ocean-crust is inferred to have begun to the west.
- IV - late Rocknest Formation deposition. The Akaitcho Group is buried beneath Epworth Group passive-margin sequence.

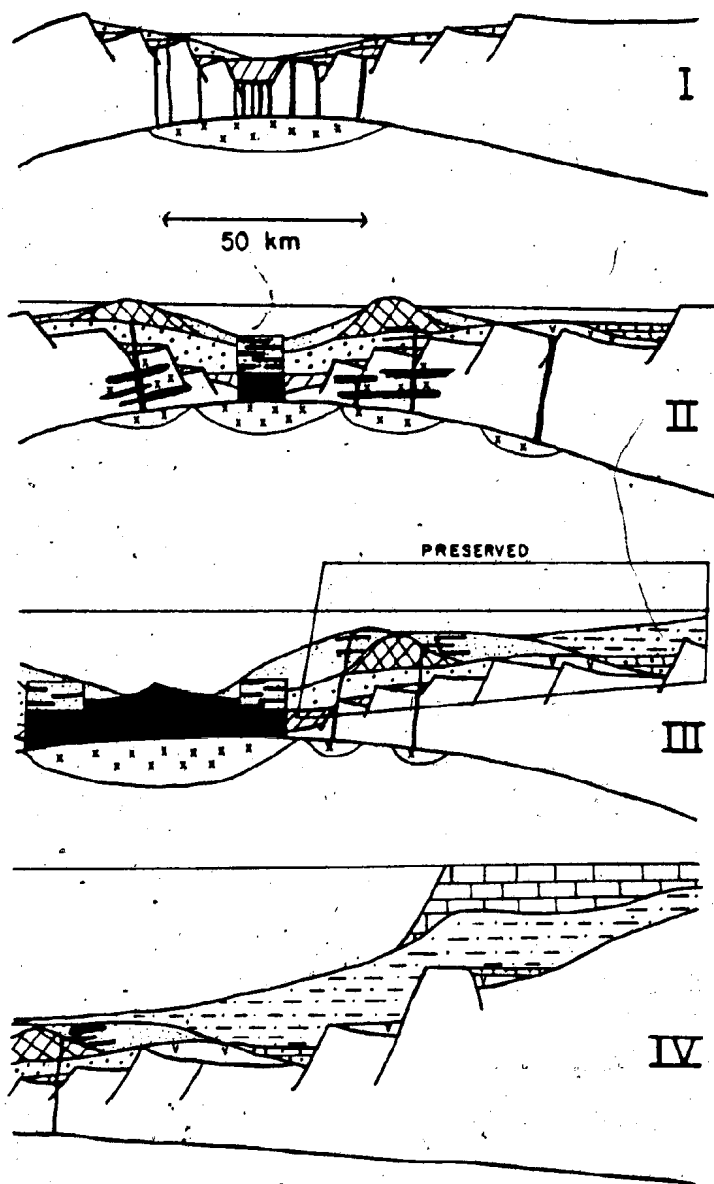
LEGEND

	Ipiutak Subgroup		rift-type ocean crust
	Zephyr Formation		
	Nasittok Subgroup		normal ocean crust
	Aglerok Formation		zones of magma generation
	Vaillant Formation		
	Stanbridge Formation		basalt feeders and sills
	Odjick Formation		
	Rocknest Formation		

AKAITCHO

GROUP

EPWORTH
GROUP



CHAPTER 7

THE AKAITCHO GROUP AND THE DEVELOPMENT OF
CONTINENTAL MARGINS7.1 INTRODUCTION

The first aim of the thesis - to determine the tectonic significance of the Akaitcho Group with respect to the Wopmay Orogen - has been addressed in Chapter 6. In this Chapter, the second aim of the thesis is examined; namely, what can the Akaitcho Group tell us about the development of continental margins and rifting processes in general, with respect to both the Proterozoic and younger plate boundaries.

7.2 CLASSIFICATION OF PROTEROZOIC RIFT SEQUENCES

In the Recent, rifts are found in a variety of tectonic settings. For example: continental collision zones (Baikal rift) (Molnar and Tapponier, 1945), left-lateral slip along transform faults (Dead Sea rift) (Hatcher et al., 1981), or spreading centres (Red Sea). Thus, in the ancient rock record, one must assume that any rift may have formed in one of several possible tectonic settings - settings that commonly form rifts with similar geological characteristics. One difficulty in working with older rift sequences is that recognition of a rift is a significant first step. The second, more difficult step, is determining the tectonic setting of that rift.

For the purpose of discussion, Proterozoic rifts in the Canadian Shield have been divided into two broad classes

(Figure 7.1). The first class of rifts are associated with orogenic belts. The rifts generally parallel the trend of the belt, and are affected by deformation and metamorphism associated with the orogenic belt. Aulacogens, which strike at high angle into orogenic belts, can be considered as a subclass of the first class of rifts. It is from the first class of rifts that we gain insight into rifting processes related to the development of continental margins. Subsequent discussion will focus on this first class of rifts.

The second class of rifts are less clearly associated with any major fold belt, or are post-orogenic. Some sequences such as the Borden and Thule basins (Figure 7.1) are magma-poor. Others, such as the Keweenaw, are magma-rich. Discussion of the class two rifts is beyond the scope of this thesis.

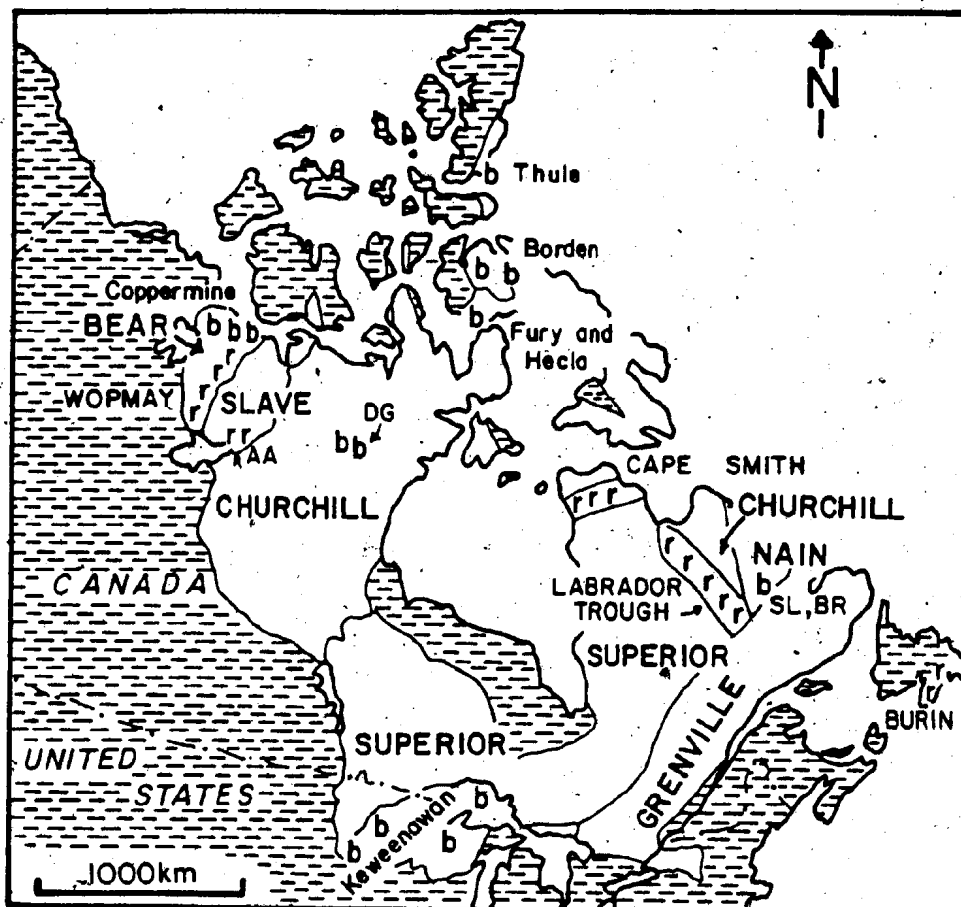
7.3 THE AKATICHO GROUP

The Akaitcho Group stratigraphic section is similar to sections drilled in the Gulf of California on DSDP Leg 64 (Curry *et al.*, 1979; Eisele *et al.*, 1980) (Figure 7.2) and the stratoid series in southern Afar (Chessex *et al.*, 1975).

The presence of the granitic rocks of the Sityok Complex, which may be basement to the Akaitcho Group, and the abundance of probable crustally-derived rhyolites in the Akaitcho Group points to the continental character of the crust underlying the Akaitcho Group. As discussed in Chapter 6.2, estimates of Akaitcho Group crustal thickness

Figure 7.1 Location of Proterozoic rifts of the Canadian Shield and adjacent areas. Class one rifts - r; Class two rifts - b. Stippled pattern - Phanerozoic rocks. Abbreviations: AA - Athapuscow Aulacogen; BR - Bruce River Group; DG - Dubwānt Group; SL - Seal Lake Group.

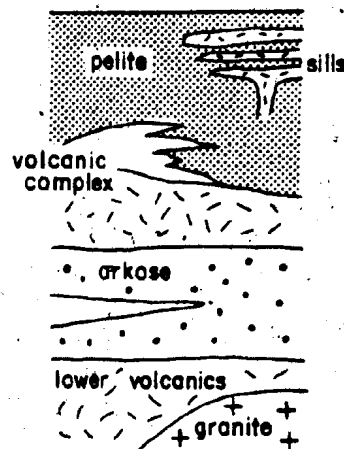
Figure 7.2 Stratigraphic sections for the Gulf of California and the Akaitcho Group. Note gross similarity between the upper part of the two sections. Gulf of California section constructed from data in Curray et al. (1979), Einsele et al. (1980). Symbols: crosses - basement rocks; hachures - basaltic flows and sills; heavy dots - coarse clastics; fine dots - mudstones; no pattern - rhyolite flows and sills.



GULF OF CALIFORNIA



AKAITCHO GROUP



during Nasittok Subgroup volcanism are 8 to 10 km less than the present (and late Archean) thickness of the Slave Craton (33.9 ± 0.9 Km, Barr (1971)). Also, as discussed in Chapter 6.2, the crustal thickness during Akaitcho Group deposition was intermediate in thickness between oceanic and continental crust, and similar to crustal thicknesses in present-day rifts such as the Gulf of California and southern Afar (Figure 6.3).

The evolution of basalt geochemistry from continental to type II ocean tholeiites indicates high degrees of partial melting in the source region for the Akaitcho Group basalts. In addition, injection of basaltic magmas into the crust in sufficient quantity to cause generation of large-volumes of crustally-derived rhyolitic magmas must have caused substantial changes to the original continental character of the crust beneath the Akaitcho Group.

As discussed in Chapter 6, the zircon dates from Zone 3 indicate that little ocean crust formed west of the rifted Slave Craton prior to the first collision. However, the Akaitcho Group probably preserves part of the crust that lay between ocean crust to the west and continental crust of the Slave Craton to the east.

The major conclusion deduced from study of the Akaitcho Group is that the crust beneath the Akaitcho Group was intermediate between continental and oceanic crust and differs from ophiolite sequences. The crustal structure of rifted continental margins therefore may be unique, as has

been suggested by recent workers (e.g. Moore, 1973; Talwani *et al.*, 1979).

7.4 CLASS ONE RIFTS - COMPARISON WITH THE AKAITCHO GROUP

7.4.1 Labrador Trough

The southern part of the Proterozoic (1.75 to 1.9 Ga) Circum-Ungava Foldbelt or Geosyncline (Dimroth *et al.*, 1970) is termed the Labrador Trough (Figure 7.1). The Labrador Trough is bounded to the east and west by the stable Archean cratons of the Nain and Superior structural provinces. The geology of the Labrador Trough has been extensively described by Dimroth (1968, 1971a, 1971b, 1972, 1978), Dimroth *et al.* (1970), Frarey (1961, 1967), Baragar (1967), Fahrig (1967), Wardle (1979), and Wardle and Bailey (1981). The following description is condensed from Wardle and Bailey (1981).

The Labrador Trough comprises a succession of sedimentary and mafic volcanic rocks (Kaniapiskau Supergroup) which is intruded by a sequence of gabbro and ultramafic sills (Montagnais Group). The Kaniapiskau Supergroup is divided into two distinct lithic assemblages: a western, predominantly sedimentary succession (the Knob Lake Group - 6500 + m) and an eastern, predominantly mafic volcanic unit (the Doublet Group - 5000 + m). The Doublet Group locally conformably overlies the Knob Lake Group on the eastern margin of the trough. A thick succession of pelitic and semi-pelitic schist and amphibolite (the Laporte Group) is an eastern lateral equivalent to the bulk of the Knob

Lake Group (Dimroth, 1978; Wardle and Bailey, 1981). The Knob Lake and the Doublet Groups were previously considered to be a miogeoclinal-eugeoclinal pair (Harrison *et al.*, 1972). Recognition of the Laporte Group as the lateral equivalent of the Knob Lake Group has required modification of this concept (see Wardle and Bailey, 1981).

Two rift assemblages are present in the trough. In the west, the lower Seward Subgroup rests unconformably on the Superior Craton and consists of coarse clastic sediments and alkaline volcanic rocks. The lower Seward Subgroup is overlain by the Knob Lake Group shelf sequence. The lower Seward Subgroup has been interpreted to represent rifting near the margin of the Knob Lake Group depositional basin (Wardle and Bailey, 1981).

The second rift assemblage is represented by the Doublet Group, which has a minimum thickness of 5000 m and overlies the Laporte Group pelitic and semi-pelitic schists. The Doublet Group is divided into three formations. The lowest, the Murdoch Formation consists of mafic pyroclastics, tuffaceous siltstones, pillow lava and minor conglomerate. The Murdoch Formation represents a period of explosive volcanism and initiated rifting (Wardle and Bailey, 1981). It is overlain by 500 to 700 m of rhythmically bedded siltstone, slate and argillite of the Thompson Lake Formation. The Thompson Lake Formation is overlain by over 3000 m of massive and pillowed low-K oceanic tholeiites of the Willbob Formation (Wardle and Bailey, 1981). The

Murdoch and Thompson Lake Formations are intruded by numerous gabbro and peridotite sills of the Montagnais Group. The Montagnais Group sills are comagmatic with the Willbob Formation basalts (Baragar, 1967; Dimroth et al., 1970); Wardle and Bailey, 1981).

Wardle (1981) and Wardle and Bailey (1981) have compared the Doublet Group to the Gulf of California, where ocean-floor spreading associated with rapid flyschoid sedimentation produces an oceanic crust very different from that present in normal spreading ridges. The conclusions reached by Wardle (1981) and Wardle and Bailey (1981) are similar to those reached by Easton (1981d) for the Akaitcho Group.

The amount of ocean-spreading which was associated with the Doublet Group is not known. Development of ocean crust in the Labrador Trough may have been less extensive than in the Wopmay Orogen, because a shelf-sequence does not post-date the Doublet Group rifting.

7.4.2 Cape Smith Foldbelt

The Cape Smith Foldbelt is also part of the Circum-Ungava Foldbelt or Geosyncline. The Cape Smith Foldbelt separates Archean gneisses of the Superior Province to the south from Churchill Province gneisses of uncertain age to the north (Figure 7.1). Supracrustal rocks of the Cape Smith Foldbelt lie unconformably on Archean gneisses to the south (Dimroth et al., 1970; Taylor, 1974). In the north-east, the supracrustal rocks lie unconformably on Churchill

Province gneiss (Schimann, 1978). The supracrustal rocks are between 1.75 and 1.9 Ga in age. Geology of the Cape Smith Foldbelt has been described by Dimroth *et al.*, (1970), Taylor (1974), Hynes and Francis (1981, 1982a, 1982b) and Francis *et al.* (1982). This account draws heavily from Hynes and Francis (1982a, 1982b).

The supracrustal rocks can be divided into two groups - the lower Povungnituk Group and the upper Chukotat Group. The Povungnituk Group lies unconformably on Archean basement and consists predominantly of sedimentary rocks. Argillaceous sandstones and siltstones are common in the lower Povungnituk Group, with turbidites being more common in the upper part of the Group. Pillowed and massive flows of continental tholeiite basalt intruded by large sills of komatiitic basalt, similar chemically to the volcanics of the overlying Chukotat Group, are present near the top of the Povungnituk Group. Locally, fragmental acidic rocks are intercalated with the basaltic flows. The Chukotat Group consists of lava flows, sills and sub-volcanic intrusions that range in composition from komatiitic basalt to ocean tholeiite. Siltstone horizons are rarely present in the Chukotat Group. The nature of the basement underlying the Chukotat Group is uncertain.

Hynes and Francis (1981, 1982, 1982b) interpret the Povungnituk Group as a rift sequence related to continental breakup. They interpret the Chukotat Group as a possible remnant of early Proterozoic ocean crust. There are few

constraints on the size of the early Proterozoic ocean. Hynes and Francis (1981) suspect that only a narrow ocean formed. No shelf sequence is present in the Cape Smith Foldbelt.

The rift rocks in the Cape Smith Foldbelt are similar to those present in the Akaitcho Group (Figure 7.3). Both have a stratigraphic sequence consisting of lower clastic rocks and continental tholeiite flows overlain by a thick sequence of ocean tholeiite flows and gabbro sill complexes. Both stratigraphic sequences have been interpreted independently to be rift sequences related to continental breakup and ocean-floor spreading.

7.4.3 Burin Group

The Burin Group is related to rifting that occurred about 760 Ma ago in the Avalon Zone of the Appalachian Orogen. Although not related to any known continental margin, the Burin Group is similar in many ways to the rift sequences described so far. The geology of the Burin Group has been described by Strong et al. (1978a, 1978b).

The Burin Group consists of 4 to 5 km of mainly volcanic rocks and sub-volcanic intrusives with minor basaltic pyroclastic rocks and fine-grained sediments. Pillowed lavas with alkaline affinities of the Pardy Island Formation form the base of the Burin Group. The Pardy Island Formation is overlain by siltstones, mafic tuffs, and stromatolitic limestones of the Port au Bras Formation. The overlying Path End and Beaver Pond Formations consist dom-

inantly of pillowed basalts with some waterlain mafic pyroclastics of ocean tholeiite composition (Strong and Dostal, 1980). The Path End and Beaver Pond Formations are intruded at their contact by the Wandsworth (Gabbro) Formation, a sill complex 1.5 km thick. The Burin Group was deformed, and overlain locally by the Rock Harbour Group, a sequence of conglomerates, sandstones, and turbidites (Hiscott, 1981).

The Burin Group is similar to the other three sequences discussed (Figure 7.3). The Burin Group basalts show a compositional evolution up-section from alkalic basalts to LREE depleted type I ocean tholeiites (Strong and Dostal, 1980). The volcanic sequence is intruded by a thick gabbro sill complex. Because of limited exposure, it is not known if a clastic sequence underlies the Burin Group. The tectonic setting of the Burin Group closely resembles the tectonic setting of the Gulf of California (Hiscott, 1981). Evidence for extensive rifting is lacking in the Burin Group (Strong *et al.*, 1978; Hiscott, 1981).

7.5 DISCUSSION: CRUSTAL STRUCTURE OF CONTINENTAL MARGINS




Figure 7.3 shows reconstructions of the four Proterozoic rift sequences discussed. Figure 7.3 is as faithful as possible to the reconstructions of the original authors. Evidence for successful rifting and formation of passive margin sequences diminishes from the Akaticho to the Burin Group.

Three of the four sequences have a recurrent stratigraphy: a lower clastic sequence overlain by a thick

Figure 7.3 Reconstructed Proterozoic margins showing inferred setting of rift sequences. Note common association of ocean tholeiites, gabbro sills, and fine-grained sedimentary sequences in all Proterozoic rift sequences illustrated.

Sources: Wopmay Orogen (Easton, 1981d); Southern Labrador Trough (Wardle and Bailey, 1981); Cape Smith Foldbelt (Hynes, 1981; Hynes and Francis, 1982a, 1982b); Burin Peninsula (Strong et al., 1978a, 1978b).

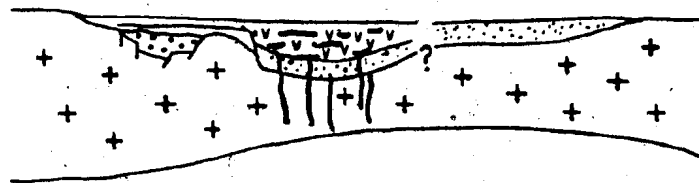
LEGEND

- + granitic basement
- coarse clastics
-  shale, siltstone
-  komatiites, ocean crust
- v tholeiites, mainly oceanic
-  tholeiitic sills

WOPMAY OROGEN

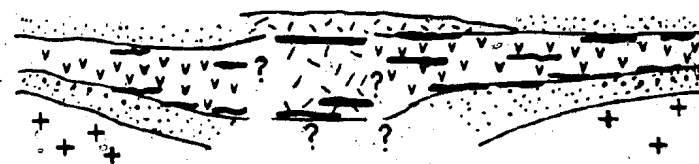


SOUTHERN LABRADOR TROUGH



50 km

CAPE SMITH FOLD BELT



BURIN PENINSULA



sequence of basaltic rocks. Gabbro sills intrude the sedimentary and volcanic rocks. The volcanic rocks show a chemical evolution up-section from either continental tholeiites or alkaline basalts to type I or type II ocean tholeiites. The Burin Group differs only in the absence of a lower clastic sequence. The stratigraphic sequence above is similar to that present in the Gulf of California, and the stratoid series of southern Afar.

In the Gulf of California, high sedimentation rates associated with ocean-floor spreading create a crustal structure different from that of normal spreading ridges. This crust is intermediate in thickness and seismic properties between continental and oceanic crust (Figure 6.3). Sedimentary rocks are abundant, and sill swarms comagmatic with oceanic tholeiite basalts are common. Note that the Gulf of California comparison applies only to the southern Gulf, and is a comparison of crustal structure and stratigraphy, not the tectonic regime.

The Proterozoic rift assemblages described above have been interpreted independently by several authors to represent the onset of ocean-floor spreading along a recently rifted cratonic block (Easton, 1981d; Wardle, 1981; Hynes and Francis, 1981). Although the evidence for generation of typical ocean crust along these continental margins is scanty, as is knowledge of the size of the resultant oceans, the similarity of stratigraphic sequences is striking.

7.6 CONCLUSIONS

Proterozoic rifts in the Canadian shield associated with orogenic belts are similar in stratigraphy and developmental history. They are characterized by a lower clastic assemblage overlain by thick piles of tholeiitic basalt, both of which are intruded by gabbro sills comagmatic with the basalts. The basaltic rocks evolve up-section from alkaline basalts or continental tholeiites to ocean tholeiites. The Proterozoic rifts are similar in stratigraphy to some modern rifted margins, indicating that as far back as 2.0 Ga, rifting processes were similar to those at present. Incipient ocean basins in the Proterozoic in areas of high sedimentation develop crustal structures similar to the Gulf of California. These preserved incipient rifts are an indication that ocean-floor spreading probably did occur in the Proterozoic, even though ophiolites are rare in the Precambrian.

CHAPTER 8

SUMMARY AND CONCLUSIONS

The following is a summary of the geological and geochemical features of the Akaitcho Group, and the conclusions inferred from these features.

1) The Akaitcho Group consists of 6 to 8 km of meta-sedimentary and metavolcanic rocks. Volcanic rocks comprise roughly half of the exposed Akaitcho Group in northern Wopmay Orogen (above 65°N). The following, generalized stratigraphic section has been recognized in the central metamorphic core zone (Zone 3) of northern Wopmay Orogen: i) a lower sequence of at least 0.5 km of basalt flows and tuffs intercalated with pelite and ortho-quartzite (the Ipiutak Subgroup), ii) a lower clastic sequence consisting of 1 to 2 km of arkosic turbidites (the Zephyr Formation) intruded by rhyolite porphyry sills (the Okrark sills); iii) several, 3 to 4 km thick, volcanic complexes consisting of subalkaline basalt and rhyolite mainly erupted subaqueously (the Nasittok Subgroup); iv) 1 to 2 km of olive-coloured pelites and volcanoclastic sediments (the Aglerok Formation), in part derived from the volcanic complexes, and locally intruded by gabbro sills (Tallerk sills).

The lower Grant Subgroup and the Drill Formation are lithologically correlated with the Zephyr Formation. The upper Grant Subgroup, and the Vaillant and Stanbridge Formations are lithologically correlated with the Nasittok

Subgroup volcanic rocks. The Union Island Group, which is located at the base of the Great Slave Supergroup in the East Arm of Great Slave Lake may be lithologically correlative with the Akaitcho Group.

The lithologies present in the Akaitcho Group, and the stratigraphic relationships between these lithologies are consistent with the Akaitcho Group being deposited in a rift.

2) The Akaitcho Group is probably overlain by the Epworth Group inferred passive-margin sequence. In two areas in Zone 3, the Akaitcho/Epworth Group contact is concordant, and may be conformable. A disconformable contact cannot be ruled out. In two areas near the boundary between Zones 2 and 3, the Epworth Group overlies, or is interbedded with basalts of the Vaillant Formation. These basalts have been lithologically correlated with the Akaitcho Group.

3) The Akaitcho Group volcanic rocks are bimodal: subalkaline basalt ($< 56\% \text{SiO}_2$; Y/Nb ratios generally > 3) and rhyolite or high-K rhyolite ($> 69\% \text{SiO}_2$).

4) Two types of basalt are present in the Akaitcho Group: Continental tholeiites and type II ocean tholeiites. The Akaitcho Group basalts change upsection from evolved continental tholeiites to type II ocean tholeiites. Some basalts of the Vaillant Formation may be transitional in chemistry between tholeiitic and alkaline basalts, but are volumetrically minor. The Vaillant Formation basalts lie

cratonward of the Ipiutak and Nasittok Subgroup volcanic rocks.

5) The Akaitcho Group rhyolites have high Fe, Ti, Mn, K, and Ba values, high $^{87}\text{Sr}/^{86}\text{Sr}$ initial ratios, and REE abundances and patterns different from the oceanic tholeiites they are associated with in the field. In addition, the rhyolites account for about 25% of the volcanic rocks in some of the Nasittok Subgroup volcanic complexes. The rhyolites were probably derived by melting of the lower (continental) crust.

6) Sedimentary rocks from the lower Akaitcho Group (the Zephyr Formation, the Ipiutak and the lower Grant Subgroups) have REE patterns similar to post-Archean sedimentary rocks worldwide, and were derived from a source terrane of overall granodiorite composition (i.e. the exposed continental crust). Sedimentary rocks from the upper Akaitcho Group (the Aglerok Formation) have REE patterns similar to the lower Akaitcho Group sedimentary rocks but with much lower total REE abundances. The REE results from the Aglerok Formation are interpreted to indicate a source terrane consisting of the continental crust (i.e. the Slave Craton) and a volcanic terrane similar to the Nasittok Subgroup.

7) All of the geochemical changes observed in the Akaitcho Group can be correlated with changes in stratigraphy or changes in the field appearance of the strata. The above interpretations (#3 through #7) are supported by the

correspondence between the field observations and the geochemical data.

8) Rb-Sr and K-Ar isotopic systems in central Wopmay Orogen have been reset. Both isotopic systems became closed to isotopic exchange about 1770 Ma, about 100 Ma after plutonism in Wopmay Orogen (based on zircon dates from granitoid rocks). Although Rb and Sr isotopes have been mobile, there is no evidence to indicate that the 'immobile' trace or the rare-earth elements were mobile.

9) The maximum age of the Akaitcho Group is unknown, and could range from 1920 to 2050 Ma. Rhyolites from the Akaitcho Group have a zircon age of 1901 ± 24 Ma (Zircon data courtesy of S.A. Bowring and W.R. Van Schmus, University of Kansas), only about 10 Ma older than plutonic rocks of the Hepburn Batholith that intrude and metamorphose the rhyolites.

10) Crustal thickness during Nasittok Subgroup deposition is estimated at 26 km based on volcano spacing. This estimate is 8 km lower than estimates of the Slave Craton thickness in the Proterozoic. Crustal thinning is consistent with a rift setting for the Akaitcho Group, and the rapid subsidence necessary to resolve Akaitcho and Epworth Group deposition and the zircon dates.

11) Aspects of the physical volcanology of the Nasittok Subgroup volcanics indicate that the basin deepened to the north and west during Nasittok Subgroup deposition. This

information can be fitted into a rift model for Akaitcho Group deposition.

12) The Akaitcho Group is best modelled as an intra-continental rift. Crustal extension caused rapid subsidence and volcanism, resulting in rapid filling of the rift.

Limited sea-floor spreading may have occurred, and a continental margin formed on which the Epworth Group inferred passive margin sequence was deposited. The rift closed soon after formation. Closure of the rift resulted in deformation, and was followed closely by plutonism.

Plutonism occurred rapidly because of the presence of thin, heated crust in the area as an aftermath of the recent rifting event. This model differs from that of Hoffman (1980c) in advocating the formation of a small ocean after initial rifting, and resolves the geology and the zircon data. The existence of plate interactions is implicit in the model presented here. Hildebrand (1981) presents evidence that the Great Bear Arc (Zone 4 of the Wopmay Orogen) is related to subduction of ocean crust, and independently documents possible plate interactions in the early Proterozoic.

13) The Akaitcho Group is similar to other Proterozoic rift sequences in the Canadian Shield that are associated with orogenic belts (e.g. the Doublet Group in the Labrador Trough; the Povungnituk and Chukotat Groups in the Cape Smith Foldbelt; and the Burin Group in the Avalon Zone of the Appalachian Orogen). Most of these rift sequences have

an association of fine- and coarse-grained clastic rocks, voluminous sequences of oceanic tholeiites, and extensive gabbro sill swarms comagmatic with the volcanic rocks. These sequences are similar to sequences present in the southern Gulf of California and the southern Afar. These sequences are interpreted to represent the remnants of crust that was transitional between continental and oceanic crust. If so, then the crustal structure of Recent rifted continental margins may be unique, as suggested by recent workers (e.g., Moore, 1973; Talwani et al., 1979).

REFERENCES

- ABBEY, S., 1980. Studies in "selected samples" for use in the general analysis of silicate rocks and minerals. Part 6: 1979 Edition of "usable" values. Geological Survey of Canada Paper 80-14. 30 pp.
- ALLAN, R.J. and CAMERON, E.M., 1973. Uranium, zinc, lead, manganese, iron and organic matter, copper, nickel, and potassium content of lake sediments, Bear-Slave Operation, District of Mackenzie. Geological Survey of Canada Maps, 9- to 15-1972.
- ALLAN, R.J., CAMERON, E.M., and DURHAM, C.C., 1973. Reconnaissance geochemistry using lake sediments of a 36,000 square mile area of the northwestern Canadian Shield. Geological Survey of Canada Paper 72-50, 70 pp.
- BAADSGAARD, H., MORTON, R.D., and OLADE, M.A.D., 1973. Rb-Sr isotopic age for the Precambrian lavas of the Seton Formation, East Arm of Great Slave Lake, N.W.T.. Canadian Journal of Earth Sciences, 10, 1579-1582.
- BADHAM, J.P.N., 1978. Has there been an oceanic margin to the western North America since Archean time? Geology, 6, 621-625.
- BALDRIDGE, W.S., 1981. Magmas as indicators of rifting process: Problems and Promise. In: Papers presented to the Conference on Processes of Planetary Rifting, pp. 199-201, Lunar and Planetary Institute, Houston.
- BALLARD, R.D. and MOORE, J.G., 1977. Photographic atlas of the mid-Atlantic ridge rift valley. Springer-Verlag, New York, 114 pp.

- BARAGAR, W.R.A., 1967. Wakuach map area, Quebec-Labrador (230). Geological Survey of Canada Memoir 344, 174 pp.
- BARAGAR, W.R.A. and DONALDSON, J.A., 1973. Coppermine and Dismal Lakes map areas. Geological Survey of Canada Paper 71-39, 20 pp.
- BARBERI, F. and VARET, J., 1977. Volcanism of Afar: Small-scale plate tectonics implications. Geological Society of America Bulletin, 88, 1251-1266.
- BARKER, F., 1981. Introduction to the special issue on granites and rhyolites: A commentary for the nonspecialist. Journal of Geophysical Research, 86, 10131-10135.
- BARR, K.G., 1971. Crustal Refraction experiment: Yellowknife, 1966. Journal of Geophysical Research, 76, 1924-1947.
- BASALTIC VOLCANISM STUDY PROJECT, 1981. Basaltic volcanism on the terrestrial planets. Pergamon Press, New York, 1286 pp.
- BICKFORD, M.E. and MOSE, D.G., 1975. Geochronology of the Precambrian rocks in the St. Francois Mountains, southeastern Missouri. Geological Society of America Special Paper, 165, 48 pp.
- BLATT, H., MIDDLETON, G., and MURRAY, R., 1980. Origin of Sedimentary Rocks. Second Edition, Prentice-Hall, New Jersey, 782 pp.
- BOTT, M.H.P., 1976. Formation of sedimentary basins of graben type by extension of the continental crust. Tectonophysics, 36, 78-87.
- BRADLEY, D.C., 1982. Subsidence in Late Paleozoic Basins in the northern Appalachians. Tectonics, 1, 107-123.

- BROOKS, C., HART, S.R., and WENDT, I., 1972. Realistic use of two-error regression treatments as applied to rubidium-strontium data. *Review of Geophysics and Space Physics*, 10, 551-577.
- BRYAN, W.B., THOMPSON, G., FREY, F.A., and DICKEY, J.S., 1976. Inferred geological settings and differentiation in basalts from the Deep Sea Drilling Project. *Journal of Geophysical Research*, 81, 4285-4303.
- BURKE, K.C.A. and DEWEY, J.F., 1973. Plume-generated triple junctions: Key indicators in applying plate tectonics to old rocks. *Journal of Geology*, 81, 406-433.
- CAMPBELL, F.H.A. and CECILE, M.P., 1975. Report on the Geology of the Kilohigok Basin, Goulburn Group, Bathurst Inlet, N.W.T.. Geological Survey of Canada Paper 75-1A, 297-306.
- CAMPBELL, F.H.A. and CECILE, M.P., 1976. Geology of the Kilohigok Basin, Goulburn Group, Bathurst Inlet, N.W.T.. Geological Survey of Canada Paper 76-1A, 369-377.
- CAMPBELL, F.H.A. and CECILE, M.P., 1981. Evolution of the early Proterozoic Kilohigok Basin, Bathurst Inlet-Victoria Island, Northwest Territories. In: Proterozoic Basins in Canada, F.H.A. Campbell (Editor). Geological Survey of Canada Paper 81-10, 103-132.
- CHESSEX, R., DELALOYE, M., MULLER, J., and WEIDMANN, M., 1975. Evolution of the volcanic region of Ali Sabieh (T.F.A.I.) in light of K-Ar age determinations. In: The Afar Depression of Ethiopia, A. Pilger and A. Rosler (Editors). I.U.C.G. Scientific Report #14, Schweizerbart'sche Verlagsbuchhandlung, Stuttgart, 221-227.

- CHRISTIANSEN, R.L. and MCKEE, E.H., 1978. Late Cenozoic volcanism and tectonic evolution of the Great Basin and Columbia Intermontane Regions. In: Cenozoic tectonics and regional geophysics of the western Cordillera, B.R. Smith and G.P. Eaton (Editors). Geological Society of America Memoir, 152, 283-311.
- COCHRAN, J.R., 1981. The Gulf of Aden: Structure and evolution of a young ocean basin and continental margin. Journal of Geophysical Research, 86, 263-288.
- CONDIE, K.C., 1976. Plate tectonics and crustal evolution. Pergamon Press, New York, 288 pp.
- CROWELL, J.C., 1974. Origin of the Late Cenozoic basins in Southern California. In: Tectonics and Sedimentation, W.R. Dickinson (Editor). Society of Economic Paleontologists and Mineralogists Special Publication 22, 190-204.
- CULLERS, R.L., YEH, L-T, CHAUDHURI, S., and GUIDOTT, C.V., 1974. Rare-earth elements in Silurian pelitic schists from N.W. Maine. Geochimica et Cosmochimica Acta, 38, 389-400.
- CUMMING, G.L., 1980. Lead isochron dating of the Seton Formation, East Arm of Great Slave Lake, N.W.T.. Canadian Journal of Earth Sciences, 17, 1591-1593.
- CURRAY, J.R., MOORE, D.M., AQUAYO, J.E., AUBRY, M-P., EINSELE, G., FORNARI, D.J., GIESKES, J., GUERRERO, J.C., KASTNER, K., KELTS, K., LYLE, M., MAOBA, Y., MOLINO-CRUZ, A., NIEMITZ, J., RUEDA, J., SAUNDERS, A.D., SCHRADER, H., SIMONEIT, B.R.T., and VACQUIER, V., 1979. Leg 64 seeks evidence on development of basins. Geotimes, 24, #7, 18-20.

- DALRYMPLE, G.B., 1979. Critical tables for conversion of K-Ar ages from old to new constants. *Geology*, 7, 558-560.
- DAVIS, D.W.; BLACKBURN, C.E., and KROGH, T.E., 1982. Zircon U-Pb ages from the Wabigoon-Manitou Lakes region, Wabigoon Subprovince, northwest Ontario. *Canadian Journal of Earth Sciences*, 19, 254-266.
- DIMROTH, E., 1968. Evolution of the central segment of the Labrador Geosyncline, Part I: Stratigraphy, facies and paleogeography. *Neues Jahrbuch für Geologie und Paleontologie Abhandlungen*, 130, 247-274.
- DIMROTH, E., 1971a. The evolution of the central segment of the Labrador Geosyncline, Part II: The ophiolitic suite. *Neues Jahrbuch für Geologie und Paleontologie Abhandlungen*, 137, 209-248.
- DIMROTH, E., 1971b. The Attikamagen-Ferriman transition in the central part of the Labrador Trough. *Canadian Journal of Earth Sciences*, 8, 1432-1454.
- DIMROTH, E., 1972. The Labrador Geosyncline revisited. *American Journal of Science*, 272, 487-506.
- DIMROTH, E., 1978. Labrador Trough area (54°30' - 56°30'). *Ministere des Richesses Naturelles, Quebec. Geological Report 193*.
- DIMROTH, E., COUSINEAU, P., LEDUC, M., and SANSCHAGRIN, Y., 1978. Structure and organization of Archean subaqueous basalt flows, Rouyn-Noranda area, Quebec, Canada. *Canadian Journal of Earth Sciences*, 15, 902-918.

- DIMROTH, E., BARAGAR, W.R.A., BERGERON, R., and JACKSON, G.D., 1970. The filling of the Circum-Ungava Geosyncline. In: Symposium on basins and geosynclines of the Canadian Shield, A.J. Baer (Editor), Geological Survey of Canada Paper 70-40, 45-158.
- DOUGLAS, R.J.W., NORRIS, D.K., and NORRIS, A.W., 1974. Geology of Horn River, District of Mackenzie. Geological Survey of Canada Map 1372A, 1:500,000 scale.
- EASTON, R.M., 1980. Stratigraphy and Geochemistry of the Akaitcho Group, Hepburn Lake map area, District of Mackenzie: An initial rift succession in Wopmay Orogen (Early Proterozoic). Geological Survey of Canada Paper 80-1B, 47-57.
- EASTON, R.M., 1981a. Stratigraphy of a Proterozoic volcanic complex at Tuertok Lake, Wopmay Orogen, District of Mackenzie. Geological Survey of Canada Paper 81-1A, 305-309.
- EASTON, R.M., 1981b. REE, U and Th contents of Proterozoic and Archean sedimentary rocks from the Bear and Slave Structural Provinces, N.W.T.. Geological Association of Canada Abstracts, 6, p. A-16.
- EASTON, R.M., 1981c. Geology of the Four Corners and Grant Lake map areas, District of Mackenzie, N.W.T.. Geological Survey of Canada Paper 81-1B, 83-84.
- EASTON, R.M., 1981d. Stratigraphy of the Akaitcho Group and the development of an early Proterozoic continental margin, Wopmay Orogen, N.W.T.. In: Proterozoic Basins of Canada, F.H.A. Campbell (Editor), Geological Survey of Canada Paper 81-10, 79-95.

- EASTON, R.M., BOODLE, R.L., ZALUSKY, L., EICHE, G., and MCKINNON, D., 1981. Preliminary geological map of the Pointless Island map area, 86H/3, H/4, H/5 and H/6, N.W.T. Department of Indian and Northern Affairs Preliminary Map EGS-1981-5a,b,c and d. 1:30.000 scale.
- EASTON, R.M. and GARCIA, M.O., 1981. Petrology of the Hilina Formation, Kilauea Volcano, Hawaii. *Bulletin Volcanologique*, 43-4, 657-673.
- EBY, G.N., 1972. Determination of rare-earth, yttrium and scandium abundances in rocks and minerals by an ion-exchange-X-ray fluorescence procedure. *Analytical Chemistry*, 44, 2137-2143.
- EICHELBERGER, J.C., 1978. Andesitic volcanism and crustal evolution. *Nature*, 283, 441-444.
- EINSELE, G., GEISKES, J.H., CURRAY, J., MOORE, D.M., AQUAYO, E., AUBRY, M-P., FORNARI, D., GUERRERO, J., KASTNER, M., KELTS, K., LYLE, M., MATOBA, Y. MOLINA-CRUZ, A., NIEMITZ, J., RUEDA, J., SAUNDERS, A., SCHRADER, H., SIMONEIT, B., and VACQUIER, V., 1980. Intrusion of basaltic sills into highly porous sediments and resulting activity. *Nature*, 283, 441-444.
- EWART, A., 1979. A review of the mineralogy and chemistry of Tertiary-Recent dacitic, latitic, rhyolitic and related salic volcanic rocks. *In: Trondhjemites, Dacites and Related Rocks*, F. Barker (Editor), Elsevier, Amsterdam, 13-121.
- FAHRIG, W.F., 1967. Shabogamo Lake map area (23G/E₄). Newfoundland, Labrador and Québec. Geological Survey of Canada Memoir 354. 23 pp.
- FLANAGAN, F.J., 1976. Description and analyses of eight new USGS rock standards. United States Geological Survey, Professional Paper 840. 192 pp.

- FLINN, D., 1962. On folding during three-dimensional progressive deformation. Quarterly Journal of the Geological Society of London, 118, 385-433.
- FLINN, D., 1978. Construction and computation of three-dimensional progressive deformations. Quarterly Journal of the Geological Society of London, 135, 291-305.
- FRANCIS, D.M., HYNES, A.H., LUDDEN, J.N., and BEDARD, J., 1982. Crystal fractionation and partial melting in the petrogenesis of a Proterozoic high-MgO volcanic suite, Ungava, Quebec. Contributions to Mineralogy and Petrology, in press.
- FRAREY, M.J., 1961. Menihék Lakes, Quebec and Newfoundland. Geological Survey of Canada Map 1087A, 4:253,440 scale.
- FRAREY, M.J., 1967. Willbob Lake and Thompson Lake map areas, Quebec and Newfoundland (230/1 and 230/8). Geological Survey of Canada Memoir 348. 74 pp.
- FRASER, J.A., 1974. The Epworth Group, Rocknest Lake area, District of Mackenzie. Geological Survey of Canada Paper 73-39. 23 pp.
- FRASER, J.A. and TREMBLAY, L.P., 1969. Correlation of Proterozoic strata in the north-western Canadian Shield. Canadian Journal of Earth Sciences, 6, 1-9.
- FRASER, J.A., CRAIG, B.G., DAVISON, W.L., FULTON, R.J., HEYWOOD, W.W., and IRVINE, T.N., 1960. North-central District of Mackenzie. Geological Survey of Canada Map 18-1960. 1:506,880 scale.

- FRASER, J.A., HOFFMAN, P.F., IRVINE, T.N., and MURSKY, G., 1972. Bear Structural Province. In: Variations in Tectonic Styles in Canada, R.A. Price and R.J.W. Douglas (Editors). Geological Association of Canada Special Paper 11, 453-503.
- FRIDLEIFSSON, I.B., 1977. Distribution of large basaltic intrusions in the Icelandic crust and the nature of the layer 2-layer 3 boundary. Geological Society of America Bulletin, 88, 1689-1693.
- FRITH, R.A., 1978. Tectonics and metamorphism along the southern boundary between the Bear and Slave structural provinces. In: Metamorphism in the Canadian Shield, J.A. Fraser and W.W. Heywood (Editors). Geological Survey of Canada Paper 78-10, 103-114.
- FRITH, R.A., 1980. Rb-Sr studies of the Wilson Island Group, Great Slave Lake, District of Mackenzie. Geological Survey of Canada Paper 80-1C, 229-233.
- FRITH, R.A. and LEATHERBARROW, R., 1975. Preliminary report on the geology of the Arseno Lake map area (86B/12), District of Mackenzie. Geological Survey of Canada Paper 75-1A, 317-321.
- FRITH, R.A., FRITH, R., HELMSTAEDT, H., HILL, J., and LEATHERBARROW, R., 1974. Geology of the Indin Lake area (86B), District of Mackenzie. Geological Survey of Canada Paper 74-1A, 317-321.
- FRITH, R., FRITH, R.A., and DOIG, R., 1977. The geochronology of the granitic rocks along the Bear-Slave Structural Province boundary, northwest Canadian Shield. Canadian Journal of Earth Sciences, 14, 1356-1373.

- FRYER, B.J., 1977. Rare-earth evidence in iron-formations for changing Precambrian oxidation states. *Geochimica et Cosmochimica Acta*, 41, 361-367.
- GASS, I.G., 1970. The evolution of volcanism in the Junction area of the Red Sea, Gulf of Aden and Ethiopian rifts. *Philosophical Transactions of the Royal Society of London, Series A*, 267, 369-381.
- GATES, T.M. and HURLEY, P.M., 1973. Evaluation of Rb-Sr dating methods applied to the Matachewan, Abitibi, Mackenzie and Sudbury dyke swarms in Canada. *Canadian Journal of Earth Sciences*, 10, 900-919.
- GOFF, S.P. and SCARFE, C.M., 1978. Preliminary report on the East Arm, Great Slave Lake, N.W.T.. In: *Mineral Industry Report 1975*, Department of Indian and Northern Affairs, EGS 1978-5, 129-134.
- GOFF, S.P., BAADSGAARD, H., MUEHLENBACHS, K., and SCARFE, C.M., 1982. Rb-Sr isochron ages, magmatic $^{87}\text{Sr}/^{86}\text{Sr}$ initial ratios, and oxygen isotope geochemistry of the Proterozoic lava flows and intrusions of the East Arm of Great Slave Lake, Northwest Territories, Canada. *Canadian Journal of Earth Sciences*, 19, 343-356.
- GROTZINGER, J.P., 1982. A preliminary account of the internal stratigraphy of the Rocknest Formation, foreland thrust-fold belt of Wopmay Orogen, District of Mackenzie. *Geological Survey of Canada Paper 82-1A*, 117-118.
- HANSON, R.E. and AL-SHAIEB, Z., 1980. Voluminous subalkaline silicic magmas related to intra-continental rifting in the southern Oklahoma aulacogen. *Geology*, 8, 480-484.

- HARRISON, J.M., HOWELL, J.E., and FAHRIG, W.F., 1972. A geological cross-section of the Labrador miogeosyncline near Schefferville, Quebec. Geological Survey of Canada Paper 70-37, 34 pp.
- HASKIN, L.A.; WILDEMAN, T.R., FREY, F.A., COLLINS, K.A., KEEDY, C.R., and HASKIN, M.A., 1966. Rare-earths in sediments. *Journal of Geophysical Research*, 71, 6091-6105.
- HASKIN, M.A. and HASKIN, L.A., 1966. Rare-earths in European shales: a redetermination. *Science*, 154, 507-509.
- HATCHER, R.D., JR., SIETZ, I. REGAN, R.D., and ABU-AJAMIEH, M., 1981. Sinistral strike-slip motion on the Dead Sea rift: Confirmation from new magnetic data. *Geology*, 9, 458-462.
- HILDEBRAND, R.S., 1981. Early Proterozoic Labine Group of Wopmay Orogen: Remnant of a continental volcanic arc developed during oblique convergence. In: *Proterozoic Basins of Canada*, F.H.A. Campbell (Editor). Geological Survey of Canada Paper 81-10, 133-156.
- HISCOTT, R.N., 1981. Stratigraphy and sedimentology of the Late Proterozoic Rock Harbour Group, Flat Islands, Placentia Bay, Newfoundland Avalon Zone. *Canadian Journal of Earth Sciences*, 18, 495-508.
- HILDRETH, W., 1981. Gradients in silicic magma chambers: Implications for lithospheric magmatism. *Journal of Geophysical Research*, 86, 10153-10192.
- HOBBS, B.E., MEANS, W.D., and WILLIAMS, P.F., 1976. *Structural Geology*. John Wiley and Sons, New York. 571 pp.

- HOFFMAN, P.F., 1968. Stratigraphy of the Lower Proterozoic Great Slave Supergroup, East Arm of Great Slave Lake, District of Mackenzie. Geological Survey of Canada Paper 68-42. 93 pp.
- HOFFMAN, P.F., 1969. Proterozoic paleocurrents and depositional history of the east arm fold-belt, Great Slave Lake, Northwest Territories. Canadian Journal of Earth Sciences, 6, 441-462.
- HOFFMAN, P.F., 1970. Study of the Epworth Group, Coppermine River Area, District of Mackenzie. Geological Survey of Canada Paper 70-1A, 144-149.
- HOFFMAN, P.F., 1972. Cross-section of the Coronation Geosyncline (Aphebian), Tree River to Great Bear Lake, District of Mackenzie. Geological Survey of Canada Paper 72-1A, 119-124.
- HOFFMAN, P.F., 1973. Evolution of an early Proterozoic continental margin: The Coronation Geosyncline and associated aulacogens of the northwestern Canadian Shield. Philosophical Transactions of the Royal Society of London, Series A, 273, 547-581.
- HOFFMAN, P.F., 1979. Comment on "Has there been an oceanic margin to western North America since Archean time?" . Geology, 7, 226.
- HOFFMAN, P.F., 1980a. Conjugate transcurrent faults in north-central Wopmay Orogen (early Proterozoic) and their dip-slip reactivation during post-orogenic extension, Hepburn Lake map area, District of Mackenzie. Geological Survey of Canada Paper 80-1A, 183-185.

- HOFFMAN, P.F., 1980b. On the relative age of the Muskox Intrusion and the Coppermine River basalts, District of Mackenzie. Geological Survey of Canada Paper 80-1A, 223-225.
- HOFFMAN, P.F., 1980c. A Wilson Cycle of early Proterozoic Age in the Northwest of the Canadian Shield. In: The Continental Crust and Its Mineral Deposits, D.W. Strangway (Editor). Geological Association of Canada Special Paper 20, 523-549.
- HOFFMAN, P.F., 1981a. Revision of Stratigraphic Nomenclature, foreland thrust-fold belt of Wopmay Orogen, District of Mackenzie. Geological Survey of Canada Paper 81-1A, 247-250.
- HOFFMAN, P.F., 1981b. Autopsy of Athapuscow Aulacogen: A failed arm affected by three collisions. In: Proterozoic Basins of Canada, F.H.A. Campbell (Editor). Geological Survey of Canada Paper 81-10, 97-102.
- HOFFMAN, P.F. and BELL, I., 1975. Volcanism and plutonism, Sloan River map area, Great Bear Lake, District of Mackenzie. Geological Survey of Canada Paper 75-1A, 331-338.
- HOFFMAN, P.F. and CECILE, M.P., 1974. Volcanism and plutonism, Sloan River map area (86K), Great Bear Lake, District of Mackenzie. Geological Survey of Canada Paper 74-1A, 173-176.
- HOFFMAN, P.F. and MCGLYNN, J.C., 1977. Great Bear Batholith: A volcano-plutonic depression. In: Volcanic Regimes in Canada, W.R.A. Baragar, L.C. Coleman, and J.M. Hall (Editors). Geological Association of Canada Special Paper 16, 169-192.

- HOFFMAN, P.F. and PELLETIER, K.S., 1982. Cloos Nappe in Wopmay Orogen: Significance for stratigraphy and structure of the Akaitcho Group, and implications for opening and closing of an early Proterozoic continental margin. Geological Survey of Canada Paper 82-1A, 109-115.
- HOFFMAN, P.F. and ST-ONGE, M.R., 1981. Contemporaneous thrusting and conjugate transcurrent faulting during the second collision in Wopmay Orogen: Implications for the subsurface structure of the post-orogenic outliers. Geological Survey of Canada Paper 81-1A, 251-257.
- HOFFMAN, P.F., BELL, I., HILDEBRAND, R.S., and THORSTAD, L., 1977. Geology of the Athapuscow Aulacogen, East Arm of Great Slave Lake, District of Mackenzie. Geological Survey of Canada Paper 77-1A, 117-129.
- HOFFMAN, P.F., DEWEY, J.F., and BURKE, K., 1974. Aulacogens and their genetic relation to geosynclines, with a Proterozoic example from Great Slave Lake, Canada. In: Modern and Ancient Geosynclinal Sedimentation, R.H. Dott, Jr. and R.H. Shaver (Editors). Society of Economic Paleontologists and Mineralogists, Special Publication 19, 38-55.
- HOFFMAN, P.F., FRASER, J.A., and MCGLYNN, J.C., 1970. The Coronation Geosyncline of Aphebian age, District of Mackenzie. In: Symposium on basins and geosynclines of the Canadian Shield, A.J. Baer (Editor). Geological Survey of Canada Paper 70-40, 201-212.
- HOFFMAN, P.F., GEISER, P.A., and GERANIAN, E.K., 1971. Stratigraphy and structure of the Epworth fold belt. Geological Survey of Canada Paper 71-1A, 135-138.

- HOFFMAN, P.F., ST-ONGE, M., CARMICHEAL, D.M., and DE BIE, I., 1978. Geology of the Coronation Geosyncline (Aphebian), Hepburn Lake Sheet (86J), Bear Province, District of Mackenzie. Geological Survey of Canada Paper 78-1A, 147-151.
- HOFFMAN, P.F., ST-ONGE, M.R., EASTON, R.M., GROTZINGER, J., and SCHULZE, D., 1980. Syntectonic plutonism in north-central Wopmay Orogen (Early Proterozoic), Hepburn Lake map area, District of Mackenzie. Geological Survey of Canada Paper 80-1A, 171-177.
- HOFFMAN, P.F., ST-ONGE, D.A., EASTON, R.M., and ST-ONGE, M.R., 1981. Preliminary geological map of Hepburn Lake, District of Mackenzie. Geological Survey of Canada Open File 784. 1:100,000 scale.
- HYNES, A., 1980. Carbonatization and mobility of Ti, Y and Zr in Ascot Formation metabasalts, S.E. Quebec. Contributions to Mineralogy and Petrology, 75, 79-87.
- HYNES, A. and FRANCIS, D.M., 1981. Tectonic evolution of the Cape Smith foldbelt, northern Ungava. In: Geological Association of Canada, Abstracts, 6, p. A-28.
- HYNES, A. and FRANCIS, D.M., 1982a. A transect of the early Proterozoic Cape Smith foldbelt, New Quebec. Tectonophysics, in press.
- HYNES, A. and FRANCIS, D.M., 1982b. Komatiitic basalts of the Cape Smith foldbelt, New Quebec, Canada. In: Komatiites, N.T. Arndt and E.G. Nisbet (Editors). Allen and Unwin, New York, in press.
- IRVINE, T.N. and BARAGAR, W.R.A., 1971. A guide to the chemical classification of the common volcanic rocks. Canadian Journal of Earth Sciences, 8, 523-548.

- JARVIS, G.T. and MCKENZIE, D., 1980. Sedimentary Basin Formation with finite extension rates. *Earth and Planetary Science Letters*, 48, 42-52.
- JELETZKY, O.L., 1974. Unroofing of the Hepburn Batholith: A petrographic study of the Aphebian Recluse Formation, Epworth Group, Northwest Territories. Unpublished B.Sc. Thesis, Carleton University, Ottawa, 73 pp.
- JONES, J.G., 1969. Pillow lavas as depth indicators. *American Journal of Science*, 267, 181-195.
- KARIG, D.E. and JENSKY, W., 1972. - The proto-gulf of California. *Earth and Planetary Science Letters*, 17, 169-174.
- KEARNS, C., ROSS, G.M., DONALDSON, J.A., and GELDSETZER, H.J., 1981. Tectonism and depositional history of the Helikian-Hornby Bay and Dismal Lake Groups, District of Mackenzie. In: *Proterozoic Basins of Canada*, F.H.A. Campbell (Editor), Geological Survey of Canada Paper 81-10, 157-182.
- KEEN, C.E., 1979. Thermal history and subsidence of rifted continental margins - evidence from wells of the Nova Scotian and Labrador shelves. *Canadian Journal of Earth Sciences*, 16, 505-522.
- KEEN, C.E. and CORDSEN, A., 1981. Crustal structure, seismic stratigraphy, and rift processes of the continental margin off eastern Canada: Ocean bottom seismic refraction results off Nova Scotia. *Canadian Journal of Earth Sciences*, 18, 1523-1538.
- LEECH, G.B., LOWDON, J.A., STOCKWELL, C.H., and WANLESS, R.K., 1963. Age determinations and geological studies (including isotopic ages - Report #4). Geological Survey of Canada Paper 63-17. 140 pp.

- LEEMAN, W.P., BUDAHN, J.R., GERLACH, D.C., SMITH, D.R., and POWELL, B.N., 1980. Origin of Hawaiian Tholeiites: Trace element constraints. *American Journal of Science*, 280-A, 794-819.
- LE PICHON, X. and SIBUET, J-C., 1981. Passive margins: A model of formation. *Journal of Geophysical Research*, 86, 3708-3720.
- LORD, C.S., 1942. Snare River and Ingray Lake map areas, Northwest Territories. Geological Survey of Canada Memoir 235. 55 pp.
- LORD, C.S. and PARSONS, W.H., 1952. Camell River, District of Mackenzie, N.W.T.. Geological Survey of Canada Map 1014A. 1:253,440 scale.
- LOWDON, J.A., 1960. Age determinations by the Geological Survey of Canada, Report 1 - Isotopic Ages.. Geological Survey of Canada Paper 60-17. 51 pp.
- LOWDON, J.A., 1961. Age determinations by the Geological Survey of Canada, Report 2 - Isotopic Ages. Geological Survey of Canada Paper 61-17. 127 pp.
- LOWDON, J.A., STOCKWELL, C.H., TIPPER, H.W., and WANLESS, R.K., 1963. Age determinations and geological studies (including isotopic ages - Report #3). Geological Survey of Canada Paper 62-17. 140 pp.
- MACDONALD, G.A. and KATSURA, T., 1964. Chemical composition of Hawaiian lavas. *Journal of Petrology*, 5, 82-133.
- MARTINEAU, M.P. and LAMBERT, R.ST.J., 1975. The Bigspruce nepheline-syenite/carbonatite complex, N.W.T.. Geological Association of Canada, Program with Abstracts, 1, 59.

- MASUDA, A., NAKAMURA, N., and TANAKA, T., 1973. Fine structures of mutually normalized rare-earth patterns of chondrites. *Geochimica et Cosmochimica Acta*, 37, 239-248.
- MAXWELL, J.A., 1968. *Rock and Mineral Analysis*. Wiley-Interscience, New York. 584 pp.
- McBIRNEY, A.R., 1963. Factors governing the nature of submarine volcanism. *Bulletin Volcanologique*, 26, 455-469.
- McGLYNN, J.C., 1964. Grant Lake area. Geological Survey of Canada Paper 64-1, 14.
- McGLYNN, J.C., 1972. Basler Lake Granite, District of Mackenzie. In: Rubidium-strontium isochron age studies, Report #1, R.K. Wanless and W.D. Loveridge (Editors). Geological Survey of Canada Paper 72-23, 15-20.
- McGLYNN, J.C., 1974. Geology of the Calder River map area (86F), District of Mackenzie. Geological Survey of Canada Paper 74-1A, 383-385.
- McGLYNN, J.C., 1975. Geology of the Calder River Map area (86F), District of Mackenzie. Geological Survey of Canada Paper 75-1A, 359-361.
- McGLYNN, J.C., 1976. Geology of the Calder River (86F) and Leith Peninsula (86E) map areas, District of Mackenzie. Geological Survey of Canada Paper 76-1A, 359-361.
- McGLYNN, J.C., 1977. Geology of the Bear-Slave Structural Provinces, District of Mackenzie. Geological Survey of Canada Open File 445.
- McGLYNN, J.C., 1980. Peninsula sill, Takijuk Lake, District of Mackenzie. Geological Survey of Canada Paper 80-1C, 227-228.

- McGLYNN, J.C. and IRVING, E., 1975. Paleomagnetism of early Aphebian diabase dykes from the Slave Structural Province, Canada. *Tectonophysics*, 26, 23-38.
- McGLYNN, J.C. and IRVING, E., 1978. Multicomponent magnetization of the Pearson Formation (Great Slave Supergroup, N.W.T.) and the Coronation Loop. *Canadian Journal of Earth Sciences*, 15, 642-654.
- McGLYNN, J.C. and IRVING, E., 1981. Horizontal motions and rotations in the Canadian Shield during the early Proterozoic. *In: Proterozoic Basins of Canada*, F.H.A. Campbell (Editor). Geological Survey of Canada Paper 81-10, 183-190.
- McGLYNN, J.C. and ROSS, J.V., 1962. The Basler Lake map area. Geological Survey of Canada Map 18-1962. 1:63,360 scale.
- McGLYNN, J.C. and ROSS, J.V., 1963. Arseno Lake map area, District of Mackenzie, 86B/12. Geological Survey of Canada Paper 63-26. 7 pp.
- McKENZIE, D., 1978. Some remarks on the development of sedimentary basins. *Earth and Planetary Science Letters*, 40, 25-32.
- McKENZIE, D. and WEISS, N., 1980. The thermal history of the earth. *In: The Continental Crust and Its Mineral Deposits*, D.W. Strangway (Editor). Geological Association of Canada Special Paper 20, 575-590.
- McKENZIE, D., NISBET, E., and SCLATER, J.G., 1980. Sedimentary basin development in the Archean. *Earth and Planetary Science Letters*, 48, 35-41.

- McLENNAN, S.M., 1981. Trace element geochemistry of sedimentary rocks: Implications for the composition and evolution of the continental crust. Unpublished Ph.D. thesis, Australian National University, Canberra, 500 pp.
- McLENNAN, S.M. and TAYLOR, S.R., 1980a. Rare-earth elements in fine-grained sedimentary rocks and ores from the Pine Creek Geosyncline. In: Proceedings of the International Symposium Pine Creek Geosyncline, pp. 175-190, International Atomic Energy Agency.
- McLENNAN, S.M. and TAYLOR, S.R., 1980b. Th and U in sedimentary rocks: Crustal evolution and sedimentary recycling. *Nature*, 285, 621-624.
- McLENNAN, S.M. and TAYLOR, S.R., 1980c. Geochemical standards for sedimentary rocks: Trace element data for USGS standards SCo-1, MAG-1, and SGR-1. *Chemical Geology*, 29, 333-343.
- McLENNAN, S.M., FRYER, B.J., and YOUNG, G.M., 1979. Rare-earth elements in Huronian (Lower Proterozoic) sedimentary rocks: Composition and evolution of the post-Kenoran upper crust. *Geochimica et Cosmochimica Acta*, 43, 375-388.
- McLENNAN, S.M., NANCE, W.B., and TAYLOR, S.R., 1980. Rare-earth element-thorium correlations in sedimentary rocks and the composition of the continental crust. *Geochimica et Cosmochimica Acta*, 44, 1833-1839.
- MOHR, P.A., 1978. Afar. *Annual Review of Earth and Planetary Science*, 6, 145-172.
- MOHR, P.A. and WOOD, C.A., 1976. Volcano spacing and lithospheric attenuation in the eastern rift of Africa. *Earth and Planetary Science Letters*, 33, 126-144.

- MOLNAR, P. and TAPPONNIER, P., 1975. Cenozoic tectonics of Asia: Effects of a continental collision. *Science*, 189, 419-426.
- MONTADERT, L., DE CHARPEL, O., ROBERTS, D., GUENOC, P., and SIBRET, J., 1979. Northeast Atlantic Passive Continental Margins: Rifting and Subsidence Process. *In: Deep Drilling Results in the Atlantic Ocean: Continental Margins and Paleoenvironment*, M. Talwani, W. Hay, and W.B.F. Ryan (Editors). Maurice Ewing Series #3, American Geophysical Union, Washington, 154-186.
- MOORE, D.G., 1973. Plate-edge deformation and crustal growth, Gulf of California Structural Province. *Geological Society of America Bulletin*, 84, 1883-1906.
- MOORE, D.G., 1965. Petrology of deep-sea basalt near Hawaii. *American Journal of Science*, 263, 40-52.
- MOORE, J.G. and FISKE, R.S., 1969. Volcanic substructure inferred from dredge samples and ocean-bottom photographs, Hawaii. *Geological Society of America Bulletin*, 80, 1191-1202.
- MORTON, W.H. and BLACK, R., 1975. Crustal attenuation in Afar. *In: Afar Depression of Ethiopia*, A. Pilger and A. Rosler (Editors). I.U.C.G. Scientific Report #14, Schweizerbart'sche Verlagsbuchhandlung, Stuttgart, 221-227.
- MURSKY, G., ALLAN, G.F., HUNT, G., TIPLEY, H.Z., and WOOLLET, G.N., 1970. Geological Survey of Canada Open File 4.
- NANCE, W.B. and TAYLOR, S.R., 1976. Rare-earth element patterns and crustal evolution - I. Australian post-Archean sedimentary rocks. *Geochimica et Cosmochimica Acta*, 40, 1939-1551.

- NANCE, W.B. and TAYLOR, S.R., 1977. Rare-earth element patterns and crustal evolution II. Archean sedimentary rocks from Kalgoorlie, Australia. *Geochimica et Cosmochimica Acta*, 41, 225-231.
- NATIONAL RESEARCH COUNCIL, 1979. Continental margins: Geological and geophysical research needs and problems. National Academy of Sciences, Washington. 302 pp.
- NEILSEN, P.A., 1978. Metamorphism of the Arseno Lake area, N.W.T.. In: Metamorphism in the Canadian Shield, J.A. Fraser and W.W. Heywood (Editors). Geological Survey of Canada Paper 78-10, 103-114.
- NEILSEN, P.A. and GHOSH, D.K., 1981a. An Rb/Sr isotopic investigation of polymetamorphic paragneisses from the SE Bear Province, N.W.T.. Geological Association of Canada Abstracts, 6, p. A-43.
- NEILSEN, P.A. and GHOSH, D.K., 1981b. Rb/Sr isotope systematics in polymetamorphic paragneiss of the Bear Province, N.W.T., Canada. Geological Society of America Abstracts with Programs, 13, 520.
- NORRISH, K. and HUTTON, J.T., 1969. An accurate X-ray spectrographic method for the analyses of a wide range of geologic samples. *Geochimica et Cosmochimica Acta*, 33, 431-451.
- PAGE, R.W., 1976. Response of U-Pb zircon and Rb-Sr total rock systems to low-grade regional metamorphism in Proterozoic igneous rocks, Mount Isa, Australia. Carnegie Institution of Washington Yearbook, 75, 813-821.

PAGE, R.W., 1978. Response of U-Pb zircon and Rb-Sr total rock and mineral systems to low-grade regional metamorphism in Proterozoic igneous rocks, Mount Isa, Australia. *Journal of the Geological Society of Australia*, 25, 141-164.

PATTISON, D.R.M., 1980. Geothermobarometry applied to garnet-bearing plutons of the Hepburn and Wentzel Batholiths, Wopmay Orogen, N.W.T.. Unpublished B.Sc. thesis, Queen's University, Kingston, 81 pp.

PATTISON, D.R.M., CARMICHAEL, D.M., and ST-ONGE, M.R. 1981. Geothermobarometry applied to garnet-bearing plutons of the Hepburn and Wentzel Batholiths, Wopmay Orogen, N.W.T.. *Geological Association of Canada Abstracts*, 6, p. A-46.

PEARCE, J.A. and CANN, J.R., 1973. Tectonic setting of basic volcanic rocks determined using trace element analysis. *Earth and Planetary Science Letters*, 19, 290-300.

PEARCE, T.H., GORMAN, B.E., and BIRKETT, T.C. (1975) The TiO_2 - K_2O - P_2O_5 Diagram: A method of discriminating between oceanic and non-oceanic basalts. *Earth and Planetary Science Letters*, 24, 419-426.

PETTIJOHN, F.J., 1975. *Sedimentary rocks*. Third edition. Harper and Row, New York, 628 pp.

PIPER, D.Z., 1974. Rare-earth elements in the sedimentary cycle: A summary. *Chemical Geology*, 14, 285-304.

PITCHER, W.S., 1979. The nature, ascent and emplacement of granitic magmas. *Quarterly Journal of the Geological Society of London*, 136, 627-662.

- RIES, A.C. and SHACKLETON, R.M., 1976. Patterns of strain variations in arcuate fold belts. Philosophical Transactions of the Royal Society of London, Series A, 283, 281-288.
- ROBERTSON, J.M. and MOENCH, R.H., 1979. The Pecos Greenstone Belt: A Proterozoic volcano-sedimentary sequence in the southern Sangre de Cristo mountains, New Mexico. New Mexico Geological Society Guidebook, 30th Field Conference, Santa Fe County, 165-173.
- ROBINSON, B.W. and MORTON, R.D., 1972. Geology and geochronology of the Echo Bay area, N.W.T., Canada. Canadian Journal of Earth Sciences, 9, 158-171.
- ROSS, J.V., 1959. Mesa Lake, District of Mackenzie, N.W.T.. Geological Survey of Canada Map 30-1959. 1:63,360 scale.
- ROSS, J.V., 1966. Structure and metamorphism of the Mesa Lake area, N.W.T., 86B/14. Geological Survey of Canada Bulletin 124. 33 pp.
- ROSS, J.V. and McGLYNN, J.C., 1965. Snare-Yellowknife relations, District of Mackenzie, N.W.T., Canada. Canadian Journal of Earth Sciences, 2, 118-130.
- ROYDEN, L. and KEEN, C.E., 1980. Rifting process and thermal evolution of the continental margin of eastern Canada determined from subsidence curves. Earth and Planetary Science Letters, 51, 343-361.

- SALISBURY, M.H., STEPHEN, R., CHRISTENSEN, N.I.,
FRANCHEATEY, J., HAMANO, Y., HOBART, M., and JOHNSON, D.,
1979. The physical state of the upper levels of
Cretaceous oceanic crust from the results of
logging, laboratory studies, and the oblique
seismic experiment at DSDP Sites 417 and 418.
*In: Deep Drilling Results in the Atlantic Ocean:
Ocean Crust*, M. Talwani, C.G. Harrison, and D.E.
Hayes (Editors). Maurice Ewing Series #2,
American Geophysical Union, 113-134.
- SCHIMMAN, K., 1978. On regional metamorphism in the
Wakeham Bay area, New Quebec. *In: Metamorphism
in the Canadian Shield*, J.A. Fraser and W.W.
Heywood (Editors). Geological Survey of Canada
Paper 78-10, 245-248.
- SCHLAGER, W., 1981. The paradox of drowned reefs and
carbonate platforms. *Geological Society of
America Bulletin*, 92, 197-211.
- SCHMID, R., 1981. Descriptive nomenclature and class-
ification of pyroclastic deposits and fragments:
Recommendations of the I.U.G.S. subcommission on
the systematics of igneous rocks. *Geology*, 9,
41-43.
- SCHOLZ, C.H., 1980. Shear heating and the state of stress
on faults. *Journal of Geophysical Research*, 85,
6174-6184.
- SCHOLZ, C.H., BEAVAN, J., and HANKS, T.C., 1979. Frictional
metamorphism, argon depletion and tectonic stress
on the Alpine Fault, New Zealand, *Journal of
Geophysical Research*, 84, 6770-6782.

- SCLATER, J.G., ROYDEN, L., HORVATH, F., BURCHFIEL, B.C., SEMKEN, S., and STEGENA, L., 1980. The formation of the intra-Carpathian Basins as determined from subsidence. *Earth and Planetary Science Letters*, 51, 139-162.
- SLEEP, N.J., 1979. Thermal history and degassing of the earth: Some simple calculations. *Journal of Geology*, 279, 671-686.
- SMITH, P.H., 1963. Mattberry Lake, District of Mackenzie. Geological Survey of Canada Map 44-1963. 1:63,360 scale.
- SMITH, R.L. and BAILEY, R.A., 1968. Resurgent cauldrons. In: *Studies in Volcanology*, R.R. Coats, R.L. Hay, C.A. Anderson (Editors). Geological Society of America Memoir, 116, 613-662.
- STEIGER, R.H. and JAGER, E., 1977. Subcommittee on geochronology: Conventions on the use of decay constants in geo- and cosmochemistry. *Earth and Planetary Science Letters*, 36, 359-362.
- ST-ONGE, M.R., 1981. Metamorphic conditions of the low pressure internal zone of north-central Wopmay Orogen, N.W.T., Canada. Unpublished Ph.D. thesis, Queen's University, Kingston, 240 pp.
- ST-ONGE, M.R., KING, J.E., and LALONDE, A.E., 1982. Geology of central Wopmay Orogen (early Proterozoic), Bear Province, District of Mackenzie, Redrock Lake and eastern portion of Calder River map areas. Geological Survey of Canada Paper 82-1A, 99-108.
- STEVEN, T.A. and LIPMAN, P.W., 1976. Calderas of the San Juan volcanic field, southwestern Colorado. United States Geological Survey, Professional Paper 958. 35 pp.

- STRECKEISEN, A., 1976. To each plutonic rock its proper name. *Earth Science Reviews*, 12, 1-33.
- STRONG, D.F., O'BRIEN, S.J., TAYLOR, S.W., STRONG, P.G., and WILTON, D.H., 1978a. Aborted Proterozoic rifting in eastern Newfoundland. *Canadian Journal of Earth Sciences*, 15, 117-131.
- STRONG, D.F., O'BRIEN, S.J., TAYLOR, S.W., STRONG, P.G., and WILTON, D.H., 1978b. Geology of the Marystown (1M/3) and St. Lawrence (1L/14) map areas, Newfoundland. Newfoundland Department of Mines and Energy, Mineral Development Division Report 77-8. 81 pp.
- STRONG, D.F. and DOSTAL, J., 1980. Dynamic melting of Proterozoic upper mantle: Evidence from rare-earth elements in oceanic crust of eastern Newfoundland. *Contributions to Mineralogy and Petrology*, 72, 165-173.
- SUN, S-S. and NESBITT, R.W., 1977. Chemical heterogeneity of the Archean mantle, composition of the earth and mantle evolution. *Earth and Planetary Science Letters*, 35, 429-448.
- TALWANI, M., MUTTER, J., HOUTZ, R., and KONIG, M., 1979. The crustal structure and evolution of the area underlying the magnetic quiet zone on the margin south of Australia. In: *Geological and Geophysical Investigations of Continental Margins*, J.L. Watkins, L. Montadert, and P.W. Dickerson (Editors). American Association of Petroleum Geologists Memoir 29, 151-175.
- TANKARD, A.J., JACKSON, M.P.A., ERIKSSON, K.A., HOBDAV, D.K., HUNTER, D.R., and MINTER, W.E.L., 1982. *Crustal Evolution of Southern Africa*. Springer-Verlag, New York, 523 pp.

- TARNEY, J., DALZIEL, I.W.D., and DE WIT, M.J., 1976. Marginal basin 'Rocas Verdes' complex from S. Chile: A Model for Archean greenstone belt formation. In: The Early History of the Earth, B.F. Windley (Editor). John Wiley and Sons, New York, 131-146.
- TAYLOR, F.C., 1974. Reconnaissance geology of a part of the Precambrian Shield, northern Quebec and Northwest Territories. Geological Survey of Canada Paper 74-21. 10 pp.
- TAYLOR, H.P. JR., 1978. Oxygen and Hydrogen isotope studies of plutonic granitic rocks. Earth and Planetary Science Letters, 38, 177-210.
- TAYLOR, S.R., 1964. Abundance of chemical elements in the continental crust: A new table. *Geochimica et Cosmochimica Acta*, 28, 1273-1285.
- TAYLOR, S.R., 1977. Island arc models and the composition of the continental crust. In: Island Arc, Deep Sea Trenches and Back-Arc Basins, M. Talwani and W.C. Pitman III (Editors). Maurice Ewing Series #1, American Geophysical Union, Washington, 325-335.
- TAYLOR, S.R., 1979. Chemical composition and evolution of the continental crust: The rare-earth element evidence. In: The Earth: Its Origin, Structure and Evolution, M.W. McElhinny (Editor). Academic Press, New York, 353-376.
- TAYLOR, S.R. and McLENNAN, S.M., 1981a. The rare-earth element evidence in Precambrian sedimentary rocks: Implications for crustal evolution. In: Precambrian Plate Tectonics, A. Kroner (Editor). Elsevier, Amsterdam, 527-548.

- TAYLOR, S.R. and McLENNAN, S.M., 1981b. The composition and evolution of the continental crust: Rare-earth element evidence from sedimentary rocks. *Philosophical Transactions of the Royal Society of London, Series A*, in press.
- TIRREL, R., 1982. Frontal thrust zone of Wopmay Orogen, Takijuk Lake map area, District of Mackenzie. Geological Survey of Canada Paper 82-1a, 119-122.
- TREMBLAY, L.P., STANTON, M.S., and YARDLEY, D.H., 1954. Chalco Lake. Geological Survey of Canada Map 1023A. 1:63,360 scale.
- TREMBLAY, L.P., WRIGHT, G.M., and MILLER, M.L., 1953. Ranji Lake. Geological Survey of Canada Map 1022A. 1:63,360 scale.
- TREUIL, M. and JORON, J.L., 1975. Etude geochemique des elements en traces dans le magmatisme de l'Afar: Implications petrogenetiques et comparaison avec le magmatisme de l'Islande et de la dorsale medio-Atlantique. In: *Afar: Between Continental and Oceanic Rifting*, A. Pilger and A. Rosler (Editors). I.U.G.C. Scientific Report #14, Volume II, Schweizerbart'sche Verlagsbuchhandlung, Stuttgart, 26-79.
- VAN SCHMUS, W.R. and BOWRING, S.A., 1980. Chronology of igneous events in the Wopmay Orogen, Northwest Territories, Canada. Geological Society of America, Abstracts with Programs, 12, 540.
- WANLESS, R.K. and LOVERIDGE, W.D., 1977. Rubidium-strontium isotopic age studies, Report #2 (Canadian Shield). Geological Survey of Canada Paper 77-14. 70 pp.

- WANLESS, R.K., STEVENS, R.D., LACHANCE, G.R., and RIMSAITE, R.Y.H., 1965. Age determinations and geological studies, Part 1 - Isotopic Ages, Report #5. Geological Survey of Canada Paper 64-17 (Part 1). 126 pp.
- WANLESS, R.K., STEVENS, R.D., LACHANCE, G.R., and RIMSAITE, R.Y.H., 1966. Age determinations and geological studies, K-Ar isotopic ages, Report #6. Geological Survey of Canada Paper 65-17. 101 pp.
- WANLESS, R.K., STEVENS, R.D., LACHANCE, G.R., and EDMONDS, C.M., 1967. Age determinations and geological studies, K-Ar isotopic ages, Report #7. Geological Survey of Canada Paper 66-17. 120 pp.
- WANLESS, R.K., STEVENS, R.D., LACHANCE, G.R., and EDMONDS, C.M., 1968. Age determinations and geological studies, K-Ar isotopic ages, Report #8. Geological Survey of Canada Paper 67-2A. 141 pp.
- WANLESS, R.K., STEVENS, R.D., LACHANCE, G.R., and DELABIO, R.N.D., 1970. Age determinations and geological studies, K-Ar isotopic ages, Report #9. Geological Survey of Canada Paper 69-2A. 78 pp.
- WANLESS, R.K., STEVENS, R.D., LACHANCE, G.R., and DELABIO, R.N.D., 1972. Age determinations and geological studies, K-Ar isotopic ages, Report #10. Geological Survey of Canada Paper 71-2. 96 pp.
- WANLESS, R.K., STEVENS, R.D., LACHANCE, G.R., and DELABIO, R.N.D., 1973. Age determinations and geological studies, K-Ar isotopic ages, Report #11. Geological Survey of Canada Paper 73-2. 139 pp.
- WANLESS, R.K., STEVENS, R.D., LACHANCE, G.R., and DELABIO, R.N.D., 1974. Age determinations and geological studies, K-Ar isotopic ages, Report #12. Geological Survey of Canada Paper 74-2. 72 pp.

- WANLESS, R.K., STEVENS, R.D., LACHANCE, G.R., and DELABIO, R.N.D., 1978. Age determinations and geological studies, K-Ar isotopic ages, Report #13. Geological Survey of Canada Paper 77-2. 60 pp.
- WANLESS, R.K., STEVENS, R.D., LACHANCE, G.R., and DELABIO, R.N.D., 1979. Age determinations and geological studies, K-Ar isotopic ages, Report #14. Geological Survey of Canada Paper 79-2. 67 pp.
- WARDLE, R.J., 1979. Geology of the eastern margin of the Labrador Trough: Newfoundland Department of Mines and Energy, Mineral Development Division, Report 78-9. 22 pp.
- WARDLE, R.J., 1981. Eastern margin of the Labrador Trough: An Aphebian proto-oceanic rift zone. Geological Association of Canada Abstracts, 6, p. A-59.
- WARDLE, R.J. and BAILEY, D.G., 1981. Early Proterozoic sequences in Labrador. In: Proterozoic Basins of Canada, F.H.A. Campbell (Editor). Geological Survey of Canada Paper 81-10, 331-359, and revised supplement.
- WENTWORTH, C.K. and MACDONALD, G.A., 1953. Structures and forms of basaltic rocks in Hawaii. United States Geological Survey Bulletin 994. 98 pp.
- WILDEMAN, T.R. and HASKIN, L.A., 1973. Rare-earths in Precambrian sediments. Geochimica et Cosmochimica Acta, 37, 419-438.
- WILLIAMS, H., 1979. Appalachian Orogen in Canada. Canadian Journal of Earth Sciences, 16, 792-807.
- WILLIAMS, H. and MCBIRNEY, A.R., 1979. Volcanology. Freeman, Cooper and Company, San Francisco. 397 pp.

WINDLEY, B.F., and DAVIES, F.B., 1976. Volcano spacing and lithospheric/crustal thickness in the Archean. *Earth and Planetary Science Letters*, 38, 291-297.

WRIGHT, G.M., 1954. Ghost Lake. Geological Survey of Canada Map 1021A. 1:63,360 scale.

ZANETTIN, B. and JUSTIN-Visentin, E., 1975. Tectonical and volcanological evolution of the western Afar margin (Ethiopia). In: *The Afar Depression of Ethiopia*. A. Pilger and A. Rosler (Editors). I.U.C.G. Scientific Report #14, Schweizerbart'sche Verlagsbuchhandlung, Stuttgart, 300-309.

APPENDIX A

ANALYTICAL METHODSA.1 SAMPLE COLLECTION AND PREPARATION

Representative specimens were collected from all stratigraphic units in the Hepburn, Four Corners, and Grant Lake map areas. The distribution of analyzed specimens between major stratigraphic units is given in Table A.1.

Sample names in this report use the following numbering scheme. The first letter refers to the collector, the numbers before the period indicate the station where the sample was collected, and the numbers after the period indicate the year the sample was collected; e.g. sample F405.78 was collected by the author at station 405 in 1978. Sample collectors are: F- the author, G- J.P. Grotzinger, H- P.R. Hoffman, R- Doug Furey and S- M.R. St-Onge.

Samples were prepared by crushing to -2 cm chips in the field. This procedure eliminated one source of laboratory contamination, and ensured that an adequate amount of fresh material was obtained. The chips were pulverized at -200 mesh in a tungsten carbide Siebtechnik "Tema" swing mill. The resulting rock powders were used in subsequent analyses.

A.2 MAJOR ELEMENT ANALYSES

Major elements were determined by atomic absorption (AA) spectrometry using a Perkin-Elmer digitized spectrometer or by X-ray fluorescence (XRF) spectrometry on fused pellets using a modification of the heavy absorber technique of Norrish and Hutton (1969). Agreement between the two

Table A.1 Distribution of analyzed samples between stratigraphic units.

Unit	total samples	major element analyses	trace element analyses	REE analyses
<u>AKAITCHO GROUP</u>				
lower volcanics	44	7	44	10
Nasittok volcanics				
basalt	134	36	134	55
rhyolite	48	14	48	8
Tallerk sills	14	2	14	2
Okrark sills	14	6	14	5
lower sediments	29	8	29	14
upper sediments	16	11	16	9
Vaillant Formation				
basalt	26	6	26	11
rhyolite	1	1	1	1
Total Akaitcho	336	94	336	118
OTHER CORONATION SUPERGROUP STRATA	16	3	16	9
PLUTONIC ROCKS (Sitiyok, Hepburn, Wentzel)	61	37	61	18
OTHER ROCKS (Dumas Group, Migration Sills, Muskox Intrusion, Mackenzie dykes)	84	16	84	10

This list does not include duplicate, repeat, or test analyses.

methods is good (Table A.2). Precision of the methods have been given in Easton and Garcia (1981). Samples collected in 1978 were analyzed by XRF, subsequent samples were analyzed by AA.

For the samples analyzed by XRF, the major elements, except Na, were determined using fused pellets made of 4.000 g of lithium tetraborate; 0.500 g of rock powder; and 0.500 g of lanthanum oxide. Na was detected as a thin film on pressed powder trace pellets. XRF samples were analyzed by the author. Samples were calibrated against pellets of international rock standards; using computer programs prepared by D. Press of Memorial University.

Samples for major element analyses by atomic absorption spectrometry were dissolved in a solution of 5 ml HF, 50 ml saturated H_3BO_3 and 145 ml H_2O on a steam bath overnight. P_2O_5 was determined by colorimetry (Maxwell, 1968) and "Loss on Ignition" after heating in porcelain crucibles at $1050^\circ C$ for 2 hours in a muffle furnace. G. Andrews, Department of Geology, Memorial University performed the atomic absorption analyses.

A.3 TRACE ELEMENT ANALYSES

Trace elements were determined with a Phillips 1450 X-ray fluorescence spectrometer calibrated against international rock standards. Samples were run as pellets prepared by subjecting a homogenized mixture of 10 g of rock powder and 1.25 g of phenol formaldehyde to a 50 MPa pressure in a 40 mm diameter die for 1 minute. The result-

ing pellets were heated in a muffle furnace for 10 minutes at 200°C. Estimates of analytical error for trace element analyses are $\pm 3\%$ to 5% or 1 ppm, whichever is greater. The effects of deliberate cross-contamination of samples is shown in Table A.3. For the samples in Table A.3, the swing mill was not cleaned between samples. The effects of this low-level contamination are within the limits of analytical uncertainty. The effects of inhomogeneity between pellets is shown in Table A.4. In this case, a set of pellets was made from a 60 g jar of rock powder. Again, any variation is within the limits of analytical uncertainty. In Table A.5, the effects of sample selection were examined. In this case a sample was split in two, and each half was crushed and powdered separately. Again, any variation is within analytical uncertainty. The effect of outcrop variation on a sample has been illustrated in Table 5.6. Again, any effect is insignificant with respect to analytical uncertainty.

A.4 RARE-EARTH-ELEMENT ANALYSES

REE were analyzed by the thin-film X-ray fluorescence method of Eby (1972) as modified by Fryer (1977). Samples were calibrated against international rock standards. Figure A.1 compares several determinations of the USGS standard rock BHVO-1, a hawaiian basalt, with published values. The MUN determinations are within 10% of the published values. The estimated precision of the XRF-REE method is $\pm 10\%$ (Fryer, 1977). Figure A.2 compares the

Table A.2 Comparison of XRF and AA methods for major element determinations on sample F405.78. - a basalt. All values as wt.%.

Element	XRF	AA	error*
SiO ₂	52.0	52.6	0.40
TiO ₂	2.38	2.26	0.03
Al ₂ O ₃	12.16	12.8	0.20
Fe ₂ O ₃ ^t	17.35	16.64	0.30
MnO	0.20	0.22	0.01
MgO	3.21	3.46	0.20
CaO	6.23	6.11	0.10
Na ₂ O	2.5	2.76	0.25
K ₂ O	1.87	1.72	0.02
P ₂ O ₅	0.46	0.56	0.02
L.O.I.	1.0	0.51	
Total	99.32	99.64	

* estimated analytical error for both methods, expressed as weight percent oxide (roughly 2%).

Table A.3 Comparison of contaminated and uncontaminated sample pellets - Note: contamination is due to unclean procedures during the powdering stage of sample preparation. Contamination is not directly quantified, but all other samples were prepared under 'clean' conditions. All values in ppm.

Element	RHYOLITE			QUARTZITE		
	F195.79 clean	F195.79 contaminated by basalt	error*	F365.80 clean	F365.80 contaminated by basalt	error*
Zr	458	442	13	191	200	7
Y	163	161	7	8	8	1
Nb	21	21	1			
Sr	124	123	6	56	56	3
U	1	4	2	0	0	2
Rb	9	10	1	33	33	2
Th	11	17	2	4	4	2
Pb	11	13	2	5	3	1
Ga	21	24	2	4	2	2
Zn	208	205	7	17	15	1
Cu	60	56	3			
V	81	77	3			
Ba	188	180	7			

* estimated analytical error in ppm, roughly 5% or 1 ppm, whichever is greater.

Table A.4 Comparison of trace element results for four pellets made from one jar of rock powder for sample F412B - a basalt. All values in ppm.

Element	Pellet #				error*
	1	2	3	4	
Zr	99	99	97	101	4
Y	36	36	36	37	2
Nb	5	6	6	6	1
Sr	159	159	160	157	8
U	3	3	0	8	2
Rb	14	15	12	15	1
Th	0	7	1	5	2
Pb	3	9	0	14	2
Zn	104	105	103	104	4
Cu	64	67	66	68	3
Cr	97	93	94	94	4
V	308	316	310	306	10
Ba	100	108	104	98	4

* estimated analytical error in ppm, roughly 5% or 1 ppm, whichever is greater.

Table A.5 Trace element variation in pellets prepared from two splits of sample F464.79 - gabbro. All values in ppm.

Element	SPLIT 1			SPLIT 2		error*
	F3	F2	F1	S1	S2	
Zr	35	31	30	31	33	2
Y	19	19	21	18	19	1
Sr	120	120	135	127	125	6
U	0	1	2	3	0	2
Rb	17	18	18	17	16	1
Th	1	5	4	3	2	2
Pb	3	5	8	8	5	1
Ga	15	15	15	13	14	1
Zn	71	74	78	72	70	3
Ni	174	175	186	172	170	8

* estimated analytical error in ppm, roughly 5% or 1 ppm, whichever is greater.

repeatability of the method on several low total REE abundance samples. Again, the samples all lie within analytical uncertainty of one another. Figure A.3 shows a comparison of determination of the REE content of a hawaiian basalt by XRF at MUN and by Instrumental Neutron Activation Analysis (INAA) by F. Frey at MIT. Again the determinations are within analytical uncertainty. Figure A.4 compares values for the USGS standard SCo-1 as determined by XRF at MUN and published values determined by McLennan and Taylor (1980c). At the time SCo-1 was analyzed at MUN, no reliable REE determinations were available for the sample. Again, the MUN determination is within analytical uncertainty of the published value. REE plots were normalized to the chondritic values reported by Masuda et al. (1973) times 1.2. The chondrite normalizing factors (in ppm) are: Ba 3.44; La 0.315; Ce 0.813; Pr 0.116; Nd 0.597; Sm 0.192; Eu 0.0722; Gd 0.259; Tb 0.0490; Dy 0.325; Ho 0.0730; Er 0.213; Tm 0.0300; Yb 0.208; Lu 0.0323; and Y 1.81.

Figure A.1 (Left) Comparison of determinations of REE abundances in BHVO-1 by the author (MUN) and published values for the rock standard (Abbey, 1980; Flanagan, 1976).

Figure A.2 (Right) Variation in analytical results for 4 separate determinations on sample F498.80, a basalt. Sample showing the most variation has the lowest chemical yield (50%).

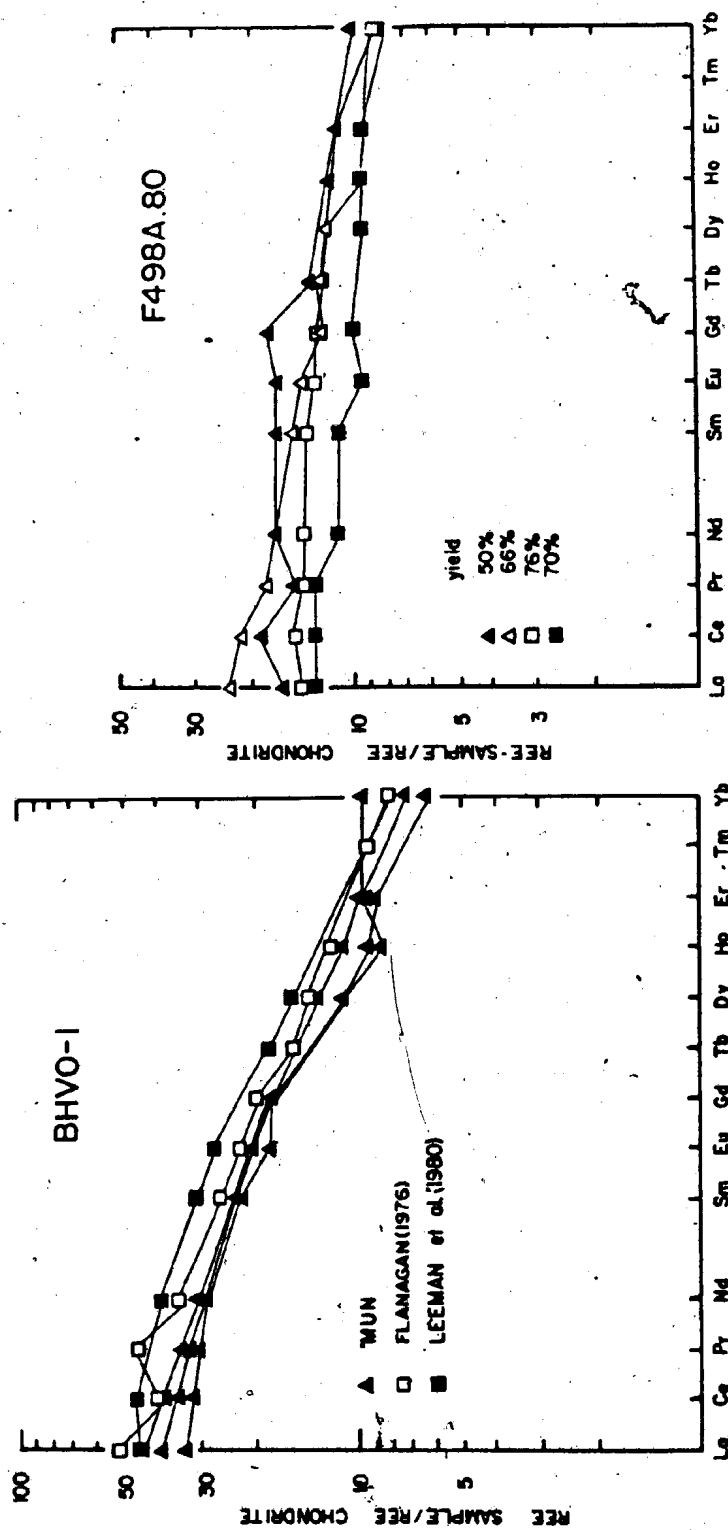
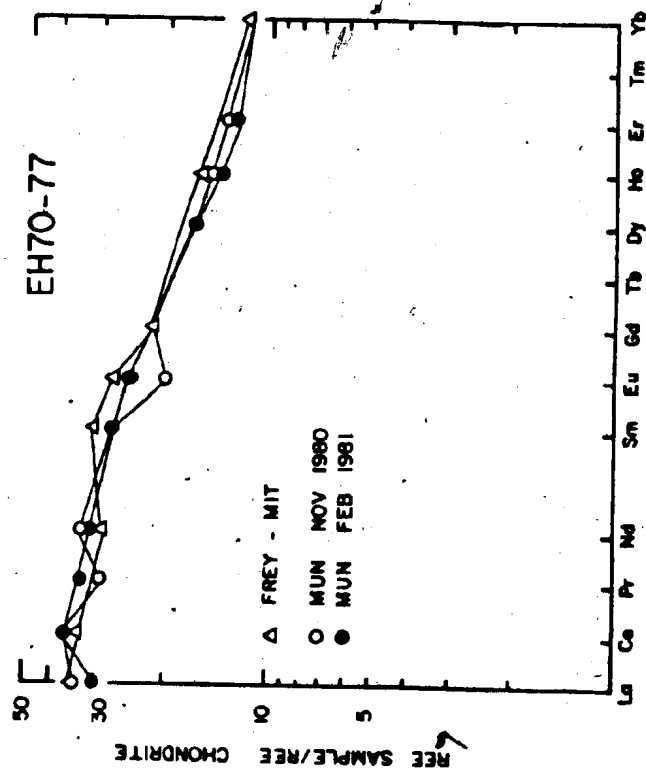
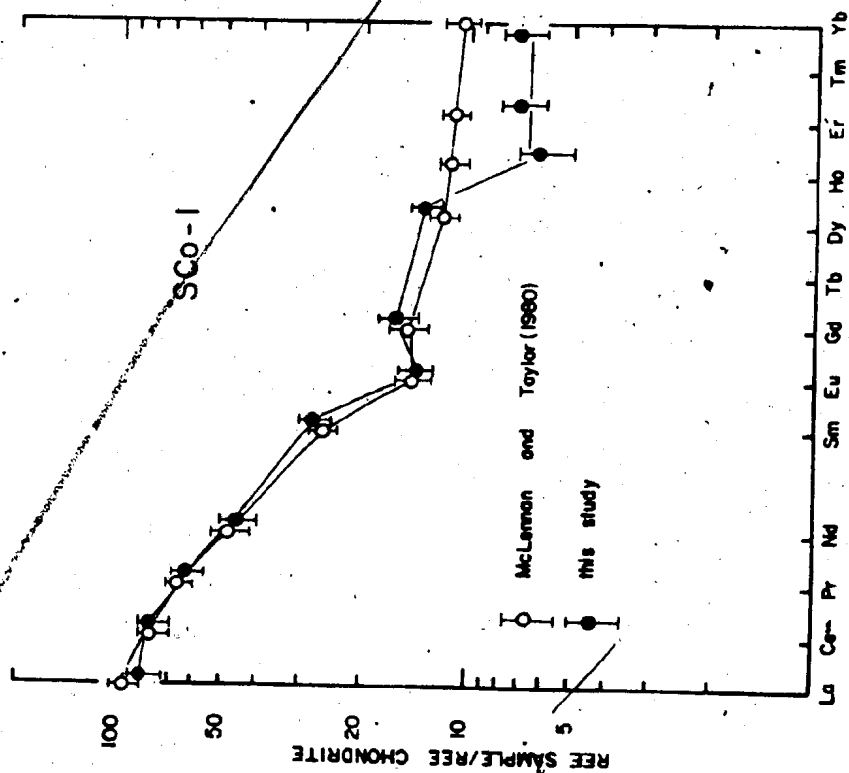


Figure A.3 (Left) Comparison of REE abundances in sample EH70-77, a hawaiian tholeiite as determined at MUN by XRF and at MIT by INAA.

Figure A.4 (Right) Comparison of REE abundances in SCo-1, a USGS rock standard as determined in this study, and the published values of McLennan and Taylor (1980c).



APPENDIX B

RUBIDIUM-STRONTIUM DATING METHODS ANDANALYTICAL RESULTSB.1 SAMPLE PREPARATION

One kilogram of chipped, fresh rock were collected in the field, and crushed under clean conditions to -1 cm size in a Braun Chipmunk Jaw Crusher. The chips were then coned and split into four quarters. One quarter was used to prime the Siebtechnik swing mill and was discarded. The second split was powdered using the swing mill. The other two splits were stored for possible future use.

B.2 STRONTIUM SEPARATION

HCL of 2N concentration (S.G. 1.035 ± 0.001) was used throughout the separation procedure. Rexyn 101, 100 to 200 mesh cation resin was conditioned in 30 ml of 2N HCl and placed in glass columns 18 x 1 cm to a height of 15 cm. One to one-half a gram of powdered sample was weighed into a teflon beaker, and dissolved overnight in a mixture of 10 ml of HF and 1 ml of HClO_4 on a hot plate @ 150°C . Next, 10 ml of 2N HCl and 2 ml HClO_4 were added and evaporated to dryness. 5 ml of 2N HCl was added to the sample, and after dissolution of the dry residue in the beaker, the sample was loaded onto the ion-exchange column. The column was eluted with 120 ml of 2N HCl to remove other ions. The final 20 ml of acid contained Sr and was collected. The final eluant was evaporated to the last drop, which was placed in a vial and dried under a heat lamp for later use.

Sr from the vial was mounted as a salt on a single tantalum filament using H_3PO_4 . Six filaments and samples were loaded onto a turret barrel and analyzed on a Vacuum Generators Micromass 30 mass spectrometer. Analytical data for the isochron diagrams and the regression tables of Chapter 5 are given in Tables B.1 to B.5. Sample locations are shown in Figures B.1 to B.5. The Tuertok Rhyolite samples were collected at $66^{\circ}40'45''N$, $115^{\circ}33'45''W$ from Unit 10 of Easton (1981c) (see also Figure 4.13). Sample F462A.79, a rhyolite from the Kapvik volcanic complex was collected at $66^{\circ}09'15''N$, $115^{\circ}37'30''W$, and is plotted with the Okrark sill samples (Figure 5.6).

B.3 RUBIDIUM-STRONTIUM ANALYSIS

Rubidium-strontium ratios were determined by X-ray fluorescence on pressed powder pellets (see Appendix A.3). Reported rubidium and strontium values and ratios are based on a minimum of ten replicate analyses and calibrated against international rock standards. Precision of rubidium-strontium ratios is estimated at 1% (2σ) or better. Precision of rubidium and strontium contents is estimated at 2% or better.

Table B.1 Results of rubidium and strontium analyses for samples from the Sityok Igneous Complex. Estimated precision for rubidium and strontium content is 2%, and 1% for rubidium-strontium ratios. Estimated precision in $^{87}\text{Sr}/^{86}\text{Sr}$ is reported at 1 σ .

Sample Number	Rb	Sr	Rb/Sr	$^{87}\text{Rb}/^{86}\text{Sr}$	$^{87}\text{Sr}/^{86}\text{Sr}$
GNEISS (Unit 1)					
F610.80	101.8	23.9	4.265	12.742	1.03418 \pm 0.000234
F611.80	67.0	44.0	1.521	4.453	0.823550 \pm 0.000152
F612.80	57.4	47.0	1.223	3.575	0.80861 \pm 0.000207
F613.80	68.0	50.8	1.340	3.918	0.811007 \pm 0.000216
F615.80	66.8	46.6	1.433	4.192	0.815975 \pm 0.000123
F616.80	22.3	53.9	0.414	1.200	0.735474 \pm 0.000028
F618.80	18.5	110.0	0.168	0.487	0.717981 \pm 0.000254
F619.80	22.9	88.5	0.259	0.751	0.723759 \pm 0.000065
F620.80	15.7	126.6	0.124	0.359	0.713968 \pm 0.000035
F614.80	19.1	93.7	0.203	0.589	0.718004 \pm 0.000077
MONZOGRAHITE (Unit 2)					
OTC 1: F608A.80	190.6	31.0	6.143	18.593	1.171225 \pm 0.000066
F608B.80	184.7	40.7	4.537	13.582	1.055064 \pm 0.000094
F608C.80	171.0	43.0	3.982	11.871	1.01160 \pm 0.000100
F608D.80	188.5	35.3	5.346	16.100	1.118210 \pm 0.000176
F608E.80	168.2	38.8	4.340	12.973	1.040043 \pm 0.000033
F608F.80	174.7	38.8	4.507	13.484	1.049153 \pm 0.000142
OTC 2: F666.80	249.3	42.4	5.882	17.793	1.165553 \pm 0.000040
F667.80	259.3	43.3	5.992	18.151	1.180236 \pm 0.000130
F668.80	256.6	42.8	6.005	18.185	1.176700 \pm 0.000129
F669.80	238.6	45.2	5.277	15.888	1.115398 \pm 0.000450
AMPHIBOLITE (Unit 3)					
F609A.80	44.8	101.1	0.443	1.285	0.73415 \pm 0.0002
F609D.80	32.7	130.4	0.251	0.727	0.72139 \pm 0.000044
F609F.80	49.7	73.5	0.676	1.967	0.753000 \pm 0.00030

Table B.2 Results of rubidium and strontium analyses for samples from the Belleau volcanic complex and the Vaillant Formation basalts. Estimated precision for rubidium and strontium content is 2%, and 1% for rubidium-strontium ratios. Estimated precision in $^{87}\text{Sr}/^{86}\text{Sr}$ is reported at 1 σ .

Sample Number	Rb	Sr	Rb/Sr	$^{87}\text{Rb}/^{86}\text{Sr}$	$^{87}\text{Sr}/^{86}\text{Sr}$
VAILLANT FORMATION					
OTC 1: F770.79	13.1	232.4	0.057	0.164	0.706915 \pm 0.000067
F771.79	1.16	86.4	0.021	0.122	0.705738 \pm 0.00014
F772.79	22.22	60.8	0.366	1.060	0.729800 \pm 0.00026
OTC 2: F775.79	21.6	53.6	0.403	1.170	0.731988 \pm 0.0001
F776A.79	12.7	59.8	0.213	0.617	0.71827 \pm 0.00053
F776B.79	15.4	90.9	0.169	0.489	0.715305 \pm 0.000052
F777.79	10.7	83.9	0.128	0.370	0.712744 \pm 0.00005
BELLEAU VOLCANIC COMPLEX					
F448.78	12.1	239.8	0.051	0.146	0.70795 \pm 0.000316
F449.78	9.7	226.5	0.043	0.124	0.70724 \pm 0.000127
F450.78	9.2	212.1	0.043	0.126	0.70722 \pm 0.000156
F452.78	9.5	202.9	0.047	0.135	0.7077 \pm 0.000756
F453.78	12.6	217.1	0.058	0.168	0.7081 \pm 0.00006

Table B.3 Results of rubidium and strontium analyses for samples from the Edjuvit mylonite zone. Estimated precision for rubidium and strontium content is 2%, and 1% for rubidium-strontium ratios. Estimated precision in $^{87}\text{Sr}/^{86}\text{Sr}$ is reported at 1 σ .

Sample Number	Rb	Sr	Rb/Sr	$^{87}\text{Rb}/^{86}\text{Sr}$	$^{87}\text{Sr}/^{86}\text{Sr}$
GRANITE					
F337E.80	136.4	133.9	1.019	2.979	0.80748 \pm 0.002
F336B.80	208.5	134.8	1.547	4.536	0.8426 \pm 0.00012
F337C.80	178.9	140.9	1.270	3.716	0.82155 \pm 0.0002
MYLONITE					
F337A.80	85.2	99.0	0.860	2.506	0.772424 \pm 0.0001
F337B.80	131.9	100.9	1.307	3.821	0.80961 \pm 0.00015
GABBRO					
F367A.80	24.2	138.7	0.174	0.505	0.7154 \pm 0.0004
F337D.80	40.3	190.9	0.211	0.612	0.72227 \pm 0.00025
F336C.80	44.4	124.9	0.356	1.032	0.72380 \pm 0.000055

Table B.4 Results of rubidium and strontium analyses for samples from the Okrark sills and a rhyolite from the Tuertok volcanic complex. Estimated precision for rubidium and strontium content is 2%, and 1% for rubidium-strontium ratios. Estimated precision in $^{87}\text{Sr}/^{86}\text{Sr}$ is reported at 1 σ .

Sample Number	Rb	Sr	Rb/Sr	$^{87}\text{Rb}/^{86}\text{Sr}$	$^{87}\text{Sr}/^{86}\text{Sr}$
OKRARK SILLS					
ORTHOCLASE PORPHYRITIC					
F458.78	164.9	185.1	0.891	2.595	0.772762 ± 0.001038
F460.78	168.0	142.0	1.183	3.452	0.792058 ± 0.000155
F420.78	199.0	145.7	1.366	3.991	0.802685 ± 0.000640
PLAGIOCLASE PORPHYRITIC					
F461A.78	218.9	91.6	2.390	7.039	0.887704 ± 0.000451
F461B.78	203.5	91.4	2.228	6.552	0.871827 ± 0.000185
F461C.78	228.3	87.4	2.611	7.697	0.893866 ± 0.000865
KAPVIK RHYOLITE					
F462A.79	133.1	89.2	1.496	4.377	0.8178 ± 0.00005
TUERTOK RHYOLITE					
F466A.80	139.7	91.7	1.524	4.460	0.820356 ± 0.00004
F466D.80	158.1	56.5	2.799	8.263	0.91017 ± 0.00005
F466E.80	131.3	51.5	2.549	7.519	0.89841 ± 0.0004
F466F.80	157.1	46.7	3.362	9.972	0.959017 ± 0.00005
F466G.80	138.8	46.5	2.985	8.830	0.93044 ± 0.00015

Table B.5 Results of rubidium and strontium analyses for samples of the Rib Pluton. Estimated precision for rubidium and strontium content is 2%, and 1% for rubidium-strontium ratios. Estimated precision in $^{87}\text{Sr}/^{86}\text{Sr}$ is reported at 1 σ .

Sample Number	Rb	Sr	Rb/Sr	$^{87}\text{Rb}/^{86}\text{Sr}$	$^{87}\text{Sr}/^{86}\text{Sr}$
OTC 1: F104.79	161.5	153.5	1.052	3.069	0.782524 ± 0.00019
F105.79	149.9	101.2	1.480	4.329	0.81565 ± 0.00029
F106.79	176.3	150.6	1.174	3.416	0.79330 ± 0.0008
F107.79	172.1	139.9	1.231	3.595	0.799674 ± 0.000095
F88.79(altered)	159.8	123.7	1.291	3.773	0.804507 ± 0.00005
OTC 2: F353.79	166.6	188.4	0.8841	2.574	0.772130 ± 0.00081
F358.79	173.3	86.5	2.004	5.883	0.8548 ± 0.0007
OTC 3: F66.79	147.4	166.3	0.8864	2.582	0.773408 ± 0.0001
F67.79	177.9	101.3	1.756	5.278	0.840667 ± 0.000031
F68.79	201.4	60.1	3.353	9.948	0.96245 ± 0.00013

Figure B.1 Rb-Sr sample location map for the Okrark sills
and the Belleau volcanic complex basalts.

Figure B.2 Rb-Sr sample location map, Vaillant Formation
basalts.

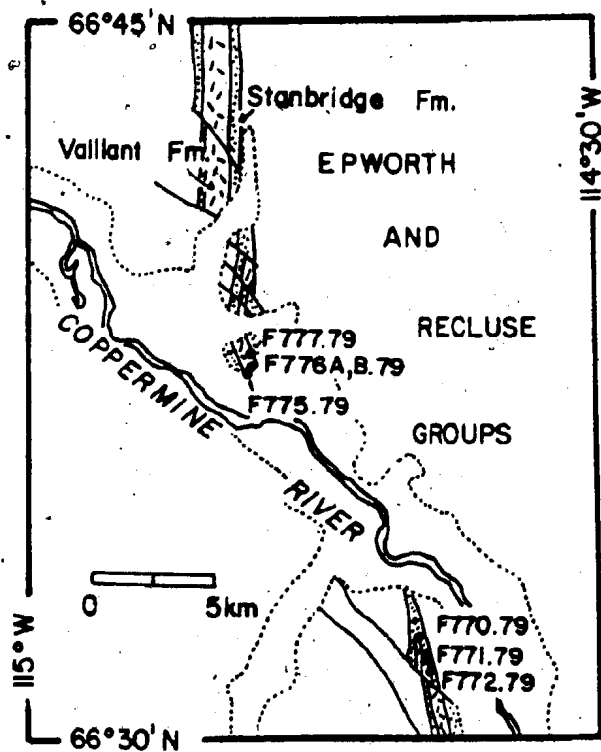
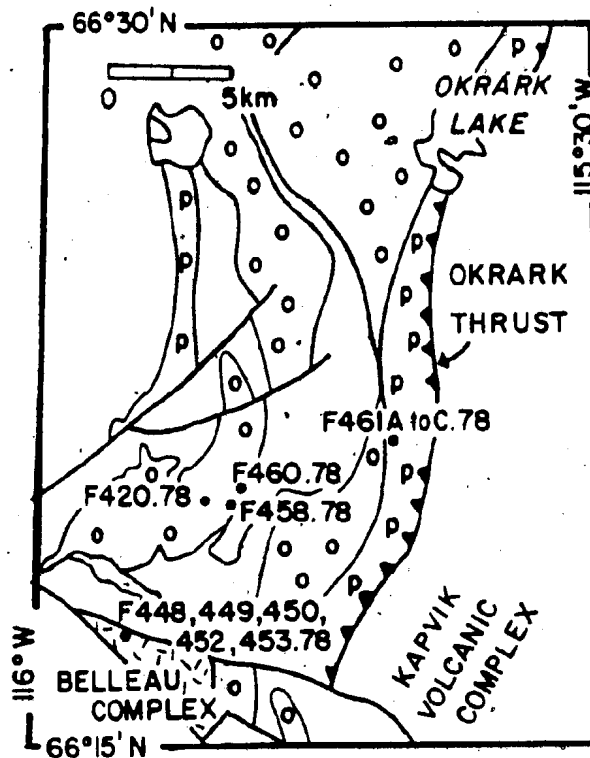


Figure B.3 Geological sketch map showing the Edjuvit mylonite zone and Rb-Sr sample locations.

LEGEND






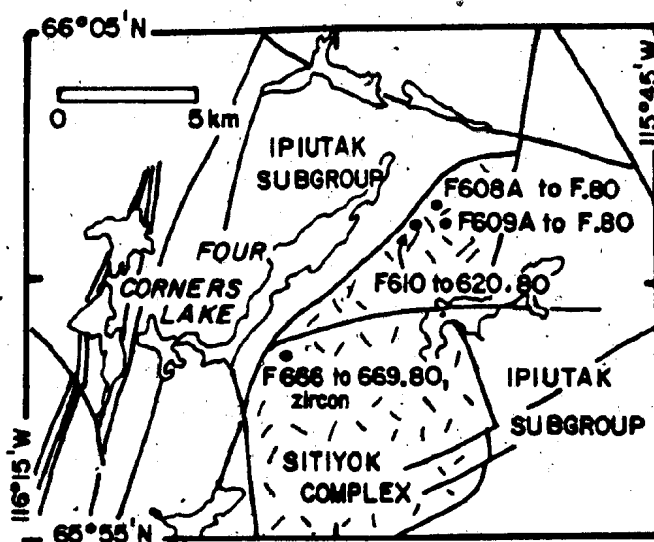
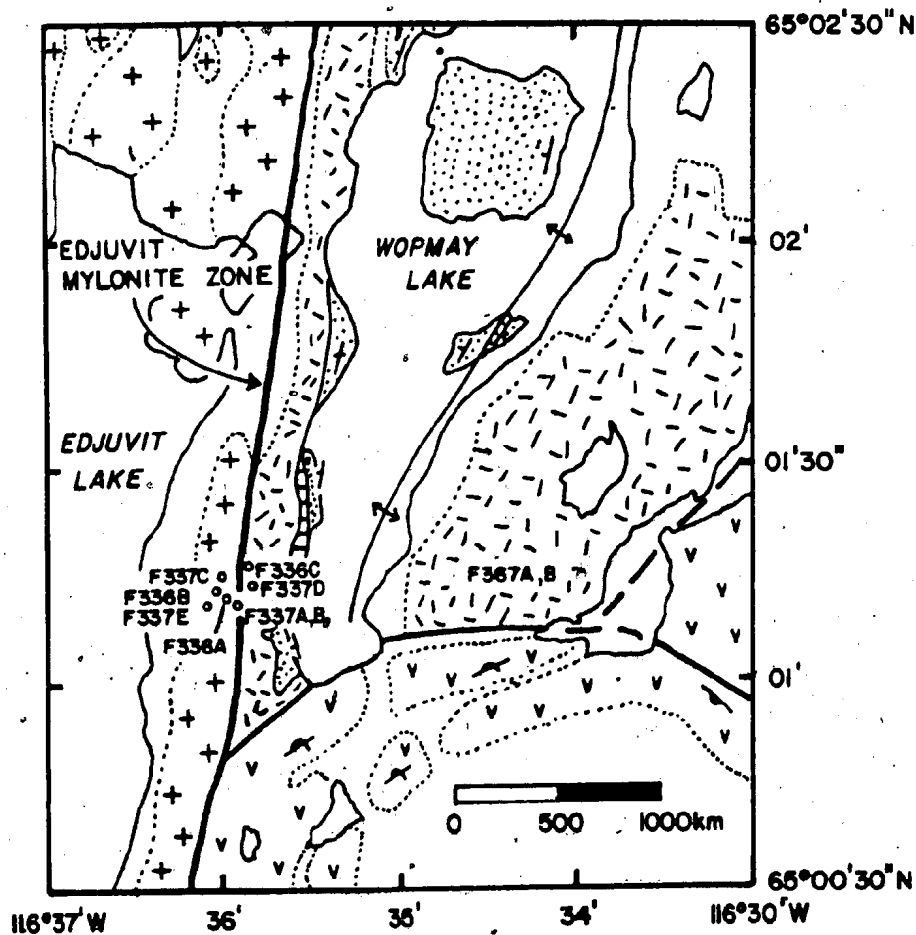
-  granite gneiss
Grant Subgroup
-  massive and pillowed basalts
-  gabbro sills
-  dolomite
-  pelite and siltstone

Figure B.4 Rb-Sr sample location map, Sityok Igneous Complex.



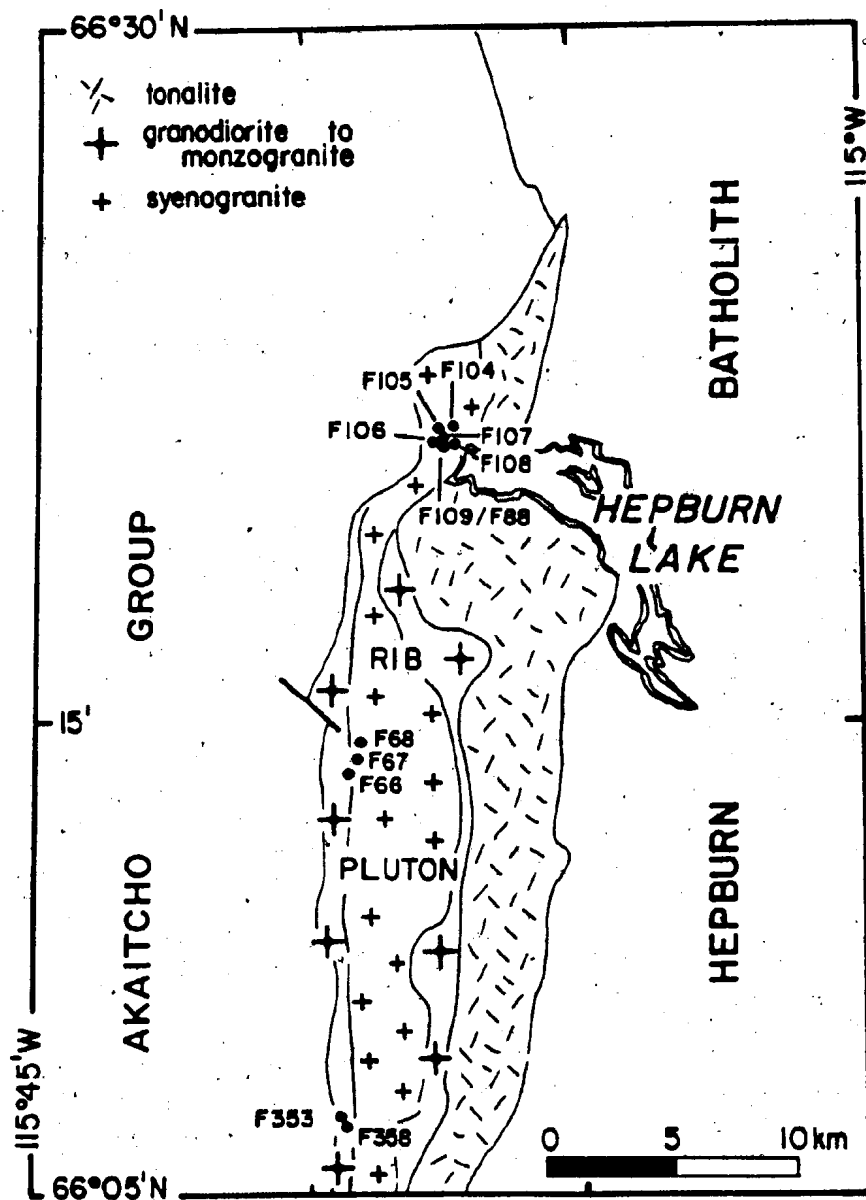


Figure B.5 Rb-Sr sample location map for the Rib Pluton.

APPENDIX C

STRAIN MEASUREMENTS ON CONGLOMERATES OVERLYING
THE TUERTOK VOLCANIC COMPLEX

METHOD 1

The equations used are:

$$V_{\text{sphere}} = V_{\text{ellipsoid}} \quad \text{or} \quad \frac{4}{3}\pi r^3 = \frac{4}{3}\pi a.b.c$$

$$\text{or} \quad r = \sqrt[3]{a.b.c}$$

where a is the half-length of the large axis, b is the half length of the intermediate axis, c is the half length of the least axis, and r is the radii of the original sphere.

Clast measurements are given in Table C.1.

METHOD 2

Assumptions and observations.

- 1) short axis is normal to the fold axes
- 2) cleavage is parallel to fold axes, intermediate axis is parallel to the fold axes,
- 3) plane strain
- 4) no volume change.

For plane strain, $k = 1$, where $k = \frac{\log_e a}{\log_e b}$ (Flinn, 1962, 1978);

$$a = \frac{\text{major axis}}{\text{intermediate axis}}$$

$$b = \frac{\text{intermediate axis}}{\text{minor axis}}$$

The intermediate axis is parallel to the fold axes, and the regional cleavage. The volcano spacings that were measured are also parallel to the strike of the regional cleavage. Under the condition of plane strain the intermediate axis

remains fixed in length, hence, no correction of the volcano spacings is necessary. For cobbles 2, 3 and 9 (Table C.1), k is close to 1, hence the assumption of plane strain is probably reasonable.

Table C.1 Measured strain ratios in conglomerate overlying the Tuertok volcanic complex.

METHOD 1						
	axis normal to cleavage (X) (cm)	axis parallel to cleavage (Y) (cm)	axis parallel to cleavage (Z) (cm)	ratio of axes to X	original sphere radius(cm)	extension relative to original k
Granite and orthoquartzite cobbles						
1	4.5	4.5	7	1/1/1.6	1.8	35% ∞
2	4	5	7	1/1.25/1.75	1.8	35% 1.6
3	1	1.5	2.25	1/1.5/2.25	0.75	50% 1
4	3.5	3.8	6	1/1.1/1.7	2.15	40% 6.4
5	3	3	5	1/1/1.7	1.78	41% ∞
6	2.25	2.5	4	1/1.1/1.8	1.5	33% 5.5
7	3	3.5	5.1	1/1.17/1.7	1.9	35% 2.7
8	2.5	3	5	1/1.2/2	1.67	50% 3.35
mean				1/1.17/1.8		40 \pm 6%
typical volcanic cobble						
9	1.5	2.5	5	1/1.67/1.35	1.3	88% 1.5

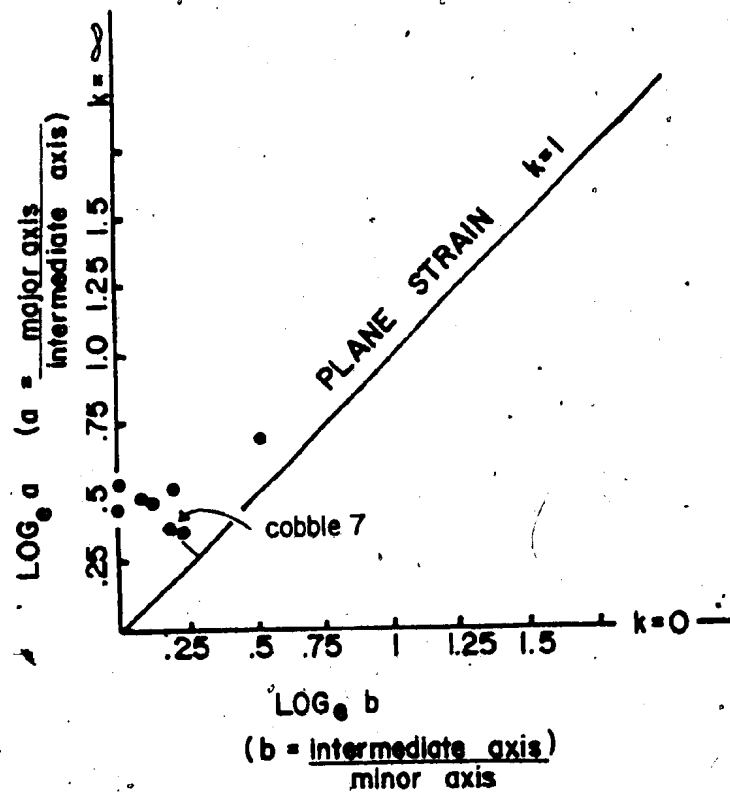


Figure C.1 $\text{Log}_e a$ versus $\text{Log}_e b$ plot for conglomerate cobbles from the upper Tuertok volcanic complex (after Flinn, 1962, 1978).

APPENDIX D

CHEMICAL ANALYSES

This appendix is a tabulation of the chemical analyses of the Akaitcho Group and related rocks that are the basis of the geochemical results discussed in Chapter 4.

Analytical methods are described in Appendix A. This appendix includes analyses that are not reported elsewhere in the thesis (namely, Tables 4.1, 4.2, 4.3, and 5.6).

Major elements are reported in weight percent; trace and rare-earth elements are reported in ppm. The analyses are tabulated in roughly stratigraphic order, from oldest (the Sityok Igneous Complex) to youngest (Tallerk sills).

Chemical analyses of Sityok Complex rocks.

	F614.80 ¹	F618.80 ¹	F619.80 ¹	F620.80 ¹	F709.80 ²	F617.80 ²
SiO ₂	48.4					
TiO ₂	2.87	2.21	3.30	2.53	1.15	
Al ₂ O ₃	11.2					
Fe ₂ O ₃ ^t	20.36					
MnO	0.32					
MgO	3.10					
CaO	8.29					
Na ₂ O	1.93					
K ₂ O	0.86					
P ₂ O ₅	1.55					
L.O.I.	0.20					
Total	99.08					
Nb	15	8	13	16	9	13
Zr	318	172	272	371	107.	376
Y	139	59	93	144	42	67
Sr	76	110	76	101	0	56
Rb	19	17	21	15	117	74
Pb	1	11	2	6	4	8
Zn	197	145	175	185	60	70
Cr	0	104	0	0	0	0
V	57	447	164	37	313	4
Ba	200	76	177	167	246	415
La	16.9	40.8	30.1	20.5		35.6
Ce	46.2	108.8	77.2	52.7		88.6
Pr	6.1	14.2	10.3	6.8		10.6
Nd	30.7	69.0	47.5	32.1		43.8
Sm	8.5	19.2	13.7	9.4		9.5
Eu	2.5	5.0	4.0	2.6		1.5
Gd	10.3	22.5	16.5	10.4		7.8
Dy	9.4	20.4	17.2	9.9		4.3
Ho	1.9	4.0	2.9	1.7		0.7
Er	4.8	10.7	8.3	5.1		2.1
Yb	3.0	8.3	4.1	2.5		1.4

¹ amphibolite (Unit 1); ² paragneiss (Unit 1)

Chemical analyses of Sityok Complex rocks.

← paragneiss (Unit 1) →

	F610.80	F611.80	F612.80	F613.80	F615.80	F616.80
Nb	20	23	22	12	14	25
Zr	307	410	421	368	329	290
Y	78	113	106	71	80	66
Sr	15	37	40	44	40	49
Rb	112	72	67	71	76	23
Pb	8	2	11	4	9	10
Zn	39	24	19	26	33	31
Cr	69	76	79	0	0	0
V	4	3	4	0	3	2
Ba	586	172	147	188	186	102
La	27.4	29.4	16.1	12.6	17.2	7.6
Ce	69.0	71.0	39.6	31.2	45.1	16.3
Pr	8.5	8.7	4.8	3.6	5.6	1.6
Nd	33.4	34.3	19.2	14.8	21.0	7.4
Sm	7.2	7.8	4.4	3.0	4.0	1.9
Eu	0.4	1.3	0.7	0.4	0.5	0.5
Gd	6.2	6.3	3.8	2.6	3.5	1.9
Dy	3.8	4.1	2.6	1.2	2.5	1.8
Ho	0.7	0.5	0.5	0.1	0.5	0.4
Er	2.2	2.3	1.5	1.3	1.6	1.6
Yb	1.6	1.9	1.3	0.8	1.6	1.6

Chemical analyses of Sityok Complex rocks.

	F608A.80 ¹	F666.80 ¹	F604A.80 ²	F604B.80 ²	F605.80 ²
SiO ₂	75.8				
TiO ₂	0.10	0.16	1.99	0.91	1.68
Al ₂ O ₃	11.5				
Fe ₂ O ₃ ^t	2.30				
MnO	0.02				
MgO	0.31				
CaO	trace				
Na ₂ O	2.69				
K ₂ O	5.00				
P ₂ O ₅	0				
L.O.I.	0.72				
Total	98.44				
Nb	26	28			
Zr	259	242	169	91	121
Y	128	132	63	36	47
Sr	32	32	130	125	103
Rb	190	276	30	58	37
Pb	5	31	15	38	14
Zn	18	50	148	152	141
Cr	0	0	0	91	69
V	2	10	387	235	376
Ba	820	553	189	136	145
Ni	0	0	0	42	21
La	42.0	52.1			
Ce	111.0	131.4			
Pr	13.5	15.6			
Nd	55.7	58.6			
Sm	13.1	12.8			
Eu	1.6	1.4			
Gd	12.7	13.1			
Dy	11.7	13.9			
Ho	2.3	2.8			
Er	6.8	8.8			
Yb	4.9	7.2			

¹ granite (Unit 2); ² amphibolite dykes (Unit 3)

Chemical analyses of Sitiyok Complex rocks.

← amphibolite dykes (Unit 3) →

	F705A.80	F705B.80	G45.79	F609B.80	F609C.80	F609D.80
TiO ₂	1.13	1.05		0.88	0.88	1.16
Nb			0			5
Zr	68	73	45	65	62	80
Y	29	30	26	26	24	36
Sr	147	167	257	103	111	112
Rb	43	39	80	53	39	33
Pb	23	67	24	5	4	9
Zn	660	170	110	81	87	108
Cr	172	139	251	352	368	202
V	317	304	295	260	249	300
Ba	207	154	152	72	68	105
Ni	50	51	115	122	121	

← amphibolite dykes (Unit 3) →

	F609E.80	F609F.80	F708.80	F712.80	R119.79	F659.80
TiO ₂	0.87	0.92	0.90	0.74		1.47
Nb	1	8	2	1	1	0
Zr	59	59	57	44	50	133
Y	25	37	25	17	24	47
Sr	101	59	116	100	120	127
Rb	39	48	57	24	119	48
Pb	8	3	1	6	6	76
Zn	92	118	119	95	85	183
Cr	371	346	114	282	393	44
V	266	256	282	239	185	335
Ba	87	68	131	66	76	171
Ni					196	22

Chemical analyses of Ipiutak Subgroup rocks.

	R116.79 ¹	E20A.78 ¹	R112.79 ¹	R124.79 ¹	J87.79 ²	F717.79 ³
SiO ₂	53.5	45.6				
TiO ₂	1.73	1.12				
Al ₂ O ₃	13.5	14.5				
Fe ₂ O ₃	12.98	13.94				
MnO	0.46	0.25				
MgO	4.98	6.94				
CaO	4.48	9.00				
Na ₂ O	0.62	2.5				
K ₂ O	2.71	1.52				
P ₂ O ₅	0.37	0.14				
L.O.I.	3.23	1.09				
Total	98.56	96.60				
Nb	13	10	9	2	12	8
Zr	206	97	208	136	212	176
Y	69	26	75	55	68	60
Sr	69	140	119	141	145	154
Rb	149	66	78	5	44	30
Pb	17	27	12	6	10	11
Zn	205	494	142	102	259	139
Cr	0	206	100	44	26	124
V	359	225	467	438	399	390
Ba	271	246	314	159	418	351
Ni	35	83	66	54	56	62
La	14.5		22.3	20.9	36.9	19.0
Ce	36.2		55.0	49.9	93.4	43.4
Pr	4.6		8.2	6.7	11.2	5.8
Nd	19.8		30.9	28.9	47.2	23.7
Sm	4.8		7.9	7.7	11.4	6.9
Eu	1.1		2.3	1.8	2.5	1.9
Gd	5.3		9.1	8.4	12.1	7.6
Dy	6.7		11.8	10.0	13.4	9.0
Ho	1.3		2.6	2.1	2.8	2.1
Er	3.5		6.6	4.5	5.8	4.9
Yb	3.0		6.8	3.8	3.9	4.0

¹ amphibolite; ² gabbro; ³ basalt

Chemical analyses of Ipiutak Subgroup rocks.

	F240A.78 ¹	F240B.78 ¹	S165.78 ¹	S168.78 ¹	E20B.78 ¹	R123.79 ¹
Nb	5	8	7	9	7	12
Zr	73	85	96	91	103	188
Y	22	27	22	25	27	72
Sr	232	174	161	191	158	134
Rb	76	51	41	71	75	25
Pb	1	20	6	10	91	10
Zn	120	230	104	163	333	137
Cr	95	122	126	252	31	35
V	270	293	249	237	326	406
Ba	365	166	128	408	535	188
Ni	55	55	32	52	40	55

	R110.79 ¹	J88.79 ¹	F588.80 ¹	F701.80 ¹	F702.80 ¹	J33.79 ²
TiO ₂			1.13	1.58		
Nb	8					10
Zr	145	42	77	116	181	170
Y	49	20	31	48	58	40
Sr	119	79	200	159	193	108
Rb	100	85	39	25	33	79
Pb	18	50	22	6	16	15
Zn	109	143	118	98	134	103
Cr	205	370	199	8		97
V	197	248	326	360		241
Ba	358	204	166	152		304
Ni	95	117	48	3	0	42

¹ amphibolite; ² basalt

Chemical analyses of Ipiutak Subgroup rocks.

	F638A.80 ¹	R80.79 ²	J95.79 ²	F593.80 ¹	F708.79 ²	J81.79 ²
TiO ₂	0.67			0.73		
Nb	17	23	16	9	23	18
Zr	236	255	238	222	224	149
Y	25	55	41	29	46	30
Sr	105	157	124	107	84	67
Rb	131	64	167	83	179	189
Pb	97	16	19	31	27	66
Zn	65	28	62	136	71	666
Cr	63	0	60	66	32	86
V	68	13	105	98	71	124
Ba	1401	370	1502	401	695	716
Ni		21	36		28	41
La	10.6	31.7	36.4	7.5	48.4	25.7*
Ce	28.0	79.3	88.4	23.7	111.0	57.6
Pr	3.9	9.5	10.1	2.9	12.4	6.8
Nd	16.3	36.8	41.5	13.3	46.7	27.3
Sm	3.8	7.5	7.6	3.9	8.8	5.3
Eu	0.8	1.3	1.4	0.6	0.9	1.0
Gd	3.1	6.3	6.2	3.6	6.6	3.5
Dy	2.1	5.2	5.2	5.1	5.4	2.7
Ho		1.0	0.9	1.1	1.1	
Er	1.3	3.1	3.0	3.7	2.2	0.5
Yb		2.5	3.7	4.1	1.6	0.6

¹quartzite; ²metapelite

Chemical analyses of Ipiutak Subgroup rocks.

	F660A.79 ¹	F660B.79 ¹	F718.79 ²	S130.79 ²	J35.79 ²	J38.79 ²
Nb	26	18	4	1	0	0
Zr	212	175	142	120	66	15
Y	45	28	58	50	31	10
Sr	213	167	121	134	132	192
Rb	133	138	3	7	20	21
Pb	32	16	6	8	4	1
Zn	24	14	123	110	76	38
Cr	1	0	52	114	171	728
V	24	27	447	412	310	180
Ba	568	583	47	113	60	38
Ni	12	4	52	51	74	116
La	55.0		29.7			
Ce	127.1		68.8			
Pr	13.1		8.2			
Nd	47.5		35.6			
Sm	7.8		8.0			
Eu	0.8		2.3			
Gd	5.1		8.4			
Dy	5.5		8.3			
Ho	1.9		1.4			
Er	3.0		5.0			
Yb	3.6		4.0			

¹metapelite; ²basalt

Chemical analyses of Ipiutak Subgroup and Zephyr Formation rocks.

	← Ipiutak Subgroup →			← Zephyr Formation* →		
	J60.79 ¹	J89.79 ¹	F637.80 ²	F715A.80 ³	F135.79 ²	F319A.79 ²
TiO ₂			0.62	0.89	0.09	
Nb	25	16	10	3	3	39
Zr	200	184	102	62	90	265
Y	40	48	46	27	10	112
Sr	75	189	73	92	18	141
Rb	214	72	70	10	77	28
Pb	19	24	297	4	47	20
Zn	110	88	266	95	34	58
Cr	141	69	78	334	6	0
V	149	120	105	261	7	2
Ba	687	585	308	99	457	548
Ni	67	40				18
La					6.0	14.6
Ce					16.2	36.0
Pr					2.1	3.3
Nd					8.5	12.1
Sm					1.7	2.8
Eu					0.2	0.7
Gd					1.3	3.1
Dy					0.6	5.6
Ho					0.1	1.4
Er					0.5	5.2
Yb					0.2	7.1

¹metapelite; ²quartzite; ³amphibolite

* see Table 4.4 for additional analyses.

Chemical analyses of Belleau volcanic complex basalts (see also Table 4.1, page 143).

	F260.78	F263.78	F266.78	F267.78	F268.78	F271.78
SiO ₂	48.2	50.5	49.7	50.3	47.4	
TiO ₂	1.35	1.60	1.02	1.42	1.06	1.2
Al ₂ O ₃	15.3	12.5	13.7	12.4	13.6	
Fe ₂ O ₃ ^t	12.17	14.68	11.65	14.22	11.35	
MnO	0.16	0.19	0.13	0.19	0.13	
MgO	5.82	5.83	8.06	5.23	7.70	
CaO	9.94	8.39	6.53	8.55	9.97	
Na ₂ O	1.3	2.2	3.1	2.5	2.6	
K ₂ O	1.20	0.36	0.14	0.152	0.24	
P ₂ O ₅	0.13	0.16	0.11	0.12	0.08	
L.O.I.	3.6	1.7	5.0	4.12	4.1	
Total	99.17	98.0	99.14	99.6	98.23	
Nb	6	12	6	8	7	6
Zr	112	142	102	127	84	99
Y	32	40	26	38	29	35
Sr	193	125	186	157	174	157
Rb	53	12	6	15	7	14
Pb	53	10	0	89	0	1
Zn	115	168	128	200	110	127
Cr	114	20	217	20	130	79
V	269	323	230	297	275	338
Ba	247	140	67	137	68	81
Ni	45	20	52	23	52	38
La	8.7	17.7	7.0	10.3	7.8	10.9
Ce	23.0	44.6	19.3	27.7	21.3	27.6
Pr	3.0	5.0	2.1	3.6	2.9	3.0
Nd	13.0	23.2	11.1	15.1	12.7	17.5
Sm	3.6	6.1	3.2	4.3	3.8	6.1
Eu	1.0	1.9	1.0	1.0	1.8	1.9
Gd	4.0	6.9	3.7	5.3	4.3	6.9
Dy	4.7	7.7	4.3	5.8	4.8	7.9
Ho	0.9	1.4	0.8	1.1	0.8	1.7
Er	2.8	4.1	2.4	3.2	2.3	4.6
Yb	2.8	3.5	1.9	2.9	1.7	2.9

Chemical analyses of Belleau volcanic complex basalts.

	F288.78	F289A.78	F300.78	F321.78	F338.78	F448.78
SiO ₂			47.8	48.9	49.7	
TiO ₂	1.55	0.8	1.17	1.29	1.14	
Al ₂ O ₃			15.0	16.2	15.1	
Fe ₂ O ₃ ^t			13.14	10.38	12.75	
MnO			0.17	0.11	0.21	
MgO			6.95	8.84	6.02	
CaO			10.48	3.85	8.57	
Na ₂ O			1.8	3.75	2.4	
K ₂ O			0.24	0.14	0.44	
P ₂ O ₅			0.10	0.07	0.09	
L.O.I.			2.84	4.2	3.10	
Total			99.69	97.73	99.52	
Nb	8	6	6	5	6	1
Zr	148	60	85	74	90	92
Y	40	22	25	24	30	33
Sr	160	170	198	105	198	242
Rb	18	9	7	5	10	13
Pb	0	9	53	15	20	52
Zn	110	103	204	438	135	260
Cr	18	283	151	119	73	162
V	310	235	249	316	268	287
Ba	148	103	89	60	67	242
Ni	17	91	78	120	37	49
La	16.3	2.8	6.6	1.6	9.0	
Ce	42.2	8.3	16.3	4.6	15.6	
Pr	5.2	0.8	1.8	0.6	2.0	
Nd	21.8	5.7	9.3	3.7	9.3	
Sm	6.0	1.8	2.7	1.6	3.0	
Eu	1.5	0.5	1.2	0.3	1.3	
Gd	6.8	2.4	3.2	2.1	3.5	
Dy	7.3	3.0	3.7	3.0	4.4	
Ho	1.0	1.0	0.7	0.7	0.7	
Er	4.0	2.1	2.1	1.5	2.1	
Yb	2.9	2.5	2.6	2.0	1.3	

Chemical analyses of Belleau volcanic complex basalts.

	F449.78	F450.78	F452.78	F453.78	F454.78
Nb	3	4	2	3	1
Zr	96	97	94	94	97
Y	34	37	34	33	35
Sr	228	214	205	215	226
Rb	10	9	8	11	13
Pb	17	21	20	23	44
Zn	122	127	149	143	138
Cr	156	161	165	161	160
V	295	296	297	293	294
Ba	213	222	238	253	315
Ni	47	45	44	49	47

Chemical analyses of Zephyr and Sinister volcanic complex rocks
(see Table 4.2 for additional analyses).

	Zephyr volcanic complex				Sinister volcanic complex	
	F733.79 ¹	F742.79 ¹	F745B.79 ¹	F755.79 ¹	F183.79 ²	F195.78 ²
Nb	7	8	1	3	16	15
Zr	91	118	127	61	245	272
Y	39	47	57	35	51	49
Sr	148	124	154	83	99	119
Rb	23	32	49	43	154	232
Pb	16	18	90	3	23	18
Zn	134	121	248	87	76	76
Cr	74	8	55	49	40	16
V	428	493	422	373	57	54
Ba	233	277	208	127	879	830
Ni	64	44	47	43	18	8

¹ amphibolite; ² orthoclase and plagioclase porphyritic rhyolite flows.

Chemical analyses of rocks from the Sinister volcanic complex.

	S592.77 ¹	F125.78 ²	F133.78 ²	F793.79 ²	F122A.78 ²	F122C.78 ²
SiO ₂	44.9	71.8	65.9			
TiO ₂	2.47	0.63	0.73			
Al ₂ O ₃	15.3	12.8	13.1			
Fe ₂ O ₃ ^t	15.50	3.20	6.15			
MnO	0.21	0.05	0.05			
MgO	6.61	0.22	1.21			
CaO	6.32	1.17	0.63			
Na ₂ O	3.12	1.2	2.0			
K ₂ O	0.83	6.65	5.41			
P ₂ O ₅	0.58	0.13	0.13			
L.O.I.	3.48	1.26	2.06			
Total	99.32	99.11	97.37			
Nb	22	17	16	20	15	15
Zr	238	282	254	148	203	255
Y	52	52	42	40	18	20
Sr	153	73	63	99	363	423
Rb	15	205	164	195	247	219
Pb	16	26	14	30	25	30
Zn	141	76	112	125	37	46
Cr	71	15	22	92	7	13
V	342	41	66	120	30	48
Ba	154	1144	888	775	1988	2121
Ni	35	10	11	61	12	15

F121.78² F122B.78²

Nb	15	16
Zr	276	255
Y	37	34
Sr	100	48
Rb	102	245
Pb	12	17
Zn	87	76
Cr	22	16
V	65	54
Ba	929	1179
Ni	8	18

¹ basalt flow² orthoclase and plagioclase
porphyritic rhyolite flows

Chemical analyses of the Okrark rhyolite porphyry sills
(see Table 4.2 for additional analyses).

← plagioclase porphyritic sills →

	F69A.78	F69C.78	F461A.78	F461B.78	F461C.78
Nb	16	15	24	23	23
Zr	276	244	320	323	331
Y	50	43	78	73	77
Sr	74	92	90	89	87
Rb	208	189	215	200	225
Pb	26	78	30	28	30
Zn	93	143	70	68	69
Cr	8	8	0	0	0
V	47	35	27	27	27
Ba	561	1323	842	800	888
Ni	11	10	47	45	45

← orthoclase porphyritic sills →

	F95.78	F216.78	F458.78	F217.78	F459.78
Nb	16	16	24	22	23
Zr	264	270	314	302	299
Y	48	48	75	74	73
Sr	136	129	182	139	150
Rb	203	198	161	158	180
Pb	53	28	33	32	24
Zn	105	93	87	91	20
Cr	18	15	5	7	6
V	59	55	45	41	44
Ba	809	850	943	736	1007
Ni	20	19	41	41	43

Chemical analyses of various Akaitcho Group rhyolites.

	F372.78 ¹	F460.78 ²	S164A.78 ³	S164B.78 ⁴	J40.79 ⁵	J47.79 ⁵
SiO ₂	69.0		72.5			
TiO ₂	0.89		0.30			
Al ₂ O ₃	13.2		13.4			
Fe ₂ O ₃ ^t	6.1		4.19			
MnO	0.08		0.08			
MgO	1.73		0.28			
CaO	1.06		0.61			
Na ₂ O	2.2		3.5			
K ₂ O	3.33		4.86			
P ₂ O ₅	0.11		0			
L.O.I.	1.9		1.14			
Total.	99.60		99.96			
Nb	16	22	23	16	29	48
Zr	308	311	412	260	335	243
Y	44	74	84	61	110	120
Sr	96	137	115	31	20	27
Rb	144	163	190	110	126	125
Pb	24	47	44	5	7	14
Zn	117	97	103	56	37	5
Cr	25	8	4	4	0	0
V	72	49	12	39	0	0
Ba	819	780	1000	923	861	576
Ni	8	44	8	5	0	0
La	25.5	37.9				
Ce	66.2	105.2				
Pr	7.8	12.6				
Nd	31.9	53.5				
Sm	7.2	11.8				
Eu	1.5	2.3				
Gd	6.6	11.8				
Dy	6.8	13.1				
Ho	1.4	5.7				
Er	3.8	5.7				
Yb	3.4	4.2				

¹ orthoclase and plagioclase porphyritic flow, Beileau volcanic complex.² Okrak sill, orthoclase porphyritic; ³ tuff, near Kingarok Lake;⁴ Lapilli tuff, near Kingarok Lake; ⁵ tuff, south of Kapvik Lake.

Chemical analyses of Kapvik volcanic complex rhyolites.*

	F236.78	R104.79	F462A.79	F345.79	F461A.79	F359.78
Nb	18	25	36	10	37	15
Zr	160	343	229	197	242	197
Y	34	108	122	29	112	58
Sr	40	121	90	1496	56	75
Rb	85	80	134	178	201	286
Pb	16	28	16	17	42	29
Zn	27	207	72	87	103	66
Cr	4	0	0	124	0	23
V	4	58	2	128	0	42
Ba	327	639	573	2479	439	650
Ni	0	19	45	100	56	19

Chemical analyses of Kapvik volcanic complex basalts.**

	F16.79	F55.79	S174.78	F540.79	F512.79	F453.79
TiO ₂	1.66					
Nb	8	15	10	3	2	16
Zr	131	147	112	148	77	193
Y	56	47	34	58	34	54
Sr	185	219	153	156	149	220
Rb	43	35	54	7	7	18
Pb	43	7	15	5	7	38
Zn	130	90	126	113	78	257
Cr	34	12	70	76	261	26
V	443	406	238	457	249	382
Ba	438	123	192	47	65	196
Ni		72	33	58	88	21

Chemical analyses of gabbros from the lower Kapvik volcanic complex.

	F456.79	F498.79	F227B.78	F317.79	F518A.79
Nb	4	10	7	11	0
Zr	118	152	65	187	34
Y	38	47	27	57	22
Sr	208	141	114	185	203
Rb	45	32	13	74	59
Pb	13	16	1	22	18
Zn	151	100	90	118	117
Cr	2	0	62	0	292
V	296	313	268	171	220
Ba	342	189	14	376	121
Ni	8	5	45	24	176

*see Table 4.2 for additional analyses

** see Table 4.1 for additional analyses

Chemical analyses of basalts and gabbros from the Kapvik volcanic complex:*

	F227A.78 ¹	F318.79 ¹	F394.78 ¹	S176.78 ²	M100.78 ²	F398.78 ²
SiO ₂	48.9	50.0	46.0		54.6	
TiO ₂	0.87	1.41	0.94	1.1	1.13	
Al ₂ O ₃	13.8	13.1	16.8		15.6	
Fe ₂ O ₃ ^t	12.89	13.51	11.18		10.53	
MnO	0.19	0.29	0.14		0.17	
MgO	9.08	6.61	6.15		4.67	
CaO	10.00	7.42	13.11		6.35	
Na ₂ O	1.2	2.92	1.6		2.3	
K ₂ O	2.18	1.18	0.66		1.81	
P ₂ O ₅	0.06	0.18	0.07		0.10	
L.O.I.	1.0	2.27	2.5		2.2	
Total	100.17	98.89	99.15		99.46	
Nb	6	3	8	4	5	8
Zr	61	105	80	73	108	90
Y	25	46	27	25	28	27
Sr	123	210	206	243	254	197
Rb	62	54	15	33	49	17
Pb	15	9	4	3	11	5
Zn	101	165	81	100	100	100
Cr	94	9	220	158	60	150
V	234	379	226	245	239	260
Ba	212	151	41	112	440	190
Ni	84	47	73	150	27	80
La	4.4		8.4			5.9
Ce	10.9		23.8			14.6
Pr	1.9		3.1			1.6
Nd	7.8		14.4			8.6
Sm	2.9		4.5			2.7
Eu	0.6		1.7			1.2
Gd	2.9		5.2			3.5
Dy	3.6		6.6			3.5
Ho	1.2		1.5			0.3
Er	2.1		3.6			1.8
Yb	2.1		5.1			1.2

* see Table 4.1 for additional analyses

Chemical analyses of Kapvik volcanic complex basalts.*

	F230.78	F231.78	F232.78	F517.79	F350.79
Nb	6	5	7	1	5
Zr	102	51	126	74	95
Y	27	24	29	31	30
Sr	172	120	205	174	146
Rb	18	27	66	75	7
Pb	1	7	20	85	15
Zn	109	99	167	225	107
Cr	100	290	22	151	0
V	290	330	255	277	443
Ba	80	105	385	372	66
Ni	46	155	8	57	7
La	10.3	5.1	16.7		
Ce	25.6	8.3	38.8		
Pr	3.4	1.6	5.0		
Nd	16.0	6.1	20.1		
Sm	5.0	2.5	4.4		
Eu	1.4	0.5	0.8		
Gd	5.7	2.3	4.9		
Dy	6.6	3.4	5.5		
Ho	1.4	0.5	1.0		
Er	2.9	2.5	3.5		
Yb	2.2	1.5	3.1		

*see Table 4.2 for additional analyses.

Chemical analyses of Tuertok volcanic complex rhyolites.*

	S38.78	H17D.78	F102.78	F784.79	F189.79	F194.79
Nb	13	27	23	21	20	21
Zr	256	188	376	301	315	280
Y	51	58	87	70	71	75
Sr	47	43	38	166	544	63
Rb	120	133	59	153	171	125
Pb	20	66	20	21	32	24
Zn	60	51	73	73	47	54
Cr	9	5	7	3	0	0
V	38	4	39	51	31	21
Ba	761	572	753	947	1130	766
Ni	10	8	25	38	48	36

Chemical analyses of Tuertok volcanic complex basalts from sites near, and south of Okrark Lake.**

	F123.79	F124.79	F125.79	F133.79	F153.79	F113A.79
Nb	11	5	4	4	7	3
Zr	186	104	127	126	149	140
Y	65	44	53	49	45	48
Sr	173	167	141	115	149	142
Rb	14	14	8	57	68	16
Pb	12	9	59	8	6	7
Zn	134	85	183	89	106	117
Cr	4	65	20	12	0	265
V	418	291	354	375	355	426
Ba	262	106	64	214	197	98
Ni	30	48	30	20	12	78

	F192.79 ¹	F195.79	F211.79 ¹	F45.79	F8C.79 ²	S48.78
Nb	13	21	41	0	1	10
Zr	255	458	251	70	79	144
Y	80	163	61	24	27	31
Sr	185	124	84	307	136	67
Rb	26	9	244	72	193	163
Pb	10	11	21	27	683	217
Zn	143	208	170	147	842	111
Cr	0	0	29	437	402	56
V	238	2	415	273	320	90
Ba	179	187	543	235	138	236
Ni	31	60	69	112	105	29

¹tuffs; ²tuff, near contact with Rib Granite, visible galena in hand specimen

* see Table 4.2 and 5.6 for additional analyses

**see Table 4.1 for additional analyses

Chemical analyses of Tuertok volcanic complex basalts from
Tuertok Lake

	F400.78	F406.78	F412C.80	F412D.80	F413B.80	F413C.80
TiO ₂	1.10	0.76	1.06	1.09	1.34	1.27
Nb	4	4	5	7	5	9
Zr	71	71	95	95	106	106
Y	29	24	32	36	43	43
Sr	165	245	154	143	146	119
Rb	11	10	17	8	9	17
Pb	13	20	8	9	7	11
Zn	105	125	90	99	111	104
Cr	310	313	89	124	41	41
V	325	169	315	308	369	342
Ba	109	84	133	108	82	116
Unit*	5	8	5	5	5	5

	F413D.80	F413E.80	F413F.80	F420B.80	F420C.80	F446.80
TiO ₂	1.31	1.38	1.27	1.33	1.30	1.20
Nb	6	7		6	7	6
Zr	114	111	112	109	111	107
Y	47	48	44	41	42	45
Sr	105	133	153	147	163	127
Rb	17	19	20	8	8	14
Pb	11	2	4	6	7	12
Zn	112	107	96	113	114	107
Cr	34	14	35	25	26	133
V	372	377	340	386	367	368
Ba	110	157	124	82	89	55
Unit*	5	5	5	8	8	9

	F451B.80	F452B.80	F452C.80*	F489B.80	F498B.80	F498C.80
TiO ₂	1.57	0.94	0.72	0.83	0.55	0.74
Nb	8					
Zr	120	67	47	47	38	46
Y	46	23	17	26	13	17
Sr	153	220	272	176	212	232
Rb	18	7	11	44	22	8
Pb	17	10	3	29	1	37
Zn	133	80	73	113	79	102
Cr	0	151	124	362	108	119
V	424	238	194	275	155	209
Ba	149	73	71	276	89	174
Unit*	5	4	4	11a	4	4

*refers to map units in Figure 4.13 and Easton (1981a)

Chemical analyses of Tuertok volcanic complex basalts from
Tuertok Lake.

	F506B.80	F521.80	F524.80	F525.80	F526.80	F529.80
TiO ₂	1.27	1.02	1.31		1.59	0.79
Nb	6	3	6	7	9	5
Zr	96	73	112	106	128	67
Y	37	24	41	42	50	24
Sr	91	238	136	86	118	114
Rb	7	1	13	18	13	4
Pb	6	6	14	14	5	45
Zn	89	95	107	112	130	142
Cr	95	285	29	30	12	295
V	342	272	367	359	386	295
Ba	109	70	131	139	124	78
Unit*	11a	5	5	6	8	9

	F530.80	F531.80	F532.80	F463.80 ¹	F36.78	F37.78
TiO ₂	1.36	1.25	1.38	1.05	0.9	1.2
Nb	6	8	5	1	5	6
Zr	103	112	112	44	77	87
Y	46	48	41	13	21	25
Sr	116	149	173	0	214	237
Rb	12	11	8	61	16	10
Pb	2	8	3	0	5	3
Zn	116	111	116	159	76	84
Cr	46	40	61	404	117	116
V	367	360	401	387	183	243
Ba	130	116	100	208	156	97
Unit*	9	9	9	3	5	5

	F510.80	F380.78	F39.78 ³	F103B.78 ²	F105.78 ²	F101.78 ⁴
TiO ₂	1.19	1.3	1.8	1.2	1.2	
Nb	5	7	14	9	7	11
Zr	80	67	175	88	91	200
Y	32	18	34	27	22	53
Sr	236	95	173	205	196	108
Rb	8	11	21	12	22	45
Pb	14	3	1	15	1	40
Zn	98	130	150	113	90	243
Cr	145	185	285	140	61	9
V	343	288	243	260	282	393
Ba	70	120	335	145	81	524
Ni		131	167	90	88	14
Unit*	6	5	9			

¹ altered basalt, near Okrark Thrust Fault; ² flow, near Okrark Lake;

³ gabbro plug, near Okrark Lake; ⁴ mafic tuff, garnet bearing

* refers to map units in Figure 4.13 and Easton (1981a)

Chemical analyses of Tuertok volcanic complex basalts,
Tuertok Lake.

	F413A.80	F420A.80	F451A.80	F452A.80	F492.80	F489A.80
TiO ₂	1.26	1.22	1.57	0.72	1.87	1.55
Nb	6		9			
Zr	105	106	126	46	140	110
Y	42	41	46	16	35	35
Sr	140	158	155	227	395	167
Rb	10	9	9	11	9	8
Pb	9	8	7	60	5	5
Zn	107	108	133	155	94	89
Cr	41	28	0	138	130	53
V	349	358	424	197	229	367
Ba	92	94	149	115	152	102
Ni		7		86	63	24
Unit*	5	8	5	4	11a	11a
La	12.0	12.9	11.2	8.5	10.5	9.2
Ce	31.0	24.4	28.0	18.4	28.9	26.2
Pr	3.7	4.3	3.4	2.0	3.8	4.0
Nd	18.7	20.5	15.9	11.4	16.4	19.5
Sm	5.3	6.2	4.5	3.2	4.5	5.6
Eu	1.2	1.9	1.3	1.1	1.7	1.6
Gd	6.8	7.5	5.2	3.4	5.0	7.2
Dy	5.9	1.1	5.4	2.4	5.2	5.9
Ho	1.0	1.1	1.1	0.6	1.0	0.7
Er	3.3	3.7	3.1	1.8	2.5	3.0
Yb	1.5	2.0	2.2	1.7	2.5	1.7

*refers to map units in Figure 4.13 and Easton (1981a)

Chemical analyses of Tuertok volcanic complex basalts, Tuertok Lake.*

	F459.80	F484.80	F506A.80	F511.80	F533.80	S39.78
SiO ₂	47.8	51.6		49.6	49.2	48.8
TiO ₂	0.73	1.67	1.27	1.43	1.43	1.18
Al ₂ O ₃	20.6	13.5		13.2	13.2	16.0
Fe ₂ O ₃ ^t	7.81	12.88		13.62	14.17	11.48
MnO	0.11	0.19		0.22	0.21	0.15
MgO	5.92	4.88		6.65	6.08	6.57
CaO	10.32	9.27		8.95	9.41	9.43
Na ₂ O	3.31	2.22		2.30	2.03	1.6
K ₂ O	0.43	0.49		1.00	0.51	1.06
P ₂ O ₅	0.06	0.17		0.12	0.15	0.11
L.O.I.	2.91	1.83		1.86	1.93	2.7
Total	100.00	98.70		98.95	98.32	99.08
Nb	2		8	4		7
Zr	39	159	101	68	117	100
Y	14	45	38	28	46	27
Sr	248	254	56	183	166	270
Rb	9	12	5	10	8	22
Pb	68	10	3	3	37	5
Zn	120	99	98	86	102	100
Cr	104	59	85	308	31	110
V	180	344	346	294	362	224
Ba	151	119	86	100	129	190
Ni					78	65
Unit*	4	11b	11a	6	9	5
La	6.1	26.8	6.4	5.1	15.1	
Ce	13.9	58.8	16.8	13.9	39.3	
Pr	1.8	7.6	2.2	1.7	4.5	
Nd	8.8	32.2	9.6	8.2	23.5	
Sm	2.5	7.6	2.6	2.6	7.1	
Eu	0.9	1.9	0.7	0.9	2.2	
Gd	2.9	8.1	3.2	3.2	8.3	
Dy	3.8	6.8	3.4	3.5	9.2	
Ho	0.6	1.1	0.7	0.7	1.8	
Er	1.8	3.2	2.1	2.0	5.5	
Yb	1.7	1.6	1.9	1.9	5.0	

* see Table 4.1 for additional analyses.

Chemical analyses of rocks from the Tuertok volcanic complex and the Tallerk sills.

	F103A.78 ¹	F48.78 ²	F85.78 ²	F592.79 ³	F445.79 ³	F446.79 ³
SiO ₂	49.3					
TiO ₂	1.23					
Al ₂ O ₃	15.9					
Fe ₂ O ₃ ^t	11.54					
MnO	0.26					
MgO	6.11					
CaO	9.11					
Na ₂ O	2.3					
K ₂ O	1.10					
P ₂ O ₅	0.11					
L.O.I.	1.16					
Total	98.12					
Nb	8	11	15	1	24	2
Zr	91	147	267	116	276	108
Y	24	30	46	50	74	40
Sr	201	87	114	175	168	193
Rb	38	127	145	31	64	27
Pb	188	9	13	38	15	15
Zn	417	44	61	171	163	86
Cr	125	15	8	44	0	160
V	246	56	62	374	465	339
Ba	241	630	860	128	290	82
Ni	55	9	15	65	88	55
La		17.6	16.1	8.7		
Ce		41.2	60.2	21.4		
Pr		5.1	9.0	2.1		
Nd		20.1	32.0	11.8		
Sm		3.7	8.8	3.6		
Eu		0.6	0.6	1.3		
Gd		3.5	8.2	4.1		
Dy		4.4	10.7	5.0		
Ho		0.6	2.4	1.1		
Er		1.8	5.8	3.0		
Yb		2.0	6.4	3.0		

¹basalt, near Okrark Lake; ²rhyolite tuff, Tuertok volcanic complex;

³Tallerk gabbro sill.

Chemical analyses of Tallerk gabbro sills and basalt tuffs
interbedded with the Aglerok Formation.*

	F381.79 ¹	F10.79 ¹	F13.79 ¹	F84.79 ¹	F74.79 ¹	F516.79 ¹
Nb	0	0	6	0	1	0
Zr	133	68	205	78	138	160
Y	53	30	63	36	58	64
Sr	110	273	230	166	219	134
Rb	10	156	38	24	41	57
Pb	11	18	8	10	22	37
Zn	194	70	119	95	105	141
Cr	0	191	102	4	22	0
V	428	266	339	315	585	491
Ba	72	332	182	66	244	153
Ni	134	65	57	64	60	
	F44.79 ¹	J7.79 ¹	F364.80 ¹	F14.79 ¹	F110.78 ²	F451.79 ³
TiO ₂	1.29	1.00	1.99	1.14		
Nb	6	3	8	6	13	20
Zr	73	56	135	80	117	279
Y	32	30	70	26	28	59
Sr	225	169	150	190	71	42
Rb	164	32	51	32	148	108
Pb	5	0	5	5	7	25
Zn	89	162	171	80	122	17
Cr	80	212	0	88	75	0
V	293	308	6	289	142	6
Ba	174	53	173	120	410	485
Ni					51	27
	F36.79 ⁴	G2B.79 ⁵	F115.79 ⁶	D26.79 ⁷		
TiO ₂	0.84	1.70				
Nb	15	9	0	13		
Zr	130	116	1	209		
Y	32	62	6	75		
Sr	83	94	34	77		
Rb	206	115	0	51		
Pb	14	12	1	4		
Zn	112	5	0	46		
Cr	103	27	0	0		
V	139	330	0	8		
Ba	1151	330	0	247		

¹Tallerk gabbro sill; ²mafic tuffaceous pelite, garnet bearing;

³staurolite bearing, mafic tuffaceous pelite; ⁴siltstone inclusion in
Hepburn Batholith; ⁵siliceous siltstone; ⁶marble, upper Tuertok complex;

⁷mafic tuff, Kapvik complex; *see Table 4.1 and 4.4 for additional
analyses

Chemical analyses of Aglerok Formation rocks.

	F261.78 ¹	F287.78 ²	F466.78 ³	F467.78 ⁴	F24.79 ⁵	F121.79 ⁵
SiO ₂	66.8	70.3	65.6			
TiO ₂	0.65	0.51	0.39			0.92
Al ₂ O ₃	14.7	13.0	11.9			
Fe ₂ O ₃ ^t	6.09	5.26	10.00			
MnO	0.04	0.03	0.1			
MgO	1.95	1.18	2.40			
CaO	0.58	0.56	0.23			
Na ₂ O	2.3	2.2	0.8			
K ₂ O	4.65	2.89	3.85			
P ₂ O ₅	0.08	0.07	0.08			
L.O.I.	2.0	2.17	2.46			
Total	99.84	98.17	97.95			
Nb	16	14	15	22	9	17
Zr	130	136	211	184	559	186
Y	21	25	37	61	20	45
Sr	45	52	29	23	24	15
Rb	172	124	161	141	52	193
Pb	27	24	15	12	26	27
Zn	162	77	72	57	36	133
Cr	76	48	17	8	22	84
V	94	66	42	8	28	128
Ba	853	612	640	1030	101	551
Ni	31	18	21	5	14	
La	17.7	21.4	39.3	13.2	22.6	16.4
Ce	47.8	55.8	96.2	35.5	54.4	47.6
Pr	5.7	6.0	10.6	4.2	5.6	5.3
Nd	22.3	22.5	42.1	18.4	21.0	21.5
Sm	4.4	4.5	8.1	4.4	3.9	4.9
Eu	1.0	0.9	0.1	0.6	0.7	1.1
Gd	3.6	3.6	5.3	4.6	2.9	4.9
Dy	3.9	3.4	4.3	6.8	2.3	6.0
Ho	0.7	0.7	1.0	1.2	0.4	1.1
Er	1.6	1.8	2.4	3.7	1.2	3.3
Yb	2.1	1.9	3.1	5.0	0.5	2.5

¹ mafic tuffaceous pelite, Belleau complex; ² sandstone, Belleau complex;

³ mafic tuffaceous pelite, Kapvik complex; ⁴ felsic tuffaceous pelite,

Kapvik complex; ⁵ pelite, Kapvik complex.

Chemical analyses of Grant Subgroup sedimentary rocks at Grant Lake.

	F47.80 ¹	F49.80 ²	F66.80 ¹	F75.80 ²	F93.80 ¹	F194.80 ¹
SiO ₂	63.7	62.7	59.9	47.6	62.5	61.0
TiO ₂	0.64	0.58	0.72	2.36	0.72	0.72
Al ₂ O ₃	18.0	14.4	20.1	13.4	18.9	19.1
Fe ₂ O ₃ ^t	6.62	10.92	8.36	16.79	6.54	7.47
MnO	0.09	0.48	0.09	0.26	0.09	0.07
MgO	2.73	2.92	2.51	6.48	2.16	2.34
CaO	0.71	1.88	0.62	8.74	0.72	0.32
Na ₂ O	0.9	1.4	1.1	0.7	1.4	0.9
K ₂ O	5.04	2.73	4.66	1.81	4.26	4.78
P ₂ O ₅	0.11	0.09	0.09	0.33	0.07	0.08
L.O.I.	2.7	1.8	2.7	3.0	3.3	3.4
Total	101.24	99.90	100.85	101.47	100.66	100.18
Nb	14	14	17	17	14	
Zr	140	131	148	194	142	
Y	25	28	35	52	37	
Sr	47	79	74	91	85	
Rb	220	98	232	71	208	
Pb	36	12	20	5	10	
Zn	114	136	106	138	101	
Cr	99	85	105	90	101	
V	111	117	134	411	139	
Ba	694	738	838	175	849	

¹ pelite; ² mafic tuffaceous pelite

Chemical analyses of Grant Subgroup sedimentary rocks from Grant Lake.

	F365D.80 ¹	F281A.80 ²	F281B.80 ²	F304.80 ²	F15.80 ²
SiO ₂	93.4				
TiO ₂	0.04	0.86	0.83	0.76	1.37
Al ₂ O ₃	3.52				
Fe ₂ O ₃ ^t	1.43				
MnO	0.02				
MgO	0.54				
CaO	trace				
Na ₂ O	0.06				
K ₂ O	0.60				
P ₂ O ₅	0.02				
L.O.I.	0.75				
Total	100.38				
Nb	2	19	19	17	14
Zr	209	165	182	145	120
Y	9	40	42	38	20
Sr	49	116	157	87	126
Rb	35	236	181	212	117
Pb	2	24	16	23	10
Zn	25	125	70	97	120
Cr	6	91	90	103	125
V	19	139	131	138	261
Ba	365	764	747	847	442
La	5.7			20.7	
Ce	14.2			54.2	
Pr	1.5			6.6	
Nd	6.2			26.7	
Sm	1.2			5.3	
Eu	0.2			1.3	
Gd	1.2			4.5	
Dy	1.1			4.2	
Ho	0.1			0.4	
Er	0.7			1.6	
Yb	0.2			2.0	

¹quartzite; ²pelite

Chemical analyses of Grant Subgroup volcanic rocks at Grant Lake.

	F367A.80 ¹	F367B.80 ¹	F8.80 ¹	F388C.80 ²	F388D.80 ²	F344.80 ²
SiO ₂	46.1	48.4	46.2	48.4	48.4	50.0
TiO ₂	3.78	0.88	3.43	2.42	2.35	1.46
Al ₂ O ₃	12.7	14.0	12.4	12.8	12.4	13.1
Fe ₂ O ₃ ^t	21.06	11.87	19.47	17.4	16.76	15.37
MnO	0.26	0.19	0.32	0.26	0.23	0.22
MgO	4.05	9.02	5.14	5.14	5.06	5.41
CaO	9.00	12.00	8.89	7.77	9.28	8.40
Na ₂ O	2.29	1.82	1.5	1.8	1.31	3.2
K ₂ O	0.71	0.28	1.05	0.48	0.52	0.57
P ₂ O ₅	0.10	0.07	0.28	0.24	0.34	0.13
L.O.I.	0.61	1.48	2.2	3.9	2.69	4.2
Total	100.66	100.01	100.88	100.61	99.34	102.06
Nb	6	3	9	7	7	4
Zr	90	55	150	148	138	100
Y	39	22	50	47	51	39
Sr	115	92	105	113	118	119
Rb	23	10	44	16	15	16
Pb	4	10	7	6	10	6
Zn	156	87	161	135	135	100
Cr	0	418	7	211	81	6
V	637	278	712	467	460	353
Ba	119	79	165	73	176	188
La	6.3	5.5				
Ce	16.3	13.1				
Pr	1.9	1.6				
Nd	11.4	8.6				
Sm	3.5	2.7				
Eu	1.4	0.7				
Gd ⁶	4.5	3.6				
Dy	4.5	3.4				
Ho	0.9	0.8				
Er	2.7	2.3				
Yb	2.2	1.0				

¹gabbro sill; ²basalt flow

Chemical analyses of Grant Subgroup volcanic rocks at Grant Lake and early Proterozoic dykes at Point Lake.

	F390C.80 ¹	F361.80 ¹	F362.80 ¹	F32.81 ²	F165.81 ³
SiO ₂	74.8	68.0	77.3	48.4	48.4
TiO ₂	0.37	0.10	0.23	0.96	2.05
Al ₂ O ₃	11.6	9.70	11.1	15.3	14.1
Fe ₂ O ₃ ^t	3.3	2.92	2.9	11.6	15.5
MnO	0.05	0.11	0.04	0.20	0.23
MgO	0.64	0.90	1.37	6.95	5.9
CaO	1.34	6.36	1.08	11.8	9.81
Na ₂ O	1.8	2.69	2.5	1.7	1.6
K ₂ O	4.56	2.40	2.55	0.81	0.84
P ₂ O ₅	0.06	0.05	0.02	0.08	0.19
L.O.I.	2.0	5.84	1.2	2.3	2.1
Total	100.52	98.87	100.29	100.10	100.72
Nb	21	27	24	3	5
Zr	385	357	408	58	149
Y	109	188	134	24	41
Sr	21	152	138	146	206
Rb	119	145	79	41	34
Pb	15	12	28	0	10
Zn	63	119	171	77	109
Cr	0	0	0	203	64
V	0	6	13	262	294
Ba	719	377	502	185	186

¹ rhyolite flow; ² east-trending dyke; ³ north-trending dyke (cuts east-trending Proterozoic dykes).

Chemical analyses of Vaillant Formation rocks.*

	Coppermine River area			Vaillant Lake area		
	F772.79	F776A.79	F776B.79	C151.77	F425A.80	F425B.80
SiO ₂	60.1	46.3			77.5	
TiO ₂	2.65	3.69		0.73	0.74	0.75
Al ₂ O ₃	11.9	13.6			3.9	
Fe ₂ O ₃ ^t	13.33	17.48			11.7	
MnO	0.11	0.33			0.06	
MgO	1.92	6.15			0.75	
CaO	2.65	4.67			3.71	
Na ₂ O	3.8	2.5			0	
K ₂ O	1.12	1.20			0.37	
P ₂ O ₅	0.36	0.41			1.4	
L.O.I.	1.6	4.3			0.06	
Total	99.5	100.6			100.2	
Nb	46	59	59	4	4	6
Zr	265	279	271	156	40	45
Y	71	75	67	61	19	14
Sr	61	61	92	91	105	95
Rb	22	12	14	58	7	10
Pb	7	3	7	9	12	5
Zn	97	195	160	156	18	26
Cr	0	0	0	103	49	70
V	255	593	610	475	159	124
Ba	215	790	259	109	43	52
Ni	24	46	40	56		

*see Table 4.3 for additional analyses

Chemical analyses of Vaillant Formation rocks from the Vaillant Lake area.

	F426.80	F428.80	F429.80	F430A.80	F430B.80	F431B.80
SiO ₂	46.4			47.4	46.0	43.4
TiO ₂	1.10	1.39	1.43	1.39	1.37	2.43
Al ₂ O ₃	16.3			14.3	13.9	14.2
Fe ₂ O ₃ ^t	14.2			12.7	14.7	20.6
MnO	0.20			0.32	0.31	0.20
MgO	7.58			8.29	7.16	4.49
CaO	3.49			6.00	7.09	3.52
Na ₂ O	4.2			3.1	3.0	4.3
K ₂ O	0.06			0.14	0.08	0.41
P ₂ O ₅	0.09			0.14	0.13	0.27
L.O.I.	7.6			7.2	7.3	6.1
Total	101.2			101.0	101.0	99.92
Nb	5	8	11	9	11	25
Zr	57	77	88	79	76	171
Y	20	28	36	26	30	64
Sr	84	39	76	104	128	94
Rb	1	0	3	1	0	8
Pb	0	0	6	6	0	9
Zn	136	174	140	117	105	155
Cr	23	11	40	120	110	34
V	248	383	356	325	356	519
Ba	35	39	57	27	27	103

Chemical analyses of Vaillant Formation rocks in the Vaillant Lake area.

	F432A.80	F433A.80	F434.80	H30A.80	H30B.80	H30C.80
SiO ₂	45.5	47.9				
TiO ₂	2.20	2.46	1.10	1.69	1.59	1.69
Al ₂ O ₃	13.7	15.6				
Fe ₂ O ₃ ^t	10.2	22.3				
MnO	0.24	0.06				
MgO	7.10	2.43				
CaO	5.82	0.89				
Na ₂ O	1.0	0				
K ₂ O	2.60	5.75				
P ₂ O ₅	0.24	0.30				
L.O.I.	11.9	4.0				
Total	100.5	101.7				
Nb	23	27	11	12	21	12
Zr	148	162	92	86	142	90
Y	43	48	31	28	43	38
Sr	34	0	12	45	37	26
Rb	36	72	59	2	32	2
Pb	0	0	10	8	9	10
Zn	113	78	61	162	117	147
Cr	108	125	74	149	98	134
V	419	272	220	393	430	403
Ba	579	233	287	32	603	58

Chemical analyses of Epworth and Recluse Group sedimentary rocks.

	F906A.79 ¹	F906B.79 ²	F12.81 ³	F28.81 ⁴	S68.78 ⁵	S107A.77 ⁶
SiO ₂	61.9	53.1	62.4			
TiO ₂	0.72	2.28	0.71			
Al ₂ O ₃	18.4	18.1	16.1			
Fe ₂ O ₃ ^t	5.90	10.96	6.55			
MnO	0.05	0.09	0.08			
MgO	2.40	2.98	2.24			
CaO	0.22	1.46	2.48			
Na ₂ O	1.42	1.0	0.2			
K ₂ O	4.95	4.99	4.23			
P ₂ O ₅	0.13	0.17	0.13			
L.O.I.	2.57	5.8	5.5			
Total	98.66	100.93	100.62			
Nb	12	22	18	13	21	18
Zr	244	244	316	183	146	119
Y	60	32	31	34	34	31
Sr	120	44	113	103	92	85
Rb	98	182	167	176	214	229
Pb	35	21	10	4	19	24
Zn	63	80	81	36	98	103
Cr	33	100	28	74	115	124
V	59	148	205	94	148	131
Ba	289	1057	588	710	700	735
La	39.3	18.0			16.2	
Ce	90.5	51.6			45.9	
Pr	10.8	7.1			5.7	
Nd	37.8	26.2			21.1	
Sm	6.7	5.2			4.7	
Eu	0.7	1.1			1.2	
Gd	4.3	3.5			3.8	
Dy	3.0	3.7			5.2	
Ho	0.5	0.6			1.2	
Er	1.5	1.4			1.9	
Yb	2.2	1.8			2.3	

¹Odjick Formation, quartzite bed; ²Odjick Formation, pelite; ³Odjick Formation, green siltstone; ⁴Odjick Formation, red mudstone; ⁵Odjick Formation, pelite; ⁶Odjick Formation, pelite.

Chemical analyses of Epworth and Recluse Group sedimentary rocks.

	F911.79 ¹	F912.79 ²	F495.78 ³	S152.78 ³	F166.81 ⁴	H101.78 ⁵
SiO ₂	51.2		60.8		58.6	72.1
TiO ₂	0.50		0.52		0.67	0.58
Al ₂ O ₃	9.82		18.3		18.5	10.6
Fe ₂ O ₃ ^t	6.16		7.27		7.8	5.08
MnO	0.08		0.05		0.12	0.09
MgO	3.52		2.72		3.89	3.11
CaO	10.65		0.09		-0.76	2.09
Na ₂ O	4.86		1.30		1.1	1.1
K ₂ O	0.26		4.09		4.86	2.86
P ₂ O ₅	0.08		0.06		0.11	0.11
L.O.I.	12.55		3.21		3.8	3.2
Total	99.68		98.41		100.21	100.92
Nb	9	7	18	20		12
Zr	100	173	168	137		185
Y	30	28	39	35		30
Sr	18	76	50	59		121
Rb	8	95	164	165		130
Pb	10	6	16	16		21
Zn	50	44	79	62		68
Cr	38	34	116	119		126
V	104	75	134	126		112
Ba	72	458	763	611		445
Ni				37		44
La	18.2	16.6	28.4	41.9		30.8
Ce	42.5	41.3	68.6	93.2		68.6
Pr	4.9	5.0	7.8	10.5		7.9
Nd	18.8	20.2	30.9	40.4		28.5
Sm	3.7	4.1	5.9	7.4		4.9
Eu	0.5	0.6	0.9	1.0		0.9
Gd	3.7	3.8	5.0	4.3		3.4
Dy	3.1	3.2	3.3	3.6		3.7
Ho	0.7	0.5	0.5	0.8		1.3
Er	2.0	1.8	1.9	1.4		1.6
Yb	1.9	1.3	1.6	1.8		2.2

¹Takiyuak Formation siltstone; ²Takiyuak Formation sandstone;³Fontano Formation pelite; ⁴Dumas Group mudstone; ⁵Recluse Formation greywacke.

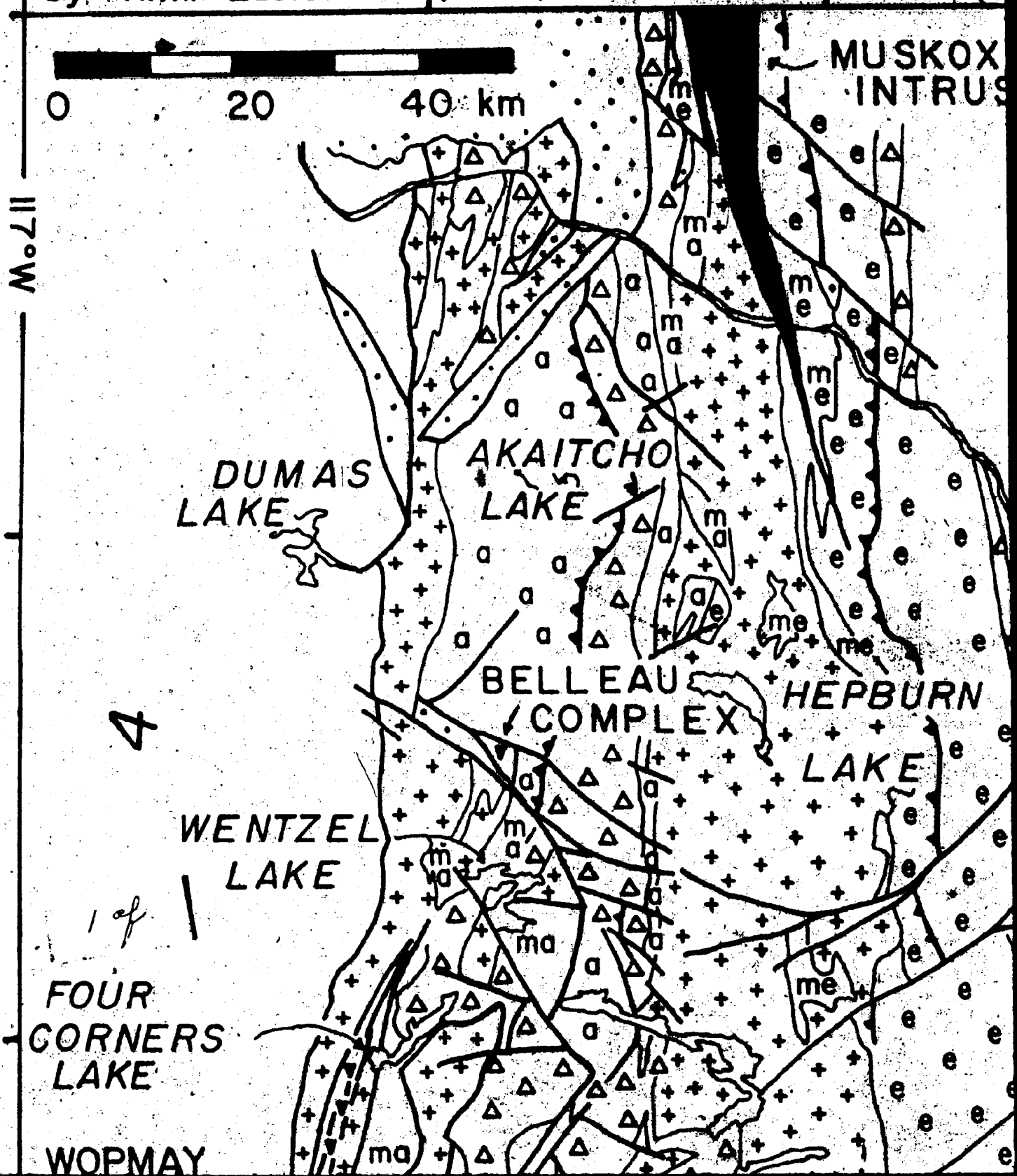
Chemical analyses of Epworth and Recluse Group sedimentary rocks.

	F910.79 ¹	D31.77 ²	F774.79 ³
Nb	5	17	0
Zr	50	159	2
Y	14	27	6
Sr	15	0	33
Rb	3	126	2
Pb	7	4	1
Zn	23	43	0
Cr	6	75	0
V	48	158	0
Ba	49	482	0
La		9.2	
Ce		24.8	
Pr		3.2	
Nd		14.8	
Sm		3.6	
Eu		0.8	
Gd		3.8	
Dy		2.8	
Ho		0.9	
Er		2.4	
Yb		2.1	

¹Rocknest Formation dolomite;²Rocknest Formation argillaceous dolomite;³Stanbridge Formation dolomite

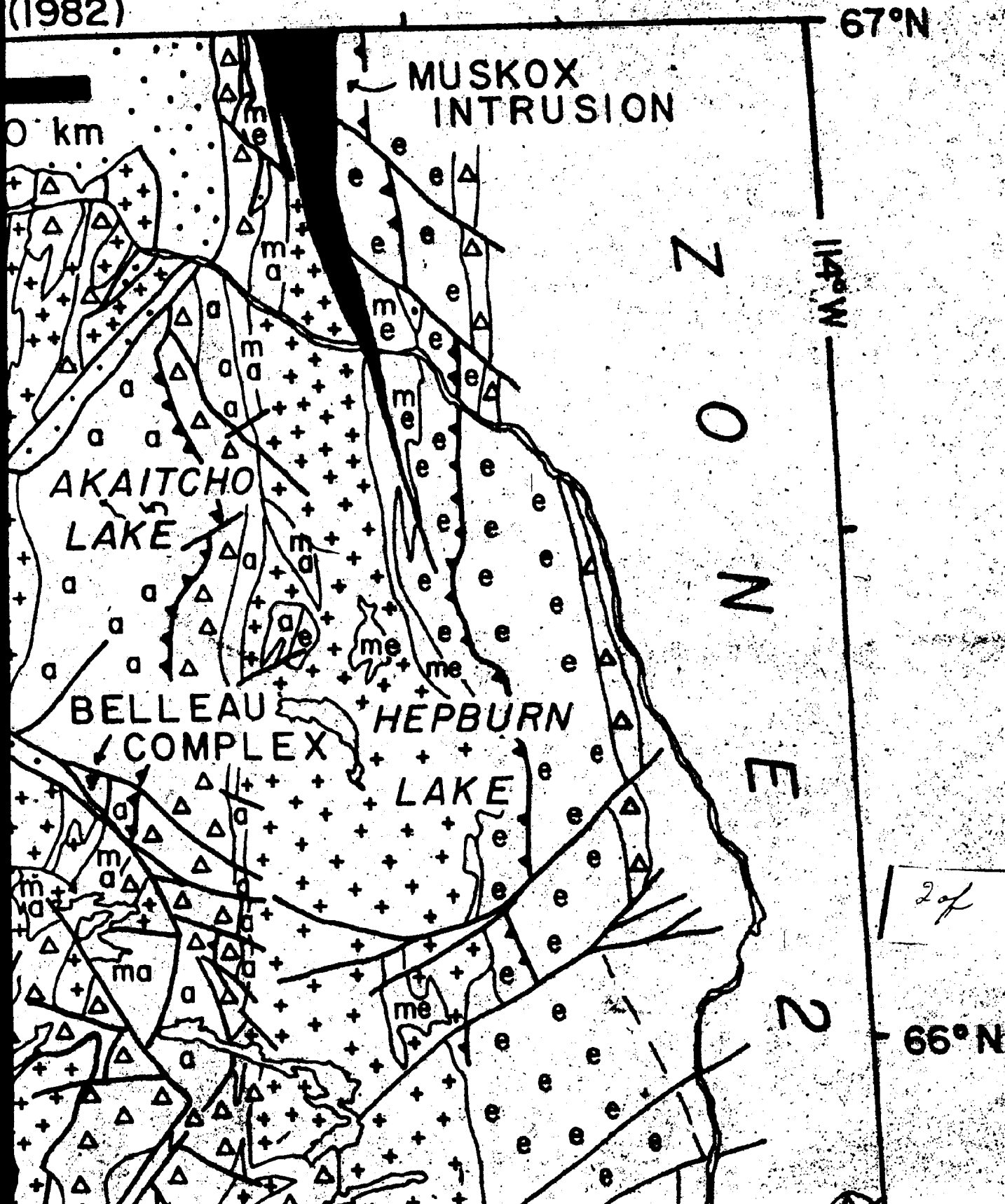
FIGURE 2.3 scale 1:500,000

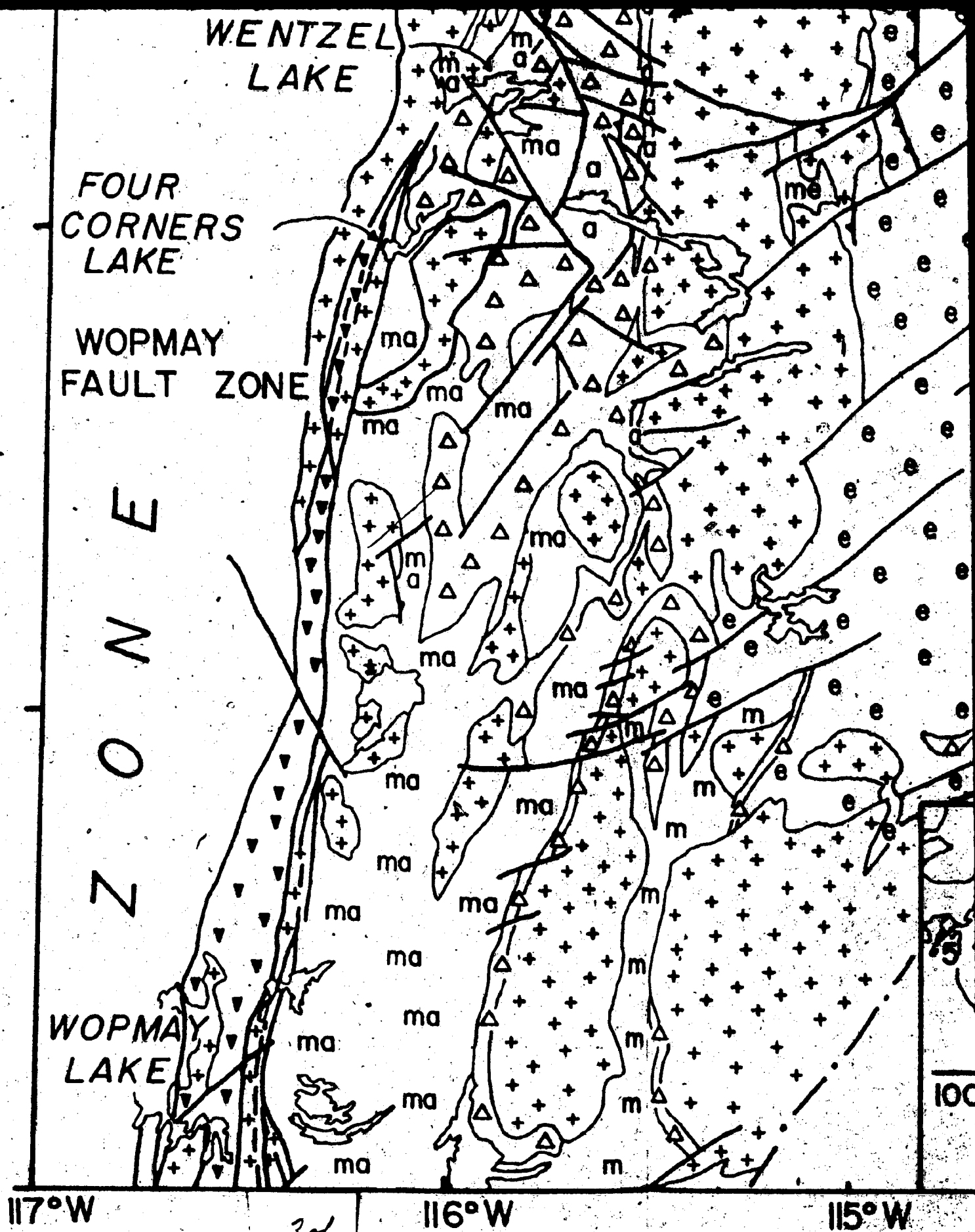
to accompany "Tectonic Significance of the Akaitcho
by R.M. Easton (1982)



scale 1:500,000

Significance of the Akaitcho Group
(1982)





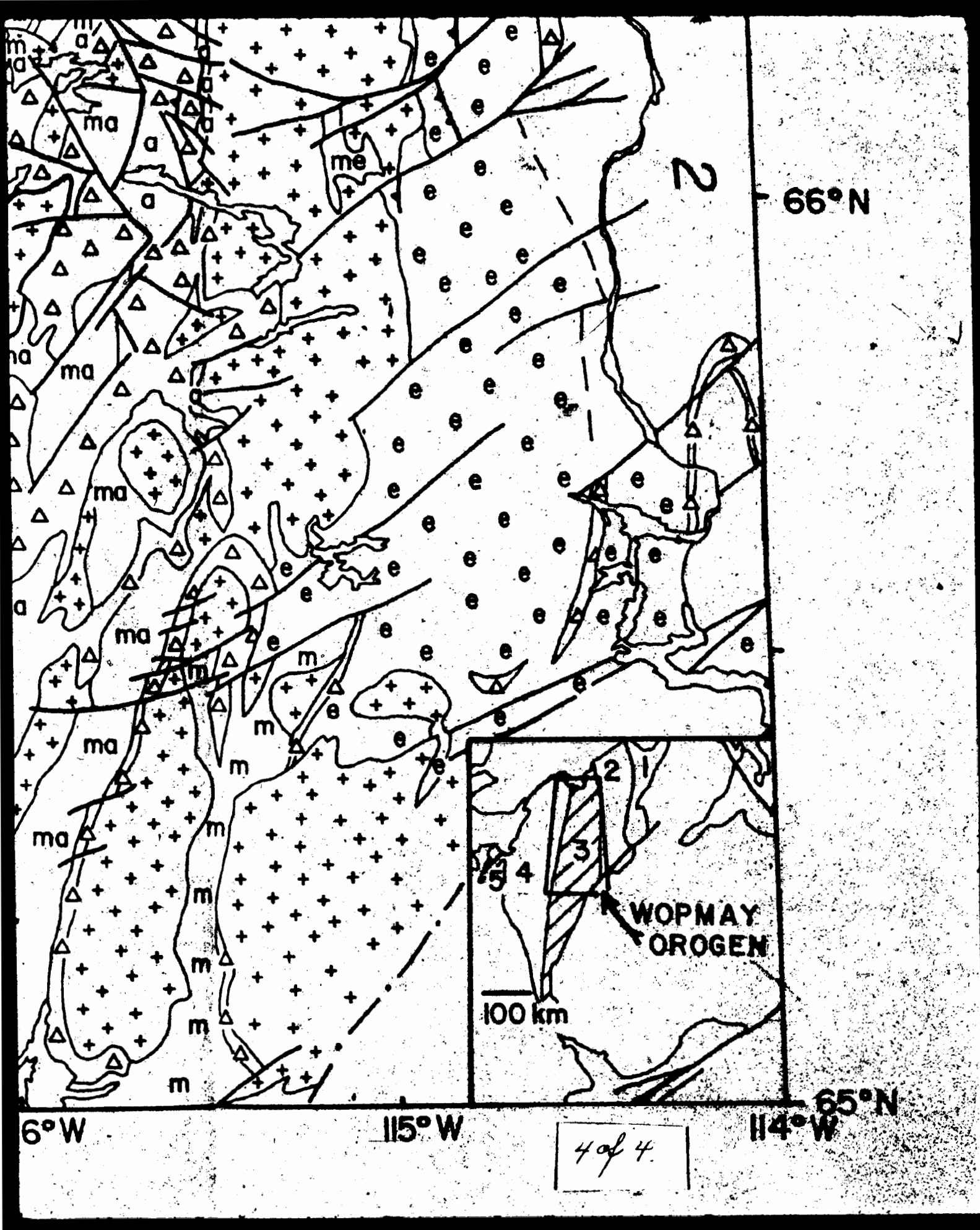
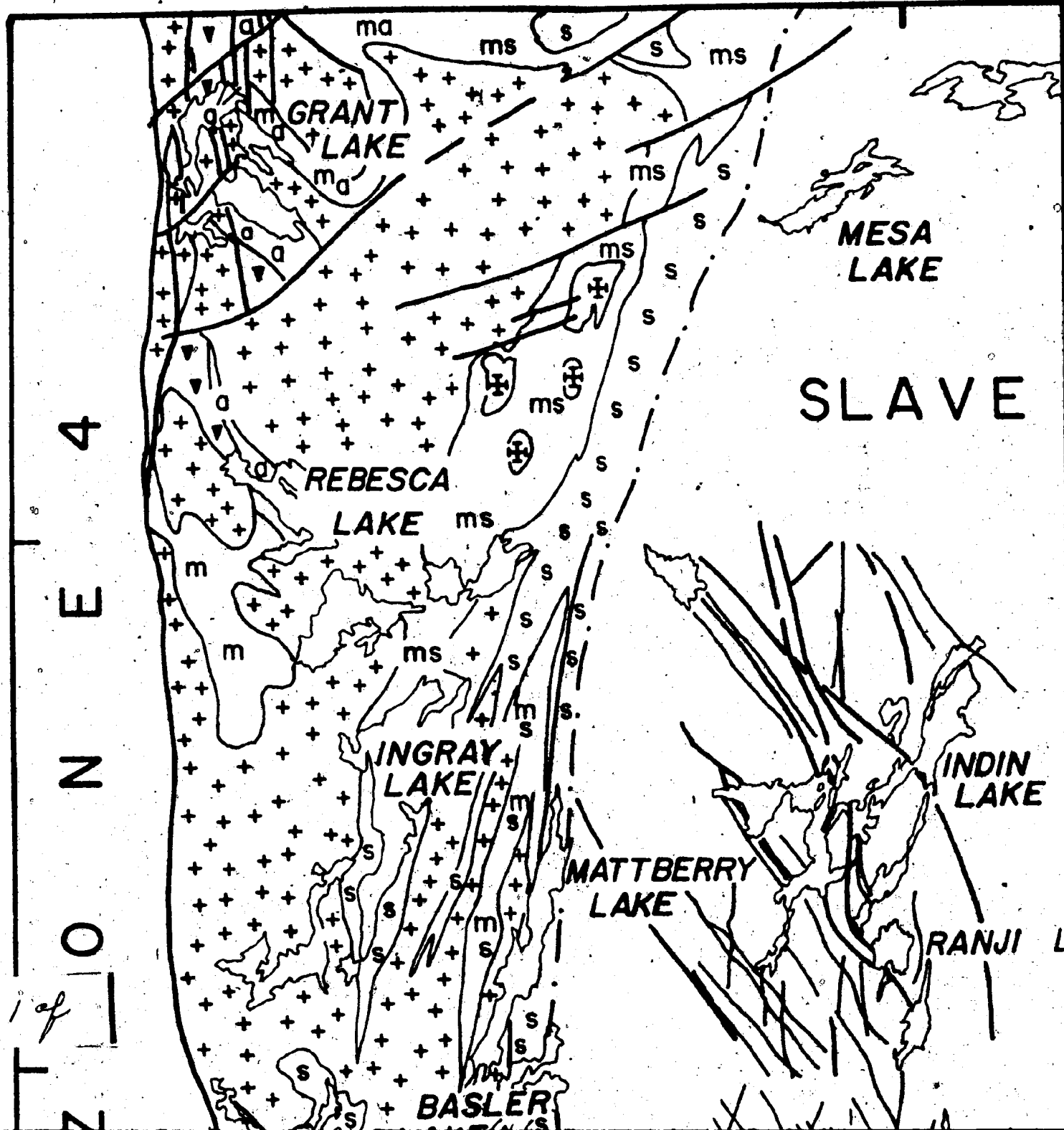


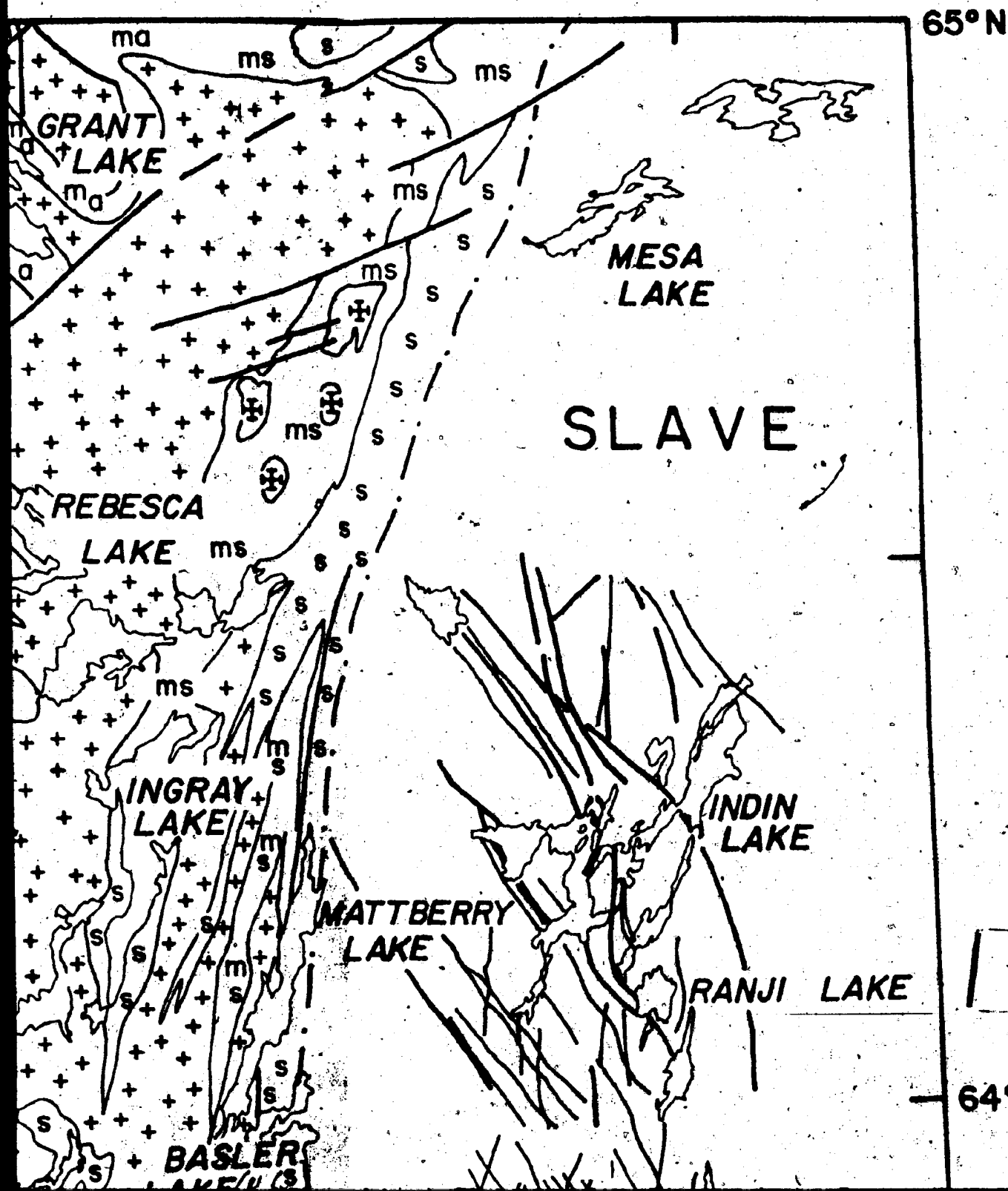
FIGURE 2.4 scale 1:500,000

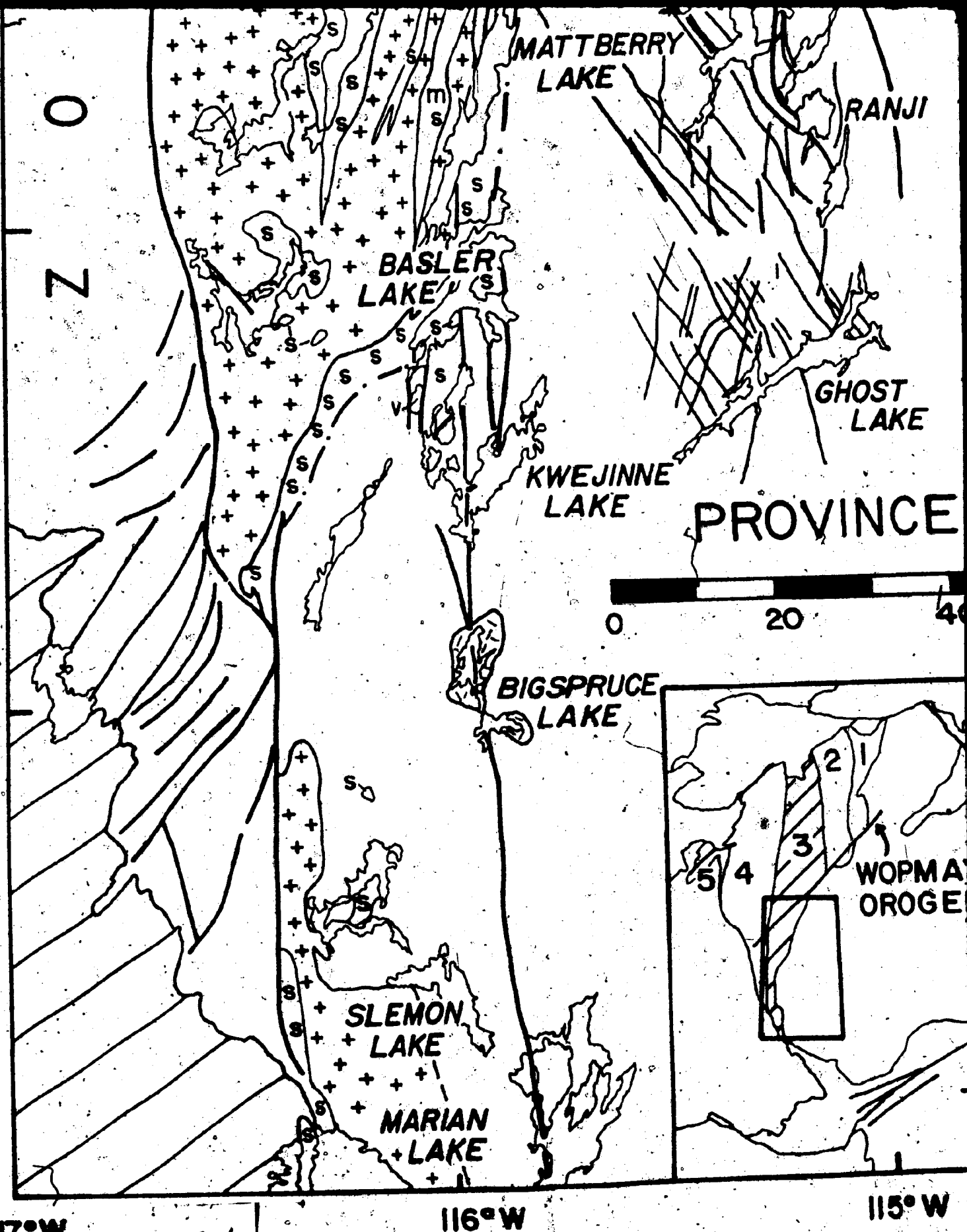
to accompany "Tectonic Significance of the
Akaitcho Group" by R.M. Easton (1982)



2.4 scale 1:500,000

by "Tectonic Significance of the
Group" by R.M. Easton (1982)



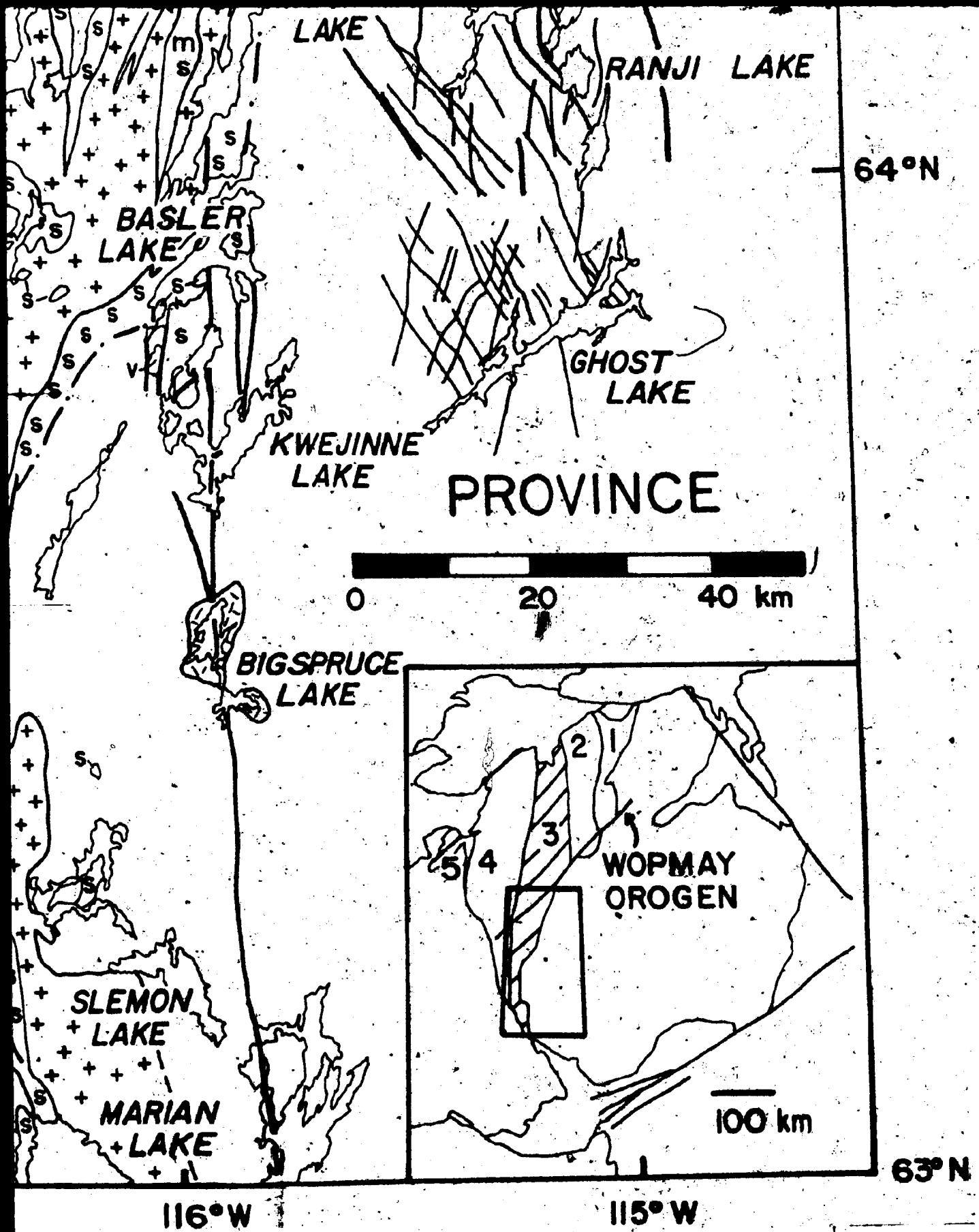


117°W

34.

116°W

115°W



4 of 4

116°
67°00'N

FIGURE 2.6 Simplified geological map of the Hepburn Lake map area (N.T.S. 86J/W4).

LEGEND

10 MUSKOKX INTRUSION

9 HORNBY BAY GROUP SANDSTONE

8 GREAT BEAR VOLCANO-PLUTONIC BELT (ZONE 4)

- 7 a) granitoid intrusions of the Hepburn Batholith
b) syenogranite and garnet granite intrusions and gneisses of the Wentzel Batholith
c) younger, mafic intrusions of the Hepburn Batholith
d) Sittiyek Igneous Complex, in-part may be older than Unit 1

6 EPHWATH GROUP a) Odjick Formation

1-5 AKALITUK GROUP

5 a) basalt flows; b) gabbro sills; c) siliceous siltstone

4 olive pelites and volcanoclastic sediments of the AGLEROK FORMATION

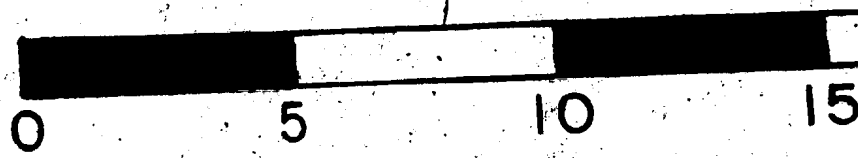
3 Nasittok Subgroup volcanic complexes

- a) aphanitic rhyolite; b) gabbro sills; c) massive and pillowed basalt flows; d) basalt tuff; e) porphyritic rhyolite flows; f) plagioclase porphyritic rhyolite sills; g) orthoclase

FIGURE 2.6 scale 1:
to accompany "Tectonic Significant
Group " by R.M. Easton

116°15'W
67°00'N

RME



Hepburn Lake

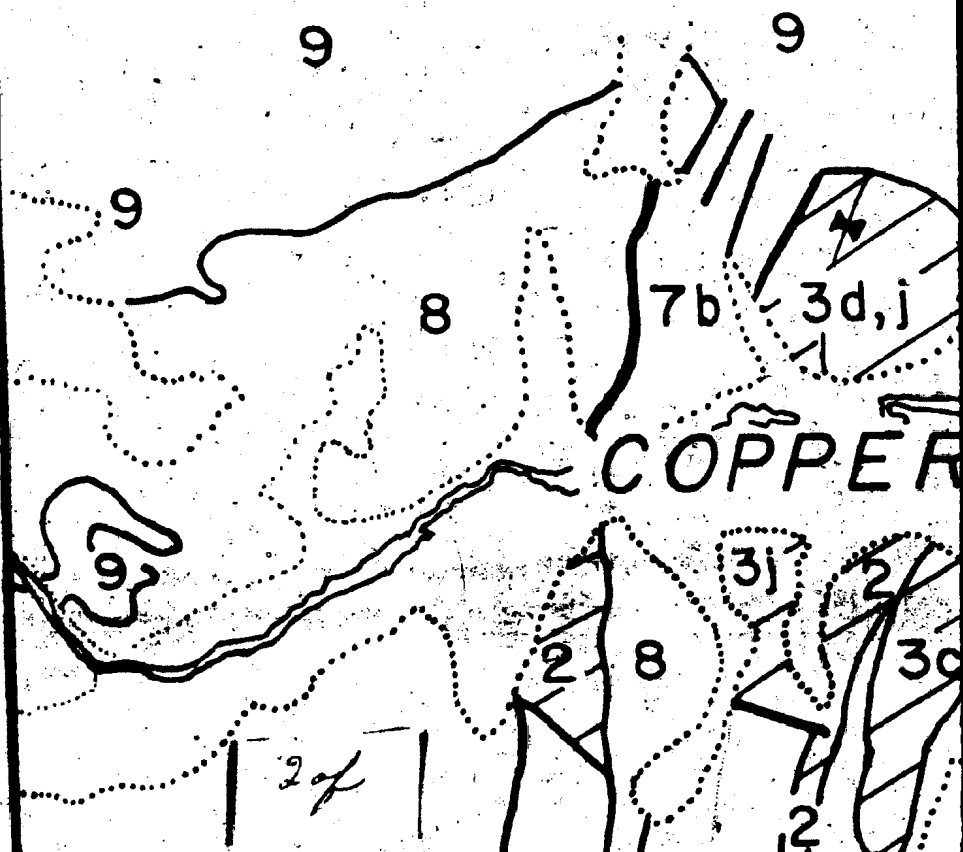
Batholith
sions and

Hepburn Batholith
be older than Unit 1

iceous siltstone

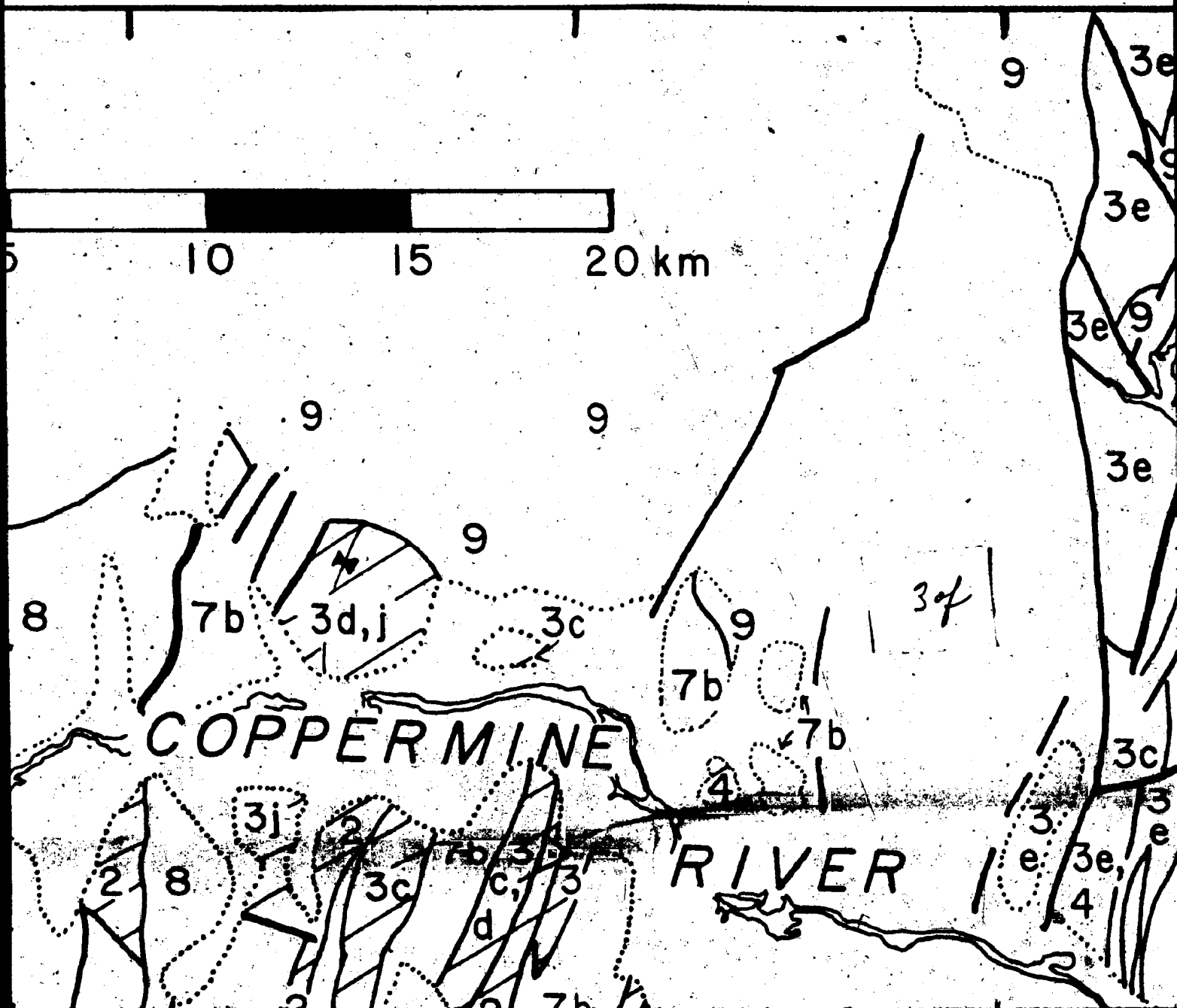
ts of the AGLEROK FORMATION

c) massive and
d) porphyritic rhyolite
e) siltstone; g) orthoclase



2.6 scale 1:125,000

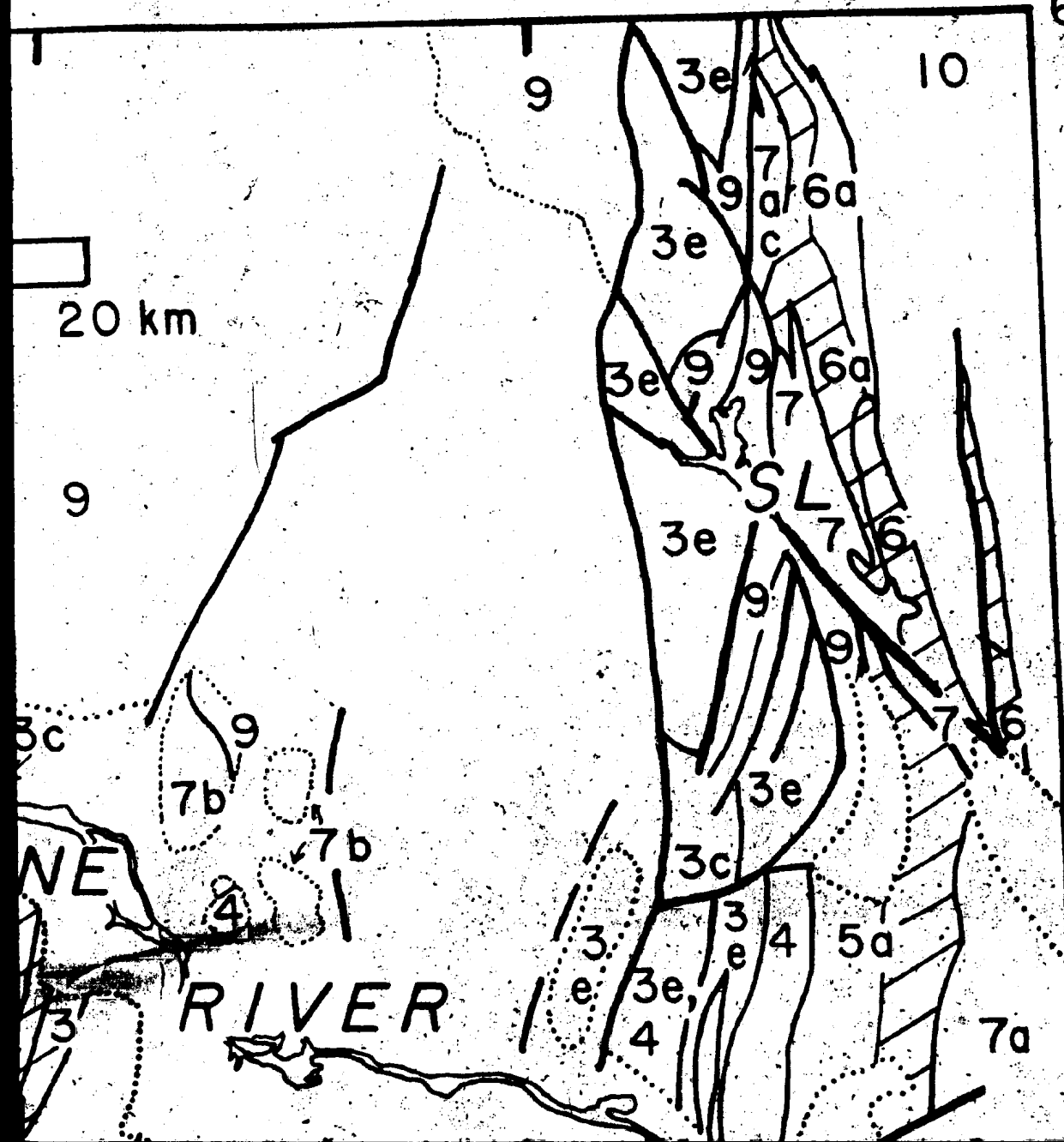
"Tectonic Significance of the Akaitcho
....." by R.M. Easton(1982)



000

of the Akaitcho
(2)

115°15' W
67°00' N



404

1-5 AKAITCHO GROUP

- 5 a) basalt flows; b) gabbro sills; c) siliceous siltstone
- 4 olive pelites and volcaniclastic sediments of the AGLEROK FORMATION
- 3 Nasittok Subgroup volcanic complexes
 - a) aphanatic rhyolite; b) gabbro sills; c) massive and pillowed basalt flows; d) basalt tuff; e) porphyritic rhyolite flows; f) plagioclase porphyritic rhyolite sills; g) orthoclase porphyritic rhyolite sills; h) conglomerate; i) siliceous siltstone; j) marble, orthoquartzite
- 2 subarkosic and arkosic turbidites of the ZEPHYR FORMATION
- 1 IPJUTAK SUBGROUP amphibolite; a) metapelite and quartzite

* / fold, of bedding, of foliation

— fault

— Okrark Thrust Fault, teeth on upper plate

— biotite isograd, mark on high T side

◻ sigmoidite (over 30% granite material)

AL	Akaitcho Lake
BL	Belleau Lake
HL	Hepburn Lake
KA	Kapvik Lake
KL	Kingrook Lake
OL	Okrark Lake
SA	Samandre Lake
SL	Sinister Lake
TL	Tuerton Lake
WL	Wentzel Lake
ZL	Zephyr Lake

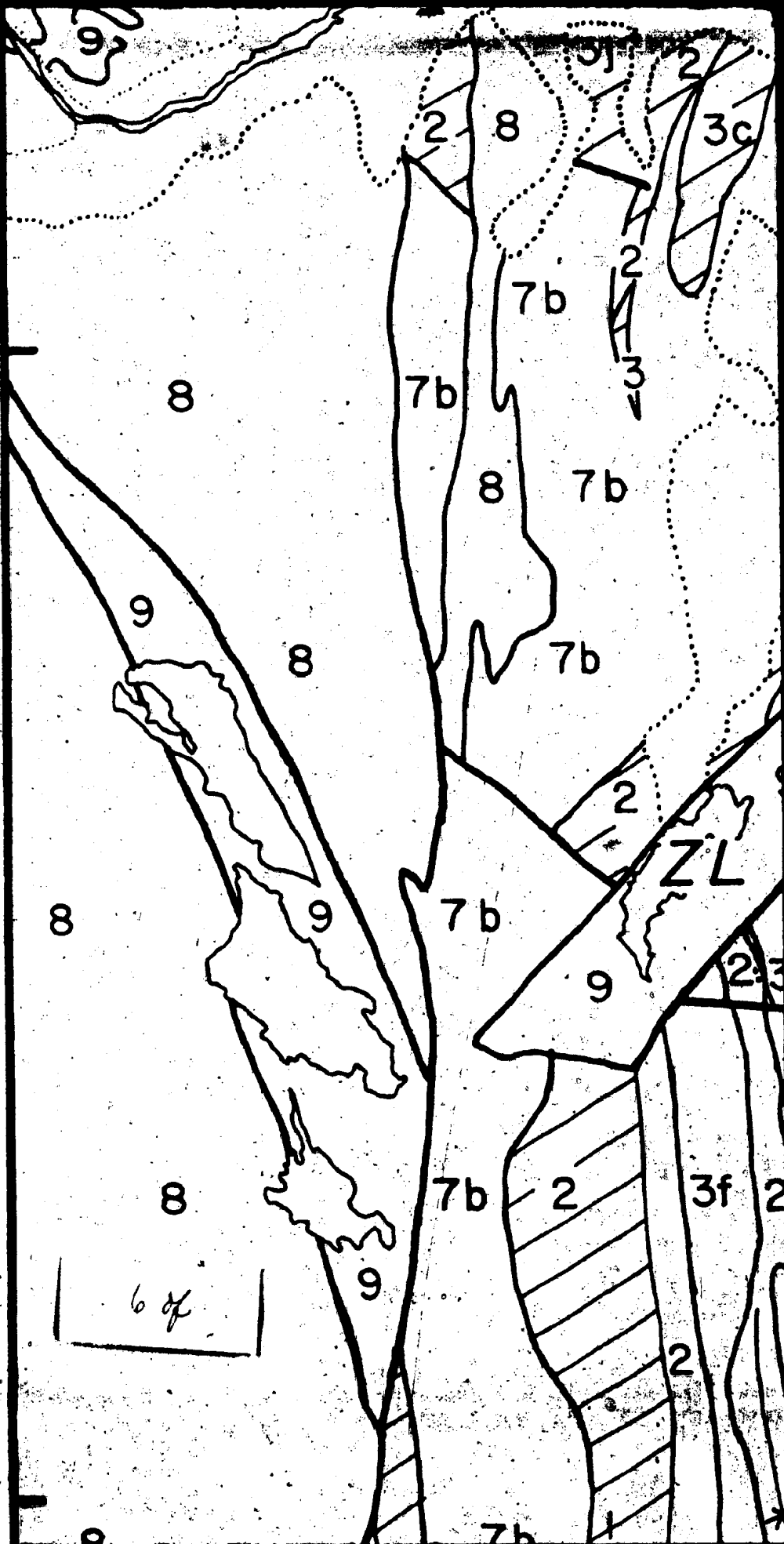
1.5 of 1

aceous siltstone
 of the AGLEROK FORMATION

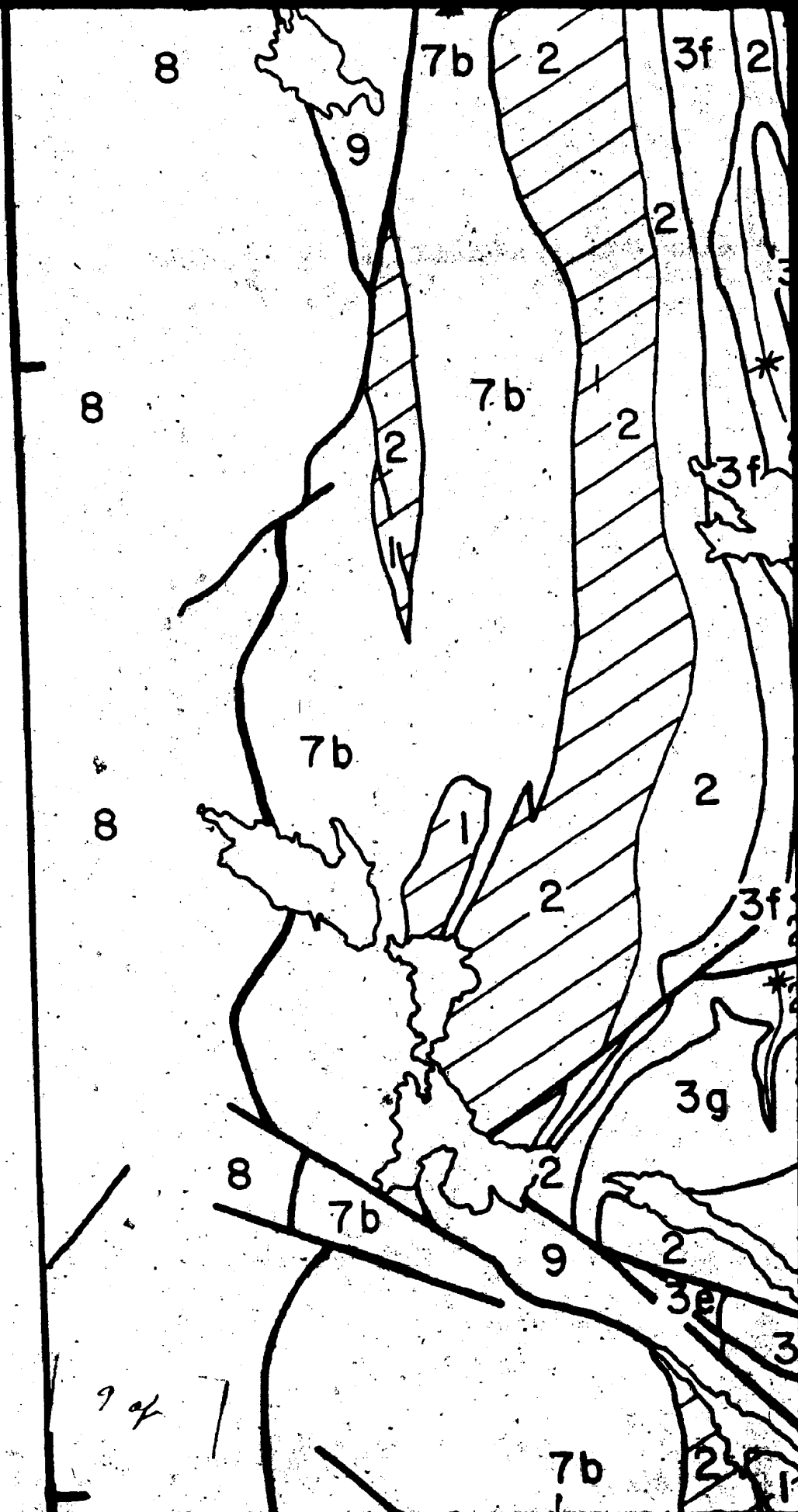
massive and
 porphyritic rhyolite.
 e sills; g) orthoclase
 te; i) siliceous

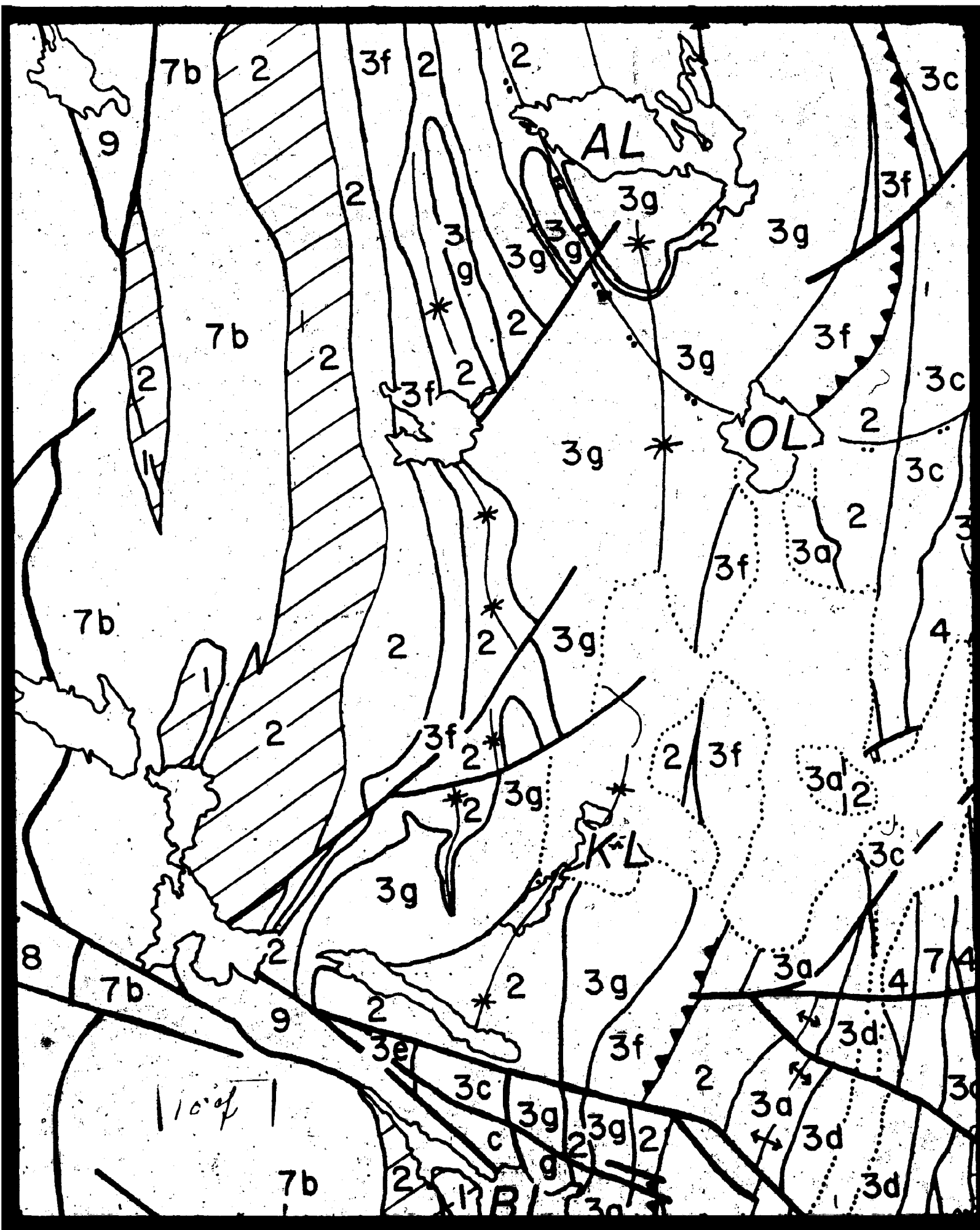
ZEPHYR FORMATION
 te and quartzite

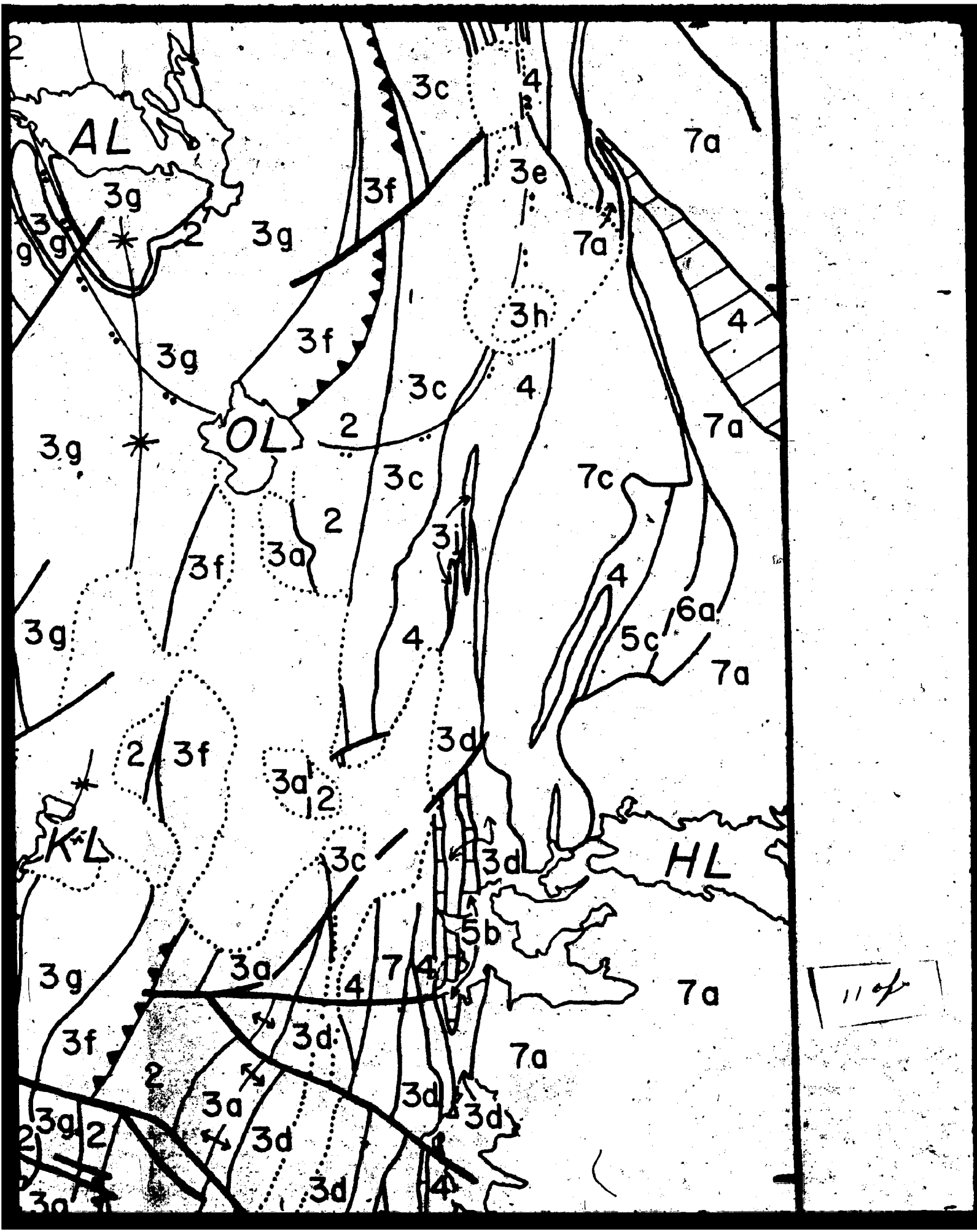
Akaltcho Lake
 Belleau Lake
 Hepburn Lake
 Kapvik Lake
 Kingarok Lake
 Krark Lake
 Samandre Lake
 Sinister Lake
 Tuerton Lake
 Wentzel Lake
 Zephyr Lake







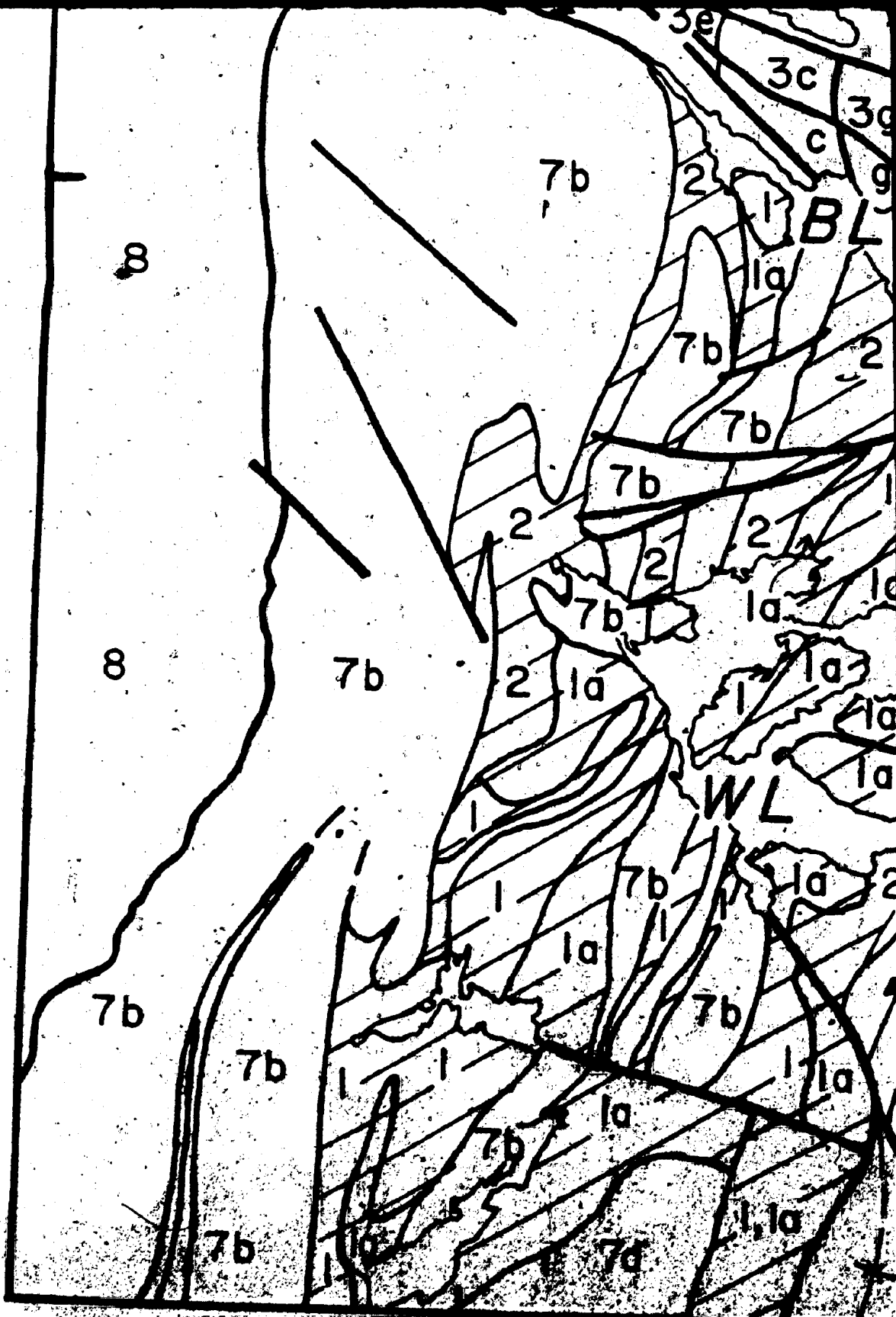


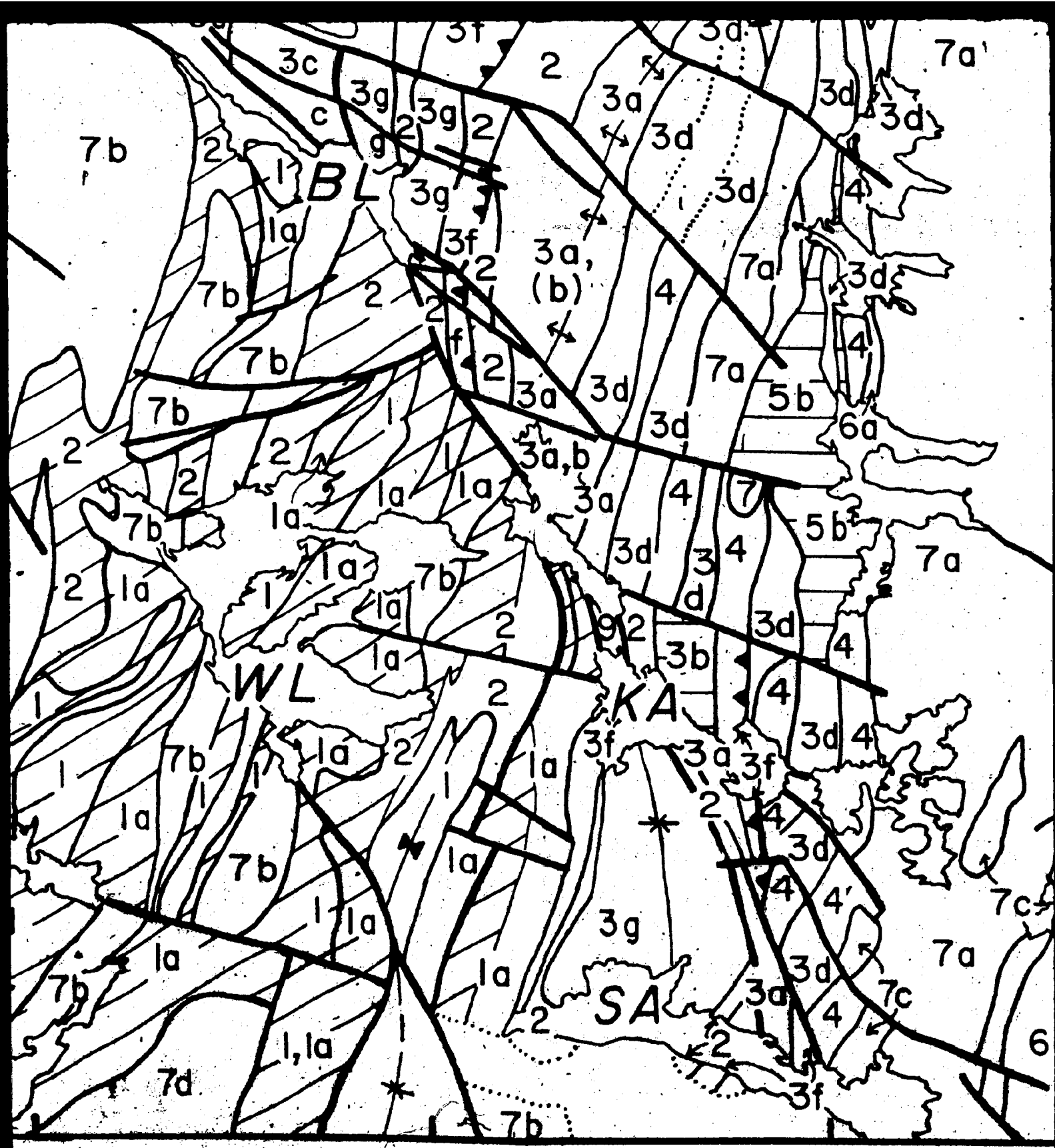


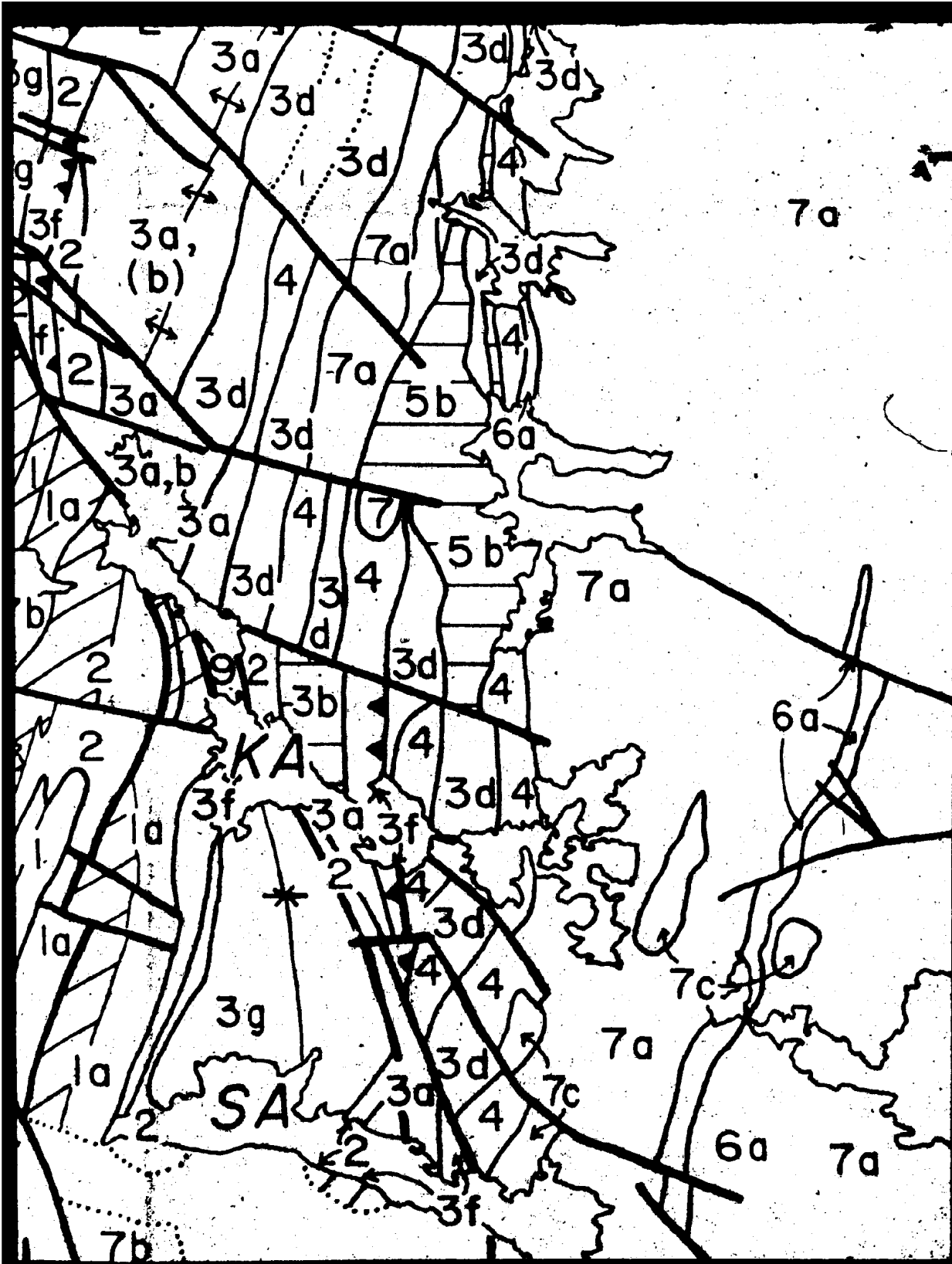
66°00'N

116°15'W

12 of







66°00'N

115°15'W

14814

C-1-2

Chemical analyses of Lower Devonian and Permian Group sedimentary rocks.

7710.754 031.752 7774.753

NO	17	0
IR	128	2
Y	27	6
ST	0	33
RB	126	2
PA	4	1
IN	43	0
CA	25	0
V	128	0
SA	487	0
LA	9.2	
LO	24.8	
SI	3.2	
PI	14.8	
RI	3.6	
TI	0.8	
VI	3.8	
VI	2.8	
VI	0.2	
VI	2.4	
VI	2.1	

1. Rockwell formation dolomite;
2. Rockwell formation argillaceous dolomite;
3. Sandridge formation dolomite.

① 9944 273 pocket

